University of Nottingham
UK | CHINA | MALAYSIA

Effect of cigarette smoke extract on allergen and viral responses in human bronchial epithelial cells

Omar Ali M Alqarni

Thesis submitted to the University of Nottingham for the degree of Doctor of Philosophy in Respiratory Medicine

Centre for Respiratory Research

School of Medicine

The University of Nottingham

June 2025

Acknowledgements

Firstly, all praise and thanks go to my god (Allah), who granted me the strength, resilience, and patience to complete my PhD and persevere through challenging times. I am deeply grateful to Allah for fulfilling my dreams and for granting me the health and life to reach this point.

Secondly, I would like to express my gratitude to the many individuals whose support and contributions have played a role in completing this thesis. I would like to express my deepest gratitude and warm thanks to my supervisor, Dr. Amanda Tatler, for believing in me and giving me the opportunity to pursue my PhD at her lab. I am deeply grateful for the invaluable support and guidance Dr. Tatler offered throughout my PhD, which words alone cannot fully express. I am sincerely thankful to Dr. Tatler for her invaluable guidance, encouragement, and patience, as well as for sharing her expertise, which played a pivotal role in shaping my development as an independent researcher. I truly couldn't have wished for a more outstanding supervisor. My sincerest gratitude and warm thanks also go to my second supervisor, Dr. Rachel Clifford, for all the valuable guidance, continued support, and advice during my PhD. Dr. Clifford's door was always open whenever I needed guidance or had questions about my research or writing. This PhD thesis would not have been completed without her endless help. I would also like to thank my former supervisor, Professor Linhua Pang, for his support and guidance at the early stages of my PhD journey. I would like to extend my warm thanks to all the members of our incredible research group (TC(A)G) in the Respiratory Medicine Department for creating such a welcoming atmosphere and for their support throughout my PhD journey. My thanks also go to the University of Nottingham for accepting me and providing me with the

resources I needed to pursue my PhD, as well as to my university in Saudi Arabia, Umm Al-Qura University and the Saudi Arabian Cultural Bureau in London for the support and funding I received during my PhD studies.

To my beloved father, who despite losing his vision recently, never lost sight of his belief in me. Thank you for your strength, love, and constant prayers that have guided me through this journey. To my great mother, thank you for shaping me into the person I am today. Your constant love, guidance, and sacrifices since my childhood have shaped every success I have achieved. My dear brothers, sisters, nephews, and nieces, your unwavering support and encouragement have been the foundation of my success. I am forever grateful for everything you have done for me, and no words can truly express how much you mean to me.

Lastly, a special thanks to my little family, my wife and my daughter (Sama), who was born in the second year of my PhD. Your unwavering support, love, and presence have provided immense strength and encouragement throughout my PhD journey. Keep smiling, little girl, you have been my greatest source of motivation and inspiration, reminding me every day why I pursued this journey.

Conference presentations and awards

Accepted abstracts for presentations at national and international meetings

Omar Alqarni, Mushabbab Alahmari, Abdulrahman Alghamdi, Laura Matthews, Linhua Pang, Rachel Clifford, Amanda Tatler. Effect of cigarette smoke extract on cell-free DNA release from bronchial epithelial cells**.** Accepted for poster presentation at the European Respiratory Society International Congress, Vienna, Austria, 2024.

Omar Alqarni, Mushabbab Alahmari, Abdulrahman Alghamdi, Linhua Pang, Rachel Clifford, Amanda Tatler. Effect of cigarette smoke extract on the inflammatory responses and cell-free DNA release from bronchial epithelial cells**.** Accepted for poster presentation at the University of Leicester and Nottingham Joint Respiratory Research Day, Leicester, United Kingdom, 2024

Omar Alqarni, Linhua Pang, Rachel Clifford, Amanda Tatler. Effect of cigarette smoke extract on the inflammatory responses of human bronchial epithelial cells in asthma. Accepted for poster presentation at Biodiscovery Institute Research Day, University of Nottingham, Nottingham, United Kingdom, 2023

Omar Alqarni, Linhua Pang, Rachel Clifford, Amanda Tatler. Effect of cigarette smoke extract on viral responses in human bronchial epithelial cells. Accepted for oral presentation at Sue Watson Oral Presentation Event, University of Nottingham, Nottingham, United Kingdom, 2023

Awards

An excellence award from Royal Embassy of Saudi Arabian Cultural Bureau, 2022 and 2023

Abbreviations

A

Adjusted P values (Padj)

Airway hyperresponsiveness (AHR)

Airway smooth muscle (ASM)

Allergic rhinitis (AR)

Allergic airway inflammation (AAI)

Alveolar macrophages (AMs)

Arachidonic acid (AA)

Activate transient receptor potential vanilloid-1 (TRPV1)

A one-way analysis of variance (ANOVA)

B

Base pairs (bp)

Bicinchoninic acid (BCA)

Bovine pituitary extract (BPE)

Bovine serum albumin (BSA)

Bronchoalveolar lavage (BAL)

Bronchoalveolar lavage fluid (BALF)

5-Bromo-2′-deoxyuridine (BrdU)

C

Cell-free DNA (cfDNA)

Cell-free microbial DNA (cfmDNA)

Cigarette smoke (CS)

Cigarette smoke condensate (CSC)

Cigarette smoke extract (CSE)

Circulating tumor cells (CTCs)

Circulating tumor DNA (ctDNA)

Cyclooxygenase (COX)

Chronic obstructive pulmonary disease (COPD)

Chronic respiratory diseases (CRDs)

Cyclic adenosine monophosphate (cAMP)

Cyclin-dependent kinase 4 (CDK4)

Coluble intercellular adhesion molecule-1 (sICAM-1)

D

Dermatophagoides pteronyssinus1 (*Der P1*)

Deoxyribonucleic acid (DNA)

Dimethyl sulfoxide (DMSO)

Double-stranded RNA (dsRNA)

Dulbecco's Modified Eagle's Medium (DMEM)

Double-distilled water (ddH_2o)

E

Elution buffer (EB)

Enzyme-Linked immunosorbent assay (ELISA)

Enhanced chemiluminescence (ECL)

Environmental tobacco smoke (ETS)

Epithelial growth factor (EGF)

Exercise-induced asthma (EIA)

Extracellular vehicles (EVs)

F

Fluticasone propionate (FP)

Foetal bovine serum (FBS)

Forced expiratory volume in one second (FEV_1)

Forced vital capacity (/FVC)

G

Gene Ontology (GO)

Glucocorticoid receptor (GR)

Glucocorticoid receptor alpha (GR-α)

Glucocorticoid receptor β isoform (GR-β)

Glucocorticoid response element (GRE)

H

Horseradish peroxidase (HRP)

House dust mite (HDM)

Human airway smooth muscle cells (HASMCs)

Human bronchial epithelial cells (HBECs)

Human rhinovirus (HRV)

I

Immortalised human bronchial epithelial cells (iHBECs)

Immunoglobulin E (IgE)

Inhaled corticosteroids (ICS)

Interferon (IFN)

Interleukin (IL)

K

Keratinocyte serum-free-medium (KSFM)

Kyoto Encyclopedia of Genes and Genomes (KEGG)

L

Leukotriene receptor antagonists (LTRAs)

Lipopolysaccharide (LPS)

Long-acting beta$_2$-agonists (LABA)

Log fold Change (LFC)

M

Matrix metalloproteinase-9 (MMP-9)

Messenger Ribonucleic Acid (mRNA)

Microsomal PGE_2 synthases (mPGES)

Mitogen-activated protein kinases (MAPKs)

N

Nanoparticle tracking analysis (NTA)

National health service (NHS)

National Research Ethics Service (NRES)

National Institute for Healthcare and Care Excellence (NICE)

Neutrophil extracellular traps (NETs)

Nitric oxide (NO)

Noncommunicable disease (NCD)

No template control (NTC)

P

Particulate matter (PM)

Pattern-recognition receptors (PRRs)

Pathogen-associated molecular patterns (PAMPs)

Phenylmethylsulphonyl Fluoride (PMSF)

Phosphate-buffered saline (PBS)

Photomultiplier tube (PMT)

Polyinosinic-polycytidylic acid (Poly (I:C)

Polyacrylamide gel electrophoresis (PAGE)

Prostaglandins (PG)

Prostaglandin H_2 (PGH_2)

Protease Inhibitor Cocktail (PIC)

Plasmacytoid dendritic cells (pDCs)

Q

Quantitative real-time PCR (qPCR)

R

Radioimmunoprecipitation assay (RIPA)

Raw quantification cycle (Cq)

Respiratory syncytial virus (RSV)

Regulated on activation, normal T cell expressed and secreted (RANTES)

Respiratory syncytial virus (RSV)

Ribonucleic acid (RNA)

Ribosomal RNA (rRNA)

Rhinovirus (RV)

RNA sequencing (RNA-Seq)

S

Short-acting beta$_2$-agonists (SABA)

T

T helper 1 (Th1)

T helper 2 (Th2)

Tetramethylbenzidine (TMB)

Telomerase enzyme reverse transcriptase (TERT)

Thymic Stromal Lymphopoietin (TSLP)

Tris-buffered saline (TBS)

Tumour necrosis factor α (TNF-α)

Type 2-high asthma (T2-high)

Type 2 innate lymphoid cells (ILC2)

Type 2-low asthma (Non-T2)

Transforming growth factor β (TGF-β)

Toll-like receptors (TLRs)

Tris buffered saline with tween 20 (TBS-T)

Transmission electron microscopy (TEM)

U

United Kingdom (UK)

United States (USA)

V

Vascular endothelial growth factor (VEGF)

Vascular cell adhesion protein 1 (VCAM-1)

W

World Health Organization (WHO)

Statement of originality

I acknowledge that RNA-sequencing methodology processes and all the analyses were done by the Deep Seq team, Centre for Genetics and Genomics, The University of Nottingham. The analysis of gene expression and functional data was carried out independently by me using Excel files obtained from the service provider. I also acknowledge the assistance from Dr. Kenton Arkill's group for performing the transmission electron microscopy (TEM) analysis of extracellular vesicles (EVs).

Abstract

Background: Asthma is a heterogeneous lung disorder characterized by airway inflammation, hyperresponsiveness, and remodeling. Airway inflammation is a primary characteristic of asthma, and the endotypes of asthma are classified into two main types based on inflammatory profiles, namely Type 2-high allergic asthma (T2-high) and non-Type 2 asthma (Non-T2). Cigarette smoke combined with asthmatic inflammation may induce important changes in asthma pathogenesis. Cigarette smoke extract (CSE) can modify the inflammatory responses in human airway smooth muscle cells (HASMCs), promoting a shift from steroid-sensitive type 2 (T2-high) eosinophilic inflammatory responses to steroid-insensitive (Non-T2) neutrophilic inflammatory responses, at least in part through a COX-2/PGE2-dependent mechanism. Human bronchial epithelial cells (HBECs) are the first line of defence against inhaled insults, including viruses and allergens, and are an important source of a group of cytokines termed alarmins, which play a key role in the initiation of allergen- and viral-induced T2 inflammatory responses in asthma. Cell-free DNA (cfDNA), refers to all non-encapsulated DNA in the bloodstream or other fluids that occurs as active secretion from the cells and during normal apoptotic and necrotic processes, and is known to be released from virally infected HBECs. Whether CSE can modify allergen and viral-induced T2 inflammatory responses and promote non-T2 neutrophilic inflammatory responses, and modulate cfDNA release from HBECs that can alter HASMCs function is unclear.

Methods: CSE was prepared from the smoke of (3R4F) research-grade cigarettes bubbled into 20 ml of culture medium. Immortalised HBECs (iHBECs) were treated with and without CSE (3%) and/or house dust mite (*Der p1*) 10 µg/ml for 24 hours, and/or viral mimic Poly(I:C) 10 µg/ml for 24 hours and 48 hours. The concentrations of alarmins (IL-25, IL-33, and TSLP), Th2 cytokines (IL-4, IL-5, and IL-13), eosinophilic chemokines (Eotaxin, RANTES, and IP-10), pleiotropic cytokine IL-6, and neutrophilic chemokine IL-8 were measured in conditioned media using a Luminex® Multiplex assay.
Quantitative real-time PCR (qPCR) for telomerase reverse transcript (TERT) and the TapeStation System were used to investigate the concentration of cfDNA released.

BrdU Cell Proliferation ELISA and PrestoBlue™ Cell Viability Reagent were used to assess HASMCS proliferation. A cell Collagen-based Contraction assay was used to assess HASMCs contraction, and transcriptome profiling using RNA-Sequence technology was used identify gene expression changes in HASMCs.

Results: I found that CSE did not modulate the inflammatory mediator response of iHBECs to *Der P1* allergen, with no interaction between CSE and *Der P1* exposure on the production of alarmins (IL-25, IL-33, TSLP), Th2 cytokines (IL-4, IL-5, IL-13), eosinophilic chemokines (Eotaxin, IP-10, RANTES). However, CSE significantly increased the production of neutrophilic chemokine IL-8 in response to *Der P1*. Notably, I found that CSE modulates the response of iHBECs to viral mimic poly (I:C) through altering inflammatory responses, suppressing epithelial-derived alarmins and eosinophil responses, and inducing neutrophilic responses. cfDNA was released in response to Poly (I:C) but not CSE. Interestingly, co-stimulation of CSE and Poly (I:C) significantly increased the concentration of released cfDNA, relative to Poly (I:C) alone, (0.03901 and 0.03696 Cq respectively $p<0.05$, $n=3$). Functional studies of iHBEC cfDNA revealed that cfDNA from poly (I:C) and CSE+poly (I:C)-stimulated iHBECs had no effect on HASMC proliferation but significantly modulated gene expression in HASMCs.

Conclusion: This thesis showed that CSE may have a minimal effect on allergen-induced inflammatory mediator response of iHBECs but did have profound effects on the inflammatory response to the viral mimic poly (I:C) through altering inflammatory responses, which may suggest a shift from eosinophilic to neutrophilic airway inflammation. cfDNA released from poly (I:C) and co-stimulation of CSE and poly (I:C)-stimulated iHBECs had no effect on remodelling of HASMCs but significantly modulated gene expression specifically in pathways related to chemokine activity and defence response to virus.

Table of Contents

List of Figures

List of Tables

Chapter 1. Introduction

1.1 Asthma Definition

Asthma is a heterogeneous lung disorder characterized by airway inflammation, hyperresponsiveness, and remodeling. Patients with asthma tend to have symptoms including expiratory wheezing, chest tightness, shortness of breath, and cough that vary over time and in intensity, together with the limitation of expiratory airflow [1]. Exposure to irritants such as cigarette smoke causes worsening of these symptoms. Many cells play an important role in asthmatic airway inflammation, such as mast cells, eosinophils, neutrophils, T lymphocytes, macrophages, and epithelial cells [2]. The currently available management of asthma includes pharmacological and non-pharmacological interventions. However, only a few of these interventions have been shown to relieve asthma symptoms and improve lung function. Globally, a significant percentage of asthma patients (5-12%) may respond poorly to the current treatments, necessitating personalized approaches and consideration of pathological changes [3]. Therefore, further studies of the underlying mechanisms of asthma are needed.

1.2 Epidemiology of Asthma

1.2.1 Prevalence and impact

Asthma is a chronic respiratory disease that affects children and adults, with higher incidence and prevalence in children, but higher morbidity and mortality rates in adults [4]. Asthma is considered a major noncommunicable disease (NCD) and the most common chronic disease among children around the world, and the prevalence of asthma has increased worldwide in the last century [5, 6]. Asthma is a global health problem that affects around 300 million people of different ages and ethnic groups in many countries, and low- and lower-middle-income countries are

most affected by asthma-related deaths [6, 7]. There are around 8 million people in the United Kingdom (UK) who have been diagnosed with asthma, 5.4 million of those people are receiving asthma treatment [8]. Each year, there are around 160,000 people in the UK diagnosed with asthma which accounts for 60,000 hospital admissions and 2-3% of primary care consultations [8]. The National Health Service (NHS) spends at least £1.1 billion annually on treating and caring for asthmatic people in the UK [9]. Furthermore, the financial burden on asthmatic patients in many Western countries ranges from $300 to $1,300 per patient annually [10].

1.2.2 Mortality and Morbidity

According to the World Health Organization (WHO), asthma affected around 262 million individuals and caused 461,000 deaths in 2019 [6]. Over the last 40 years, there has been a significant increase in morbidity, mortality, and economic burden globally associated with asthma, mostly in children [11]. Asthma is responsible for considerable morbidity in the UK [9]. The UK has the highest prevalence rate in the world for asthma symptoms in children, with every classroom in the UK having on average three children with asthma [12]. In addition, the UK has one of the highest rates of death due to asthma in Europe, with an average of 3 deaths every day from asthma attacks [12].

1.2.3 Risk Factors

Asthma is associated with many risk factors which may contribute to asthma phenotype, including environmental and genetic factors. Environmental factors such as air pollutants, occupational exposures, respiratory viruses, tobacco smoke, and allergens in the air have been suggested to contribute to allergic asthma pathogenesis [13, 14]. Globally, smoking was the primary risk factor, followed by air

pollution and occupational exposure, responsible for the age-standardised rates of disability-adjusted life years from chronic respiratory diseases (CRDs) [15]. Many studies have been conducted showing a correlation between smoking and the development of asthma [16, 17]. Continued exposure to cigarette smoke (CS) can modify the balance between T helper 1 (Th1) and T helper 2 (Th2) cells in the lung [18]. In addition, studies of asthmatic patients stated that up to 85% of asthma exacerbations in children and about one-half of asthma episodes in adults are caused by viral infection [19, 20]. Asthma is also influenced by genetic predisposition. A study of twins, their siblings, and parents showed that genetic factors accounted for 70% of the association between asthma and allergens and were the primary cause of the association [21]. Another finding showed that 118 different genes had been associated with asthma in a review study of genes associated with asthma/atopy phenotypes [22]. Furthermore, a family history of asthma was identified as a risk factor in asthma pathogenesis, suggesting that genetics play a role in asthma development [23].

1.3 Asthma diagnosis and treatment

1.3.1 Diagnosis of asthma

Asthma is characterized by clinical symptoms such as cough, wheezing, and shortness of breath [24]. Clinical diagnosis of asthma is based on the combination of the presence of asthma symptoms and objective lung function tests [25]. Spirometry test with bronchodilator reversibility remains the mainstay lung function test for the diagnosis of asthma in both children and adults [26]. A ratio of forced expiratory volume in one second to forced vital capacity (FEV_1/FVC) of less than 70% indicates

an airway obstruction and is considered a positive test for asthma. Moreover, bronchodilator reversibility is considered positive if there is an increase of 12% or more and an increase of volume by 200 ml or more in FEV_1/FVC after inhalation of a bronchodilator [27]. After confirming a diagnosis of asthma, a treatment plan is developed to control the symptoms of the disease.

1.3.2 Treatment

The goals for asthma treatment are to reduce symptoms, maintain normal activity levels, prevent exacerbation and emergency department visits, and achieve long-term control of asthma [28]. Steroids and other anti-inflammatory drugs, together with bronchodilators, are currently the key treatment for asthma control and prevention of attack by reducing inflammation, mucus production, and swelling in the airways [29].

1.3.2.1 Corticosteroids

Corticosteroids are by far the most effective treatment of asthma and the only drugs that suppress inflammation in asthmatic airways, even with low doses [30]. Inhaled corticosteroids (ICS) improve asthma control and reduce exacerbations [31]. Type 2 airway inflammation (allergic inflammation) is usually suppressed by corticosteroids, which have been the mainstay medication to control allergic asthma [32].

Corticosteroids reduce inflammation by either activation or suppression of different genes [33]. Airway inflammation in asthma is driven by increased expression of inflammatory genes, including cytokines, chemokines, inflammatory enzymes, and receptor genes. Corticosteroids switch off multiple inflammatory genes mainly by reversing histone acetylation of these inflammatory genes, which is

mediated through the binding to the corticosteroid receptors, leading to reduced inflammatory gene expression [34, 35]. ICS targets gene transcription by interacting with the glucocorticoid receptor (GR) at the glucocorticoid response element (GRE) [36]. Fluticasone propionate (FP) is an example of ICS treatment of asthma for children and adults. Most respiratory societies and organizations recommend in their management guidelines a dose titration approach to the use of FP and other ICS treatments [37]. Budesonide is another ICS treatment used to treat airway inflammation in asthma, able to improveFEV_1 values in severe asthma patients, and reduce exacerbations in moderate to severe asthma [38]. Additionally, Budesonide inhibited the production of vascular endothelial growth factor (VEGF)-stimulated by T helper 2 (Th2) cytokines, including interleukin-4 (IL-4), IL-5, and IL-13 in airway smooth muscle cells *in vitro* [39]. Beside ICS, systemic corticosteroids (oral or intravenous) are another approach to manage uncontrolled asthma. They are more frequently used in severe asthmatic patients than in those with mild asthma [40], and reduce the need for hospital admission in patients with acute asthma [41].

1.3.2.2 Other anti-inflammatory drugs

No other anti-inflammatory treatment is as effective to control asthma as corticosteroids. However, other treatments may reduce the need for a high dose of ICS [42]. Leukotriene receptor antagonists (LTRAs) are drugs used to reduce the function of leukotrienes, which are inflammatory mediators that cause bronchoconstriction and airway hyperresponsiveness (AHR). Zafirlukast and Montelukast are LTRAs useful for the long-term management of asthma in addition to ICS. They are most valuable for asthma patients complicated by exercise-induced asthma (EIA) or allergic rhinitis (AR). The use of LTRAs results in a significant improvement in respiratory function and asthma symptoms by inducing

bronchodilation action and airway inflammation inhibition [43].

Cromolyn sodium and nedocromil sodium are other approaches for the treatment of asthma. They are prophylactic mast cell stabilizer agents used to inhibit the activation of mast cells in asthma [44]. Cromolyn sodium inhibits the release of inflammatory mediators induced by specific antigens and nonspecific mechanisms, such as exercise, from mast cells. Cromolyn sodium can control mild to moderate chronic asthma symptoms in 60-70% of patients and may allow the reduction of corticosteroid dosage in severe steroid-dependent asthmatics [45]. Nedocromil sodium has anti-inflammatory effects *in vitro* and *in vivo* by inhibiting cell activation and mediator release of inflammatory cells in early and late allergen-induced AHR and bronchoconstriction [46].

1.3.2.3 Bronchodilators

Bronchodilators are central in the management of airway disorders and play a critical role in symptomatic asthma management [47] by reducing airway constriction during an asthma exacerbation. Inhaled short-acting β_2-agonists (SABA) such as albuterol are the most frequently used rescue or relief bronchodilator medications which reverse bronchoconstriction leading to a relaxation of airway smooth muscle and improvement of airflow [48]. Long-acting beta$_2$-agonists (LABA) such as salmeterol and formoterol are bronchodilators with a longer duration of action than SABAs, with effects lasting for more than 12 hours after a single dose. Nevertheless, LABAs are not used as monotherapy and should be used in combination with ICS as maintenance therapy to lower the dose of ICS in combination for long-term control and to prevent symptoms in asthma [49].

Other short-acting bronchodilators are anticholinergic bronchodilators such as ipratropium bromide, which target the parasympathetic nervous receptors and inhibit

their function in the airway, leading to bronchodilation of the airway [50]. Also, the use of long-acting anticholinergic medications such as tiotropium bromide as a maintenance therapy is effective in moderate to severe asthmatic patients who are uncontrolled on combination therapy with LABA and ICS [51].

1.4 Airway inflammation in asthma

Airway inflammation is the key marker of asthma, and the severity of asthma is reflected by the degree of the inflammation [52, 53]. Currently, asthma is considered an umbrella diagnosis that contains a variable clinical presentation (phenotype) and pathophysiological mechanism (endotype) [54, 55]. Traditional phenotyping classifies asthmatic individuals based on triggers, clinical presentations, and inflammatory markers. Endotyping refines these groups and classifies asthmatic individuals based on their pathophysiologic mechanisms involving specific cytokines and chemokines [56, 57]. Cytokines are described as extracellular signaling proteins produced by different cell types acting through receptors on the surface of target cells. They act on the target cells, leading to activation, proliferation, immunomodulation, and release of other cytokines or mediators of the cells [58]. Chemokines are small cytokines with low molecular weights that contribute to regulating the number, intensity, and activation of leukocyte migration in asthma [59]. Endotypes of asthma are classified as Type 2-high asthma (T2-high), which is characterized by eosinophilic inflammation, and non-Type 2 asthma (Non-T2) or Type 2-low asthma, which is characterized by neutrophilic or paucigranulocytic inflammation. The patients with T2-high asthma characterized by eosinophilic airway inflammation, tend to respond well to the routine use of ICS [60]. However, non-T2

asthma might exhibit nearly absent eosinophils with increased neutrophils counts and may have poor responses to ICS [61, 62]. (Figure 1.1) illustrates the main phenotypes and endotypes of asthma [63].

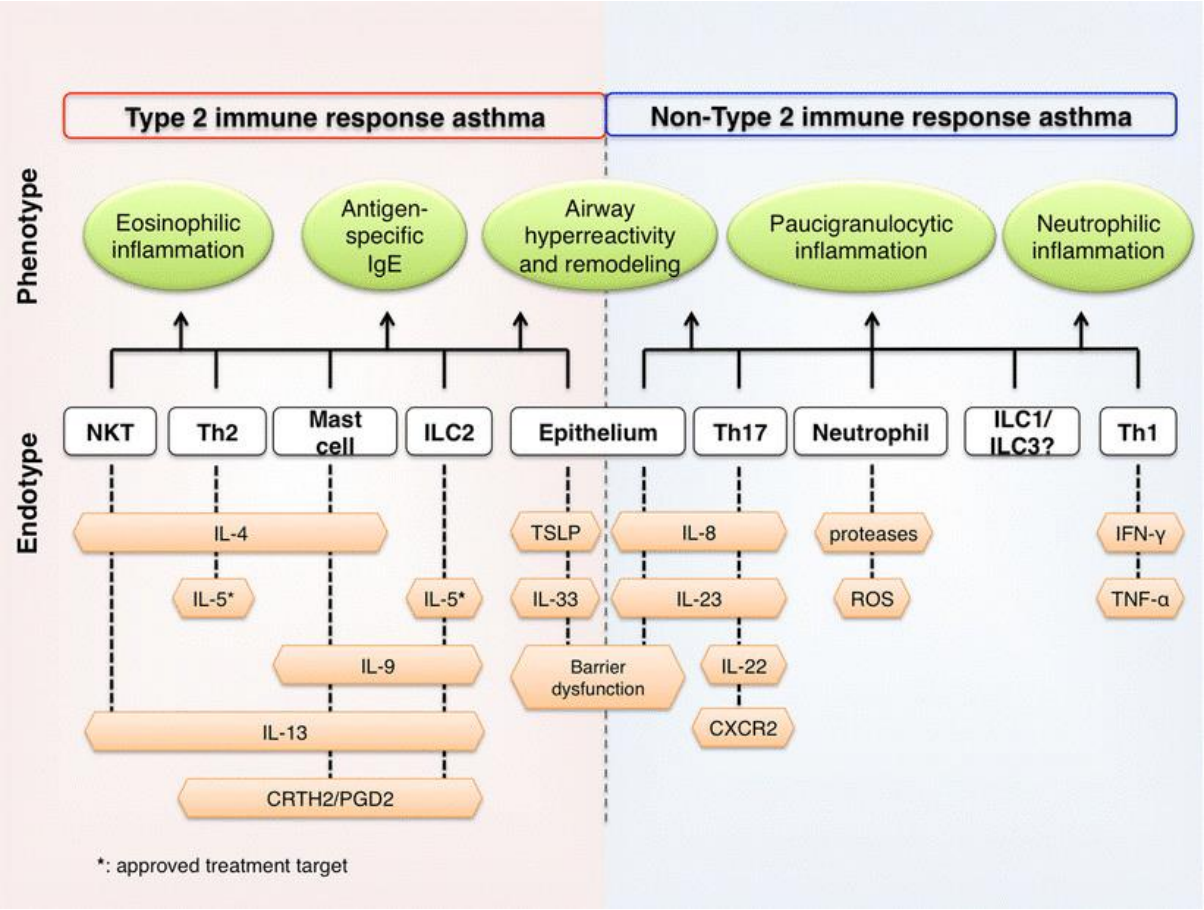

Figure 1.1 T2-high and non-T2 phenotype and endotype immune response in asthmatic patients

The main phenotypes in T2-high asthma are eosinophilic inflammation and allergic sensitization with evidence of antigen-specific IgE. T2-high asthma endotypes are characterized by the production of Th2 cytokines and alarmins from epithelial cells. The main phenotypes in non-T2 asthma are based on the inflammation pattern, e.g., neutrophilic or paucigranulocytic inflammation. Non-T2 asthma endotypes are characterized by a lack of type 2 biomarkers and the presence of neutrophils. Airway hyperreactivity and remodeling are seen in both phenotypes. The innate and acquired immune responses may contribute to the underlying asthma endotypes for types of immune responses in T2-high and non-T2. Figure adapted from Tan et al. 2016 [63].

1.4.1 Type 2 airway inflammation (T2-high)

Allergic asthma or T2-high asthma is the most common type of asthma endotype with an early onset, often in childhood, sensitivity to an allergen, and Th2-mediated background related to immunoglobulin E (IgE) [64]. Allergen exposure promotes the activation of Th2 cytokines, including IL-4, IL-5, and IL-13, which orchestrate and amplify the type 2 response [65]. There is a complex network between Th2 cytokines such as IL-4, IL-5, and IL-13, which are secreted from Th2 cells, driving eosinophil recruitment and IgE production, and alarmins such as IL-25, IL-33, and Thymic Stromal Lymphopoietin (TSLP) which are released from epithelial cells [66]. Th2 cytokines regulate the inflammatory processes and play an important role in managing allergic asthma. IL-4 is a pleiotropic cytokine produced by activated T cells and is essential for IgE production and allergic sensitization. IL-5 is responsible for maturation and releasing eosinophils in the bone marrow and helps with eosinophil survival. IL-13 is involved in switching B cells to IgE-producing cells. IL-13 also has a central role in airway hyperresponsiveness development, the remodeling of tissue, and the increase of eosinophil counts [61, 67]. The alarmin IL-25 (also known as IL-17E) is a member of the IL-17 cytokine family and has been shown to favour a Th2 type response when released from airway epithelial cells. IL-33 also plays an important role in activating basophils and eosinophils and inducing the expression of Th2 cytokines [61, 68]. TSLP is an upstream alarmin expressed in airway epithelial cells, which drives dendritic cells to attract Th2 cells in asthmatic patients [69].

Among chemokines, eotaxin, and regulated on activation, normal T cell expressed and secreted (RANTES), are valuable chemoattractants for eosinophils that play a key role in the induction of allergic inflammation in asthma [70].

Eosinophils also tend to accumulate at allergic inflammation sites and contribute to bronchial asthma development [71]. Mast cells originate in the bone marrow, where their maturation is influenced by the binding of stem cell factor to the receptor c-kit along with the influence of other cytokines, including IL-4, IL-9, IL-10, and IL-13. These cytokines promote the differentiation and proliferation of mast cells. In addition, mast cells are essential in the development of allergic asthma. They have effects on airway smooth muscle, tissue remodeling, and mucus hyper-secretion by releasing proteases like tryptase and growth factors [72]. Prophylactic mast cell stabilizer agents such as cromolyn sodium and nedocromil sodium are used to inhibit the activation of mast cells in asthma [44].

IgE is responsible for the early phase of an allergic asthma reaction and has a minor role in the late phase allergic reaction [73]. The biological roles of IgE are related to the ability to influence the functions of immune and structural cells that are involved in chronic allergic inflammation pathogenesis via specific receptors [73]. Inhalation of allergens such as house dust mites (HDM) may lead to the induction of allergen-specific Th2 responses, elevated serum IgE, and increased eosinophil counts [74]. Continued exposure to HDM is associated with chronic eosinophilic airway inflammation, bronchial hyperresponsiveness, and tissue remodeling, which are all considered hallmarks of allergic asthma [75]. (Figure 1.2) shows an overview of Th2 cytokine-driven asthma responses to airway inflammation [76].

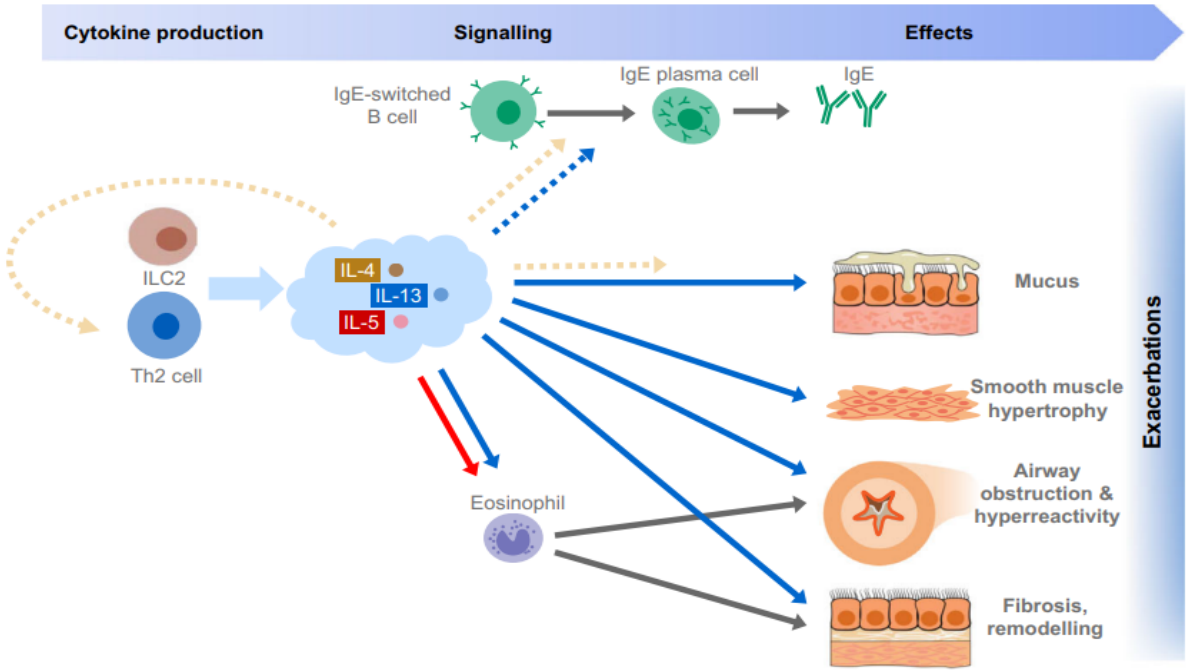

Figure 1.2 Type 2-driven asthma response to airway inflammation

Th2 cytokines drive the recruitment of the effector cells (e.g. eosinophils) and switching B cells to secrete IgE once exposed to antigens. In addition, they are critically involved in multiple characteristic aspects of asthma, including mucus production, bronchial remodeling, subepithelial fibrosis, smooth muscle hypertrophy, airway obstruction, and hyperresponsiveness. Figure adapted from Robinson et al. 2017 [76].

1.4.2 Non-Type 2 airway inflammation (Non-T2)

The definition of nonallergic or non-T2 asthma includes a subset of individuals whose asthma allergic sensitization cannot be demonstrated [77]. Non-T2 endotypes of asthma are also defined by the absence of eosinophilia in the sputum and blood [78]. It occurs in about 10% to 33% of asthmatic individuals and has a later onset than allergic asthma [77]. Non-T2 asthma endotypes are characterized by paucigranulocytic or neutrophil-dominated inflammation with a high level of cytokines such as IL-6, IL-17A/F, IL-22, interferon-gamma (IFN-γ), tumor necrosis factor α (TNF-α) and chemokines such as CXCL8, known as IL-8 [78].

IL-8 is a member of the family of C-X-C chemokines that plays an important role in

airway inflammation by activation of neutrophils, T-lymphocytes, eosinophils, basophils, and monocytes [79]. IL-6 is a pleiotropic cytokine that acts as a pro-inflammatory mediator as well as acute-phase response inducer [80]. IL-17 is associated with neutrophils and AHR. IL-17A, and IL-17F are upregulated in the lungs of asthmatic individuals and correlated with steroid resistance and asthma severity [81]. Typical clinical conditions that are usually associated with neutrophilic inflammation in asthmatic individuals include smoking, obesity, and the elderly [82]. Patients with non-T2 endotype of asthma respond poorly to corticosteroids [78]. Furthermore, neutrophilic nonallergic asthmatic individuals have corticosteroid resistance and absence of eosinophilia, which correlate with smoke, pollution, and viral-induced exacerbation [66]. Table 1.1 shows the clinical and laboratory characteristics differentiating T2-high from Non-T2 asthma [83].

Table 1.1 Clinical and laboratory characteristics differentiating T2-high vs. non-T2 asthma. Adapted from Chiu et al. 2021 [83].

	Allergic Asthma (Th2-High)	Non-Allergic Asthma (Th2-Low or Non-Th2)
Prevalence [14]	60%	10–33%
Age of onset	Occurs early in life	Mostly occurs later in life
Triggers	House dust mites, pollen, pet dander and cockroaches, etc.	More diverse. Cold air, smoke, obesity, occupational exposure, and exercise
Inflammatory mediators	IL-4, IL-5, IL-13, IL-25, IL-33 and TSLP	IL-1β, IL-6, IFN-γ, TNF-α and IL-17
Severity	Milder than Th2-low	More severe than allergic asthma
Treatment	Responds well to ICS	Require higher doses of ICS or non-responsive to ICS [15,16]
Recruiting cells in the airway	Eosinophilic inflammation [17]	neutrophilic or pauci-granulocytic inflammation [18–20]
Serum total IgE	High	Normal
Skin prick test	Positive	Negative

ICS: inhaled corticosteroids.

1.4.3 Biological approaches targeting T2-high airway inflammation

The use of monoclonal therapies to target specific inflammatory pathways improves asthma control, especially in the management of severe and uncontrolled asthma. Eosinophils are known to play a crucial role in the pathogenesis of allergic asthma [84]. IL-5 is an essential cytokine for the terminal differentiation, maturation, and migration of eosinophils [85]. Using anti-IL-5 Mepolizumab as an add-on maintenance therapy for severe asthma can target eosinophils by binding to IL-5 and preventing the bonding to the IL-5Rα chain. Therefore, it can reduce the growth, differentiation, activation, and survival of eosinophils [86, 87]. Benralizumab is also an IL-5 antagonist that binds to IL-5R. It has been shown to decrease eosinophil count in the airway mucosa/submucosa, sputum, and blood after administration in a multicenter study [88]. Currently, anti-IL-5 targeted agents, including Mepolizumab, Benralizumab, and Reslizumab, have been approved for severe eosinophilic asthma treatment from 6 years of age, subject to country-specific approvals [89]. Conversely, blocking IL-13 could be an important approach to treating allergic asthma as there are wide ranges of pathogenic effects induced by IL-13 such as AHR, mucus production, and enhanced IgE production [90]. Lebrikizumab is an example of an IL-13 antagonist that showed a significant decrease of 60 % in the exacerbation rate and improved lung function in patients with uncontrolled moderate-to-severe asthma [91]. In addition, Dupilumab, among other treatments, is a very promising drug that effectively addresses the pathophysiology of Th2 allergic asthma and can inhibit the biological effects of IL-4 and IL-13 by preventing IL-4/13 interactions with the α-subunit of the IL-4 receptors complex [92]. It has been approved in the United States since 2017 and has been under clinical trials in the UK since 2019 for adults and adolescents aged > 12 years with moderate-to-severe

asthma and eosinophilia. It received approval by the National Institute for Healthcare and Care Excellence (NICE) in late 2021 for the treatment of severe asthma in the UK [89, 93]. IL-25 has been implicated in the regulation of type 2 immunity, which has essential roles in AHR and antigen-driven airway inflammation [94]. It has been shown that blocking IL-25 by administration of anti-IL-25 mAb resulted in a significant reduction of the production levels of IL-5 and IL-13, eosinophil infiltration, and serum IgE secretion, and prevented AHR in mice with allergic airway disease [94].

Elevated serum levels of IgE correlate with atopic diseases, including allergic asthma. It has been estimated that more than 50% of poorly controlled asthmatic have allergic IgE-mediated asthma [95]. Omalizumab is an example of a biological anti-IgE agent used to treat asthma by binding to circulating IgE in the blood and interstitial space and promoting a depletion of circulating IgE. It also inhibits high-affinity and low-affinity receptors from binding to IgE on basophils, mast cells, and dendritic cells [95]. Omalizumab is currently the recommended treatment for children with severe asthma who have elevated serum IgE [89]. Quilizumab is another anti-IgE targeting IgE-switched B cells. One study found that using Quilizumab can reduce the production of IgE and inhibit asthmatic responses [96].

1.5 Role of airway structural cells in asthma pathogenesis

1.5.1 Human bronchial epithelial cells (HBECs)

The airway epithelium is a pseudostratified layer in the airway that contains a variety of cell types, such as ciliated cells, basal cells, and goblet cells. It plays a crucial role in maintaining lung homeostasis and serves as the first physical barrier against inhaled harmful stimuli of the external environment. This forming a

continuous, self-cleaning barrier with considerable resistance against chemical, physical, or biological stressors [97]. Additionally, the airway epithelium plays an active role in innate immunity and inflammatory regulation by expressing pattern recognition receptors, inducing cytokines, integrating innate and adaptive immunity, and driving allergic sensitization and inflammatory responses in asthma [98]. The airway epithelium utilizes various mechanisms to sense environmental stimuli such as bacterial lipopolysaccharide (LPS), fungi, viruses, cigarette smoke, and allergen-derived proteases such as HDM and reacts by secreting multiple cytokines and other substances to modulate immune responses [99-101].

In response to environmental insults, the epithelium releases a variety of cytokines termed alarmins, including TSLP, IL-25, and IL-33. Alarmins promote innate immune and adaptive type 2 responses and are, therefore, implicated in asthma pathogenesis [102]. TSLP is expressed in basal cells of the airway and induced by many stimuli, including rhinovirus (RV), diesel particles, and cigarette smoke extract (CSE) [103]. TSLP activates type 2 innate lymphoid cells (ILC2) and stimulates dendritic cells that promote the differentiation of Th2 cells in asthma and allergic disease [104, 105]. The alarmin IL-25 is expressed by epithelial tuft cells and promotes type 2 responses via effects on ILC2s [106]. Bronchial epithelial cell expression of IL-25 is increased in asthmatic patients and correlates with type 2 inflammation [107, 108]. IL-33 plays a key role in asthma pathogenesis by activating ILC2s leading to an increase in the production of Th2 cytokines, which are key mediators in Type-2 inflammatory responses [109]. Administration of an antibody to IL-33 receptors after an allergen challenge led to rapid resolution of airway hyperreactivity and a significant reduction in IL-4 levels, which suggests an important role for IL-33 in asthma persistence flowing allergen exposure by modulation of Th2

cell function [110]. Release of IL-25 and IL-33 from tuft and basal cells, respectively, activates ILC2s, potent producers of Th2 cytokines IL-5 and IL-13, propagating early type 2 immune responses. In addition, TSLP, among alarmins, primes antigen-presenting dendritic cells to promote type 2 immune responses by activating Th2 cells to secrete Th2 cytokines such as IL-4, IL-5, and IL-13 [102]. (Figure 1.3) illustrates the responses of airway epithelial cells to allergen stimuli by secreting alarmins, which promote the production of Th2 cytokines [111].

In addition to releasing alarmins, HBECs can release cytokines and chemokines to recruit immune cells to the airway. As described above, eosinophilia is a key feature of T2-high asthma and airway epithelial cells can secrete the eosinophil chemokines eotaxin and RANTES. These chemokines have been shown to promote eosinophil recruitment during respiratory syncytial virus (RSV) infection, contributing to the development and exacerbations of asthma mostly in children [112].

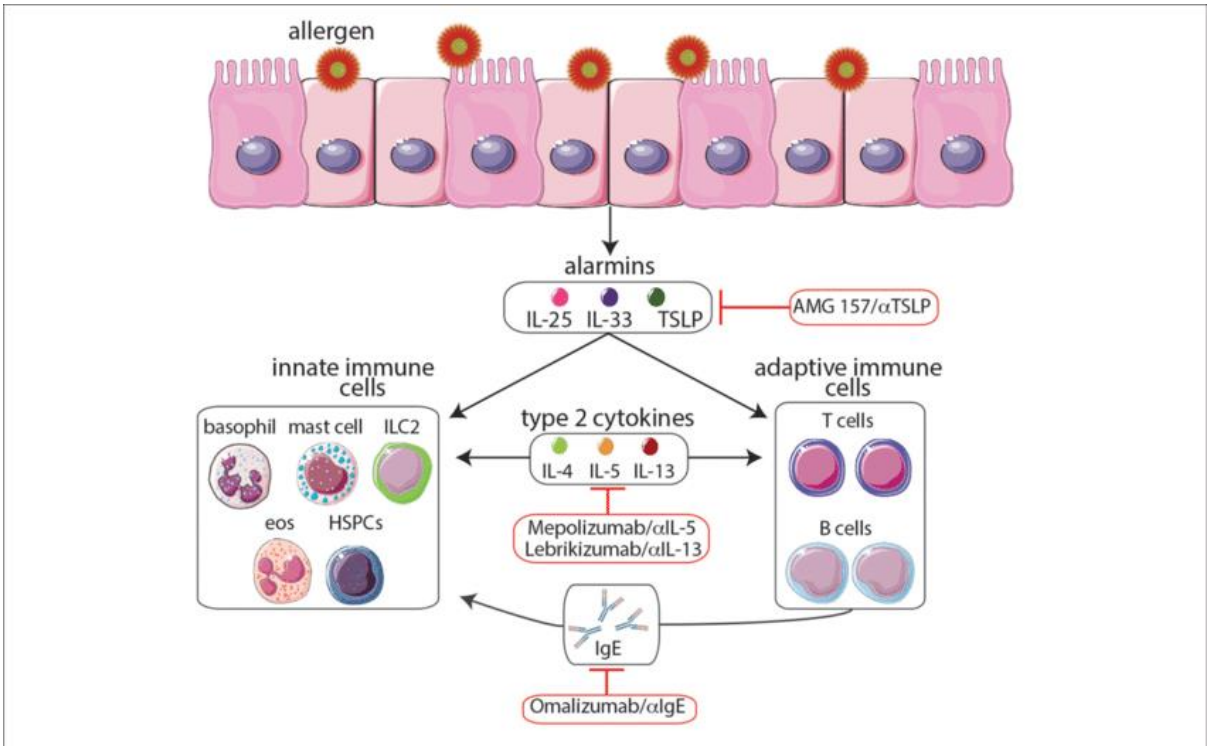

Figure 1.3 Epithelial cells' response to allergen stimulation

Following exposure to allergens, epithelial cells release cytokines termed alarmins (IL-25, IL-33, and TSLP). Alarmins promote the production of type 2 cytokines, including IL-4, IL-5, and IL-13, by immune cells of the innate and adaptive immune system. Figure adapted from Sy et al. 2016 [111].

1.5.2 Human airway smooth muscle cells (HASMCs)

Human airway smooth muscle cells (HASMCs) plays a significant role in asthma pathogenesis and constitute an important target for treatment by controlling muscle tone and regulating the opening of the airway lumen as well as secreting cytokines, chemokines, and growth factors [113]. HASMCs participate in airway hyperresponsiveness, inflammatory, and remodeling processes observed in asthmatic individuals in conjunction with other cells [114].

1.5.2.1 HASMCs role in airway inflammation

Similar to HBECs, HASMCs can release various inflammatory cytokines and chemokines contributing to airway inflammation in asthma. For example, HASMCs

from asthmatic individuals express increased levels of alarmin IL-33 and neutrophil chemoattractant (IL-8) compared to non-asthmatic controls [115, 116]. Moreover, Th2 cytokines IL-4 and IL-13 induce eotaxin release in HASMCs and TNF-α augments this effect [117]. HASMCs also released RANTES when stimulated with TNF-α and IL-1β [118]. These findings suggest that HASMCs are important in producing proinflammatory cytokines and chemokines in airway inflammation.

1.5.2.2 HASMCs role in Contraction

HASMC contraction and proliferation significantly participate in the pathogenesis of asthma as they have a role in the development of airway remodeling and AHR, in addition to their involvement in immune responses [119]. Contraction of HASMCs refers to the process by which these cells, located in the airway walls, can regulate appropriate airway tone, mainly through their contractile and synthetic activities. The balance between contraction and relaxation of HASMCs is essential for regulating airway diameter. AHR is a key feature of asthma, leading to airway obstruction, the main asthma symptoms result from exaggerated HASMC contraction [120]. Different stimuli, including inflammatory mediators, neural signals, and mechanical factors such as airway wall stretching, can trigger ASM contraction through multiple signaling pathways [121]. These stimuli induce the opening of cation channels in the nerve terminal membrane, resulting in membrane depolarisation. [121].

Regulating airway muscular tone is quite complex, requiring the integration of several signaling pathways and stimuli. One important signaling mechanism driving ASM contraction involves increased intracellular calcium concentration (Ca^{2+}) which results in the activation of phospholipase A_2 and the release of intracellular arachidonic acid [121]. The lipoxygenation of arachidonic acid generates

messengers that can subsequently activate transient receptor potential vanilloid-1 (TRPV1), which mediates calcium uptake into smooth muscle, leading to contraction [122, 123]. In addition, a small guanosine triphosphatase Rho pathway has been found to be involved in numerous cellular functions including cell adhesion, motility, migration, growth regulation, and cell contraction, and is essential in modulating the force and velocity of actomyosin cross-bridging in both smooth muscle and non-muscle cells by inhibiting the dephosphorylation of the regulatory chain of myosin II-mediated by myosin phosphatase [124]. Dysregulation of HASMC contraction can lead to airflow limitation and AHR, as seen in asthma [125]. Therefore, understanding the mechanism of HASMC contraction and targeting these pathways may provide an approach to modulating HASMC contraction and is essential for therapeutic targets.

1.5.2.3 The role of HASMC proliferation in asthma

Airway remodeling plays a crucial role in the pathogenesis of asthma, involving structural changes in the airway wall in response to diseases. The thickening of the HASMC layer is a key characteristic of airway remodeling, leading to greater force generation when the HASMCs contract [126]. The proliferation of HASMCs has an important role in asthma, characterized by increasing HASMC size (hypertrophy) and increasing cell number (hyperplasia), leading to changes in airway wall structures. These changes can contribute to increased AHR, airway narrowing, and worsening asthma symptoms. [127].

Chronic inflammation in the asthmatic airway promotes the release of inflammatory mediators, including cytokines, chemokines, and growth factors, which can directly stimulate HASMC proliferation, leading to increased airway thickness [118, 128]. Bronchoconstriction and mechanical forces can also influence the

proliferation, resulting in a thickening of the ASMC layer. It has been shown that transforming growth factor β (TGF-β), which plays a critical role in airway remodeling, induces messenger Ribonucleic Acid (mRNA) and protein levels for connective tissue growth factor in asthmatic HASMCs compared with non-asthmatic *in vitro* [129]. Additionally, Th2 cytokines and TGF-β have been shown to stimulate HASMCs release of vascular endothelial growth factor (VEGF) that has a role in the remodeling characteristic of asthma by increased airway wall vascularity [39]. The altered extracellular matrix protein profile in asthmatic HASMCs increases cell proliferation by an autocrine mechanism, leading to airway wall remodelling in asthma [130]. The complexity of the HASMCs proliferation process that leads to airway remodeling and how this contributes to the heterogeneity of asthma is an area of research that needs further studies to understand the mechanisms and identify novel targets of asthma therapeutics.

1.5.3 Intercellular communication between human bronchial epithelial cells and human airway smooth muscle cells

The intracellular communication between HBECs and HASMCs is crucial for maintaining lung function. HBECs and HASMCs play a major role in asthma pathogenesis, particularly in airway inflammation and AHR, and studying the interaction between these two cells and investigating how they contribute to asthma pathogenesis is essential. Epithelial cell mediator release, including cytokines, chemokines, growth factors, and extracellular matrix proteins, can act directly on HASMC's to affect inflammatory responses, contraction, and proliferation [131]. In a study using ex vivo lung tissue slices and a laser ablation method, investigators precisely ruptured single epithelial cells in small airways and found that localized epithelial injury contributes to the hyperresponsiveness and induced airway

constriction of HASMCs via Ca2+-dependent smooth muscle shortening [132]. While injured, HBECs release higher levels of cytokines and chemokines, including IL-6 and IL-8, and soluble mediators, including matrix metalloproteinase-9 (MMP-9), which correlates with the enhanced proliferation of HASMCs [132]. In addition, *in vitro* and *in vivo* studies found that inhibition of MMP-9 release results in a significant reduction in HASMCs proliferation indicative of direct role of MMP-9 of epithelial origin on HASMCs proliferation [133]. The same study found that repeated injury to rabbit tracheal epithelium also led to an increase in MMP-9 levels and HASMCs proliferation [133].

HASMCs can also influence HBECs through several mechanisms involving the release of cytokines and signaling pathways that impact HBECs function. B. Allard et al. showed that asthmatic bronchial smooth muscle co-culture with HBECs increases chemokine ligand 5 (CCL5) (also known as RANTES) expression in HBECs after human rhinovirus (HRV) infection and that the use of anti-CCL5 blocking antibody significantly reduced monocyte migration caused by HRV-infected HBECs [134]. Deacon et al. also reported that HASMCs increased the production of amphiregulin in response to bradykinin exposure. This increase in amphiregulin levels contributed to the production of IL-8, VEGF, and cyclooxygenase-2 (COX-2) in HBECs [135] The interaction between HBECs and HASMCs plays a crucial role in asthma pathogenesis, and targeting their intercellular communication could open the door for a potential therapeutic target. (Figure 1.4) illustrates the pathways that can be targeted to influence the interaction between HBECs and HASMCs, potentially help for a new therapeutic approach for treating airway diseases such as asthma [131].

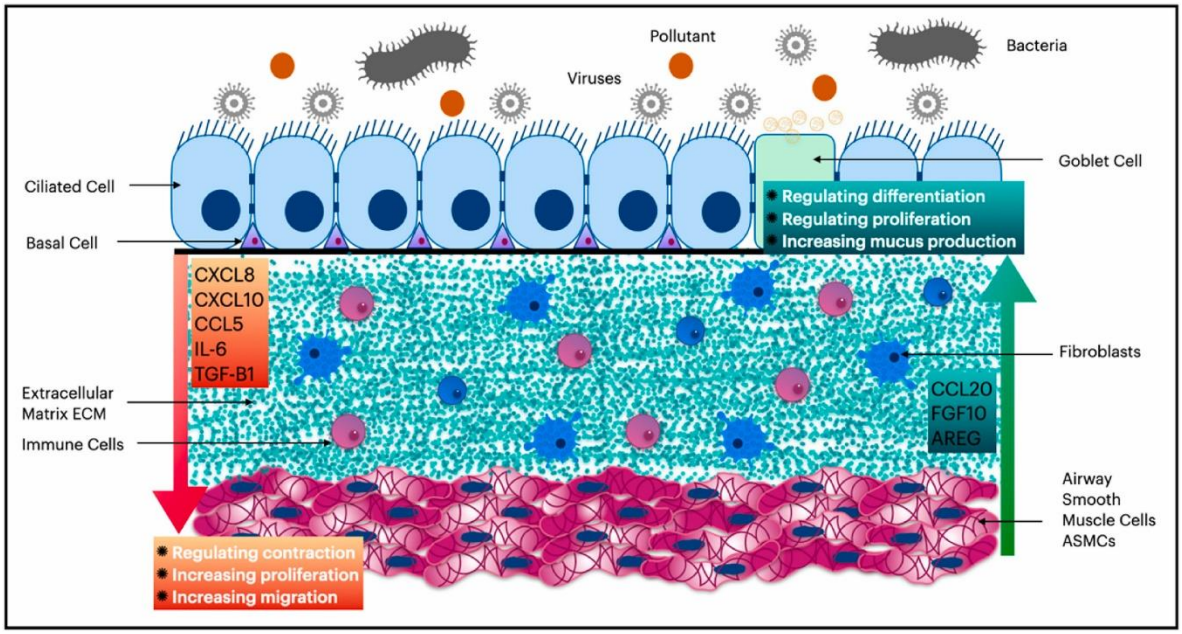

Figure1.4 Potential interaction pathways between HBECs and HASMCs

HBECs interact with the ECM, fibroblasts, and HASMCs through the release of cytokines and growth factors. HBECs can release various cytokines such as IL-8, CXCL10, RANTES, IL-6, and TGF-β1 which influence the ECM and regulate HASMCs contraction, proliferation, and migration. Environmental stimuli such as pollutants, viruses, and bacteria influence HBEC activation, leading to the overall inflammatory response. The interactions between these cell types may play a key role in airway remodeling and asthma pathogenesis, and targeting these pathways may provide potential therapeutic approaches in asthma. Figure adapted from Abohalaka et al. 2023 [131].

1.6 Role of inhaled insults on airway inflammation

The respiratory system is regularly exposed to airborne particles, allergens, pollutants, and viruses that may lead to airway inflammation. Inhaled insults, such as cigarette smoke, viruses, and allergens such as HDM, activate innate and adaptive immune responses in the airway, leading to increased inflammatory cytokine production and altered immune cell functions. This contributes to airway remodelling, mucus hypersecretion, and bronchial hyperresponsiveness, key features of asthma. Understanding the implications of inhaled exposures on the airway is essential for

developing targeted therapies to mitigate airway inflammation and key strategies to improve asthma management.

1.6.1 Cigarette smoke

1.6.1.1 Cigarette smoke and asthma

Cigarette smoke combined with asthmatic inflammation may induce important changes in the asthma endotype with a predominance of activated macrophages and increased neutrophils in the airway, sputum, and the lung parenchyma as seen in early chronic obstructive pulmonary disease (COPD) [136, 137]. The majority of asthmatic smokers have non-eosinophilic endotypes such as non-T2 inflammation in the airway compared to asthmatic non-smokers [32, 138], with increased neutrophils and decreased eosinophils [139], suggesting cigarette smoke (CS) changes the asthma endotype from eosinophilic T2-high to neutrophilic non-T2 type in asthmatic smokers. *In vivo* studies, CS causes significant lung function impairments, leads to increased lung inflammation, elevated neutrophil counts, inhibits the pulmonary T-cell response to influenza virus, and compromises adaptive immune responses to infections [140, 141]. Supporting this, *in vitro* CSE increases the release of IL-8 and CXCL1 from HASMCs, which act as neutrophilic attractants [142]. CS also has been shown to increase IL-6, IL-8, and TNF-α, all of which contribute to the upregulation of GRβ, and may elucidate the poor response to ICS treatment [143, 144].

1.6.1.2 Role of cigarette smoke in cytokine/chemokine production

1.6.1.2.1 Th2 cytokines and eosinophil chemokines

CS increases the expression of IL-4, which is a representative of Th2 cytokines, and decreases the expression of IFN-γ in a rat *in vivo* model of asthma [145]. In addition, CS is associated with airway hyperactivity, and the neutralization of IL-4 decreases the levels of IgE and airway hyperactivity [146-148]. Cigarette

smoke condensate (CSC) induces IL-5 production but not IL-13 in mouse macrophage cell lines [149]. Furthermore, cigarette smoke extract (CSE) induces the synthesis of TSLP, a known activator of dendritic cells promoting Type 2 allergic inflammation, in the mouse lung [150]. Airway epithelial cells are considered the main source of alarmins (IL-25, IL-33, and TSLP), which promote Type 2 inflammatory cytokines (IL-4, IL-5, and IL-13) that eventually induce Th2-type immune response to environmental stimuli [151]. Therefore, increased TSLP production is a potential mechanism in the airway by which cigarette smoke may prime allergic inflammation [150, 152].

On the contrary, our group found that CSE suppressed the production of Th2 cytokines IL-4 and IL-13, as well as eosinophil chemokines eotaxin, IP-10, and RANTES, but induced the neutrophil chemoattractant IL-8 production in HASMCs *in vitro* (manuscript in preparation) [153]. In line with our group findings, *in vivo* studies showed a reduced expression of IL-4 and IL-5 in bronchoalveolar lavage fluid (BALF) of mice exposed to CS, which also inhibited the production of eosinophilic chemokine eotaxin in mouse lungs exposed to HDM [154, 155],and sputum eosinophil counts are reduced in mild asthmatic smokers compared with non-smokers [136]. These findings demonstrate varied effects of CS on the production of proinflammatory cytokines and chemokines in different cell types, which could be explained using different study models. However, the effect of CSE on Th2 cytokines and eosinophil chemokines in HBECs *in vitro* has not been fully explored and remains to be investigated.

1.6.1.2.2 Non-T2 cytokines and chemokines

Asthmatic smokers develop neutrophilic inflammation of the airway [156]. BALF from asthmatic smokers increases alveolar macrophage (AM) and neutrophil

counts compared to non-smokers [157, 158]. In addition, asthmatic smokers have higher expression of IL-17A, IL-6, and IL-8 and higher neutrophil counts in the bronchial mucosa compared to asthmatic non-smokers [156]. This is supported by the findings of our group that CSE promoted the release of IL-6, IL-8, and VEGF in HASMCs *in vitro,* suggesting that CS may alter the inflammatory responses from T2 to non-T2 in asthmatic smokers (manuscript in preparation) [153]. In line with this, CSE induces the release of potent neutrophil chemoattractant IL-8 from cultured HBECs, which may contribute to neutrophilic airway inflammation seen in smokers [159]. Furthermoee, chronic exposure to CSE in vitro (20 μg/ml) for 20 weeks can induce the production of IL-6 in HBECs [160]. These findings suggest that CSE can induce the production of non-T2 cytokines and chemokines. Whether CSE can modify the inflammatory responses and cause a shift from T2 to non-T2 inflammation in HBECs is unclear and remains to be explored.

1.6.1.3 Role of cigarette smoke on COX-2/PGE_2 pathway

Prostanoids play an essential part in the inflammatory process of the airways in patients with asthma. Cyclooxygenase (COX) is an enzyme responsible for the formation of prostanoids via their respective downstream synthases [161]. There are two isoforms of COX, including COX-1, a housekeeping enzyme that is constitutively expressed in most cells, and COX-2,an inducible enzyme enhanced by cytokines and other inflammatory stimuli [162]. COX enzyme converts arachidonic acid (AA) to prostaglandin H_2 (PGH_2) [163]. The expression of COX-2 increases in response to inflammation [164]. Inflammation causes an increase in the production of prostaglandins (PG), such as prostaglandin E_2 (PGE_2), via the microsomal PGE_2 synthases (mPGES). Therefore, the expression of mPGES-1, the terminal enzyme downstream of COX, is rapidly upregulated during inflammation [165].

Inflammation is a common feature in the pathogenesis of lung diseases associated with cigarette smoke [166]. The effects of cigarette smoke on lung inflammation may result from the enhancement of COX-2 expression and PG generation in the airway [167]. COX-2 expression, mPGES-1 expression, and PGE_2 production are induced after exposure to CSE in normal human lung fibroblasts [168]. Short-term exposure to CS in vivo induces COX-2 expression in the small airway epithelial cells in mouse lungs [169]. *In vitro*, treatment with 10% CSE increases COX-2 expression in normal human bronchial epithelial cells [170]. CSE also induces COX-2 mRNA expression in pulmonary microvascular endothelial cells *in vitro* [171]. These findings are supported by our group showing that CSE-induces IL-6, IL-8, and VEGF production via COX-2 associated PGE_2 synthesis in HASMCs (manuscript in preparation) [153]. Our group demonstrated that CSE could modify inflammatory responses in HASMCs by shifting from T2-high eosinophilic inflammatory responses to non-T2 neutrophilic inflammatory responses through COX-2/PGE2/E-prostinoid receptor (EP_2 and EP_4)/Cyclic adenosine monophosphate (cAMP) pathway, mediated by oxidative stress. Whether the COX-2/PGE_2 pathway mediates the effect of CSE on Th2 cytokines and eosinophil chemokines in HBECs *in vitro* remains unclear and needs further investigation.

1.6.2 House dust mite (HDM)

1.6.2.1 HDM and airway inflammation

Allergens play an important role in asthma by triggering an excessive immune response, resulting in prolonged airway inflammation and AHR [172]. Asthmatic individuals exposed to home allergens to which they are sensitized encounter more severe symptoms of asthma [173]. Many common sources of airborne allergens, such as HDM, cockroaches, and fungi, contain proteolytic enzymes, which represent

an important mechanism in the initiation of allergic inflammation [174]. HDM among allergens is a complex of constituents that include proteases from both cysteine and serine families. The cysteine protease family contains bacterial components that activate the innate immune system, such as Dermatophagoides pteronyssinus 1 (Der P1), while the serine protease family contains allergens with potent proteolytic potential, such as *Dermatophagoides pteronyssinus 3,6*, and *9* [175, 176]. HDM is an aeroallergen that promotes the Th2 type of airway inflammation in asthmatic individuals [177]. Continued exposure to HDM is associated with chronic eosinophilic airway inflammation, bronchial hyperresponsiveness, and tissue remodeling, all considered hallmarks of allergic asthma [75]. HDM can also induce proinflammatory expression of cytokines and chemokines [178]. For example, HDM increases IL-5 levels and induces allergic sensitization, AHR, goblet cell hyperplasia, and eosinophilic airway inflammation in mouse lung tissue *in vivo* [178]. Supporting this, in another *in vivo* experiment, the production of IL-4, IL-5, and IgE were significantly increased in BAL fluids of mice injected with *Der P1* [179]. *In vitro, Der P1* and *Der P9* induce the production of IL-6 and IL-8 in HBECs [180]. In agreement with these findings, a clinical study showed a single bronchial allergen challenge with HDM and the major components *Der P1* and *Der P2* significantly increased the level of allergen-specific IgE for HDM in serum and significantly increased the production of Th2 cytokines (IL-4, IL-5, and IL-13) [181]. These results suggest that HDM can play a role in the development of airway inflammation through upregulating the production of inflammatory mediators.

1.6.2.2 HDM and human bronchial epithelial cells

Pro-inflammatory cytokines and chemokines are predominantly produced by activated airway epithelial cells [182]. *Der P1* induces the production of IL-5 and

eotaxin in HBECs from allergic subjects with asthma *in vitro* [178, 183], while *Der F 2* induces the production of IL-13 in the epithelial BEAS-2B cell line *in vitro* [184] . Additionally, the protease activity of HDM leads to the production of alarmins, including IL-25, IL-33, and TSLP, from airway epithelial cells of an asthma mouse model, leading to activate $ILC2_s$ and release of Th2 cytokines such as IL-5, IL-9, and IL-13 [185]. In addition to eosinophilic inflammatory responses, *Der P1* and *Der P9* induce the production of IL-6 and IL-8 in primary HBECs and HBECs (BEAS-2B) cell line *in vitro* [180]. These results suggest that bronchial epithelial cells can release the production of Th2 cytokines, alarmins, and other inflammatory cytokines such as IL-6 and IL-8 in response to HDM allergen. (Figure 1.5) illustrates the response of HBECs to various stimuli by releasing alarmins that activate ILC2, thereby triggering the release of Th2 inflammatory responses [185].

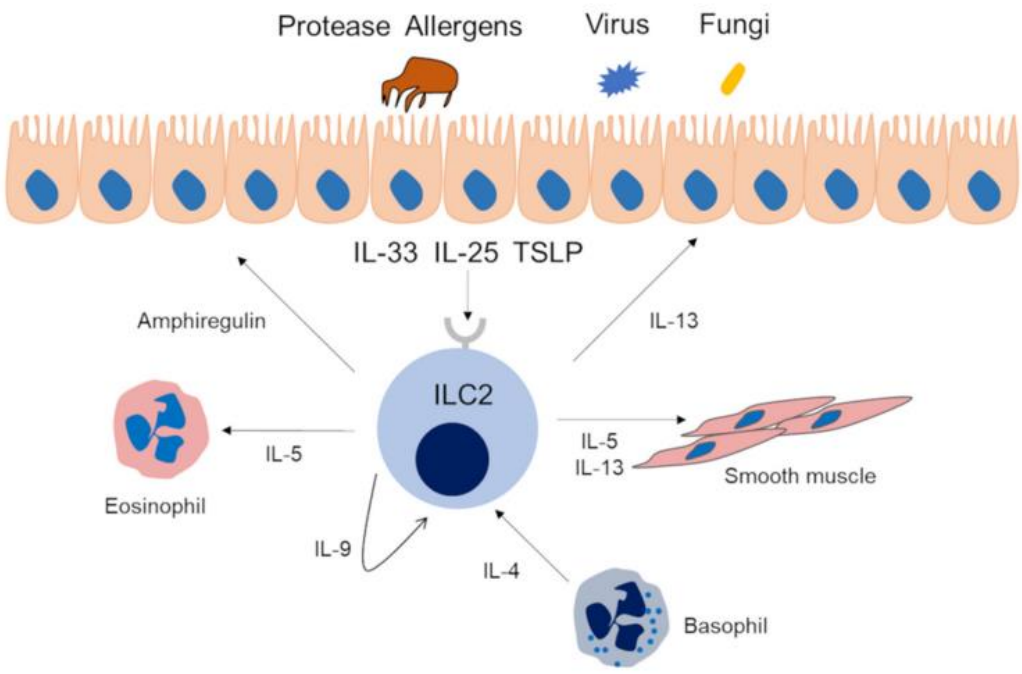

Figure 1.5 Type 2 immune response to allergen by airway epithelial cells in asthma

Allergens with protease activity, such as HDM, viruses, and fungi, promote the production of alarmins (IL-25, IL-33, and TSLP) by airway epithelial cells. These alarmins activate ILC2. Activated ILC2 releases Th2 cytokines such as IL-4, IL-5, and IL13 in asthma patients. IL-4 is involved in the differentiation of B cells into IgE-producing cells. IL-5 is responsible for the maturation and release of eosinophils and helps with eosinophil survival. IL-13 has a central role in airway hyperresponsiveness development and remodeling of the tissue and increasing eosinophil counts. Figure adapted from Yasuda et al. 2020 [185].

1.6.2.3 Interactions between HDM and cigarette smoke

Cigarette smoke and exposure to HDM allergens are associated with increased airway inflammation [177, 186, 187]. An *in vitro* study of the interaction of *Der P1* allergen and cigarette smoke on primary HBECs showed that *Der P1* and short-term exposure to CS for 20 minutes led to significantly increased release of IL-8, IL-1β, and soluble intercellular adhesion molecule-1 (sICAM-1), while longer exposure for 1-6 hours to CS led to a decrease in the amount of these mediators detected in the culture medium [188]. This study suggests that short-term exposure to CS may induce inflammation by releasing inflammatory mediators from HBECs,

an effect that Der P1 may potentiate. However, prolonged exposure to CS enhances the release of sodium chromate (^{51}Cr) from pre-loaded cells, indicating potential damage to HBECs [188]. . Furthermore, HDM and CS exposed mice show significantly attenuated eosinophilia in the BAL compared with animals exposed only to HDM. This study concluded that CS down-regulated the expression of the HDM-induced eosinophil-recruiting factors, eotaxin-1, and vascular cell adhesion protein 1 (VCAM-1), and reduced the activation of B cells and the production of IgE [154]. Moreover, mice exposed to a low-dose of HDM combined with CS for the duration of 3 weeks demonstrated an asthmatic phenotype with increased airway eosinophilia, goblet cell metaplasia, and hyperresponsiveness compared to sole HDM or CS exposure [189]. Together, these studies show that CS might have both inhibitory and exacerbating effects on eosinophil counts and airway inflammation, depending upon factors including exposure duration, dosage, and immune responses.

The interaction between CS and HDM also has an impact on alarmin production. 3 weeks of HDM and CS exposure cause a significant increase of IL-25 and IL-33 production *in vivo* [189]. When stopping CS exposure after the initial sensitization, no differences in these alarmins were found 2 weeks after smoke cessation, suggesting that CS exposure can enhance the production of these alarmins during exposure. Also, this study showed that the protein levels for Th2 cytokines (IL-4, IL-5 and IL-13) were significantly increased in mice exposed to HDM and CS compared to sole HDM or CS exposure. This might suggest a synergistic role for CS during the ongoing allergic response [189]. Alongside the interaction between CS and HDM, a study showed that a fine particulate matter (PM2.5) can enhance the *Der P1* antigen-induced HBECs innate immune response through the expression of IL-25, IL-33, and TSLP [190]. In this study, co-exposure of PM2.5 and

Der P1 antigen has synergetic effects on the regulation of cytokine expression levels compared to PM2.5 alone. The role of interactions between HDM and CSE *in vitro* on the expression and production of Th2 cytokines and chemokines in HBECs has not been fully explored. Therefore, further studies of the interaction between HDM and CSE in HBECs need to be investigated.

1.6.3 Viral infection

1.6.3.1 Viral infection and airway inflammation

Respiratory viral infections are associated with 85% of asthma exacerbations [191]. Clinical evidence indicates the substantial impact of viruses, especially Rhinovirus (RV) and Respiratory Syncytial Virus (RSV), in exacerbating asthma, leading to worsening symptoms and increased morbidity in asthmatic patients [192-194]. Viral infections are substantial causes of airway inflammation, especially in individuals with underlying respiratory diseases such as asthma. Respiratory viruses, such as RV, can enhance the inflammatory response, resulting in AHR and increased mucus production [195], damage to the airway epithelium and increased production of interferons and pro-inflammatory cytokines, including IL-6 and IL-8 [196]. This leads to mucus hypersecretion and worsening asthma symptoms by obstructing the airways. Furthermore, eosinophils are considered to play a key role in the pathogenesis of asthma exacerbation induced by viruses. RSV-infected children have a more significant number of eosinophils in their nasopharyngeal secretion, which was associated with asthma attack severity [197]. Besides the effect of viruses on asthma severity, viral infection may also contribute to airway remodeling in asthma. *In vitro* HBEC HRV infection may contribute to airway remodeling by upregulating the production of growth factors such as VEGF. These findings suggest that viral infections play a crucial role in airway inflammation in

asthma pathogenesis by triggering immune responses and worsening disease symptoms.

1.6.3.2 HBECs role in viral infection

HBECs play a key role in response to viral infection due to their location in the respiratory tract, acting as the primary target cells for infection and replication sites for various respiratory viruses, including RV, influenza, and RSV. HBECs react to viral infection via specific pattern-recognition receptors (PRRs) and regulated antiviral signaling mechanisms [198]. They express PRRs that are classified into three main groups, identical to other surveillance cells. These groups include nucleotide-binding oligomerization domain (NOD)-like receptors (NLRs), retinoic acid-inducible gene 1 (RIG-1)-like receptors (RLRs), and toll-like receptors (TLRs) [198].

TLRs, among other groups, are a family of integral proteins in the membrane that identify an extensive range of pathogen-associated molecular patterns (PAMPs) and signals via common Toll/interleukin-1 (IL-1) receptor domain-containing intermediate molecules, which play an important role in recognizing pathogens and activating innate immunity. [199, 200]. There are at least ten members of the TLR family that recognize unique microorganism-conserved components. TLR activation not only induces inflammatory responses but also promotes the formation of antigen-specific adaptive immunity [200]. Among the known TLR receptors, TLRs 3, 7, 8, and 9 tend to respond to virus-associated molecular structures, particularly viral nucleic acids, with recognition occurring largely within intracellular endosomes [201]. TLR 3 appears to be particularly important in the response of epithelial cells of the airway to respiratory viruses, including RSV and RV [202, 203]. TLR3 is stimulated by double-stranded RNA (dsRNA) during the replication of numerous respiratory viruses,

including RSV, RV, and influenza. Upon activation, TLR3 on HBECs stimulates downstream signaling pathways such as mitogen-activated protein kinases (MAPKs) and NF-kB, resulting in the release of pro-inflammatory cytokines such as IL-6, IL-8, and TNF-α [112, 202]. These cytokines and growth factors are essential for the antiviral immune response because they promote inflammation and recruit immune cells to the infection site. This helps to regulate viral replication but can also contribute to worsening airway inflammation, particularly with chronic respiratory diseases such as COPD or asthma.

TLR7 recognizes single-stranded RNA and has antiviral efficiency when combined with its homologue TLR8, which both helps to regulate interferon synthesis and activate T1 antiviral responses. This has a key role in viral-induced airway inflammation through regulating the T1/T2 immunomodulatory homeostasis by reducing T2 cytokines release such as IL-4, IL-5, and eotaxin, and promoting T1 cytokines, thus limiting airway eosinophilia [204, 205]. TLR9 recognizes cytosine-phosphate-guanine (CpG) patterns, which are common in microbial DNA but rare in mammalian DNA, thus making it an important sensor for identifying foreign DNA, particularly in viral and bacterial infections [206]. TLR9 is predominantly expressed in immune cells' endosomal compartments, including B cells and plasmacytoid dendritic cells (pDCs). It can detect viral DNA, and upon detecting it, the immune system is triggered, producing pro-inflammatory cytokines, including IL-6 and TNF-α, as well as type I interferons. This is essential for limiting the spread and replication of viruses [207].

HBECs are uniquely positioned and wired to react to respiratory viral infections. Because of their unique structure, HBECs are able to both make and react to cytokines, which control the activation and trafficking of immune cells

downstream and ultimately lead to the removal of viruses.

1.6.3.3 Interaction between viral infection and cigarette smoke

The respiratory tract's defense against respiratory infection is altered by cigarette smoke [208], which is described in more detail in section 1.6.1. CS weakens the lung's defenses against viral infections by disrupting the activity of innate immune cells, including epithelial cells and macrophages. Also, the ability of the body to produce interferons, which are essential for the antiviral response, is weakened by smoking. This makes it easier for viruses to spread throughout the lung tissues [209, 210]. This is evident in the fact that smokers are more prone to respiratory viral infections, including influenza, RSV, and coronaviruses.

CS can damage the airway epithelium, reduce mucociliary clearance, and facilitate viral transmission and infection. Because this damage inhibits effective immune clearance, viral infections are prolonged [211]. *In vitro* CSE reduces antiviral immunity by inhibiting interferon alpha (IFN-α), which is produced by the innate immune system in response to viral infections and other pro-inflammatory cytokines, including IL-6 and TNF-α, but it can also augment the pathophysiology of COPD by increasing neutrophil recruitment driven by IL-8 [212]. In addition, CSE alters the response of epithelial cells to HRV, leading to suppression of RANTES and CXCL10 cytokine production and increased viral RNA [213].

As described in section 1.5.1, HBECs are important sources of alarmins, including IL-25, IL-33, and TSLP [214], and viral infection induces the production of alarmins. Alarmin release in response to viral infection can promote Th2 allergic inflammation through TLR7, TLR8, and TLR9, among other TLRs on immune cells that are capable of detecting double-stranded DNA (dsDNA) [215-217]. The role of interactions between viral infection and CSE *in vitro* on the expression and

production of alarmins in HBECs has not been fully explored but studies outlined above suggest that CSE might attenuate the response of alarmins to viral infection in HBECs. Therefore, further studies are needed to better understand the effect of CSE on viral infection in terms of alarmin release and the response mechanism of HBECs. A better understanding of these effects has the potential to lead to a deeper understanding and may result in the development of novel therapy targets for various respiratory diseases.

1.7 Cell-free DNA (cfDNA)

1.7.1 Origins of cfDNA

Mandel & Metais were the first to report on the presence of circulating cell-free DNA (cfDNA) in human blood in 1948 [218]. cfDNA refers to the fragments of DNA that circulate freely in bodily fluids, sputum, plasma, and bloodstream. The source of cfDNA can vary depending on pathological and physiological processes and is still unclear and poorly understood. To date, the applications of integrating cfDNA analysis into clinical practice, along with its molecular profiling for the detection, prognosis, and treatment of cancer and other disorders, have been extensively researched [219-221]. Various biological aspects can not only contribute to the overall cfDNA profile, but they can also interact to create a cascade of reactions that result in further, and frequently indirect, cfDNA release [222]. Although cfDNA is a non-specific marker in inflammatory diseases, it can still provide insight into the underlying inflammatory responses. cfDNA concentrations rise significantly and track with disease intensity and other specific markers of inflammation [223]. cfDNA levels in plasma and nasal secretions were significantly higher in allergic

rhinitis patients compared to healthy controls, indicating its association with inflammatory responses and severity of allergic rhinitis [224].

Apoptosis is an innate form of controlled cell death during a regular cellular cycle. During apoptosis, the cell's DNA is broken down into pieces, some of which are released into the bloodstream. Apoptotic cfDNA is frequently fragmented in a precise pattern, with a length of roughly 180 base pairs (bp), indicating the action of nucleases [225]. During DNA damage-induced apoptosis, cells release apoptotic regulators and undergo changes in DNA integrity. This process includes the fragmentation of DNA into large fragments (50 kbp) before it breaks down into smaller, internucleosomal fragments. These early fragmentations are linked to the presence of cell-free DNA observed during apoptosis [226, 227].

Necrosis, as opposed to apoptosis, results from uncontrolled cell death caused by injury or disease, including infections, trauma, or ischemia. Necrotic cells, unlike apoptotic cells, release more irregular and bigger fragments of cfDNA into the bloodstream. Necrosis is especially relevant in cancer and sepsis diseases [228]. In cancer patients, cfDNA can be derived from circulating tumor cells (CTCs) or directly from the tissue of tumors via apoptosis, necrosis, or active release. This fraction of cfDNA, known as circulating tumor DNA (ctDNA), contains mutations of modifications specific to the tumor, making it a useful biomarker for diagnosis, prognosis, and monitoring of cancer [229].

It has also been shown that in infectious diseases, cfDNA can be produced by some pathogens like bacteria or viruses, as well as host immune cells that are undergoing apoptosis or necrosis. This source of cfDNA is highly valuable for detecting bloodstream infections through analysis and is referred to as cell-free microbial DNA (cfmDNA) [230]. In addition, cfDNA can also originate during

pregnancy from the fetal placenta, with fetal DNA fragments identified within the maternal bloodstream earlier during the first trimester. This fetal cfDNA is commonly utilized in non-invasive prenatal testing (NIPT) to identify chromosomal disorders such as Down syndrome [231]. There are various sources of cfDNA and causes that contribute to cfDNA release in the human body, which provide insightful information about a range of physiological and pathological conditions. Therefore, cfDNA has become an essential diagnostic and disease-monitoring tool. (Figure 1.6) demonstrate the interactions among biological mechanisms that participate in the release of cfDNA [222].

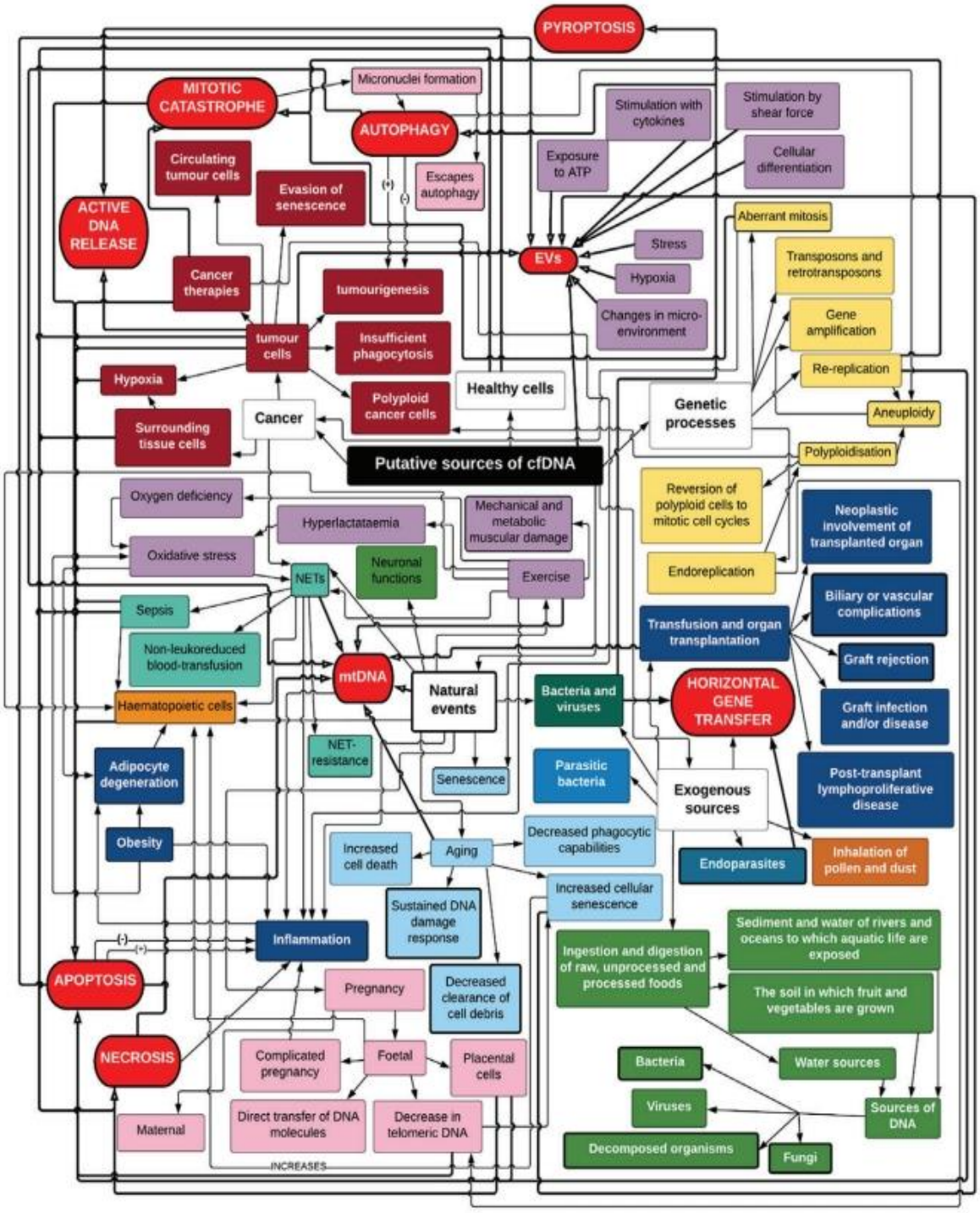

Figure 1.6 Complex interactions among biological mechanisms that participate in the release of cfDNA

The figure demonstrates the several biological and environmental origins of cfDNA. The figure displays the complex interaction of internal and external factors that influence cfDNA release and how different interactions could make it more complicated to understand the origins and biological roles of cfDNA and identify new biological markers. Figure adapted from Aucamp J et al. 2018 [222].

1.7.2 cfDNA in lung diseases

cfDNA has been identified as an important biomarker for pathogenesis, including in respiratory diseases. Concentrations of cfDNA reflect tissue damage and can predict the severity of COVID-19 patients' condition [232]. The level of cfDNA in the plasma and serum of lung cancer patients has been widely used for early detection, assessment, and characterization of lung cancer, which reflects the disease progression and offers a tracking progression to the treatments [233-235]. In asthma, neutrophil extracellular traps(NETs) and their associated extracellular double-stranded DNA (dsDNA) could contribute to the pathogenesis of asthma and serve as therapeutic targets for rhinovirus-induced asthma exacerbation *in vivo* [236]. Furthermore, elevated cfDNA levels are associated with allergic airway inflammation (AAI), including allergic asthma, due to increased turnover of cells and damage resulting from heightened inflammatory responses [224]. Notably, elevated plasma cfDNA levels have been linked to increased disease severity, frequent exacerbations, and a higher risk of mortality in COPD [237]. Lung epithelial cells release cfDNA into BAL fluid during normal cell turnover, and lung-specific cfDNA is increased in plasma in various lung diseases, significantly increasing in exacerbating versus non-exacerbating COPD [238]. I

Despite evidence that cfDNA is released in asthma and COPD, there has been little research to date on the functional role of cfDNA in asthma pathogenesis. Considering its molecular weight, cfDNA may be able to transfer genetic material from several genes in the host to the target cell [239]. Eosinophils can produce exosomes, and eosinophil-derived exosomes may carry cfDNA, suggesting a potential role in mediating inflammation and contributing to asthma pathogenesis. Exosomes derived from eosinophils in asthma patients can alter specific eosinophil

functions linked to asthma pathogenesis, potentially playing a key role in the onset and persistence of asthma [240]. Therefore, investigating cfDNA as a signaling molecular with functional impact of adjacent cells, in addition to the work already being done to investigate its role as a biomarker could open the door and have substantial promise for improving asthma management. It may provide novel tools for determining disease severity, predicting exacerbations, and modifying therapy. Expanding this research could transform how asthma is tracked and treated, providing a more precise and adaptive approach to disease management.

1.7.3 cfDNA and inhaled insults

cfDNA is released into the bloodstream as a response to different inhaled insults and pathogens. Cigarette smoke, a major inhaled insult and a well-established risk factor for COPD, induces oxidative stress, inflammation, and immune responses, ultimately leading to lung damage and the release of cfDNA. In addition, cfDNA is increased in smoke inhalation injury [241], and can be increased by CSE in endothelial cells [242], which appears to be a potentially useful biomarker for inhaled smoke and related lung damage.

In addition to cigarette smoke, cfDNA is increased following viral infection, which is correlated with disease severity and might contribute to lung injury [243, 244]. cfDNA is shown to be released by lung cells in response to various pathogens and inhaled insults, which might have potential pathogenic effects. However, studies of cfDNA as a signaling molecule with a functional impact on adjacent cells and its functional role in immune response to inhaled insults are still limited, particularly in asthma. Therefore, expanding studies on cfDNA associated with inhaled insults as a potential functional signaling molecule may provide new understanding of disease mechanisms and novel therapeutic targets for asthma management.

1.7.4 Cell-free DNA and extracellular vesicles

All living cell types are known to produce extracellular vehicles (EVs) [245], which are important intercellular communication mediators that contain a varied range of cargo, such as proteins, metabolites, lipids, and nucleic acids, that can be absorbed by other cells [246, 247]. EVs can function as mediators of intercellular communication and may influence the function of the recipient cell by transmitting biological signals and information [248].

EVs have heterogeneous functions and are generally distinguished into two main types: exosomes and ectosomes [249]. Exosomes originate from endosomes and are produced in intraluminal vesicles called multivesicular bodies. Once formed, these bodies can combine with the plasma membrane to release their contents as exosomes [249, 250]. Ectosomes are another route of biogenesis that involves the release of plasma membrane-derived EVs, which include macrovesicles [249]. Due to their role in cell-cell communication, EVs have been linked to immunological responses in various diseases [251].

In addition to being freely available in the bloodstream and other fluids, cfDNA can be associated with EVs, including exosomes and macrovesicles. cfDNA has a complex function in EVs and is crucial for normal physiological functions and pathological conditions, such as cancer, inflammation, and immunological responses, through activation of the immune response, modulation of cellular functions, promotion of tumor growth, and enhancement of metastasis [248, 252]. EVs, particularly exosomes, can carry cfDNA between cells within their cargo. This is essential for communication between cells and may influence processes such as tissue repair, immunological response, and disease progression [248]. EVs containing cfDNA can also play a role in modulating immune responses. In some

inflammatory disorders, EVs may carry DNA fragments that activate immunological responses through TLRs, resulting in chronic inflammation or autoimmune disorders [253].

In cancer, cfDNA contained within EVs is being studied as a potential biomarker for early detection and an important diagnostic tool for disease progression and treatment response, which may hold promise as a non-invasive diagnostic target [254]. The body may interpret the release of EV-bound cfDNA as a warning sign, activating immunological responses and prolonging inflammation. Because of its stability, cfDNA in EVs is being investigated as a diagnostic tool. As EVs protect cfDNA from enzyme breakdown, they provide a dependable source of genetic material for identifying genetic changes in various diseases, including cancer, cardiovascular diseases, and neurological disorders [255]. Therefore, studying the role of EVs in carrying cfDNA could offer new insights into asthma pathogenesis and may reveal novel therapeutic targets, while also highlighting their potential as biomarkers for asthma diagnosis and monitoring.

1.9 Summary

Asthma is a heterogeneous lung disorder that is characterized by inflammation of the airway. There are two major endotypes of asthma; T2-high, which is associated with eosinophilic airway inflammation, and non-T2, which is associated primarily with less eosinophils but a predominance of neutrophils and paucigranulocytic immune cells. Cigarette smoke combined with asthmatic inflammation may induce important changes in the asthma endotype with a predominance of activated macrophages and increased neutrophils in the airway, suggesting that cigarette smoke might contribute to endotype switching in asthma. Cigarette smoke extract (CSE) can alter inflammatory responses in human airway smooth muscle cells (HASMCs), promoting a shift from steroid-sensitive type 2 high (T2-high) eosinophilic inflammatory responses to steroid-insensitive Type 2 low (Non-T2) neutrophilic inflammatory responses, at least partially via COX-2/PGE_2-dependent mechanism.

Human bronchial epithelial cells (HBECs) are the first line of defence against inhaled insults, including cigarette smoke, viruses, and allergens such as house dust mites (HDM), and are an important source of a group of cytokines termed alarmins. Alarmins, including IL-25, IL-33, and thymic stromal lymphopoietin (TSLP), promote innate immune and adaptive T2-high inflammatory responses and are released during the epithelial layer response to viral infection and other inhaled insults.

In addition to the release of alarmins, exposure to inhaled insults is likely to cause the release of cell-free DNA (cfDNA) from lung epithelial cells. cfDNA refers to all non-encapsulated DNA in the bloodstream or other fluids, which consists of small extracellular nucleic acid fragments released from cells due to apoptosis, active cellular secretion, and impaired clearance mechanisms. Crucially, cfDNA

concentrations are often associated with the extent of tissue damage and/or inflammation in various pathologies. Whether CSE alters the responses of HBECs to inhaled insults such as HDM and viruses through altered release of alarmins, cytokines, and cfDNA, and alter remodeling and gene expression in HASMCs is unclear and remains to be explored.

1.10 Hypothesis and aims

1.10.1 Hypothesis

CSE alters the responses of human bronchial epithelial cells (HBECs) to inhaled insults such as HDM and viruses through the altered release of alarmins, cytokines, and cell-free DNA (cfDNA), contributing to the pathogenesis of asthma.

1.10.2 Aims

The general aims of the study are:

- To investigate the effect of cigarette smoke extract (CSE) on the expression and production of alarmins, (IL-25, IL-33, TSLP), Th2 cytokines (IL-4, IL-5, IL-13), eosinophilic chemokines (Eotaxin, IP-10, RANTES), pleiotropic cytokine IL-6, and the neutrophilic chemokine IL-8 in HBECs.
- To assess the effect of house dust mite (HDM) allergen alone and in combination with CSE on the expression and production (release) of the above cytokines and chemokines, and assess the role of COX-2 expression in response to inflammatory stimuli.
- To investigate how CSE alters inflammatory responses to viral infection using the viral mimic (poly (I:C)) by measuring the release of alarmins, (IL-25, IL-33, and TSLP), Th2 cytokines (IL-4, IL-5, and IL-13), eosinophilic chemokines (eotaxin, IP-10, and RANTES), and neutrophilic chemokine IL-8 in HBECs, and assess the role of oxidative stress in the production of inflammatory mediators .
- To determine whether CSE and poly (I:C) alone and in combination cause the release of cell-free DNA (cfDNA), an active participant in driving inflammation and immune signaling, from HBECs and understand the functional effects of released cfDNA on HASMC function by studying how cfDNA might contribute

to epithelial-HASMC crosstalk in asthma, specifically HASMCs proliferation, contraction, and gene expression.

Chapter 2. General methods and materials

2.1 Introduction

This chapter outlines the general methods used in the course of this thesis. All medium recipes, reagents, buffers, kits, and materials are listed in the Appendix.

2.2 Cell culture

2.2.1 Culture conditions

All culture medium and their supplements were made and maintained according to the manufacturer's instructions (Appendix 7.1.1-2). The cells were maintained in a humidified incubator at 37°C with 21% O_2 and 5% CO_2. The medium was changed every 48 hours until the cells reached 90-100% confluence. The cells were then growth-arrested in unsupplemented medium for 24 hours prior to experimentation.

2.2.1 Immortalised human bronchial epithelial cells (iHBECs)

Experiments of immortalised human bronchial epithelial cells (iHBECs) were performed on immortalised human bronchial epithelial cells (iHBECs; a gift from Prof. Jerry Shay, University of Texas, USA). Immortalized cell lines of HBECs were generated by a serial introduction of retroviral expression vectors for cyclin-dependent kinase 4 (CDK4) gene, followed by human telomerase reverse transcriptase (hTERT) [256] prior to receiving and using them in our lab. iHBECs were cultured in keratinocyte serum-free medium (KSFM) supplemented with 25 µg/ml bovine pituitary extract (BPE), 0.2 ng/ml recombinant epithelial growth factor (EGF), 250 ng/ml puromycin dihydrochloride, and 25 µg/ml G418 sulfate (Appendix 7.1.2).

2.2.1 Human airway smooth muscle cells (HASMCs)

HASMCs from four donors were obtained from a cell bank at the University of Nottingham NIHR Respiratory Biomedical Research Centre. The demographic details for the donors from which HASMCs were derived are shown in Table 2.1. The National Research Ethics Service (NRES) Committee East Midlands-Nottingham has granted approval for the use of lung tissue samples under ethics number 08/H0407. HASMCs were cultured in Dulbecco's Modified Eagle's Medium (DMEM) supplemented with 10% Foetal Bovine Serum (FBS), (4nM) L-glutamine, (100 unit/ml) penicillin, (0.1 mg/ml) streptomycin, and (250 mg/ml) amphotericin-B. (Appendix 7.1.2). The cells in this study were used at passage 6 in all experiments.

Table 2.1 Demographic details of HASMC donors

Donor ID	Sex	Phenotype	Age at collection	Smoking status	Inhaled corticosteroids
AZAC05	Female	Non-asthmatic	27	Never	No
AZAC11	Male	Non-asthmatic	47	Never	No
AZAC12	Male	Non-asthmatic	28	Never	No
159	Male	Non-asthmatic	36	Never	No

2.2.2 Cell subculture

To achieve passage 6 of HASMCs for all experiments, early passage of cells was cultured in a T-225 flask for 7-9 days. Immortalized HBECs were used at various passages in the experiments, as the cells were modified to retain continuous proliferation while maintaining genotypic and phenotypic characteristics. iHBECs

were also cultured in a T-225 flask for 7-9 days prior to experimentation. The supplemented medium for all cells was changed every other day until 90% confluence was reached. After the cells became confluent, the culture medium was removed, followed by washing the flask with 10 ml of PBS. Then, 10 ml of 0.25% Trypsin-EDTA solution (Appendix 7.1.1) was added to the cells and incubated for 3-4 minutes at 37 °C in a 21% O_2 and 5% CO_2 humidified incubator. Following incubation, the cells were checked under the microscope to ensure that detachment had occurred. Trypsin-EDTA was neutralized by adding 10 ml of fresh FBS into the flask. The contents were then transferred into a 50 ml Falcon® tube, and the cells were centrifuged at 1200 rpm for 5 minutes. After centrifugation, the supernatant was removed by the aspirator, leaving the cell pellet at the bottom of the Falcon® tube. Then, 10 ml of fresh medium was added to the Falcon® tube. The cells then were counted, and either the cells at a density of 0.5×10^6 cells per ml were stored in a cryogenic tube with a freezing solution (90% FBS and 10% DMSO), or the cells were seeded into a new flask for the following passage. The cryogenic tubes were placed in a Mr Frosty™ Freezing Container (Thermo Fisher Scientific) filled with 100% isopropyl alcohol. The container was immediately placed in a -80°C freezer for 24 hours to ensure slow cooling. The cryogenic tubes were transferred to liquid nitrogen storage on the following day for long-term cell storage.

2.2.3 Cell counting

Cell counting was performed using a glass haemocytometer and a coverslip. A 10 µl sample of cells was mixed with 10 µl of Trypan blue solution (Appendix 7.1.1) in a 1:1 ratio to distinguish live from dead cells. A microscope was used to visualize the glass haemocytometer, and all four squares were observed. The number of live cells was counted in each quarter. Live (viable) cells with an intact cell membrane

excluded the blue Trypan dye and appeared as bright cells under the microscope, while the dead cells took up the dye and appeared blue. Then, the average number of live cells in all four squares was multiplied by the dilution factor and then multiplied by 10^4 to provide the total number of live cells.

2.2.4 Cell viability assay

The 3-(4, 5-dimethylthiazol-2-yl)-2, 5-diphenyltetrazolium bromide (MTT) assay was used to assess the cytotoxicity of the various treatments toward cells. Following specific cell treatments, the medium was removed, and 250 µl per well of 1 mg/ml MTT solution in warm unsupplemnted medium was added. The culture plate was then incubated in a humidified incubator at 37 °C for 30 minutes. The MTT solution was removed and the plate was dried at room temperature overnight. The following day, 250 µl DMSO was added to each well, and 100 µl, placed in duplicate, was transferred to a 96-well plate. The absorbance was measured at 550 nm using a FLUOstar Omega microplate reader (BMG LABTECH). The viability data of treated values were presented as a percentage relative to the control group (100%).

2.3 Cigarette smoke extract (CSE) preparation

3R4F research-grade cigarettes (Appendix 7.1.3) were used to prepare a cigarette smoke extract (CSE). Two cigarettes, with the filters removed, were connected to an 80 ml sterile glass bottle containing 20 ml of unsupplemented KSFM medium via a rubber tube, and the bottle was connected to another big glass bottle to direct the smoke via another tube to a vacuum pump DA7C (see Appendix 7.1.3). The cigarette filters were placed between the rubber tube and the cigarette pump. The vacuum pump pressure was set to 0.2 bar to maintain a consistent cigarette

burning rate and ensure adequate bubbling in the medium. After the cigarettes were burnt, the medium was filtered into a 50 ml Falcon® tube using a 0.02 µm pore syringe filter. The absorbance of CSE was measured using a NanoDrop™ 2000 Spectrophotometers (ThermoFisher) at 320 nm to measure CSE strength (1.5=100%) (Figure 2.1). This CSE preparation was then diluted in unsupplemented medium to the desired concentration. A fresh CSE for all experiments was made on the same day of the experiment and used immediately after preparation.

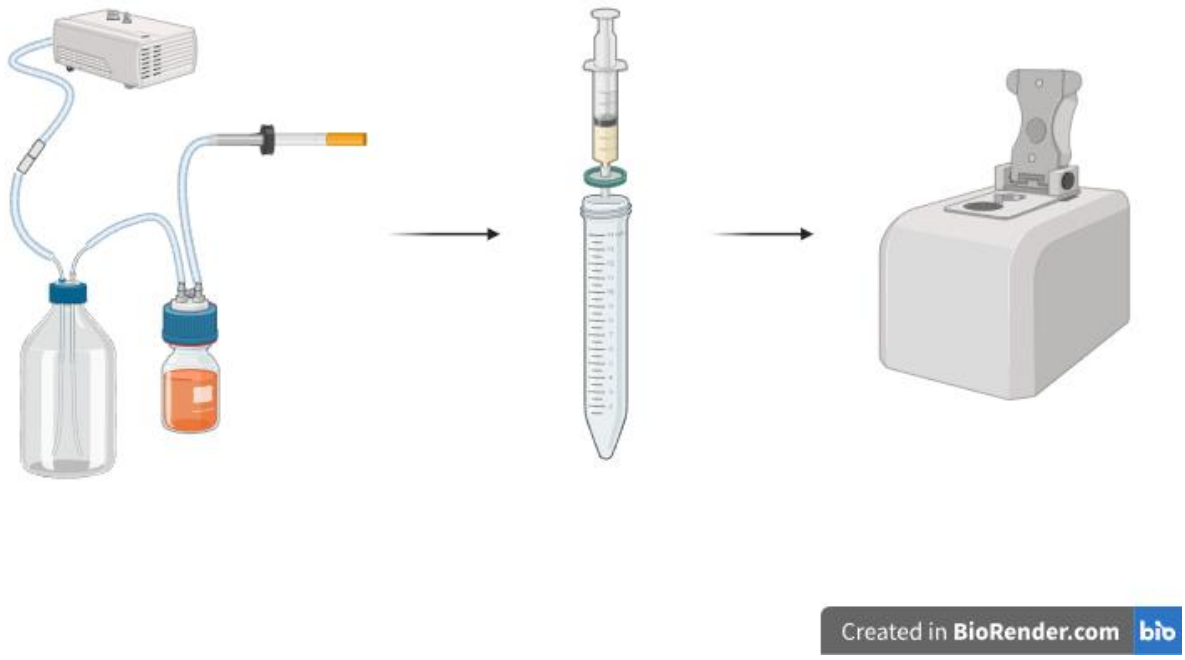

Figure 2.1 *In vitro* cigarette smoke model

3R4F research-grade cigarettes were connected to 80 ml sterile glass bottle containing 20 ml of unsupplemented medium via a rubber tube and the bottle was connected to another big glass bottle to direct the smoke via another tube to vaccum pump. The medium was then filtered into a 50 ml Falcon® tube and the absorbance of CSE was measured using a NanoDrop™ 2000 at 320 nm.

2.4 *Der P1* preparation

The Dermatophagoides pteronyssinus1 (*Der P1*) is one of the major allergens of house dust mites produced by Dermatophagoides pteronyssinus that plays a key role in allergenic responses [257]. 732 µg *Der P1* protein was dissolved in 292.3 µl unsupplemented KSFM medium to make a stock solution with a final concentration of 25 µg/ml (Appendix 7.2). Sub-aliquots of this stock solution were distributed into 0.5 ml Eppendorf tubes and stored in a -20°C freezer to avoid repeated freeze and thaw cycles until further use. The 25 µg/ml was then diluted 1:2.5 in unsupplemnted KSFM medium to a working concentration of 10 µg/ml, which was used in our experiments.

2.5 Poly (I:C) preparation

Polyinosinic-polycytidylic acid (Poly (I:C)) is a toll-like receptor 3 (TLR3) agonist, that is structurally identical to the double-stranded RNA found in some viruses and found to be a “natural” activation of TLR3 [258]. 10 mg purified white solid Poly (I:C), was dissolved in 10 ml distilled water as per the manufacturer’s instructions to make the original stock of 1 mg/ml, which was aliquoted and stored at -20°C to avoid repeated freeze and thaw cycles until further use. In my experiments, the original stock of 1 mg/ml was diluted in unsupplemented KSFM medium in 1:1000 dilution ratio to generate the final working concentration of 10 µg/ml before treating the cells (Appendix 7.3).

2.6 L-Glutathione (GSH) preparation

L-Glutathione reduced (GSH) functions as a key endogenous antioxidant, playing a vital role in reducing reactive oxygen species. GSH was dissolved and prepared according to the manufacturer's instructions (Appendix 7.4). Solid GSH was dissolved in deionised water to reach the original stock concentration of 0.05 M. Sub-aliquots of this stock solution were stored in a -20°C freezer to avoid repeated freeze and thaw cycles until further use. GSH was then dissolved in deionised water to reach a final working concentration of 100 µM, which was used to treat the cells in our experiments.

2.7 Cell lysate preparation

After a specific cell treatment, the conditioned media were collected from the wells and stored in a -20°C freezer until further use. The plates were then washed with PBS and 50 µl of complete radioimmunoprecipitation (RIPA) buffer (Appendix 7.6) added to each well. Cell scrapers were utilized to scrape the cells. The cell lysates were then collected from each well into 1.5 ml Eppendorf tubes and stored in a -80°C freezer until further use. The protein concentration was measured by a bicinchoninic acid (BCA) assay kit.

2.8 Bicinchoninic acid protein assay

The total concentration of protein was measured using a bicinchoninic acid (BCA) assay kit (Thermo Fisher Scientific). Bovine serum albumin (BSA) standards (2000-0 µg/ml) were prepared according to the manufacturer’s instructions. After preparation, the BSA standards and protein samples (5 µl of each) were placed in

duplicates into a 96-well plate. The BCA working reagents A and B were then prepared and mixed in the ratio of 1:50, and 95 µl of the mixture reagents were added to all the wells containing BSA standards and protein samples. The plate was covered and incubated for 30 minutes at room temperature. Following the incubation, the absorbance was measured using a FLUOstar Omega microplate reader (BMG LABTECH) with an optical density reading at 562 nm. The protein concentrations were measured and calculated as µg/ml using the Omega analysis software.

2.9 Enzyme-Linked immunosorbent assay (ELISA)

The concentration of IL-8 in the collected supernatant was assessed and measured using a Human IL-8/CXCL8 DuoSet ELISA kit (R&D System), which was used according to the manufacturer's instructions.

2.9.1 Assay procedure

For each ELISA experiment, 96-well plates designed for high binding were used. The capture antibody (mouse anti-human IL-8) was diluted in PBS. Immediately, 100 µl of the diluted capture antibody was added to each well. The plate was sealed with a plate sealer and incubated overnight at room temperature. The following day, the plate was washed with a wash buffer (0.05% Tween 20 in PBS) by filling each well with 400 µl wash puffer for a total of three washes. The plate was then kept upside down on a clean paper towel for drying (5-10 minutes). Subsequently, the plate was blocked by adding 300 µl of blocking buffer (1% BSA in PBS) and incubated for one hour at room temperature. Then, the plate was rewashed with wash buffer for a total of three washes. Human IL-8 standards were

diluted in reagent diluent to create a seven-point standard curve (0.1% BSA, 0.05% Tween 20 in TBS) using 2-fold serial dilutions with a concentration from 2000 to 31.3 pg/ml. In addition, blank wells containing only reagent diluent served as a negative control. After washing, 100 µl of samples and the diluted standard were added to the wells, placed in duplicates, and incubated for two hours at room temperature. After incubation, the plate was washed with wash buffer, as described previously. Next, 100 µl of diluted biotinylated goat anti-human detection antibody (specific for IL-8) at a final concentration of 10 ng/ml was added to each well, covered, and incubated for two hours at room temperature. After incubation, the plate was rewashed with wash buffer, and 100 µl of the working dilution of streptavidin-horseradish peroxidase (HRP) was added to each well and incubated for 20 minutes at room temperature in a dark place. The plate was rewashed with wash buffer and 100 µl of substrate solution (hydrogen peroxide and tetramethylbenzidine) was added to each well and incubated at room temperature for 20 minutes in a dark place. Finally, 50 µl of stop solution (2N sulfuric acid) was added to each well, and the plate was gently tapped to ensure thorough mixing. The absorbance of IL-8 was measured using a FLUOstar Omega microplate reader (BMG LABTECH) with an optical density reading set at 450 nm of each well. Following the reading, MARS software was used to analyse the obtained data. All the data were normalized to the total amount of protein measured by BCA assay. IL-8 concentrations (pg/ml) were averaged and then divided by the total protein amount (mg/ml). The divided values were multiplied by the total volume of protein lysate (0.05 ml) and expressed as pg/mg protein.

2.10 Human Luminex® Discovery Assay

Human Premixed Multi-Analyte Kit, Luminex® Discovery Assay (R&D System) was used to assess the production and concentration of alarmins (IL-25, IL-33, and TSLP), Th2 cytokines (IL-4, IL-5, and IL-13), eosinophils chemokines (Eotaxin, IP-10, and RANTES), pleiotropic cytokine IL-6, and neutrophil chemokine IL-8 from the cell supernatant. All the reagents provided in the kit were placed at room temperature before use and prepared according to the instructions of the manufacturer. The calibrator diluent provided in the kit was used to reconstitute 7 unique standard cocktails for the specific analytes selected for the above cytokines before mixing and combining them into one standard tube, which serves as the high standard. Standard was then diluted to obtain a six-point standard curve using a 3-fold dilution series. 50 µl of the prepared standard and supernatants were added into 96 well-plate, and a plate layout was written to record standard and samples assayed. Then, 50 µl of the microparticle cocktail (mix of dyed microsphere beads) was added to each well. A foil plate sealer was used to cover the plate, which was then incubated at room temperature on a horizontal shaker at 800 rpm for 2 hours. After incubation, the plate was placed on a round bottom microplate magnetic device and incubated for 1 minute. Then, the liquid was removed, while the plate remained in contact with the magnetic device to avoid the loss of magnetic beads. Each well then was filled with 100 µl wash buffer and allowed 1 minute before removing the liquid again, this procedure was repeated for total of three washes. After washing, 50 µl of diluted Biotin-Antibody Cocktail were added to each well, covered with a foil plate sealer and incubated at room temperature for 1 hour on a horizontal shaker at 800 rpm. After the incubation, the wash procedure was performed three times as previously described, and 50 µl of diluted Streptavidin-PE was added to each well,

covered with a foil plate sealer and incubated at room temperature for 30 minutes on a horizontal shaker at 800 rpm. Then, the wash was performed three times, and the beads were resuspended by adding 100 µl of wash buffer to each well. The final step was to incubate the plate at room temperature for 2 minutes on a shaker at 800 rpm. The plate was immediately read using the Bio-Plex™ 200 System (Bio-Rad), and the Bio-Plex manager 6.1 Software was used to measure the concentration of multiple biomarkers. A photomultiplier tube (PMT) with a low threshold was utilised to detect the lowest concentration range of 7-17 pg/ml. The average concentrations of the targeted cytokines (pg/ml) were divided by the total amount of protein (mg/ml). Then the divided values were multiplied by the total volume of protein lysate (0.05 ml) and expressed as pg/mg protein.

2.11 Western blotting

Western blotting was used to detect proteins of interest within a complicated mixture of proteins collected from lysed cells [259]. Proteins were separated by polyacrylamide gel electrophoresis (PAGE) according to their molecular weight using a NuPAGE mini gel tank system (Invitrogen). The experimental protocol, including running and transferring steps, blocking and antibody incubation, and detection, is described in detail below.

2.11.1 Running and transferring steps

Cellular proteins were collected and their concentration was measured using the BCA assay described in section 2.7. Protein samples were diluted at a 1:4 ratio in 4x Laemmli buffer containing 5 µl of reducing agent (Appendix 7.6). The protein samples were subsequently mixed and incubated at 80°C for 10 minutes to denature

the protein. The Bolt Bis-Tris gel (Appendix 7.6), a pre-cast polyacrylamide gel with a 4-12% concentration gradient was utilised to separate the protein of interest by their molecular weight. 10 µl of the pre-stained protein marker and 20 µg of the samples were then loaded to the gel's wells. The electrophoresis tank was filled with running buffer (Appendix 7.6), connected to the electrical supply, and electrophoresed at 160 volts for 60 minutes.

After electrophoresis, the gel was taken out of the tank and submerged in 1x transfer buffer (Appendix 7.6) to facilitate the transfer of protein to nitrocellulose blotting membrane (Appendix 7.6). A “sandwich” of sponge, filter paper, gel, blotting membrane pre-soaked in 100% methanol, filter paper, and another sponge was subsequently made accordingly in 1x transfer buffer. It was inserted between the positive and negative electrodes in the mini blot module, which was then placed in the electrophoresis tank. The tank was filled with 1x transfer buffer, and electrophoresis was run at 10 volts for 90 minutes.

2.11.2 Blocking and antibody incubation

Upon completion of the transfer, Ponceau Red staining (Appendix 7.6) was applied to the membrane to confirm protein transfer. Three washes of the membrane were performed using 1x TBS-T (tris-buffered saline with Tween 20) (Appendix 7.6) before the membrane was incubated with blocking buffer (Appendix 7.6) for 1 hour at room temperature to minimize the non-specific binding of antibodies to the membrane. The membrane was placed into a 50 ml Falcon® tube, and the primary antibody (mouse anti-human COX-2 monoclonal antibody) at 1:1000 dilution and rabbit anti-human β-Actin antibody at 1:50000 dilution (Appendix 7.6) were added and incubated at 4°C overnight on the roller.

The following day, the membrane was washed three time with 1x TBS-T, each wash lasting for 10 minutes followed by adding the secondary antibodies with the 10 ml blocking buffer and incubated at room temperature for 1 hour. In this study, we used polyclonal goat anti-mouse immunoglobulins/HRP antibody in 1:2500 ratio for mouse anti-human COX-2 monoclonal antibody and polyclonal goat anti-rabbit immunoglobins/HRP antibody in 1:2500 ratio for rabbit anti-human β-Actin antibody as secondary antibodies (Appendix 7.6).

2.11.3 Detection

Following the incubation with secondary antibodies, the membrane was washed three times, each time for 10 minutes with 1x TBS-T. Lastly, the membrane was immersed with a mixture of enhanced chemiluminescence solutions (Clarity™ Western ECL substrate) (Appendix 7.6) for 5 minutes. ECL substrate is used to detect and visualize the band of proteins in WB. The membrane was then scanned using Odyssey LI_COR scanner. Using Image Studio 5.2 software, the density of protein bands on the membrane was measured, normalized against β-Actin, and compared to the control. The outcomes were presented as fold changes compared to the control.

2.12 Cell-free DNA (cfDNA) isolation

iHBEC conditioned media was collected after each experiment in Eppendorf tubes, and centrifuged for 10 minutes at 10,000 xg. The supernatants were transferred to new Eppendorf tubes and were immediately stored in a -20°C freezer for a cfDNA isolation while the pellet was discarded.

The QIAamp®DNA Blood Mini Kit (Qiagen) was used to isolate cfDNA present in the conditioned media according to the manufacturer's instructions. Initially, 200 µl of cell lysate was lysed with 20 µl proteinase K (Appendix 7.6), and 200 µl lysis buffer AL in an Eppendorf tube. The lysate was homogenized by vortexing and incubated at 56°C for 10 minutes then briefly centrifuged to remove drops from Eppendorf's lid. 200 µl 100% ethanol was added to the lysate and mixed thoroughly by vortexing. The lysate was then transferred to the QIAamp mini-spin column in a 2 ml collection tube and centrifuged for 1 minute at 8000 rpm to bind cfDNA. The flow-through was discarded, and the QIAamp mini-spin column was placed in a new 2 ml collection tube. 500 µl of membrane desalting buffer AW1 was added, and the column was centrifuged for 1 minute at 8000 rpm to remove impurities. The flow-through was discarded, and the QIAamp mini-spin column was placed in a new 2 ml collection tube. 500 µl of desalting buffer AW2 was added, and the column was centrifuged for 3 minutes at 14,000 rpm. The column was then placed in a new 2 ml collection tube and centrifuged at 14,000 rpm for 1 minute to eliminate the chance of possible desalting buffer AW2 carryover. Finally, 100 µl of elution buffer was added to the QIAamp mini-spin column and incubated for 5 minutes at room temperature prior to the final centrifugation at 8000 rpm for 1 minute. Eluted cfDNA was placed in a -20°C freezer.

2.13 Cell-free DNA (cfDNA) quantification

2.13.1 Quantitative real-time PCR

A quantitative real-time PCR (qPCR) targeting telomerase enzyme reverse transcriptase (TERT) gene was used to quantify cfDNA from iHBEC samples. TERT is rich in cfDNA fractions and has been an extensively reported target for assessing the theoretical cfDNA concentration [260]. A 10 µl reaction mixture was made by combining the components shown in Table 2.2. qPCR was performed using Ariamx Real-Time PCR System (Agilent®). Table 2.3 shows the thermocycling conditions that were used for each experiment. iHBEC genomic DNA was used to obtain a seven-point standard curve; a 1:100 dilution of genomic DNA in nuclease free water generated the top standard, with remaining standards generated by 1:2 serial dilutions. All standards, no template control (NTC), and samples, were run in triplicate. The cfDNA level of the treatment groups was shown in relation to the cfDNA of control samples, and Raw quantification cycle (Cq) values were presented relative to the control group. A higher quantification cycle (Cq) value reflects lower cfDNA levels. Therefore, 1/Cq was plotted to represent cfDNA concentration, where higher 1/Cq values indicate more cfDNA release. Primer sequences used were (TERT) gene (Appendix 7.5):

Forward Primer 5'- CCTCACATAAATGCTACCAAACGA-3'

Reverse Primer 5'-TTCCAAGAAGGAGGCCATAGTC-3

Table 2.2 Components for quantitative real-time PCR reaction mixture.

Reaction components	Volume
Forward primer (10uM)	0.5 µl
Reverse primer (10uM)	0.5 µl
PerfeCTa® SYBR® Green FastMix™	5 µl
DNA	2 µl (Standard) 4 µl (Samples)
Nuclease free water	2 µl (Standard) ~ (Samples)

Table 2.3Thermocycling conditions for measuring gene expression using quantitative real-time PCR.

Steps	Temperature °C	Time (minutes, seconds)
1- Hot start (1 cycle)		
Initial denaturation	95	10:00
2- Amplification (40 cycles)		
Denaturation	95	00:10
Annealing	60	00:30
Extension	72	00:20
3- Melt (1 cycle)		
Denaturation	95	01:00
Annealing	55	00:30
Extension	95	00:30

2.13.2 TapeStation

The concentration of DNA isolated from conditioned media samples was also measured using Agilent 4200 TapeStation system (Agilent). A cfDNA screen tape assay was used, which was designed for the analysis of cfDNA fragments ranging from 50 to 800 bp in length. Samples were prepared according to the Quick Guide of Agilent 4200 TapeStation system. After allowing the cfDNA screen tape assay reagents to be equilibrated for 30 minutes at room temperature, the screen tape and the required pipette tips were inserted into the instrument. 2 µl of sample buffer was mixed with 2 µl of each cfDNA sample in a 96-well sample plate. 15 µl of size marker ladder was combined with a 15 µl sample buffer and added to the 96 well plate. The plate was covered with a foil seal and vortexed at 2000 rpm for 1 minute, centrifuged for 1 minute, and loaded into the Tapestation instrument. The TapeStation results were analyzed using TapeStation Analysis 5.1 Software.

2.14 RNA isolation

HASMCs were stimulated with cfDNA from iHBECs for 24 hours in 12-well plates. The supernatants were collected in Eppendorf tubes and stored in a -20°C freezer for downstream analysis. AllPrep DNA/RNA Mini Kit (Qiagen) was used for RNA and DNA isolation processes. After removing the supernatant, each well was washed with PBS. A 300 µl of RNA lysis buffer (RLT+) + β-mercaptoethanol (10 µl/ml) (Sigma-Aldrich) was then added to each well, and the plates were immediately stored in a -80°C until further use. The homogenized lysate was mixed well by pipetting and transferred to AllPrep DNA/RNA spin column in a 2 ml collection tube. The spin columns were centrifuged at 10,000 rpm for 30 seconds, and 300 µl of 70% ethanol was then mixed with the flowthrough. The mixture was transferred to the

RNeasy spin column, placed in a 2 ml collection tube, and centrifuged at 10,000 rpm for 15 seconds to bind RNA. The flowthrough was discarded after centrifugation. After that, 350 µl buffer RW1 was added and centrifuged at 10,000 rpm for 15 seconds to wash the spin column membrane. The flowthrough was discarded, and 95 µl of DNase mixture was directly added to the RNeasy spin column membrane and incubated at room temperature for 15 minutes. 350 µl buffer RW1 was added to then the RNeasy spin column and centrifuged at 10,000 rpm for 15 seconds. The flowthrough was discarded, and two washes with RPE to the RNeasy spin column membrane were performed at 10,000 rpm for 15 seconds and 2 minutes, respectively. The flowthrough was discarded, and the RNeasy spin column was placed in a new 2 ml collection tube and centrifuged at 14,000 rpm for 1 minute to eliminate any possible carryover of RPE. The RNeasy spin column was placed then in a new 1.5 ml collection tube, and 30 µl RNase-free water was directly added to the spin column membrane and incubated at room temperature for 5 minutes prior to centrifuging at 10,000 rpm for 1 minute to elute the RNA. The eluted flowthrough was placed back into the spin column and centrifuged again at 10,000 rpm for 1 minute to elute a higher RNA concentration. The RNA samples were immediately stored in a -80°C freezer. The DNA was also extracted from the samples according to the manufacturer's instructions and stored in a -20 freezer until further use.

2.15 Extracellular vesicles (EVs)

2.15.1 Cell culture

To isolate enough EVs for these experiments, iHBECs were cultured in T75 flasks (Thermo Fisher Scientific) rather than well-plates. The cells were cultured in

12 ml of KSFM+ medium, and followed the same culture conditions described previously (Section 2.2.1).

2.15.2 EVs isolation

The cells were treated with CSE (3%), Poly (I:C) (10 µg/ml), and a combination of CSE and Poly (I:C) for 24 hours and incubated in a humidified incubator. The next day, the supernatant was collected in 15 ml Conical Centrifuge tubes and centrifuged at 300xg for 10 minutes, 2000xg for 10 minutes, and 10 000xg for 30 minutes, respectively. The supernatants were immediately stored in a -80°C freezer for 24 hours.

The supernatant was then removed from the 15 mL conical tube and concentrated to 500 µl using Vivaspin 20 centrifugal concentrator (Appendix 7.9) by centrifugation at 2000xg for 2 minutes to pre-clear cell culture supernatant. EVs were then isolated manually by size exclusion chromatography using qEV original 35 columns (Appendix 7.9), which collects EVs ranging from 35 nm to 350 nm. Fractions 1-6 of 0.5 ml were then collected, pooled, and concentrated again using Vivaspin 20 centrifugal concentrator at 2000xg for 2 minutes. EV fractions (approximately 200-300 µl) were then transferred into Eppendorf tubes, covered with parafilm to prevent drying, and immediately stored in a -80°C freezer for analysis.

2.15.3 EVs Nanoparticle tracking analysis (NTA)

Nanoparticle tracking analysis (NTA) is a light-scattering technique used to size and identify EVs rapidly [261]. As previously described, EVs for NTA analysis were isolated using size exclusion chromatography (Section 2.15.2).
NTA was performed using a ZataView® Particle Tracking Analyzer (Appendix 7.9) with the technical help of Miss Mariana Rodrigues at the Biodiscovery Institute at the

University of Nottingham. All the instrument's instructions were followed accordingly. Prior to analysis, a dilution of 1:100,000 and 1:250,000 in particle-free water of alignment suspension polystyrene beads was used to test the instrument's sensitivity. 100 µl of EV samples were then diluted to a final volume of 2 ml in PBS. For each measurement, three cycles were performed by scanning 11 positions. The particle drifts were checked, and a high-resolution video was selected under the following settings: 30 frames per position, automatically sensed cell temperature and Scattering Intensity detected automatically. Focus: autofocus; Camera sensitivity for all samples: (80-90); Shutter: 160-257); analysis parameters: Maximum area: 1000, Minimum area 10, Minimum brightness: 30. The data and the distribution of particle size were analyzed by the in-built ZetaView Software (version 8.06.01).

2.15.4 Transmission electron microscopy (TEM)

TEM was carried out with the help of Dr. Kenton Arkill's group at the Biodiscovery Institute at the University of Nottingham. 10 µl of EV samples were used per condition. EVs were fixed by adding 8 µl of 4% formaldehyde (Appendix 7.6) and incubated for 10 minutes. TEM carbon film 200 mesh copper grids (Appendix 7.6) were placed onto fixed EV samples and incubated for 30 minutes in a closed humidity chamber. After incubation, TEM grids were removed using a tweezer, all excess solution was blotted away using filter paper, and TEM grids were positioned upright with their face exposed. EV samples were then washed by placing TEM grids onto double-distilled water (ddH_2o) droplets face down on a parafilm strip for a total of two washes. The EV samples were then stained with 2% filtered uranyl acetate (UA) and incubated for 1 minute. The excess UA solution was blotted away using filter paper, and the TEM grids were air-dried for 10 minutes. TEM was performed using Technai T12 (nmRC) with an accelerating voltage of 100 kV.

2.15.5 Exo-Check™ Exosome Antibody Arrays

The presence of EV markers was assessed using Exo-Check™ Exosome Antibody Arrays kit (Appendix 7.7). 12 pre-printed spots, including eight EV antibodies for known exosome markers including tetraspanin (CD63) and (CD81), Programmed cell death 6 interacting protein (ALIX), Flotillin-1 (FLOT1), Intercellular adhesion molecule 1 (ICAM1), epithelial cell adhesion molecule (EpCam), Annexin A5 (ANXA5), and Tumor susceptibility gene 101 (TSG101) (see Table 2.4), were already embedded in the kit's membrane and all the manufacturer's instructions were followed. Initially, EV proteins were measured using a BCA assay (Section 2.8) 50 µl of the EV samples were lysed by lysis buffer, and the lysate was homogenized by vortexing for 30 seconds. Labelling reagent was added to the lysate, vortexed, and incubated at room temperature for 30 minutes. After incubation, the mixed lysate was combined with 5 mL blocking buffer in a 15 mL conical tube. The exosome membrane was gently removed using forceps and briefly wetted in 5 mL distilled water for 2 minutes. The membrane was placed into a 50 ml Falcon® tube, and a 5 ml labelled exosome lysate/blocking buffer mixture was added to the membrane and incubated overnight at 4°C on the roller. On the next day, the lysate/blocking mixture was removed, and the membrane was washed with a wash buffer provided in the kit for 5 minutes and placed on the roller for a total of 3 washes. Subsequently, a 5 ml Detection Buffer was added to the membrane and incubated at room temperature for 30 minutes on the roller. The membrane was washed 3 times with a wash buffer as previously described. The membrane was then immersed with a developer mixture in a 1:1 ratio for 5 minutes Clarity™ Western ECL substrate (Appendix 7.6) for better detection and visualization for the band of proteins. The membrane was then scanned using Odyssey LI_COR scanner, and the density of EV markers on the

membrane was measured using Image Studio 5.2 software.

Table 2.4 Pre-printed spots for Exosome protein targets.

Location	ID	Protein Name
A1	Positive	Labeled positive control for HRP detection
A2	Blank	Negative control for background
A3	FLOT1	Flotillin-1
A4	ICAM1	Intercellular adhesion molecule 1
A5	ALIX	Programmed cell death 6 interacting protein (PDCD6IP)
A6	CD81	Tetraspanin IGSF8, Immunoglobulin superfamily, member 8
B1	CD63	Tetraspanin CD63, LAMP-3
B2	EpCam	Epithelial cell adhesion molecule; often found in cancer-derived exosomes
B3	ANXA5	Annexin A5
B4	TSG101	Tumor susceptibility gene 101
B5	GM130	Cis-golgi matrix protein – control for cellular contamination in exosome preparation
B6	Positive	Labeled positive control for HRP detection

2.16 Cell proliferation

Cell proliferation of HASMCs was assessed using two methods: the BrdU Cell Proliferation ELISA kit and PrestoBlue™ Cell Viability Reagent.

2.16.1 BrdU Cell Proliferation ELISA Kit

The gold standard method for evaluating cell proliferation is to measure the proportion of cells engaged in DNA synthesis during a specific timeframe [262]. Since the early 1980s, more sensitive and nonradioactive techniques, particularly those using the thymidine analog 5-bromo-2′-deoxyuridine (BrdU), have been developed [263]. BrdU ELISAs have become a widely used assay for assessing cell proliferation. A BrdU Cell Proliferation ELISA Kit (Abcam), was used in this study. All the reagents provided were prepared according to the manufacturer's instructions. Initially, cells were resuspended and seeded at $2x10^4$ cells/ml in an unsupplemented DMEM medium in a 100 µl/well in a 96-well plate. The cells were subsequently incubated overnight in a humidified incubator set to 37°C with 21% O2 and 5% CO2. The cells were then stimulated with 33.33 µl of cfDNA from iHBECs on the top of individual wells and placed in the humidified incubator for 2 hours. This was calculated as the final volume of 1000 µl cfDNA generated from iHBECs experiments were carried out in 6 well plates with a surface area of 9.6 cm^2, and the surface area of the HASMC cell-culture plates for the proliferation assay was 0.32 cm^2. Subsequently, 20 µl of BrdU label was added to each well, and the plate was incubated in a humidified incubator for 22 hours. After incubation, the culture medium was removed from the plate wells, and the plate was blotted on an absorbent paper towel. 200 µl/well of fixing solution was added, and the plate was incubated at room temperature for 30 minutes. The fixing solution was removed, and the plate was then blotted dry on an absorbent paper towel. On the next day, the

plate was washed with a wash buffer that was provided with the kit for a total of three washes before adding 100 µl/well anti-BrdU monoclonal Detector Antibody to each well and incubated at room temperature for 1 hour. The plate was washed as previously described, and 100 µl/well Peroxidase Goat Anti-Mouse IgG Conjunction was added to each well and incubated at room temperature for 30 minutes. The plate was then washed as previously described, and a final water wash was performed by flooding the entire plate with distilled water, and the plate was blotted dry on an absorbent paper towel. Subsequently, 100 µl/well of Tetramethylbenzidine (TMB) peroxidase substrate was added to each well and incubated at room temperature for 30 minutes in the dark before stopping the reaction by adding 100 µl/well of stop solution. Measurement of absorbance was performed using a FLUOstar Omega microplate reader (BMG LABTECH) with an optical density reading set at 450 nm of each well.

2.16.2 PrestoBlue™ Cell Viability Reagent

The second method for assessing cell proliferation of HASMCs was performed using PrestoBlue™ Cell Viability Reagent (Appendix 7.7). PrestoBlue® is a cell-permeable resazurin-based solution that functions as a cell viability indicator by quantitatively measuring cell proliferation utilizing the reducing power of living cells. Applying the PrestoBlue® reagent to cells causes the reducing environment of live cells to change color to red and emit fluorescence, which can be quantified using absorbance or fluorescence techniques. Initially, cells were resuspended and seeded at $2x10^4$ cells/ml in an unsupplemented DMEM medium in 100 µl/well in a 96-well plate. The cells were then incubated overnight in a humidified incubator at 37°C with 21% O2 and 5% CO2. The cells were stimulated with 33.33 µl of cfDNA from iHBECs on the top of individual wells and incubated in a humidified incubator at

37°C for 24 hours. After incubation, 11µl PrestoBlue® reagent was added to the top of individual wells and incubated in a humidified incubator at 37°C for 10 minutes. Measurement of fluorescence was performed using a FLUOstar Omega microplate reader (BMG LABTECH) with a dual wavelength of 560/590 nm for each well.

2.17 Cell contraction

HASMC contraction was assessed using a Cell Collagen-based Contraction Assay kit (Appendix 7.7) according to the manufacturer's protocol. Cells were harvested and resuspended in unsupplemented DMEM medium at $2x10^6$ cells/ml. The collagen lattice was prepared by mixing the HASMCs suspension with the cold Collagen Gel Working Solution at 1:4. 0.5 ml of the mixture was then dispensed into individual wells in a 24-well plate and incubated in a humidified incubator at 37°C for 1 hour to allow for collagen polymerization. After incubation, 1 ml of unsupplemented DMEM medium was added to each collagen gel lattice. Subsequently, the cells were incubated for two days in a humidified incubator at 37°C with 21% O_2 and 5% CO_2. After incubation, the collagen gels were gently released from the side of each well of the plate with a sterile spatula, and the circumference size of the collagen gels was captured by EVOS Cell Imaging System (ThermoFisher Scientific). The cells were then stimulated with 197 µl of cfDNA from iHBECs added on the collagen gel lattice for 24 hours. The EVOS Cell Imaging System then captured the circumference size of the collagen gels change. The diameter of gel contraction at zero hours and at 24 hours after the stimulation was measured using ImageJ software, and the difference between the baseline and 24 hours was expressed as a percentage of gel contraction.

2.18 RNA sequencing (RNA-Seq)

2.18.1 Principles

The Deep Seq Core facility, Centre for Genetics and Genomics at the University of Nottingham, performed RNA-Seq methodology steps and RNA-seq data analysis in this thesis. I isolated RNA samples from HASMCs exposed to iHBEC-released cfDNA following iHBEC stimulation with CSE, Poly I:C, or CSE + Poly I:C and handed the samples to Deep Seq for RNA-Seq process. The aim was to determine whether HASMCs gene sets show significantly different expressions in response to iHBEC derived cfDNA generated in response to poly (I:C) and co-stimulation of CSE and poly (I:C).

2.18.2 Samples quality control, library preparation, and sequencing

According to the report of the RNA-Seq data by Deep Seq facility, the Qubit Fluorometer and the Qubit RNA BR Assay Kit (ThermoFisher Scientific) were used to measure the concentration of RNA. QuantSeq 3' mRNA-Seq library prep kit for Illumina (FWD) (Lexogen) was used to generate complementary DNA (cDNA) from 10ng of total RNA for each sample. The Lexogen i7 6nt Index Set (Lexogen) was then used to create indexing sequencing libraries. All samples underwent 17 PCR cycles. The Qubit Fluorometer and the Qubit dsDNA HS Kit (ThermoFisher Scientific) were used to quantify the libraries. The Agilent High Sensitivity D1000 ScreenTape Assay (Agilent) and the Agilent TapeStation 4200 were used to analyze library fragment-length distributions. Libraries were pooled in equimolar proportions, and final library quantification was carried out with the KAPA Library Quantification Kit for Illumina (Roche). The library pool was sequenced on the Element Biosciences

Aviti platform, with an Aviti 2x75 Sequencing Kit - Cloudbreak FS Medium Output (Element Biosciences), generating about 5 million 150bp single-end reads per sample.

2.18.3 Quality Control

All primary bioinformatics analysis of sequence data was carried out using the Lexogen QuantSeq procedure, designed particularly for data obtained by Illumina's QuantSeq 3' mRNA-Seq library prep kits including AVITI. Raw readings were trimmed of Polyadenylation (poly(A)) tails and Illumina NextSeq adapters using Cutadapt during the Lexogen QuantSeq [264]. The STAR aligner was used to align the trimmed reads to the human reference genome (Homo sapiens GRCh38_ensembl_release_107_ERCC_SIRV) [265]. Aligned reads were then passed to 'featureCounts' [266], which classified and counted each alignment against the reference using the proper annotation data. Genes with fewer than ten readings across all samples were removed. Using the annotation data, genes coding for lncRNA, rRNA, and mt_tRNA were excluded from further study.

2.18.4 Differential expression analysis

Differential expression analysis was performed outside of the Lexogen QuantSeq approach to allow for more customized studies. Comparisons were made between the contrasts and assessed using the 'R' package ‘DESeq2’ [267, 268]. Genes with substantial differential expression (adjusted p-value < 0.05) were analysed in each contrast. Log2 fold changes were shrunk using the 'apeglm' method. The extent of clustering of different cell lines and separation of different treatments, was analysed using PCA analyses.

2.18.5 Pathway analysis

Genes showing significant differential expression (adjusted $p < 0.05$) with a baseMean value of > 50 and log2FoldChange of +/- > 0.5 were selected for Gene Ontology (GO) analysis. The 'enrichGO' function of the R package 'clusterProfiler' [269, 270], was used to assign enrichment GO categories to each collection of genes, with annotations from the R package 'org.Hs.eg.db' as the annotation source [271]. Cellular component sub-ontologies, biological processes, and molecular functions were calculated for each set. Gene lists also underwent a Kyoto Encyclopedia of Genes and Genomes (KEGG) enrichment analysis, again using ‘clusterProfiler’.

2.19 Statistical analysis

Besides the RNAseq analysis described above, all the data were analysed using GraphPad Prism 10.3 software. Data were expressed as mean ± standard error of the mean (SEM) from repeated experiments or from experiments conducted in the specified number of cell lines. An unpaired Student's t-test was used to compare two data sets. A one-way analysis of variance (ANOVA) followed by Dunnett’s multiple comparisons test was used to determine whether the differences between the control and the treated cells were significant. Results with p-values under 0.05 were considered statistically significant.

Chapter 3. Effect of cigarette smoke extract on house dust mite (*Der P1*) inflammatory responses in human bronchial epithelial cells

3.1 Introduction

As previously described in section 1.4, airway inflammation is a primary characteristic of asthma, and the endotypes of asthma are classified into two main types based of inflammatory profiles, namely Type 2-high allergic asthma (T2-high) and non-Type 2 asthma (Non-T2) [272]. Cigarette smoke combined with asthmatic inflammation may induce important changes in the asthma endotype with a predominance of activated macrophages and increased neutrophils in the airway [136]. In addition, cigarette smoke may contribute to lung inflammation by upregulating COX-2 expression in the airways [167]. An expanding body of evidence indicates that the majority of asthmatic smokers have non-eosinophilic endotypes in the airway compared with asthmatic non-smokers who have largely eosinophilic-driven inflammation [138, 273]. Crucially, asthmatic smokers have poor responses to inhaled steroids, the primary anti-inflammatory treatment for asthma management [274].

HBECs are the first line of defence against inhaled insults, including cigarette smoke, viruses, and allergens such as HDM, and are an important source of a group of cytokines termed alarmins. Alarmins, including IL-25, IL-33, and TSLP, promote innate immune responses, which lead to the downstream production of T2-high inflammatory responses that are characterized by inducing the production of Th2 cytokines, including IL-4, IL-5, and IL-13, and eosinophilic inflammation [214].

HDM is one of the main sources of persistent allergens and an essential contributor to allergic rhinitis and allergic asthma [275]. An expanding body of evidence indicates that HDM is one of the most common allergens in asthma pathogenesis leading to exacerbation and poorly controlled asthma [276-278]. Continued exposure to HDM is associated with chronic eosinophilic airway

inflammation, bronchial hyperresponsiveness, and tissue remodeling, all considered hallmarks of allergic asthma [75]. HDM particles can induce sensitization, and mite proteases have direct effects on epithelial cells, including the stimulation of protease-activated receptors, which leads to epithelial dysfunction and release of cytokines [277]. The epithelium is important as an orchestrator of immune responses in asthma, acting as a barrier against environmental stimulants such as HDM allergens through crosstalk with immune cells to maintain homeostasis and activation of innate and adaptive immunity against allergens [98].

Evidence suggests that increased non-T2 inflammation among asthmatic patients positively correlates with increased neutrophilic chemoattractant IL-8 [279]. CSE can induce the production of IL-8 in HBECs [280, 281]. In addition, our group has reported that CSE can modify the inflammatory responses in HASMCs, favouring a switch from steroid-sensitive type 2 high (T2-high) eosinophilic inflammatory responses to steroid-insensitive Type 2 low (Non-T2) neutrophilic inflammatory responses, at least partially via a cyclooxygenase-2 (COX-2)/PGE_2-dependent mechanism (manuscript in preparation) [153].

Several studies have investigated the interaction between CSE and HDM. Short term exposure of HBECs to CSE (20 minutes) increases IL-8 and IL-1beta release, while longer exposure of CSE (1-6 hours) cause damage to epithelial cells [188]. Moreover, combined CSE and HDM leads to a loss of epithelial cell barrier integrity [282]. *In vivo,* CS increased HDM-induced eosinophils and neutrophils of the airway and increased the production of IL-4, IL-5, and IL-13 in BAL fluid of mice [283]. On the contrary, a separate study found that CSE and HDM significantly attenuated eosinophilia in BAL of mice compared to HDM alone treatment while the expression of IL-5, IL-13, and TGF-β had were not affected by CSE [154]. The

studies in the current literature on the interaction between CSE and HDM on the release of inflammatory mediators from HBECs are still limited. Therefore, whether CSE can modify HDM allergen-induced alarmins and T2-high eosinophilic inflammatory responses and promote non-T2 neutrophilic inflammatory responses in HBECs is not fully clear and remains to be explored.

3.2 Hypothesis and Aims

Within this chapter, I hypothesized that CSE modifies HDM allergen-induced T2-high inflammatory responses and promotes non-T2 neutrophilic inflammatory responses in HBECs.

The specific aims for this chapter were:

- To investigate the effect of cigarette smoke extract (CSE) on the expression of alarmins (IL-25, IL-33, TSLP), Th2 cytokines (IL-4, IL-5, IL-13), eosinophilic chemokines (Eotaxin, IP-10, RANTES), non-T2 inflammatory cytokines, including pleiotropic cytokine (IL-6) and the neutrophilic chemokine (IL-8) in iHBECs.
- To assess the effect of HDM allergen (*Der P1)* alone and combined with CSE, on the expression of the above cytokines and chemokines.
- To investigate the potential role of the COX-2 pathway in CSE-induced production of non-T2 neutrophilic inflammatory responses in iHBECs.

3.3 Methods

CSE was generated by bubbling the smoke from two 3R4F research-grade cigarettes into 20 ml of cell culture medium as described in the general methods and materials (section 2.3). A pilot investigation of an extended range of CSE and *Der P1* concentrations was conducted before the optimal concentrations were chosen for the following experiments. Fresh aqueous CSE was prepared on the day of the experiment and used immediately for all experiments.

Cells were distributed into 24-well plates at a density of 41,666 per well. Following seeding, the fresh medium was changed every 48 hours until 90-100% confluence was reached. The cells were then growth-arrested with unsupplemented KSFM medium for 24 hours prior to each experiment. The cells were treated with CSE (3%), *Der P1* (10 µg/ml), and a combination of CSE and *Der P1 for* 24 hours. After collecting the supernatant, 50 µl RIPA buffer (Appendix 7.6) was added to the cells and stored in a -20°C freezer until further use. ELISA (General methods, section 2.9) and Luminex® Discovery Assay (General methods, section 2.10) were used to detect the concentration of the desired cytokines and chemokines in the collected supernatants. COX-2 protein expression was assessed using a Western Blot (section 2.11), with β-actin serving as a loading control to ensure equal loading of samples.

3.4 Results

3.4.1 Effect of CSE and Der P1 on the production of neutrophilic chemokine IL-8 in iHBECs

In this chapter, pilot studies were initially conducted to determine the optimal concentration of CSE and *Der P1* for subsequent experiments. Four CSE concentrations: 2%, 3%, 4%, and 5% (Figure 3.1), and three *Der P1* concentrations: 1 μg/ml, 10 μg/ml, and 25 μg/ml (Figure 3.2), were used. I assessed the effect of different CSE concentrations on the production of neutrophilic chemoattractant IL-8 in iHBECs. IL-8 was basally produced by iHBECs (884.2 ± 277.5 pg/mg protein, Figure 3.1). CSE 3% and CSE 4% significantly increased the production of IL-8 (3075 ± 379.1 pg/mg protein, $^{**}P<0.01$, and 2276 ± 145.6 pg/mg protein, $^{*}P<0.05$, respectively, Figure 3.1) compared with control. No decrease in the cell viability was observed when iHBECs were treated with CSE concentration 2% and 3% compared to the control (Figure 3.2). However, a significant reduction was seen with CSE concentration 4% and 5%, ($^{*}P<0.05$ and $^{****}P<0.0001$, respectively, Figure 3.2). CSE 3% was then chosen as the optimal CSE concentration, which showed the highest significance of IL-8 production and had no decreases in the cell viability.

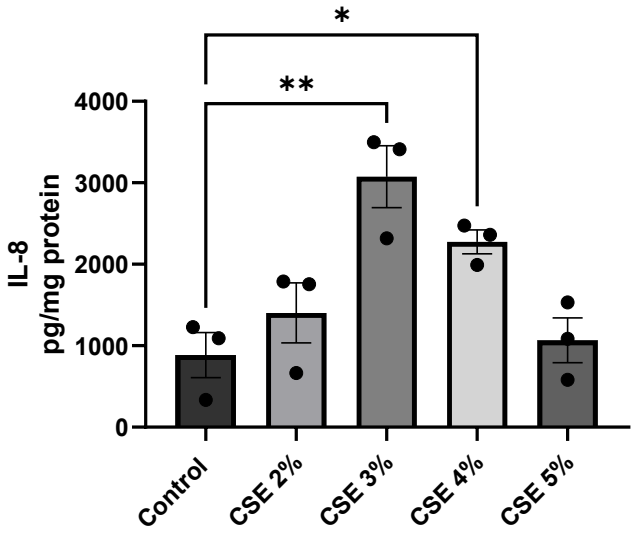

Figure 3.1 Effect of increasing CSE concentrations on IL-8 production

iHBECs were treated with varying concentrations of CSE (0%, 2%, 3%, 4%, and 5%) for 24 hours. The concentration of IL-8 in cell supernatants was measured by ELISA. Data were normalised to total protein and presented as pg/mg protein. Each data point represents mean ± SEM of three independent experiments, each performed with triplicate samples. **P*<0.05 and ***P*<0.01, compared with untreated cells (control).

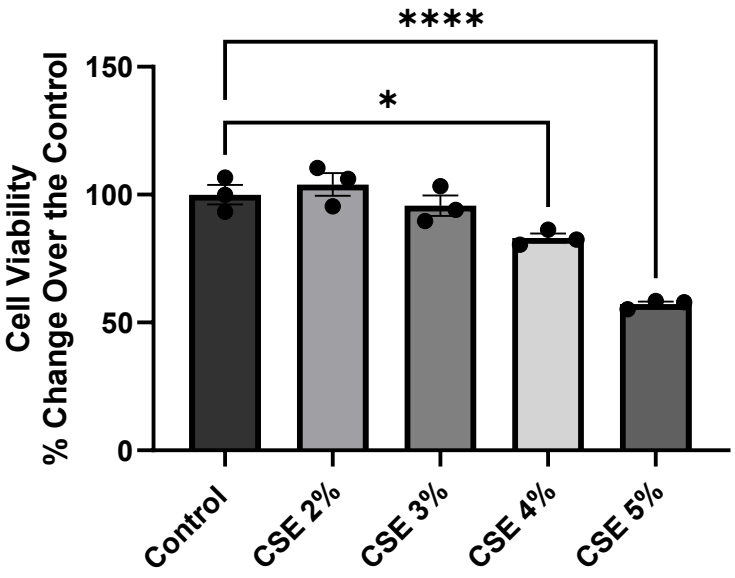

Figure 3.2 Effect of increasing CSE concentrations on cell viability in iHBECs

iHBECs were treated with varying concentrations of CSE (0%, 2%, 3%, 4%, and 5%) for 24 hours. MTT was used to assess the cell viability, and was expressed as % change over the control. Each data point represents mean ± SEM of three individual experiments carried out in triplicate samples. **P*<0.05 and *****P*<0.0001 compared with untreated cells (control).

Having confirmed that 3% CSE induced IL-8 release without significantly affecting iHBEC viability, I next investigated the effect of 3% CSE plus varying *Der P1* concentrations on the production of IL-8 in iHBECs. Confirming previous data (Figure 3.1), IL-8 was basally produced by iHBECs (681.7 ± 148.5 pg/mg protein), and CSE significantly increased IL-8 release (2496 ± 243 pg/mg protein, $^{**}P<0.01$, Figure 3.3) compared with control. Treatment of iHBECs with 10 µg/ml and 25 µg/ml *Der P1* alone significantly increased the production of IL-8 (2510 ± 592.8 pg/mg protein, $^{**}P<0.01$ and 2310 ± 164 pg/mg protein,$^{*}P<0.05$, respectively, Figure 3.3) compared with control. Co-stimulation of iHBECs with 3% CSE and 10µg/ml *Der P1* significantly increased the production of IL-8 (3844 ± 232.5 pg/mg protein, $^{****}P<0.0001$, Figure 3.3) compared with control but had no significant additive effect compared to each individual treatment alone. These results suggest that CSE and *Der P1* can promote (Non-T2) neutrophilic inflammatory responses by inducing the production of neutrophilic chemoattractant IL-8 in iHBECs. Based on these data CSE 3% and *Der P1* 10 µg/ml were used in the following experiments.

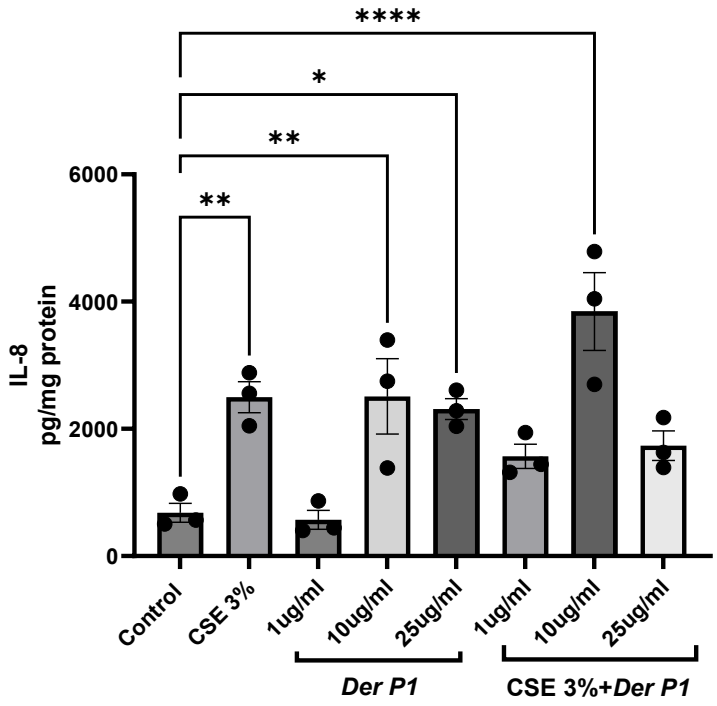

Figure 3.3 Effect of CSE and varying concentrations of Der P1 on IL-8 production

iHBECs were treated with or without CSE (3%), different concentrations of *Der P1* (1 µg/ml, 10 µg/ml, and 25 µg/ml), or CSE + different concentrations of *Der P1* for 24 hours, and the concentration of IL-8 in cell supernatants was measured by ELISA. Data were normalised with total protein and presented as pg/mg protein. Each data point represents mean ± SEM of three individual experiments carried out in triplicate samples. **P*<0.05, ***P*<0.01, and *****P*<0.0001 compared with untreated cells (control).

3.4.2 Effect of CSE and *Der P1* on the production of alarmins in iHBECs

HBECs are well known to play a vital role in airway inflammation, in part through the release of alarmins, including IL-25, IL-33, and TSLP, in response to allergens, which contributes to activating Th2 cytokines and eosinophilic inflammation [284, 285]. I sought to explore the effect of CSE and *Der P1* on the release of alarmins from iHBECs. IL-25 (Figure 3.4 A), IL-33 (Figure 3.4 B), and TSLP (Figure 3.4 C) were basally produced by iHBECs at low levels (169.2 ± 8, 309.5 ± 6.3, 339.2 ± 6.2 pg/mg protein, respectively). CSE, *Der P1*, and CSE+ *Der P1* did not affect the production of IL-25, IL-33, and TSLP. Overall, these results

suggest that combined treatment of iHBECs with CSE and *Der P1* does not alter alarmin production.

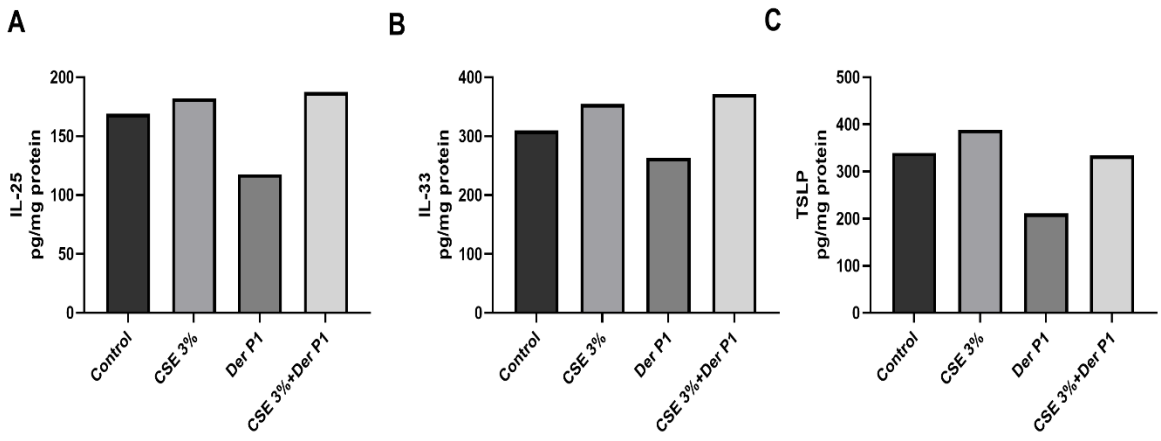

Figure 3.4 Effect of CSE and Der P1 on the production of alarmins

iHBECs were treated with or without CSE (3%), *Der P1* 10µg/ml, or CSE + *Der P1* for 24 hours. The supernatants were collected, and the concentration of **(A)** IL-25, **(B)** IL-33, and **(C)** TSLP were measured by Luminex® Discovery Assay. Data were normalised with total protein and presented as pg/mg protein. Each data point represents the mean of one experiment carried out in triplicate samples.

3.4.3 Effect of CSE and *Der P1* on the production of Th2 cytokines in iHBECs

Type 2 inflammation is mediated by Th2 cells and characterised by the production of Th2 cytokines including IL-4, IL-5, and IL-13 [32]. I assessed the effect of CSE and *Der P1* on the release of Th2 cytokines. IL-4 (Figure 3.5 A), IL-5 (Figure 3.5 B), and IL-13 (Figure 3.5 C) were basally produced by iHBECs at low levels (157.3 ± 5.8, 141.9 ± 6.4, 247.7 ± 8 pg/mg protein, respectively) but CSE, *Der P1*, and CSE+ *Der P1* did not affect their release. Together, these results show that similar to alarmin production, CSE, *Der P1*, and combined treatment of CSE and *Der P1* did not affect the production of Th2 cytokines in iHBECs.

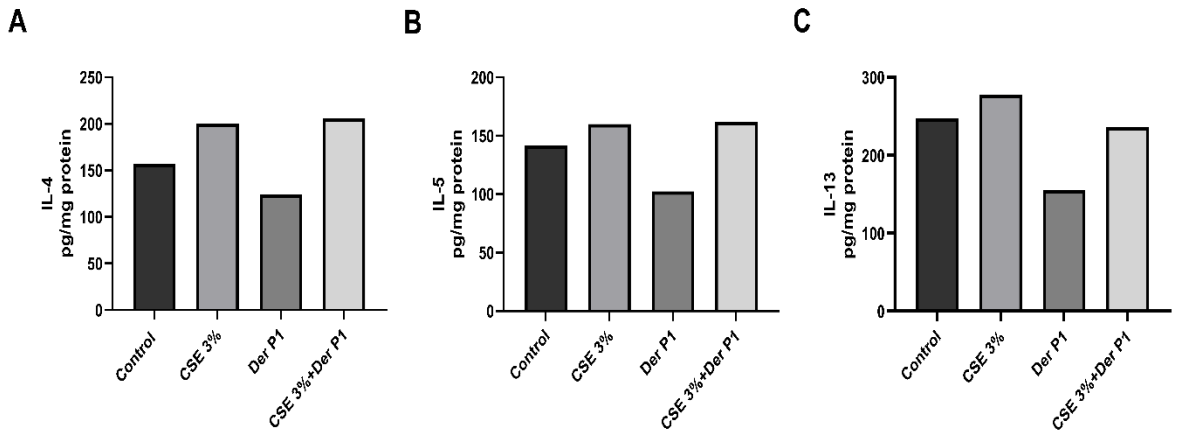

Figure 3.5 Effect of CSE and Der P1 on the production of Th2 cytokines

iHBECs were treated with or without CSE (3%), *Der P1* 10µg/ml, or CSE + *Der P1* for 24 hours. The supernatants were collected, and the concentration of **(A)** IL-4, **(B)** IL-5, and **(C)** IL-13 were measured by Luminex® Discovery Assay. Data were normalised with total protein and presented as pg/mg protein. Each data point represents the mean of one experiment carried out in triplicate samples.

3.4.4 Effect of CSE and *Der P1* on the production of eosinophil chemokines in iHBECs

Chemokines such as eotaxin, IP-10, and RANTES play a vital role in recruiting and activating eosinophils in response to inflammatory stimulation [286]. I sought to assess the effect of CSE and *Der P1* on the release of eosinophil chemokines. Eotaxin (Figure 3.6 A), IP-10 (Figure 3.6 B), and RANTES (Figure 3.6 C) were basally produced by iHBECs at low levels (222.9 ± 9.2, 226.1 ± 5.4, 142.1 ± 8.6 pg/mg protein, respectively) but neither CSE, *Der P1*, nor CSE plus *Der P1* altered the production of eotaxin, IP-10, and RANTES. The data presented here suggests that CSE and *Der P1* do not alter the production of eosinophil chemokines in iHBECs.

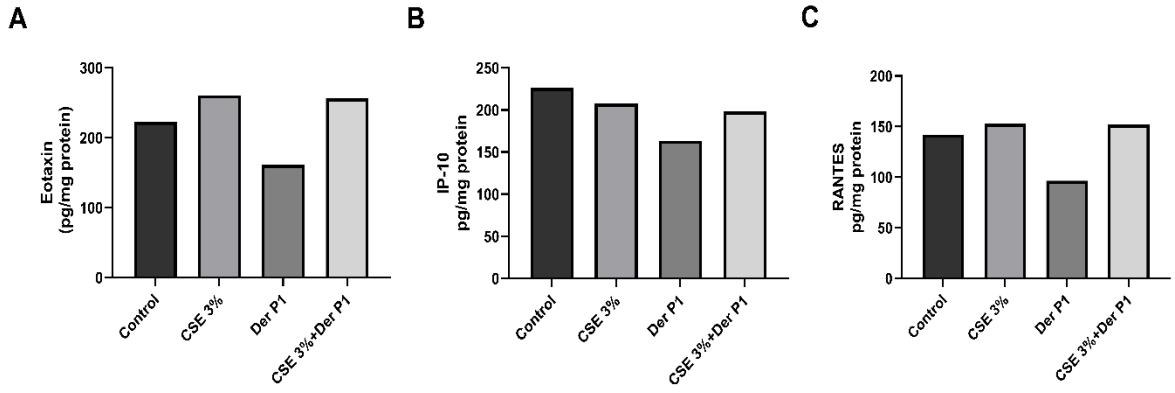

Figure 3.6 Effect of CSE and Der P1 on the production of eosinophil chemokines

iHBECs were treated with or without CSE (3%), *Der P1* 10µg/ml, or CSE + *Der P1* for 24 hours. The supernatants were collected, and the concentration of **(A)** Eotaxin, **(B)** IP-10, and **(C)** RANTES were measured by Luminex® Discovery Assay. Data were normalised with total protein and presented as pg/mg protein. Each data point represents the mean of one experiment carried out in triplicate samples.

3.4.5 Effect of CSE and *Der P1* on the production of non-T2 inflammatory cytokines in iHBECs.

Non-T2 inflammatory cytokines, such as IL-6 and IL-8, are associated with the presence of neutrophilic airway inflammation in respiratory diseases [287, 288] and CSE is known to cause neutrophilic inflammation in asthma [289]. I investigated the effect of CSE and *Der P1* on the release of proinflammatory cytokine IL-6 (Figure 3.7 A). IL-6 was basally produced by iHBECs at low levels of 152.4 ± 3.36 pg/mg protein. CSE and CSE + *Der P1* increased the production of IL-6 (235.6 ± 8.5 and 184.8 ± 8.6 pg/mg protein, respectively). As this result from n=1 experiment, I was unable to perform a statistical significance of the treatment groups compared to the control.

IL-8 was also included in the Luminex® Discovery Assay and mirrored the previous findings of IL-8, which was originally assessed by ELISA (Figure 3.3). IL-8

(Figure 3.7 B) was basally produced by iHBECs (4827 ± 526 pg/mg protein), and CSE, *Der P1,* and CSE + *Der P1* increased the production of IL-8 (14630 ± 262.4, 9727 ± 477.4, and 16866 ± 1536 pg/mg protein, respectively). These results suggest that CSE may promote neutrophilic inflammation in iHBECs by increasing non-T2 inflammatory cytokines, including IL-6 and IL-8.

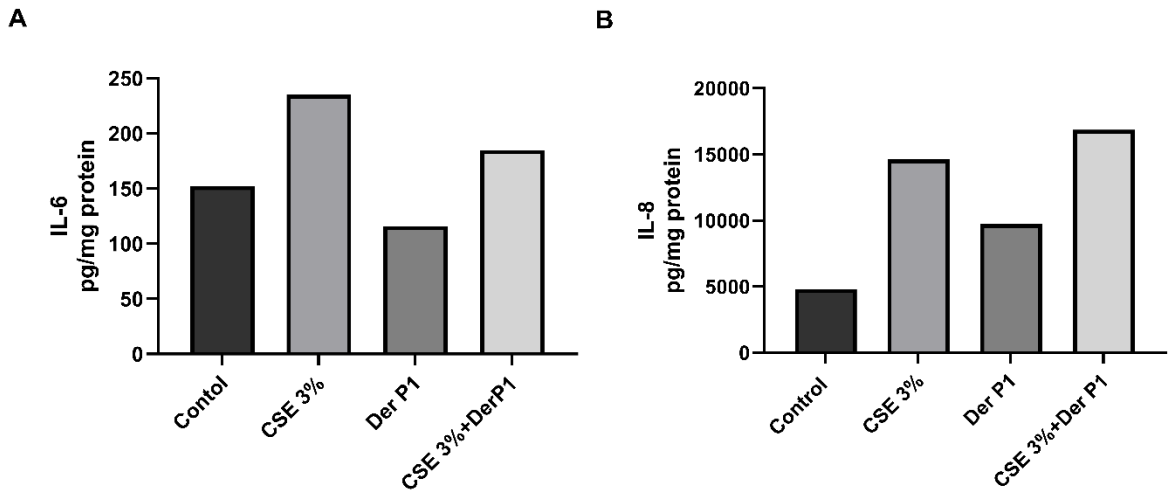

Figure 3.7 Effect of CSE and Der P1 on the production of non-T2 inflammatory cytokines

iHBECs were treated with or without CSE (3%), *Der P1* 10μg/ml, or CSE + *Der P1* for 24 hours. The supernatants were collected, and the concentration of **(A)** IL-6 and **(B)** IL-8 were measured by Luminex® Discovery Assay. Data were normalised with total protein and presented as pg/mg protein. Each data point represents the mean of one experiment carried out in triplicate samples.

3.4.6 More cellular protein was measured in response to DerP1 in iHBECs stimulated with CSE, Der P1, and CSE+Der P1

It was observed from all the data measured by Luminex® Discovery Assay that more cellular protein was measured in response to *Der P1,* which may have affected the results given the manner in which data were normalised to total cell protein. The mean of total cell protein for control, CSE, and CSE + *Der P1* was 1296, 1279, and 1265 µg/ml, respectively, while the mean of total cell protein for *Der P1* was 1987 µg/ml (Figure 3.8). The measurements of the total cell protein were used to control for the differences in the protein concentration between conditions. The results of Luminex® Discovery Assay on the production of all cytokines tested were normalised for the total protein from the same experiment, which show that DerP1 reduces the production of tested cytokines when expressed in pg/ml protein. Nevertheless, there was no interaction between CSE and *Der P1* on the production of the inflammatory mediators assessed. The main findings by Luminex® Discovery Assay of the chapter are summarized in (Figure 3.9).

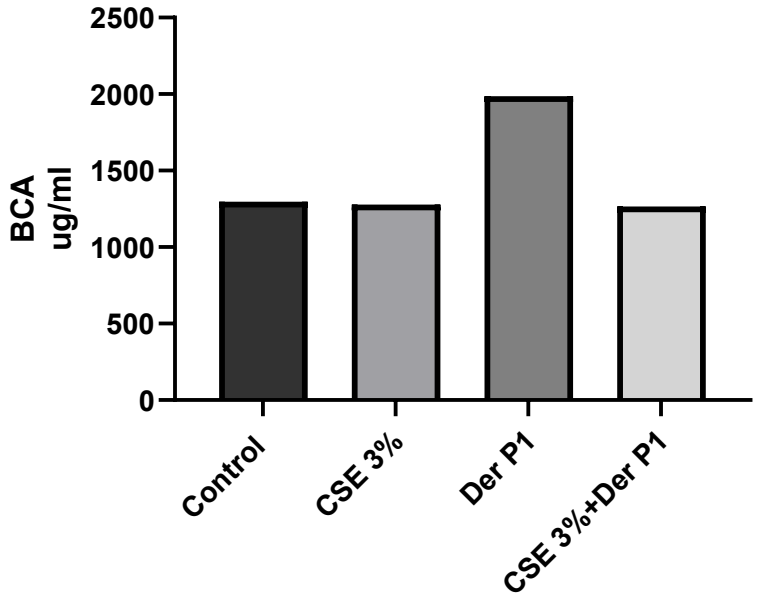

Figure 3.8 Effect of CSE and Der P1 on the total concentration of the protein

iHBECs were treated with or without CSE (3%), *Der P1* 10μg/ml, or CSE + *Der P1* for 24 hours. The supernatants were collected, and the total concentration of the protein was measured using a bicinchoninic acid (BCA) assay kit. Data were presented as μg/ml. Each data point represents the mean of one experiment carried out in triplicate samples.

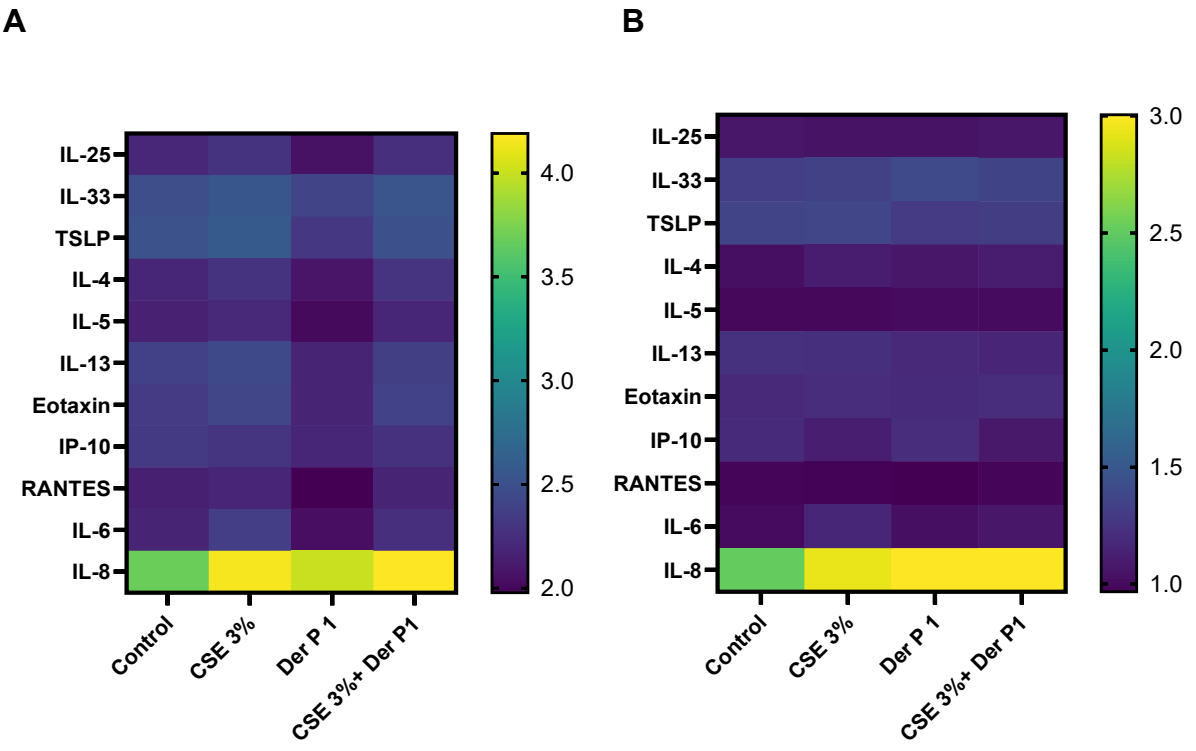

Figure 3.9 Heat map summarized the main findings on the effect of CSE and Der P1 on the expression of alarmins, cytokines, and chemokines

The summary of Luminex® Discovery Assay results data were log-transformed and plotted in heat maps showing the effect of CSE and *Der P1* on the production of alarmins (IL-25, IL-33, and TSLP), Th2 cytokines (IL-4, IL5, and IL-13), eosinophil chemokines (Eotaxin, IP-10, and RANTES), pro-inflammatory cytokine IL-6, and neutrophilic chemokine IL-8 in iHBECs. **A,** After data were normalised with total protein and presented as pg/mg protein. **B,** Data were not normalised with total protein and presented as pg/ml. Each data point represents the mean of one experiment carried out in triplicate samples. Data were $\log_{10}$-transformed, and the heatmap colour intensity reflects the relative expression levels on a $\log_{10}$ scale.

3.4.6 Effect of CSE and *Der P1* on the protein expression of COX-2 in iHBECs.

CSE has been shown to induce COX-2 expression in many cells [290], including HASMCs [291] and HBECs [292]. In this part of the study, it was of interest to assess whether effect of CSE on COX-2 expression in the iHBECs utilised in this thesis. The protein expression of COX-2 was undetectable in iHBECs at the basal level (Figure 3.10 A and B), however, CSE and CSE + *Der P1* significantly induced COX-2 protein expression (fold change 8.38 ± 0.9, ***P<0.001 and 9.25 ± 1.2 ***P<0.001, respectively) over the basal level. These findings of increased COX-2 expression raise the possibility that CSE-induced non-T2 inflammatory cytokines were via COX-2 upregulation.

A

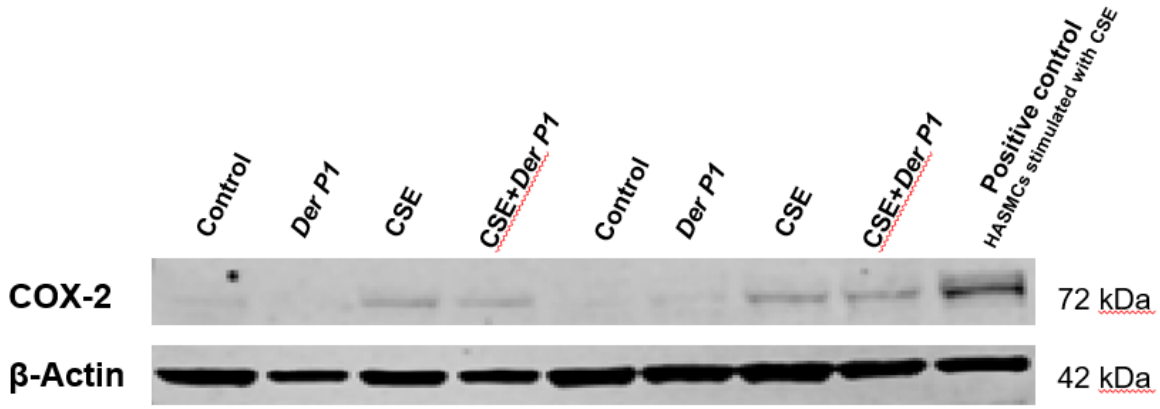

B

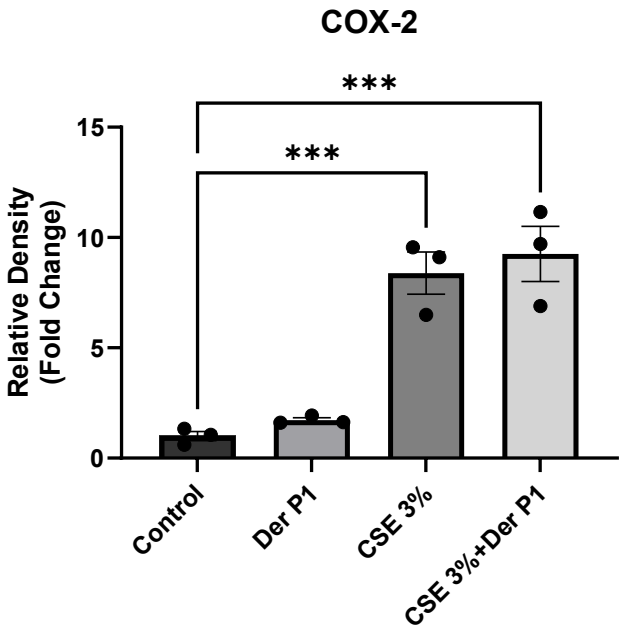

Figure 3.10 Effect of CSE and Der P1 on COX-2 protein expression

iHBECs were treated with or without CSE (3%), *Der P1* 10μg/ml, or CSE + *Der P1* for 24 hours. The collected cell lysates were used to assess COX-2 protein expression by Western Blot analysis. **A**, a representative Western Blot showing two experiments out of the three individual experiments exhibiting the effect of CSE, *Der P1*, and combined CSE+*Der P1* on the protein expression of COX-2. Sample of HASMCs stimulated with CSE was used as a positive control. **B,** a densitometry analysis of Western blotting bands from at least three individual experiments. ****P*<0.001, compared with untreated cells (control).

3.5 Discussion

The main aim of this chapter was to explore the impact of CSE on the expression and production of alarmins, Th2 cytokines, eosinophilic chemokines, and non-T2 cytokines in response to HDM in iHBECs. HBECs are the primary source of alarmins, including IL-25, IL-33, and TSLP [293]. The release of alarmins from HBECs plays a crucial role in orchestrating T2 inflammatory responses by releasing Th2 cytokines such as IL-4, IL-5, and IL-13 to amplify the recruitment of eosinophils [294]. An expanding quantity of evidence indicates that HDM stimulates HBECs to release alarmins [295-297]. Therefore, I sought to use the allergen protease HDM, particularly *Der P1*, as a potent allergen that can exacerbate alarmins and T2 inflammatory responses, and to assess the impact of CSE on the production and release of alarmins, Th2 cytokines, eosinophilic chemokines, and non-T2 cytokines on the effect of *Der P1* in iHBECs. Contrary to my hypothesis, CSE and *Der P1* showed no synergistic or additive effect on the production of alarmins, Th2 cytokines, and eosinophilic chemokines.

Der P1 can induce alarmin production. For example, exposure to HDM increases IL-25, IL-33, and TSLP release from HBECs, which are critical in driving allergic airway inflammation and remodeling [295, 298, 299]. Alarmins act as an upstream activator of T2 high responses driven by Th2 cytokines, including IL-4, IL-5, and IL-13 [300]. Th2 cytokines play essential roles in developing allergic asthma. IL-4 promotes Ig isotype switching in B cells, leading to the production of IgE and IgG [288]. IL-5 is an essential cytokine for eosinophil survival, differentiation, and migration, whereas IL-13 promotes mucus metaplasia and induces airway hyperresponsiveness [288]. Moreover, Th2 cytokines are essential for inducing eosinophilic inflammation and enhancing the production of IgE, resulting in AHR in

asthma [301]. An animal model of allergic airway inflammation found that HDM significantly increased expression of IL-4 and IL-13 following 2 and 8 weeks of exposure to HDM [302]. The same study also found that the expression of eotaxin-1 showed progressively increased expression with more prolonged exposure to HDM in 2, 4, and 8 weeks of exposure, while IL-6 showed a significant expression only in 2 weeks of exposure to HDM [302]. Additionally, *Der P1* dose-dependently increases the production of IL-6 and IL-8, and the action of *Der P1* is inhibited by cysteine-protease inhibitors in a human airway-derived epithelial cell line (A549) [303]. It is well known from the literature that continued exposure to HDM is associated with chronic eosinophilic airway inflammation, bronchial hyperresponsiveness, and tissue remodeling, and HDM particles can induce sensitization. Mite proteases have direct effects on epithelial cells, including the stimulation of protease-activated receptors, which leads to epithelial dysfunction and release of cytokines, all considered hallmarks of allergic asthma [75, 277]. Contrary to these findings, our results showed that *Der P1* had no effects on the release of alarmins, Th2 cytokines, eosinophilic chemokines, and pleiotropic cytokine IL-6 in iHBECs. However, *Der P1* signifacntly increased the production of the neutrophilic chemoattractant IL-8 in iHBECs. In support of this finding, *Der P1* stimulation caused a significant elevation in IL-8 production in primary cultured nasal epithelial cells (NECs) but also caused a significant elevation of IL-6, which is in opposition to our findings [304]. The lack of effect of *Der P1* on alarmin and cytokine production in our study may be attributed to several factors, including cell type, exposure duration, and experimental model, as our *in vitro* iHBECs were exposed to purified *Der P1* rather than the full HDM extract.

On the other hand, CSE can cause the release of TSLP from primary HBECs, which is associated with increased oxidative stress [305]. While mice exposed to CS

have significantly reduced IL-4 and IL-5 and eosinophils in BALF [155]. Furthermore, CSE reduces Lipopolysaccharide (LPS)-induced production of eosinophilic chemokine IP-10 in the HBEC line,16-HBE [306]. Similar to the effect of *Der P1* in our study, the results from this investigation showed that CSE had no effects on the release of alarmins, Th2 cytokines, and eosinophilic chemokines but increased the production of IL-6 and IL-8 in iHBECs. In line with our findings, CSE significantly increased the production of IL-6 and IL-8, and the production was further increased when CSE was combined with an air pollutant, particulate matter (PM) in HBECs (BEAS-2B) cell line [307]. Oltmanns et al. also showed that CSE can enhance the production of IL-8 and that TNFα-induced eotaxin and RANTES production was inhibited by CSE in HASMCs [308]. Furthermore, our group also showed that CSE significantly increased the production of IL-8 in HASMCs (manuscript in preparation) [153].

Several studies investigated the interaction between CSE and HDM, showing a synergistic effect on the combination of CSE and HDM in exacerbating airway inflammation leading to increased severity of asthma. The BALF of mice exposed to 3 weeks of HDM and CS exposure displays a significant increase in airway eosinophilia and significant release of IL-25 and IL-33 but not TSLP when HDM and CS were combined compared to sole HDM or CSE exposure [189]. In addition, a combination of CSE and HDM induced IL-33 in a murine model of CSE asthma and caused upregulation of gene expression of IL-33 and IL-13 *in vivo* [309, 310]. *In vivo* CS increases HDM-induced eosinophils and neutrophils of the airway and the production of IL-4, IL-5, and IL-13 in the BAL fluid of mice [283]. Supporting this, an *in vivo* study showed that IL-5 was increased in BAL fluid leading to increase eosinophils in mouse model of allergic asthma exposed to environmental tobacco

smoke (ETS) and HDM [311]. On the contrary, a study found that a combination of CSE and HDM significantly attenuated eosinophilia in BAL of mice compared to HDM alone treatment, while the expression of IL-5, IL-13, and TGF-β were not affected by CSE [154]. The effect of combined CSE and HDM in airway structural cells, particularly HBECs has not been well explored *in vitro*. Therefore, it was of interest to investigate the impact of CSE on the release of alarmins, Th2 cytokines, eosinophilic chemokines, and non-T2 cytokines in iHBECs.

Taking together the findings of this chapter, the results did not align with the original hypothesis and the literature findings, as there was no synergistic effect between CSE and Der P1 on the release of the alarmins, Th2 cytokines, and eosinophilic chemokines, but they increased the production of neutrophilic chemokine IL-8 in our study model. Several reasons could explain the lack of effects of CSE and *Der P1* in our study model. I utilised an immortalised HBEC cell line in these studies, which was generated by a serial introduction of retroviral expression vectors for cyclin-dependent kinase 4 (CDK4) gene and human telomerase reverse transcriptase (hTERT) [256]. iHBECs have many normal features of primary airway epithelial cells, including inflammatory responses and the ability to differentiate. However, these cells are still limited by the genetic manipulations that give them immortality, but are more relevant than other HBEC cell lines, particularly once of cancerous lineage, that often have an abnormal number of chromosomes [256]. Different cell lines can exhibit varied responses to treatments. For example, A549 and BEAS-2B cells differ in their expression of proinflammatory cytokines and interferons following stimulation with recombinant RSV [312]. iHBECs were selected for the experiments in this study due to their ease of culture and the fact that they

have been shown to exhibit phenotypic similarities with primary HBECs [256], and it was aimed to confirm the findings on the primary cells.

The composition of HDM could be another potential reason for the observed different responses between this study and other published studies. HDM is a complex of constituents that include proteases belonging to the cysteine protease family, such as *Dermatophagoides pteronyssinus1* (*Der P1*), and serine protease family, such as *Der P3, 6*, and *9* [175]. Different HDM extracts vary extensively in their effect on airway inflammation and remodeling, as well as the release of cytokines in normal HBECs,16HBE cell lines, and in a mouse model [313]. *Der P1* is a major allergen in allergic airway inflammation and was the focus of this study. However, its effects are regulated by protease activity, cell variability, concentration, and exposure time. HDM extracts showed marked variation in their biochemical profiles and triggered diverse responses in vitro and in vivo [313]. The observed variability in the biochemical properties and corresponding responses of HDM extracts may, in part, arise from factors such as incorrect protein folding or differences in the preparation of major allergens like *Der P1*. Employing a cocktail or 'matrix' of HDM allergens could provide a more standardized and robust stimulus in experimental models. A study of A549 and BEAS-2B cell lines found that the effect of *Der P1* on protease inhibitors can vary depending on treatment duration and the presence or absence of Th2 cytokines [314]. Therefore, mitigation strategies of this variance by controlling protease-independent effects and using chronic exposure models could be a potential way to address the variability on *Der P1* effects. Furthermore, as a lack of protease function could potentially explain the absence of cytokine responses observed in this study, the significant increase in IL-8 production following *Der P1* stimulation suggests that the allergen retained some functionality.

COX-2 expression is increased in response to inflammatory stimuli, including CSE, and is important in asthma pathogenesis due to its role in promoting airway inflammation through the production of pro-inflammatory prostaglandins [290]. CSE induces COX-2 expression in airway cells via different mechanisms [315, 316]. Zhang et al. reported that CSE induced the production of IL-6 and TNF-α, and increased the protein expression level of COX-2 and in HBECs 16HBE cell line [292]. They also reported that CSE-mediated an increase in oxidative stress, and the use of oxidative stress inhibitor (FAPB4) blocked the effect, which may suggest that oxidative stress may mediate COX-2 expression induced by CSE in HBECs [292]. Additionally, our group has previously demonstrated that CSE alters Th2 cytokines production in HASMCs through a COX-2/PGE_2/EP_2/EP_4 pathway via oxidative stress (manuscript in preparation) [153]. Supporting these previous studies, here I show that CSE increased COX-2 protein expression, raising the possibility that CSE-induced non-T2 inflammatory cytokines in iHBECs were via COX2 upregulation.

In conclusion, there was no interaction between CSE and *Der P1* expression on the production of alarmins (IL-25, IL-33, TSLP), Th2 cytokines (IL-4, IL-5, IL-13), eosinophilic chemokines (Eotaxin, IP-10, RANTES). However, CSE significantly increased the production of IL-8, which might suggest that CSE may promote neutrophilic inflammation in iHBECs by increasing non-T2 inflammatory cytokines, and the effect of CSE on the production of non-T2 inflammation might be mediated by COX-2 expression. In the next chapter, I will assess the effect of CSE on the inflammatory responses from iHBECs in response to viral infection.

Chapter 4. Effect of cigarette smoke extract on viral responses in human bronchial epithelial cells

4.1 Introduction

In addition to investigating HDM, this thesis also aimed to assess the effect of CSE on the inflammatory responses of iHBECs in response to viral infection using the viral mimic Polyinosinic:polycytidylic acid **(**poly (I:C)). Viral respiratory infections are a major trigger of asthma and the most common cause of asthma exacerbation in children and adults [194, 317]. Pathological changes related to viral infections in asthma are generally characterised by increased virus replication and altered innate immune responses, with augmented Th2 cytokine responses leading to heightened inflammation and more severe asthma exacerbation [193, 318]. HBECs are the first line of defence against viruses and are capable of mounting innate immune and other biological responses [319]. In this study, I used the viral mimic Poly (I:C) to study the effect of CSE on viral responses in iHBECs. Poly (I:C) is a synthetic double-stranded RNA (dsRNA) that mimics viral RNA, which induces inflammatory responses in the cells [320]. Poly (I:C) can modulate the responses of HBECs by enhancing the release of cytokines such as IL-6, IL-8, TNFα and TSLP [321], and upregulate the expression of anti-viral genes such as IFN-α [322].

An expanding body of evidence indicates that cigarette smoke increases susceptibility to viral infection [323-325]. Nasal epithelial cells from smokers express more TSLP than cells from non-smokers in response to influenza infection [326]. Cigarette smoke decreases innate immune responses and cytokine production of HBECs to viral infection. Eddleston et al. found that CSE altered the responses of HBECs (BEAS-2B) to HRV infection, leading to the suppression of RANTES and IP-10 production [213]. In addition, CS exposure-induced disruption of epithelial barrier function was enhanced by challenge with poly (I:C) or infection with influenza H1N1 in a mouse model [327]. *In vivo*, CS increases IL-33 expression and exacerbates the

effect of viral infection [328]. Collectively, these findings suggest that cigarette smoke may influence immune responses to viral infections. While existing literature demonstrates that CSE can modulate immune function, it remains unclear whether such modulation contributes to inflammatory endotype switching in asthma.

Cell-free DNA (cfDNA), a small extracellular fragment, refers to all non-encapsulated DNA in the bloodstream or other fluids that occurs via active secretion from the cells and during normal apoptotic and necrotic processes. The concentration of cfDNA is associated with the extent of tissue damage and/or inflammation in various pathologies [329]. Extracellular vesicles (EVs) play a crucial role in carrying cfDNA, and a large proportion of cfDNA in human blood plasma is found within EVs [330]. Airway structural and immune cells secrete EVs containing cfDNA, along with various lipids, proteins, and nucleic acids, that can alter normal airway function and initiate respiratory disease processes [331-333]. The discovery of cell-free DNA (cfDNA) as a biologically active molecule that can enhance oxidative stress, promote proinflammatory cytokine synthesis, and activate signalling pathways in various cell types has led to its characterization as a signalling molecule in disease processes [334-336]. The lung epithelium releases cfDNA into bronchoalveolar lavage (BAL) fluid during normal cell turnover, and lung-specific cfDNA is increased in various lung diseases, including exacerbated COPD, compared to stable COPD [238], following viral infection [244, 337], and in response to smoke inhalation injury [241], Crucially, *in vitro* CSE activates innate immune responses and significantly increases the release of cfDNA into the culture medium from human endothelial cells, as quantified by qPCR [242].

As HBECs play a central role in viral-induced asthma pathogenesis through the release of alarmins that can activate type 2 immune responses, the impact of

CSE on viral infection in the context of releasing alarmins and other inflammatory mediators, and the release of cfDNA from HBECs is still limited. and requires further investigation.

4.2 Hypothesis and Aims

Within this chapter, I hypothesized that CSE modulates the inflammatory responses of iHBECs to poly (I:C) and causes enhanced release of cfDNA.

The specific aims for this chapter were:

- To understand how combined CSE and poly (I:C) affects the release of alarmins, (IL-25, IL-33, and TSLP), Th2 cytokines (IL-4, IL-5, and IL-13), eosinophilic chemokines (Eotaxin, IP-10, and RANTES), pleiotropic cytokine IL-6, and neutrophilic chemokine IL-8 from iHBECs.
- To investigate the potential role of oxidative stress in CSE-mediated effects on inflammatory cytokine and alarmin production by applying the oxidative stress inhibitor GSH.
- To determine whether CSE, poly (I:C) and CSE + poly (I:C) cause the release of cfDNA from iHBECs.
- To assess whether cfDNA released in response to CSE and poly (I:C) is found within EVs.

4.2 Methods

CSE was generated by bubbling the smoke of two cigarettes (3R4F) into 20 ml of cell culture medium as described in the general methods and materials (Section 2.3). Cells were distributed into 24-well plates at a density of 41,666 per well. Following the seeding, the medium was changed every 48 hours until 90-100% confluence was reached. The cells were then growth-arrested with unsupplemented KSFM medium for 24 hours prior to each experiment. To explore the effect of CSE and poly (I:C), iHBECs were treated with and without CSE (3%) and/or Poly(I:C) 10 µg/ml for 24 hours. The supernatant was then collected, and 50 µl cell lysis (RIPA) buffer (Appendix 7.6) was added to the cells and stored in a -20°C freezer until further use. To assess the role of oxidative stress on the effect of CSE and Poly (I:C), growth arrested iHBECs were treated as above but with or without antioxidant GSH (100 µM) for 1 hour before incubation with CSE and Poly(I:C) for 24 hours. ELISA and Luminex® Discovery Assay were used to detect the concentration of the desired cytokines and chemokines in the collected supernatants. Quantitative real-time PCR for telomerase reverse transcript (TERT) and TapeStation were used to investigate the concentration of cfDNA released (general methods and materials, section 2.13).

To assess the effect of CSE and poly (I:C) on the release of EVs, iHBECs were cultured in T75 flasks. The cells were treated with and without CSE (3%) and/or Poly(I:C) 10 µg/ml for 24 hours and followed the same culture conditions as in well plates. The supernatant was collected and centrifuged at 300xg for 10 minutes, 2000xg for 10 minutes, and 10,000xg for 30 minutes, sequentially. The supernatants were immediately stored in a -80°C freezer until further use. EVs were isolated manually by size exclusion chromatography using qEV original 35 columns and

concentrated using Vivaspin 20 centrifugal concentrator. Nanoparticle tracking analysis (NTA) and transmission electron microscopy (TEM) were used to characterize and visualize EVs in the samples. The presence of EV markers was assessed using Exo-Check™ Exosome Antibody Arrays kit. Detailed EVs methodology was previously explained in general methods and materials (section 2.15).

4.4 Results

4.4.1 Effect of CSE and poly (I:C) on the total protein concentration and cell viability in iHBECs

As previously reported in Chapter 3, CSE 3% was chosen in the experimental models of this thesis because it was the highest concentration that showed no toxicity on the iHBECs. In this chapter, poly (I:C) 10 µg/ml was chosen based on studies from the literature as a viral mimic to assess the impact of CSE on viral responses in iHBECs [338, 339]. I initially assessed the effect of CSE 3%, poly (I:C) 10 µg/ml, and a combination of CSE and poly (I:C) on the total cell protein concentration and evaluated the cytotoxicity of these stimulants on iHBECs to ensured that observed effects were not due to cell death or compromised viability. Cells were stimulated with or without CSE 3%, poly (I:C) 10 µg/ml or CSE+poly (I:C) for 24 hours. The results showed that all conditions caused the release of similar amount of protein in the region of 1200 µg/ml, indicating that there was no significant difference between untreated and treated cells on the total protein concentration (Figure 4.2 A). Cell viability was then assessed by MTT (General methods, section 2.2.4). There was no decrease in cell viability when iHBECs were treated with CSE,

poly (I:C) and a combination of CSE + poly (I:C) compared with control (Figure 4.2 B). However, a stimulation of CSE 3% alone showed an 8.2% increase in viability compared with control (*P<0.05), indicating a small but statistically significant increase. CSE 3% and poly (I:C) 10 µg/ml were then used for further experiments in this chapter.

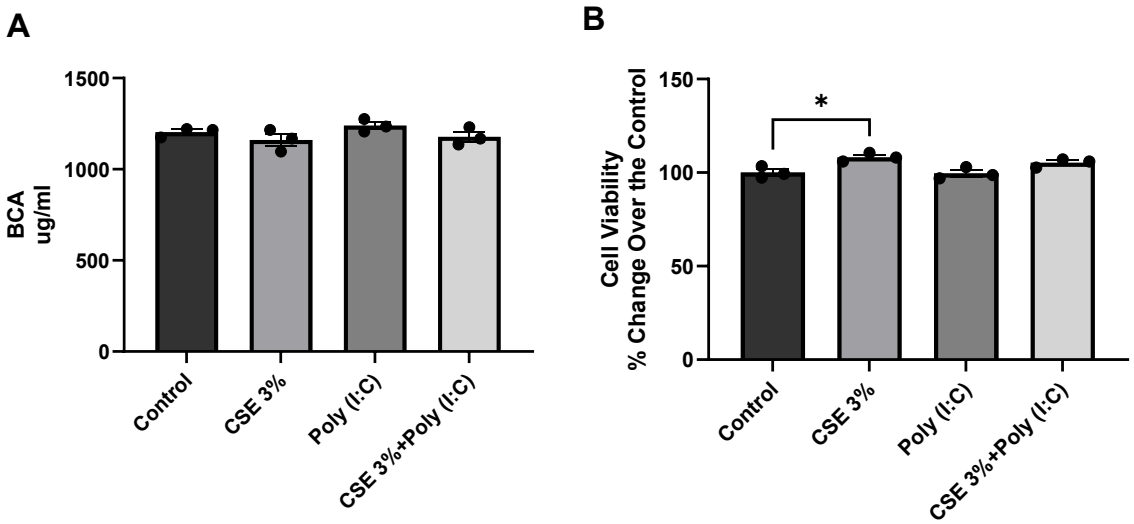

Figure 4.1 **Effect of CSE and poly (I:C) on the total protein concentration and cell viability in iHBECs**

iHBECs were treated with or without CSE (3%), poly (I:C) (10 µg/ml), or CSE + poly (I:C) for 24 hours. (**A)** BCA assay was used to measure the total protein concentration. (**B)** MTT was used to assess the cell viability and was expressed as % change over the control. Each data point represents mean ± SEM of three individual experiments carried out in triplicate samples. *P<0.05 compared with untreated cells (control).

4.4.2 Effect of CSE and poly (I:C) on the production of neutrophilic chemokine IL-8 in iHBECs

In order to understand the impact of CSE on virus-induced neutrophilic inflammation, I next explored the effect of CSE and poly (I:C) on the neutrophilic chemoattractant IL-8 production at 24 and 48 hours. IL-8 was basally produced by iHBECs at 24 and 48 hours (442.3 ± 27.55 and 468.6 ± 24.39 pg/mg protein, respectively) (Figure 4.2). As shown in Chapter 3 (Section 3.4.1), CSE significantly increased the production of IL-8 at 24 and 48 hours (2104 ± 86.11 and 5867 ± 461 pg/mg protein, *P<0.05, respectively) (Figure 4.2A) compared with the control. Stimulation with poly (I:C) also caused a significant increase in IL-8 production at 24 and 48 hours (5473 ± 244.3 and 44096 ± 896.1 pg/mg protein, ****P<0.0001, respectively) (Figure 4.2A and B) compared with control. Interestingly, a synergistic effect was observed when cells were stimulated with CSE and poly (I:C) in combination at 24 hours' time point (6251 ± 623.9 pg/mg protein, ***p<0.001) compared to poly (I:C) alone, while CSE inhibited poly (I:C)-induced production of IL-8 by 40% (**p<0.01) compared with poly (I:C) alone at 48 hours. These findings suggest that both CSE and poly (I:C) can induce the neutrophilic chemoattractant IL-8 production in iHBECs at different time points of 24 and 48 hours, and the combination of CSE and poly (I:C) suggests a potential synergistic effect between the CSE and poly (I:C) at an early exposure on the inflammatory response. However, a time-dependent regulatory role of CSE on IL-8 production and large production of IL-8 after stimulation with poly (I:C) at a later exposure (48 hours) might explain the inhibitory effect of CSE on poly (I:C)-induced the production of IL-8.

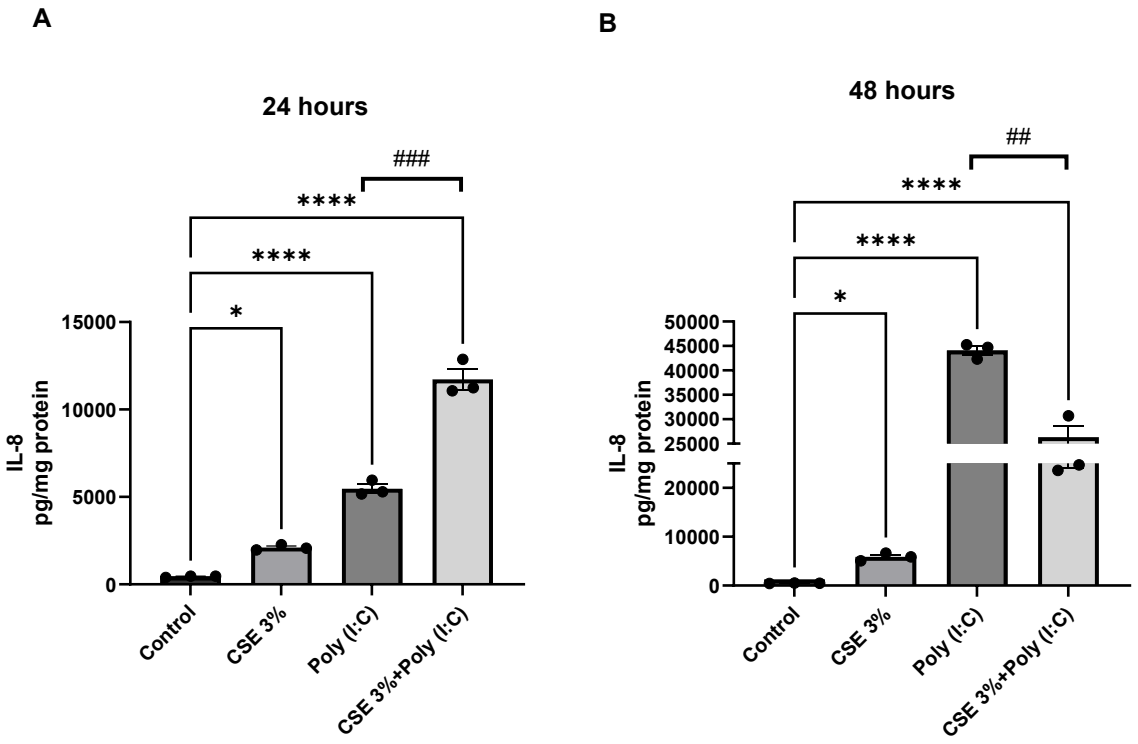

Figure 4.2 Effect of CSE and poly (I:C) on IL-8 production

iHBECs were treated with or without CSE (3%), poly (I:C) (10 µg/ml), or CSE + poly (I:C) for 24 and 48 hours. The concentration of IL-8 for **(A)** 24 hours and **(B)** 48 hours in cell supernatants was measured by ELISA. Data were normalised with total protein and presented as pg/mg protein. Each data point represents mean ± SEM of three individual experiments carried out in triplicate samples. **P*<0.05 and *****P*<0.0001 compared with untreated cells (control), ##*p*<0.01 and ###*P*<0.001 compared with poly (I:C) alone.

4.4.3 Effect of CSE and poly (I:C) on the production of alarmins in iHBECs

HBECs release alarmins, including IL-25, IL-33, and TSLP, in response to viral infection to maintain tissue immunity [340, 341]. The impact of CSE on viral-induced alarmins in HBECs has not been widely investigated. Therefore, I investigated the effect of CSE and poly (I:C) on the production of IL-25, IL-33, and TSLP in iHBECs. iHBECs basally produced low levels of IL-25 at 24 hours (155.2 ± 1.74 pg/mg protein, Figure 4.3 A) and at 48 hours (170.3 ± 5.8 pg/mg protein, Figure

4.3 B), IL-33 at 24 hours (311.6 ± 4.9 pg/mg protein, Figure 4.3 C) and at 48 hours (324.5 ± 10.72 pg/mg protein, Figure 4.3 D), TSLP at 24 hours (243.2 ± 7.67 pg/mg protein, Figure 4.3 E) and at 48 hours (297.2 ± 6.14 pg/mg protein, Figure 4.3 F). CSE significantly increased IL-25 at 24 hours (188.8 ± 1.7 pg/mg protein, ****p<0.0001) and IL-33 at 48 hours (536 ± 45.16 pg/mg protein, ***p<0.001) without affecting TSLP. Stimulation with poly (I:C) alone significantly increased production of all the alarmins, IL-25 at 24 and 48 hours (250 ± 1.5 pg/mg protein, ****p<0.0001 and 466.9 ± 17.65 pg/mg protein,****p<0.0001, Figure 4.3 A and B), IL-33 at 24 and 48 hours (602.9 ± 70.72 pg/mg protein, **p<0.01 and 1519 ± 18.65 pg/mg protein, ****p<0.0001, Figure 4.3 C and D) and TSLP at 24 and 48 hours (1143 ± 73.86 pg/mg protein, ****p<0.0001 and 1729 ± 137.6 pg/mg protein, ****p<0.0001, Figure 4.3 E and F), compared with untreated cells (control).

Interestingly, poly I:C-induced production of alarmins at 24 and 48 hours was inhibited by CSE. Specifically, IL-25 production was reduced by 26%, ****p<0.0001 at 24 hours and 18%, *P<0.05 at 48 hours (Figure 4.3 A and B), IL-33 production was reduced by 39%, *P<0.05 at 24 hours and 20%, ***p<0.001 at 48 hours (Figure 4.3 C and D), and TSLP production was reduced by 70%, ***p<0.001 at 24 hours and 62%, **p<0.01 at 48 hours (Figure 4.3 E and F), compared with poly (I:C) alone stimulation. These findings showed that CSE inhibits the release of alarmins in response to poly (I:C), which might affect the inflammatory response of iHBECs to viruses by suppressing the production of alarmins.

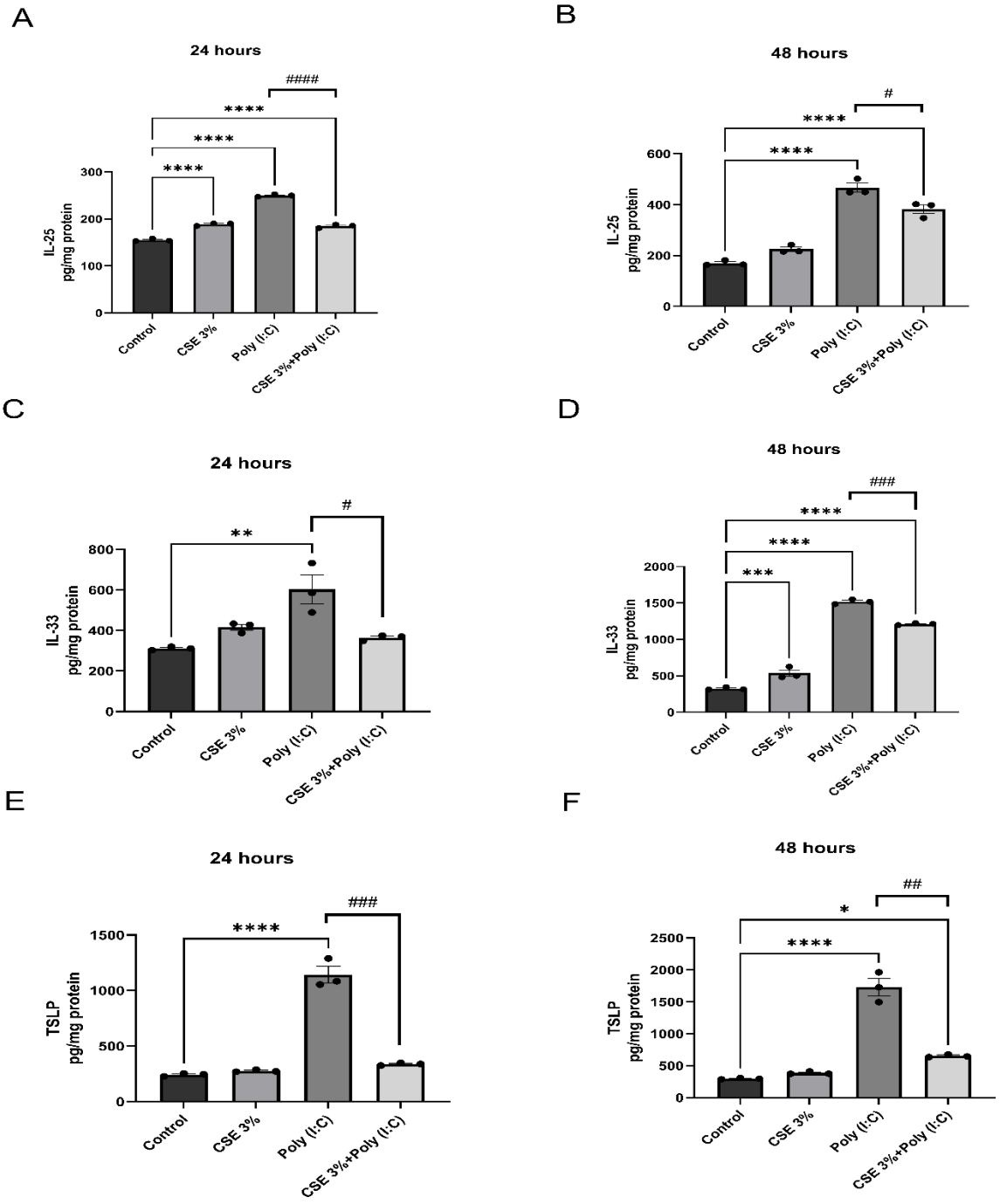

Figure 4.3 Effect of CSE and poly (I:C) on the production of alarmins

iHBECs were treated with or without CSE (3%), poly (I:C) 10µg/ml, or CSE + poly (I:C) for 24 and 48 hours. The supernatants were collected, and the concentration of IL-25 for **(A)** 24 hours, **(B)** 48 hours, IL-33 for **(C)** 24 hours, **(D)** 48 hours, and TSLP for **(E)** 24 hours, **(F)** 48 hours were measured by Luminex® Discovery Assay. Data were normalised with total protein and presented as pg/mg protein. Each data point represents mean ± SEM of three individual experiments carried out in triplicate samples. *p<0.05, **p<0.01, ***p<0.001, and ****p<0.0001 compared with untreated cells (control), and #p<0.05, ##p<0.01, ###p<0.001, and ####p<0.0001 compared with poly (I:C) alone.

4.4.4 Effect of CSE and poly (I:C) on the production of Th2 cytokines in iHBECs

Alarmins such as IL-25, Il-33, and TSLP can promote Th2 cytokine responses by activating innate immune response in HBECs [284]. Therefore, I sought to assess the effect of CSE and poly (I:C) on the production of Th2 cytokines, IL-4, IL-5, and IL-13. iHBECs basally produced IL-4, IL-5, and IL-13 at low levels at 24 and 48 hours. The production of IL-4 at 24 hours (Figure 4.4 A) and 48 hours (Figure 4.4 B) was 92.91 ± 3.15 and 203.9 ±5.28, pg/mg protein, respectively. The production of IL-5 at 24 hours (Figure 4.4 C) and 48 hours (Figure 4.4 D) was 128 ± 2.35 and 388.5 ± 3.6, pg/mg protein, respectively, and the production of IL-13 at 24 hours (Figure 4.4 E) and 48 hours (Figure 4.4 F) was 190 ± 4.7 and 218.8 ± 7.2, pg/mg protein, respectively.

CSE significantly increased the production of IL-4 at 24 hours (121.5 ± 2.29 pg/mg protein, $^{**}p<0.01$, Figure 4.4 A) and at 48 hours (442.9 ± 54.17 pg/mg protein, $^{**}p<0.01$, Figure 4.4 B), IL-5 at 24 hours (152.9 ± 1.4 pg/mg protein, $^{**}p<0.01$, Figure 4.4 C), and IL-13 at 48 hours (302.5 ± 11.26 pg/mg protein, $^{**}p<0.01$, Figure 4.4 F). Poly (I:C) alone significantly increased the production of IL-4 at 24 hours (156.2 ± 2.29 pg/mg protein, $^{****}p<0.0001$, Figure 4.4 A) and 48 hours (1530 ± 21.86 pg/mg protein, $^{****}p<0.0001$, Figure 4.4 B), IL-5 at 48 hours (28382 ± 606 pg/mg protein, $^{****}p<0.0001$, Figure 4.4 D), and IL-13 at 48 hours (528.7 ± 6.13 pg/mg protein, $^{****}p<0.0001$, Figure 4.4 F), compared with control. A synergistic effect was observed in IL-4 at 24 hours when cells were co-stimulated with CSE and poly (I:C) (216.7 ± 7.1 pg/mg protein, $^{****}p<0.0001$, Figure 4.4 A), compared to control, and increased by 27%, compared to poly (I:C) alone ($^{**}p<0.01$, Figure 4.4 A). On the contrary, CSE inhibited poly (I:C)-induced IL-4 at 48 hours by 21%, ($p<0.001$, Figure 4.4 B) and IL-5 at 48 hours by 45%, ($p<0.01$, Figure 4.4 D), compared to poly (I:C)

alone stimulation. There was no significant effect of co-stimulation of CSE and poly (I:C) on IL-13 production observed at either 24 or 48 hours. These findings suggest that CSE may modulate some of the Th2 responses. However, CSE may have dual-phase effects on poly (I:C)-induced Th2 cytokines responses at early and late exposures.

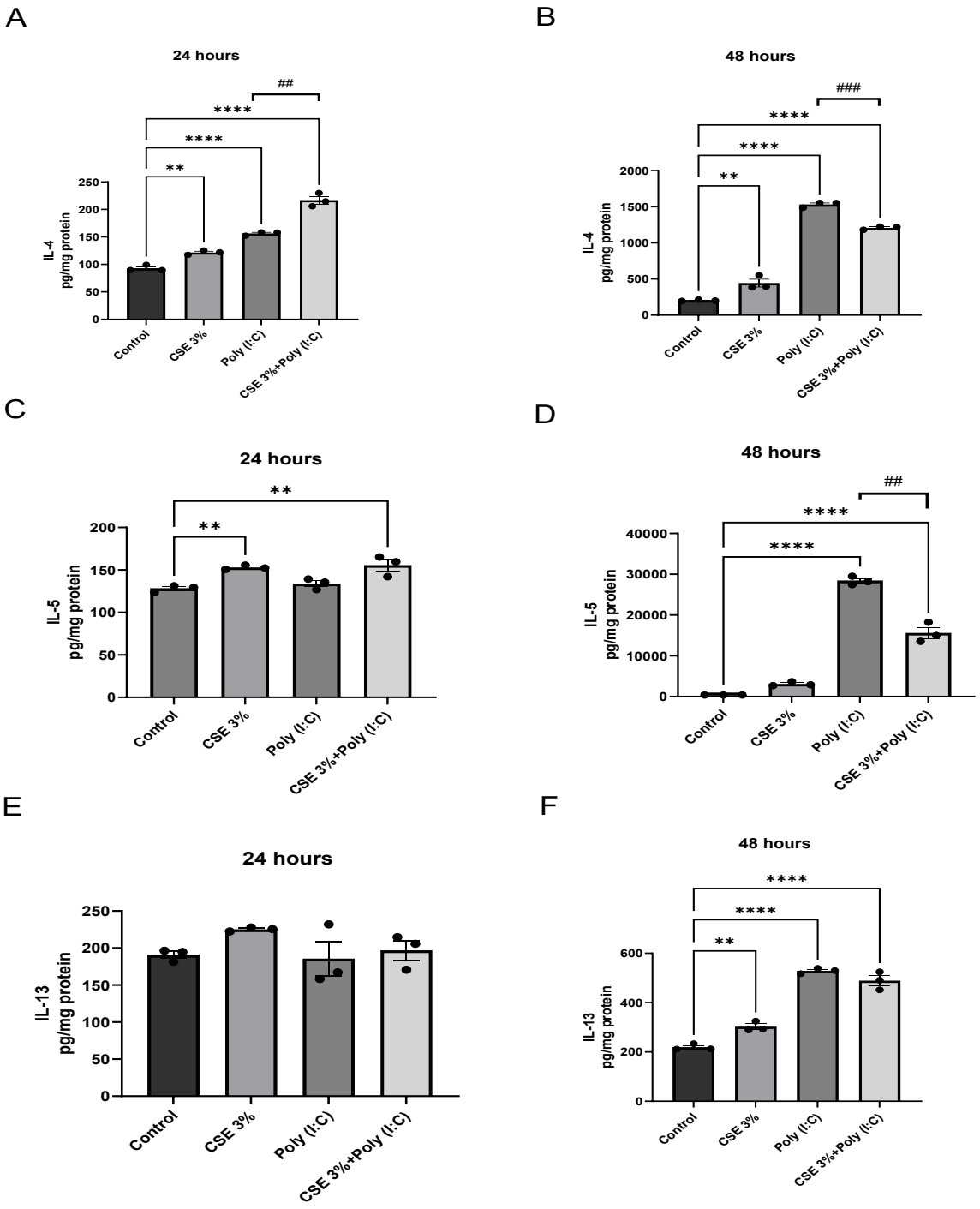

Figure 4.4 Effect of CSE and poly (I:C) on the production of Th2 cytokines

iHBECs were treated with or without CSE (3%), poly (I:C) 10μg/ml, or CSE + poly (I:C) for 24 and 48 hours. The supernatants were collected, and the concentration of IL-4 for **(A)** 24 hours, **(B)** 48 hours, IL-5 for **(C)** 24 hours, **(D)** 48 hours, and IL-13 for **(E)** 24 hours, **(F)** 48 hours were measured by Luminex® Discovery Assay. Data were normalised with total protein and presented as pg/mg protein. Each data point represents mean ± SEM of three individual experiments carried out in triplicate samples. **p<0.01 and ****p<0.0001 compared with untreated cells (control), and ##p<0.01 and ###p<0.001 compared with poly (I:C) alone.

4.4.5 Effect of CSE and poly (I:C) on the production of eosinophil chemokines in iHBECs

To further elucidate the effect of CSE on poly (I:C)-induced production of Th2 mediators, I investigated the effect of CSE and poly (I:C) on eosinophil chemokines, including eotaxin, IP-10, and RANTES. The results revealed that iHBECs produced relatively low levels of eotaxin at 24 and 48 hours (210 ± 2.38 and 242.5 ± 7.23 pg/mg protein, respectively) (Figure 4.5 A and B), IP-10 at 24 and 48 hours (162 ± 4.4 and 207 ± 3.3 pg/mg protein, respectively) (Figure 4.5 C and D), and RANTES at 24 and 48 hours (100.4 ± 2.8 and 143 ± 3.6 pg/mg protein, respectively) (Figure 4.5 E and F). CSE significantly increased eotaxin release at 24 and 48 hours (248.1 ± 9.2 pg/mg protein, $^{**}p<0.01$ and 288.8 ± 7 pg/mg protein, $^{**}p<0.01$, respectively, Figure 4.5 A and B) compared with control, but had no effect on the production of IP-10 (Figure 4.5 C and D) and RANTES (Figure 4.5 E and F). Poly (I:C) significantly increased the production of all tested eosinophil chemokines including eotaxin (273.2 ± 5.7, $^{***}p<0.001$ and 425.4 ± 4.9 pg/mg protein, $^{****}p<0.0001$, respectively at 24 and 48 hours, Figure 4.5 A and B), IP-10 (79000 ± 7327, $^{****}p<0.0001$ and 281661 ± 4109 pg/mg protein, $^{****}p<0.0001$, respectively at 24 and 48 hours, Figure 4.5 C and D), and RANTES (13942 ± 1659, $^{****}p<0.0001$ and 121342 ± 418 pg/mg protein, $^{****}p<0.0001$, respectively at 24 and 48 hours, Figure 4.5 E and F). Interestingly, CSE inhibited Poly (I:C)-induced eotaxin at 24 hours by 15%, $^{**}p<0.01$, (Figure 4.5 A), IP-10 at 24 and 48 hours by 99.7%, $^{****}p<0.0001$ and 99.8%, $^{****}p<0.0001$, respectively (Figure 4.5 C and D), and RANTES at 24 and 48 hours by 78%, $^{**}p<0.01$ and 64%, $^{***}p<0.001$, respectively (Figure 4.5 E and F) compared with poly (I:C) alone stimulation. These findings suggest that CSE suppresses eosinophil chemokines in iHBECs.

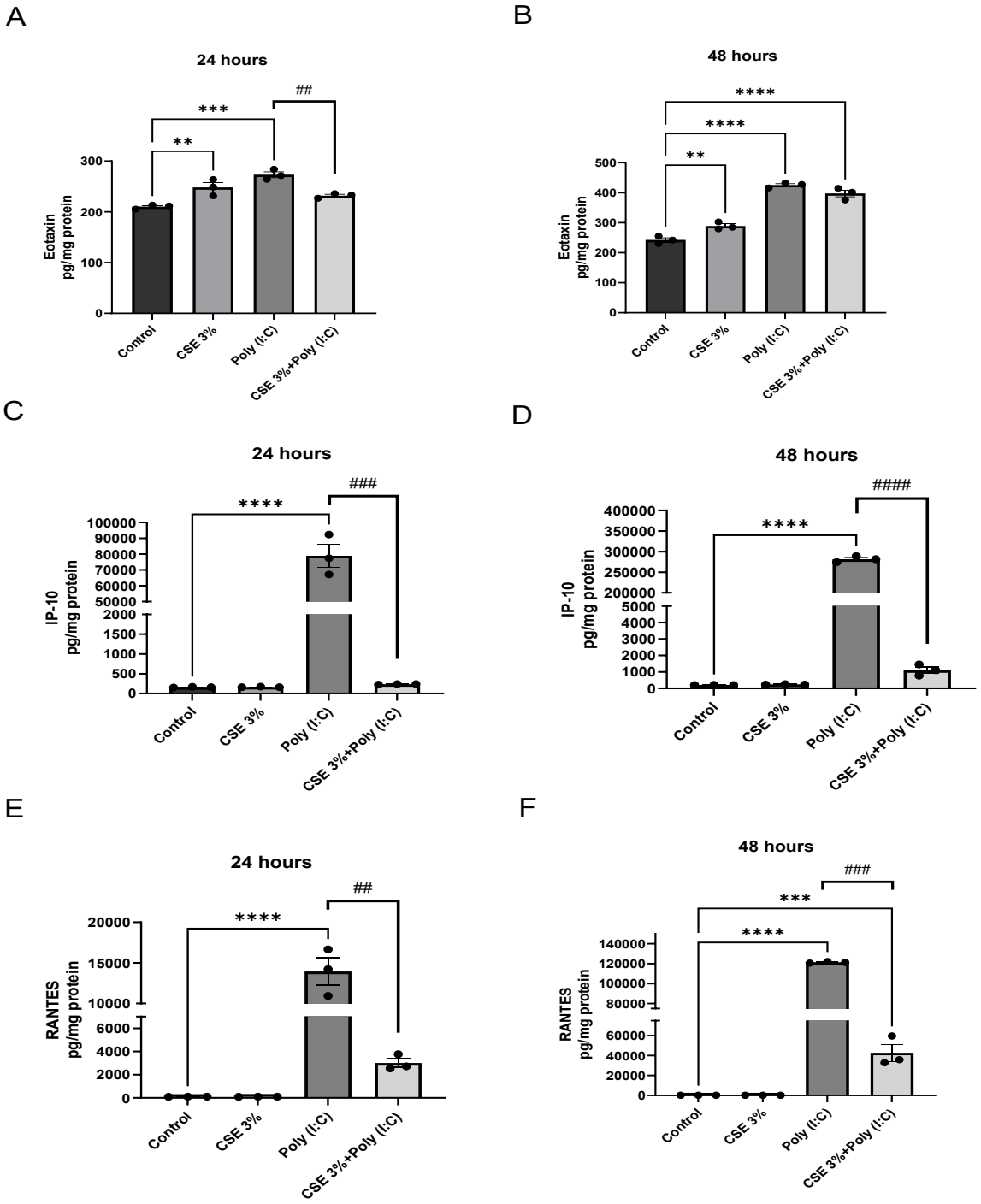

Figure 4.5 Effect of CSE and poly (I:C) on the production of eosinophil chemokines

iHBECs were treated with or without CSE (3%), poly (I:C) 10μg/ml, or CSE + poly (I:C) for 24 and 48 hours. The supernatants were collected, and the concentration of eotaxin for **(A)** 24 hours, **(B)** 48 hours, IP-10 for **(C)** 24 hours, **(D)** 48 hours, and RANTES for **(E)** 24 hours, **(F)** 48 hours were measured by Luminex® Discovery Assay. Data were normalised with total protein and presented as pg/mg protein. Each data point represents mean ± SEM of three individual experiments carried out in triplicate samples. **p<0.01, ***p<0.001, and ****p<0.0001 compared with untreated cells (control), and ##p<0.01, ###p<0.001, and ####p<0.0001 compared with poly (I:C) alone.

4.4.6 Effect of CSE and poly (I:C) on the production of non-T2 inflammatory in iHBECs

The data presented in Chapter 3 suggested that CSE may promote neutrophilic inflammation in iHBECs by increasing non-T2 inflammatory cytokines, including IL-6 and IL-8. I therefore investigated the effect of CSE on poly (I:C)-induced non-T2 inflammatory mediators in iHBECs. IL-8 was included in the Luminex® Discovery Assay and mirrored the previous findings of IL-8, which was originally assessed by ELISA (Figure 4.2). IL-6 and IL-8 were produced basally in iHBECs, 94.32 ± 0.8 and 145.4 ± 0.7 pg/mg protein, respectively at 24 and 48 hours for IL-6 (Figure 4.6 A and B), and 3751 ± 247 and 5129 ± 304 pg/mg protein, respectively at 24 and 48 hours for IL-8 (Figure 4.6 C and D). In line with the previous findings (Figure 4.2), CSE significantly increased the production of IL-8 at 24 hours (16374 ± 21382 pg/mg protein, *p<0.05) compared with control (Figure 4.6 C) but had no effect on the production of IL-8 at 48 hours (Figure 4.6 D) or IL-6 at 24 and 48 hours (Figure 4.6 A and B). Poly (I:C) significantly increased the production of IL-6 at 24 and 48 hours (270 ± 22 pg/mg protein, ****p<0.0001, and 844.3 ± 50 pg/mg protein, ****p<0.0001, Figure 4.6 A and B) and IL-8 at 24 and 48 hours (44799 ± 3505 pg/mg protein, ****p<0.0001 and 195176 ± 8653 pg/mg protein, ****p<0.0001, Figure 4.6 C and D), compared with control. A significant synergistic effect was observed in IL-8 production at 24 hours when CSE was combined with poly (I:C) (58741 ± 5026 pg/mg protein, ***p<0.001) compared to poly (I:C) alone (Figure 4.6 C). On the contrary, CSE significantly inhibited IL-6 at 24 and 48 hours by (48%, p<0.01 and 52%, ***p<0.001, respectively) (Figure 4.6 C and D). These findings were in line with the previous findings in this chapter on the IL-8 production assessed by ELISA, which showed a synergistic effect of CSE and poly (I:C) on the

IL-8 production at early exposure. However, the results suggest that CSE may promote neutrophilic inflammation in iHBECs by increasing neutrophilic chemokine IL-8, especially at an early exposure, but may also lead to an inhibition of other non-T2 cytokine such as a pleiotropic cytokine IL-6 in iHBECs.

Taken together, the results presented here suggest that CSE may impair antiviral responses in HBECs through inhibiting alarmins and eosinophil chemokines and may contribute to shifting the inflammation from eosinophilic to neutrophilic inflammation through the production of neutrophilic chemokine IL-8. The main findings of the investigation of the effect of CSE on poly (I:C) in iHBECs by Luminex® Discovery Assay are summarized in (Figure 4.7).

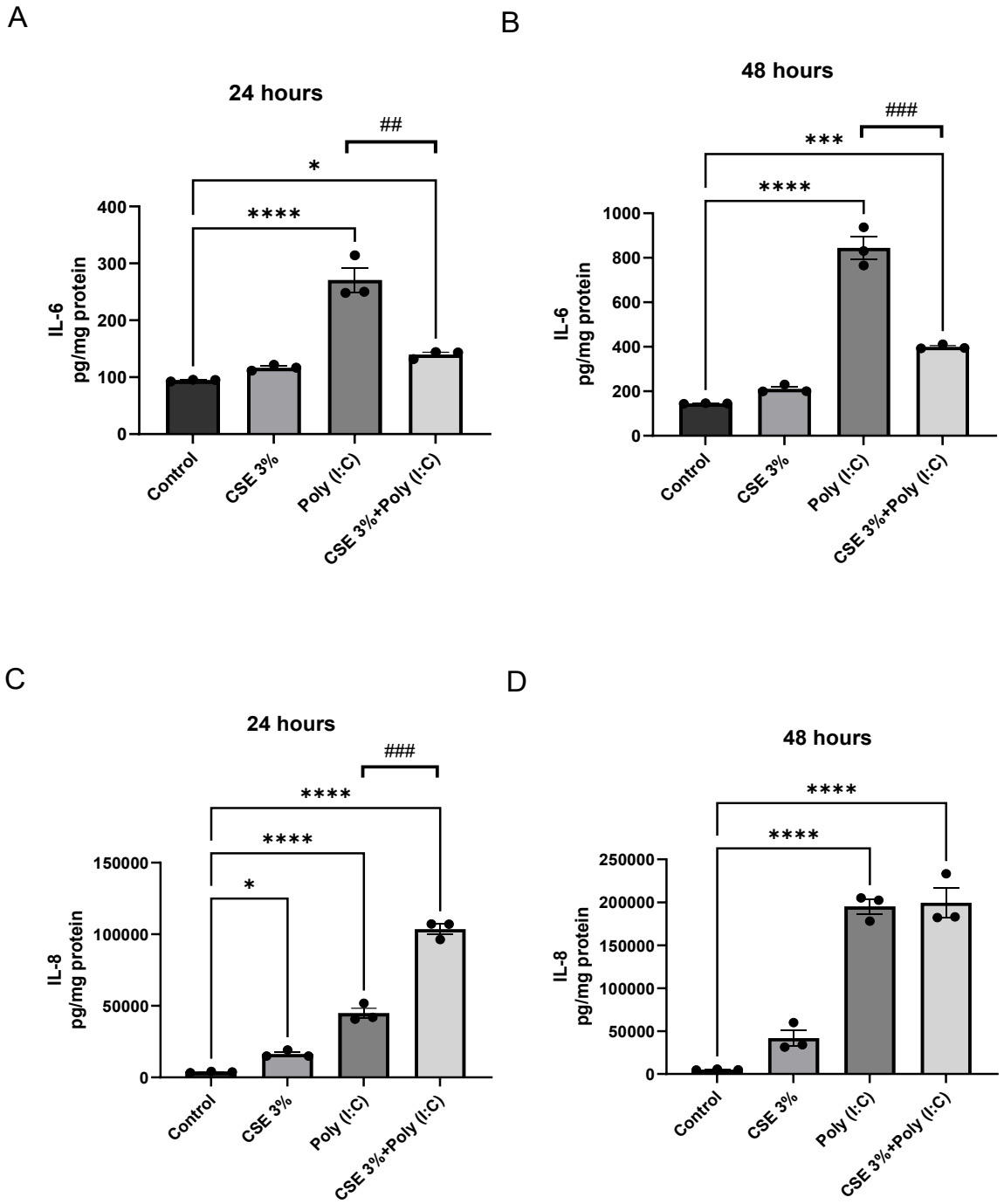

Figure 4.6 Effect of CSE and poly (I:C) on the production of non-T2 inflammatory cytokines

iHBECs were treated with or without CSE (3%), poly (I:C) 10µg/ml, or CSE + poly (I:C) for 24 and 48 hours. The supernatants were collected, and the concentration of IL-6 for **(A)** 24 hours, **(B)** 48 hours, and IL-8 for **(C)** 24 hours, **(D)** 48 hours were measured by Luminex® Discovery Assay. Data were normalised with total protein and presented as pg/mg protein. Each data point represents mean ± SEM of three individual experiments carried out in triplicate samples. *p<0.05, ***p<0.001, and ****p<0.0001 compared with untreated cells (control), and ##p<0.01 and ###p<0.001 compared with poly (I:C) alone.

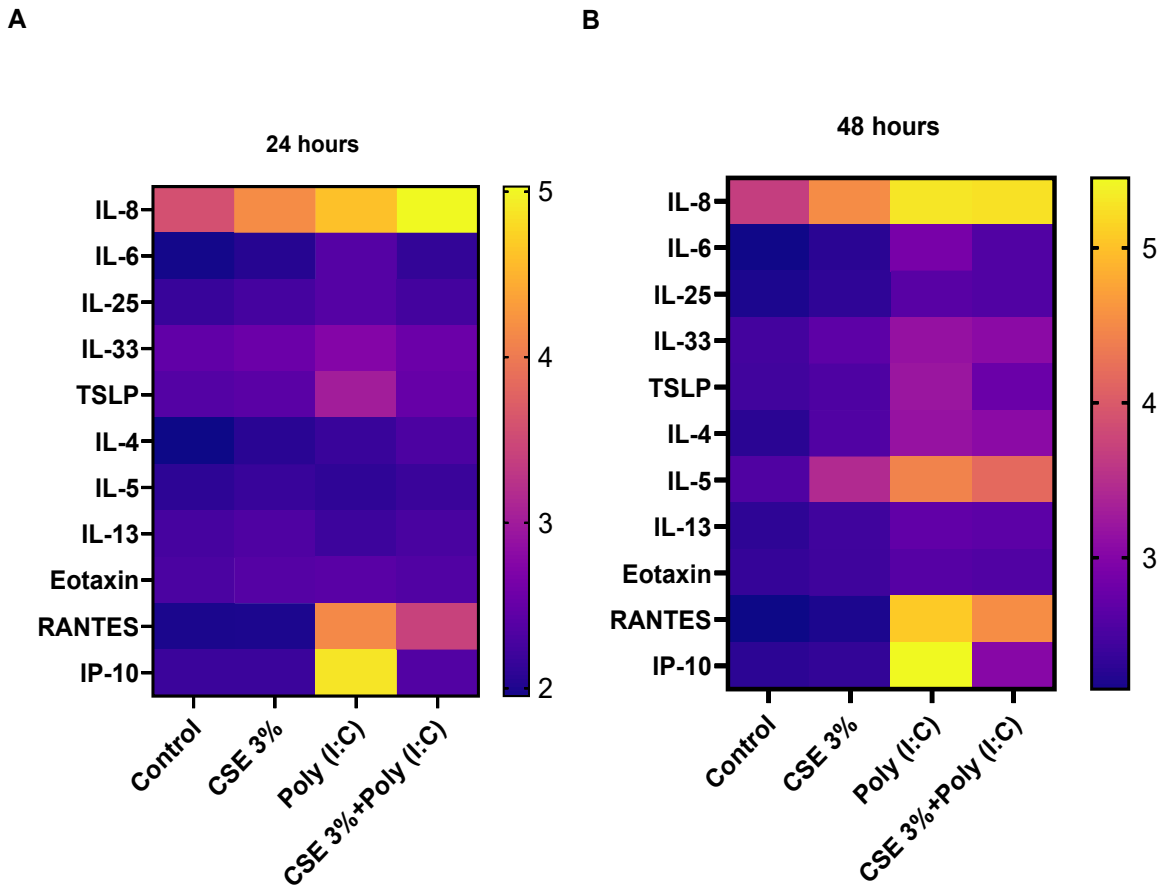

Figure 4.7 Heat map summarized the main findings on the effect of CSE and poly (I:C) on the expression and production of alarmins, cytokines, and chemokines

The summary of Luminex® Discovery Assay results data were log-transformed and plotted in heatmap showing the effect of CSE and poly (I:C) on the production of alarmins (IL-25, IL-33, and TSLP), Th2 cytokines (IL-4, IL5, and IL-13), eosinophil chemokines (Eotaxin, IP-10, and RANTES), pleiotropic cytokine IL-6, and neutrophilic chemokine IL-8 in iHBECs for **A,** 24 hours and **B,** 48 hours of stimulation. Data were $\log_{10}$-transformed, and the heatmap colour intensity reflects the relative expression levels on a $\log_{10}$ scale.

4.4.7 Effect of CSE and poly (I:C) on cfDNA release from iHBECs

cfDNA release has been linked to inflammation and disease progression, which might be associated with the extent of inflammation and may serve as a potential biomarker for tissue damage in several diseases [342, 343]. Yet its role in asthma and/or viral-induced exacerbations of asthma is largely unexplored. In this study, TERT was selected as a reference gene for cfDNA quantification due to its stable and ubiquitous expression across various biological conditions, making it a reliable control, which has been used previously to standardize cfDNA quantification [260]. I sought to explore the effect of CSE and poly (I:C) on the release of cfDNA from iHBECs at two different time points of 24 and 48 hours. QPCR targeting TERT gene was used to quantify the level of cfDNA secreted by iHBECs into conditioned supernatants. Since a higher quantification cycle (Cq) value reflects lower cfDNA levels, 1/Cq was plotted to represent cfDNA concentration, where higher 1/Cq values indicate more cfDNA release. cfDNA was secreted into culture medium basally by iHBECs at 24 and 48 hours, with the highest concentration of cfDNA released after 48 hours (0.03337 and 0.03492 Cq, respectively for 24 and 48 hours) (Figure 4.8 A and B). cfDNA release was significantly increased in response to poly (I:C) at 24 and 48 hours, as signified by (0.03696 Cq, ****p<0.0001 and 0.03778 Cq, ***p<0.001, respectively, Figure 4.8 A and B). CSE alone did not significantly release cfDNA compared to control, but co-stimulation of iHBECs with CSE and poly (I:C) at 24 and 48 hours led to a significant increase in cfDNA (0.03901 Cq and 0.04001 Cq, ****p<0.0001 for both, respectively (Figure 4.8 A and B) compared with control. Interestingly, co-stimulation of CSE and poly (I:C) significantly increased the concentration of released cfDNA compared to poly (I:C) alone stimulation by 37%

(***p<0.001) and 49% (*p<0.05), respectively for 24 and 48 hours (Figure 4.8 A and B).

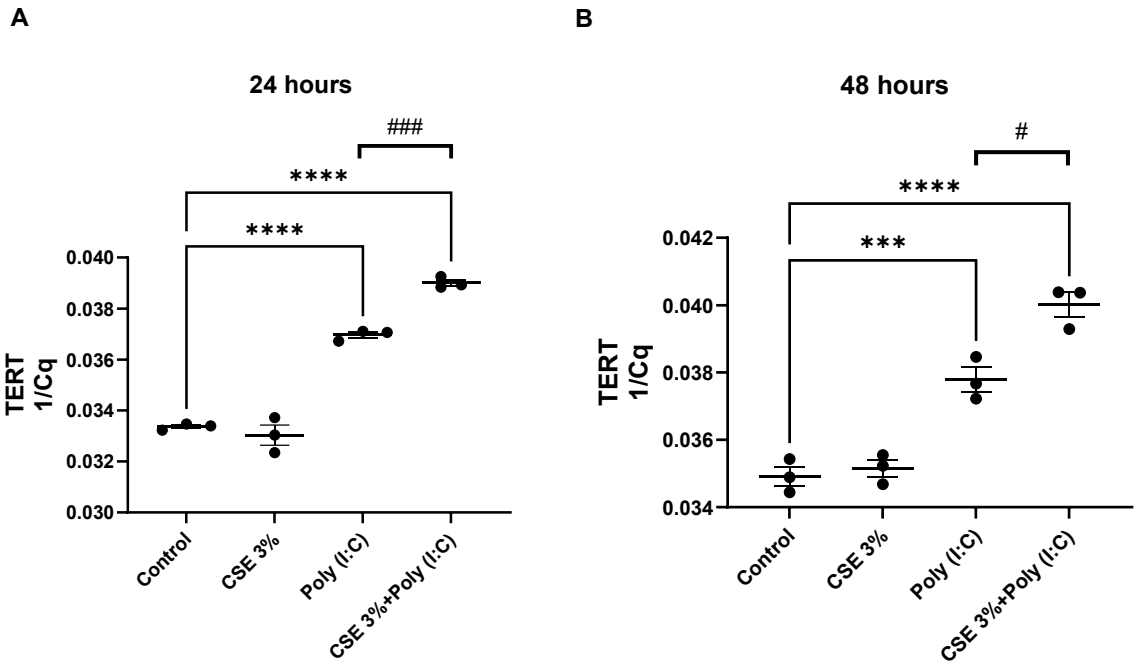

Figure 4.8 Effect of CSE and poly (I:C) on cfDNA release from iHBECs

iHBECs were treated with or without CSE (3%), poly (I:C) 10µg/ml, or CSE + poly (I:C) for 24 and 48 hours. DNA was isolated from the collected supernatant, and qPCR targeting TERT gene was used to quantify cfDNA from iHBECs samples for **A)** 24 hours and **(B)** 48 hours using Ariamax Real-Time PCR System (Agilent®). Data were presented as 1/Raw quantification cycle (1/Cq). Each data point represents mean ± SEM of three individual experiments carried out in triplicate samples. ***p<0.001 and ****p<0.0001 compared with untreated cells (control), and #p<0.05 and ###p<0.001 compared with poly (I:C) alone.

To validate the qPCR findings, cfDNA released from iHBECs following stimulation with CSE, poly (I:C), or their combination was analyzed using the TapeStation system. Basal cfDNA concentrations in the conditioned medium at 24 and 48 hours were 15.5 ± 2.9 and 12.63 ± 1.3 pg/µl, respectively (Figure 4.9 A and

B). Confirming the TERT qPCR data shown in Figure 4.8, the TapeStation demonstrated that CSE alone did not significantly increase the concentration of cfDNA released at both 24 and 48 hours. Poly (I:C) significantly increased the concentration of cfDNA released at 24 hours (31.84 ± 5.3 pg/µl, *p<0.05) compared with control (Figure 4.9 A), but no significant increase in the concentration of cfDNA was observed at 48 hours. Co-stimulation of CSE and poly (I:C) also led to a further increase in cfDNA release at 24 and 48 hours (78.9 ± 3.3, ****p<0.0001 and 89.22 ± 15.2 pg/µl, **p<0.01, respectively (Figure 4.9 A and B) compared with control. Importantly, co-stimulation of CSE and poly (I:C) significantly increased cfDNA concentration at 24 hours compared to poly (I:C) alone by 53% (**p<0.01) (Figure 4.9 A). Differences in the fragment size of cfDNA are associated with distinct pathological conditions [222, 344]. The cfDNA fragment sizes of the tested samples showed that cfDNA released in response to Poly (I:C) and co-stimulation of CSE and Poly (I:C) were larger than 1000 bp bases in length, which might indicate the DNA is packaged as part of extracellular vesicles (EVs) (Figure 4.10).

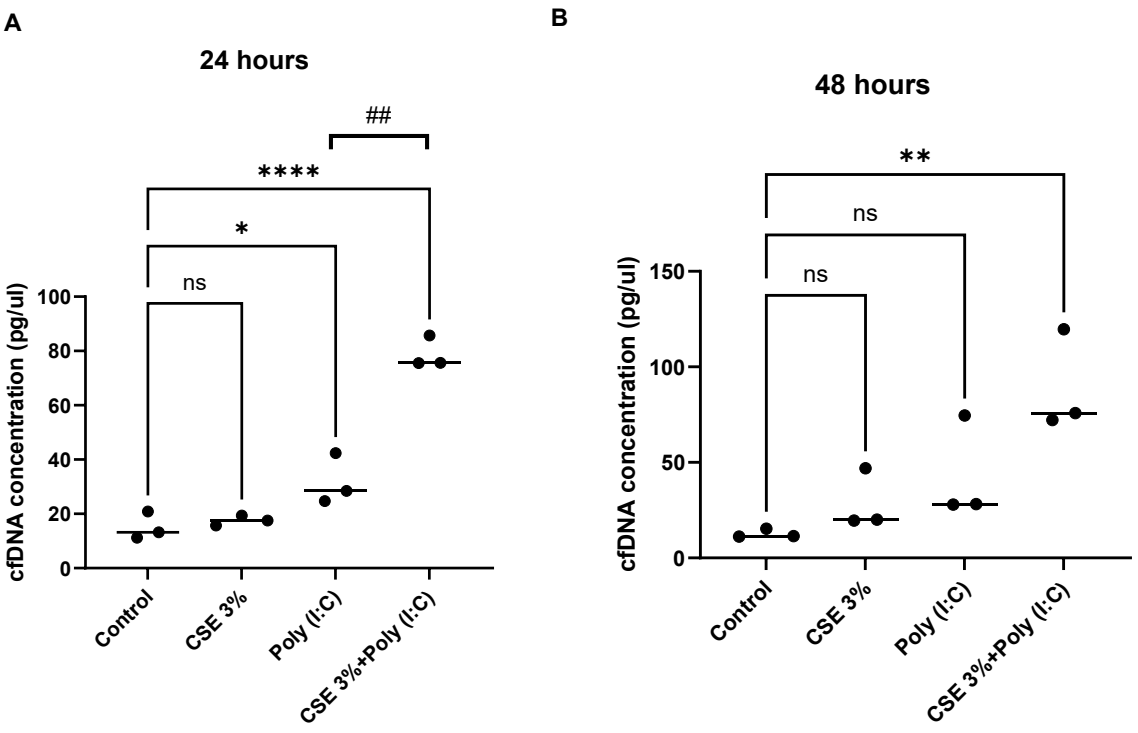

Figure 4.9 Effect of CSE and poly (I:C) on cfDNA concentration from iHBECs

iHBECs were treated with or without CSE (3%), poly (I:C) 10µg/ml, or CSE + poly (I:C) for 24 and 48 hours. DNA was isolated from the collected supernatant, and the concentration of released cfDNA from conditioned samples was measured for **A)** 24 hours and **(B)** 48 hours using Agilent 4200 TapeStation system. Data were presented as pg/µl. Each data point represents mean ± SEM of three individual experiments carried out in triplicate samples. *p<0.05, **p<0.01, and ****p<0.0001 compared with untreated cells (control), and ##p<0.01 compared with poly (I:C) alone.

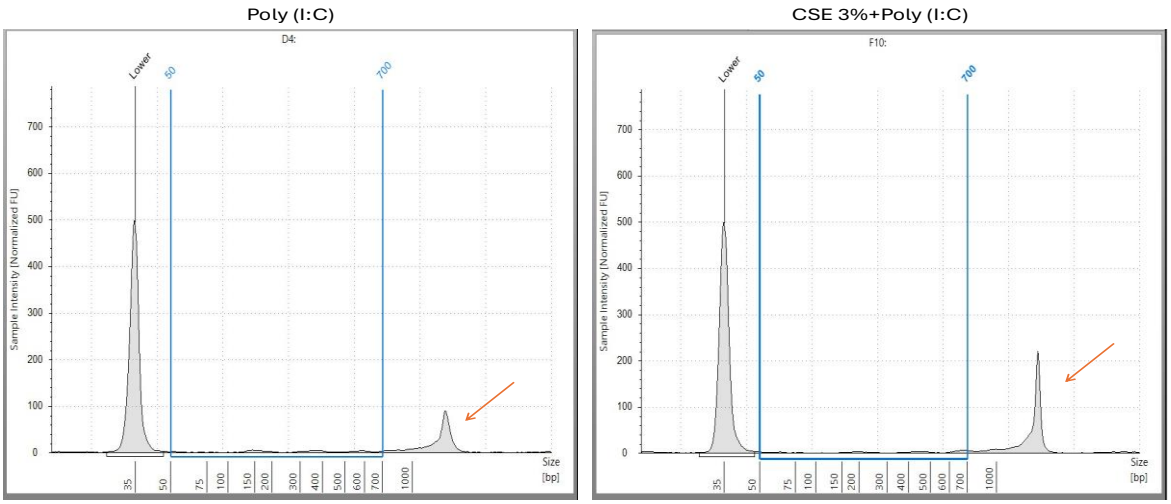

Figure 4.10 Characterization of cfDNA fragment size in iHBECs following poly (I:C) and CSE + poly (I:C) stimulation

Samples of TapeStation data show that the released cfDNA of Poly (I:C) and co-stimulation of CSE and Poly (I:C) were larger than 1000bp bases in length.

4.4.8 CSE, Poly (I:C) and CSE + poly (I:C)-stimulated iHBECs cause the release of EVs

Having demonstrated that the cfDNA release from Poly (I:C) and CSE + Poly (I:C) stimulated iHBECs was of a size that suggests it may be packaged within EVs, I investigated whether the same treatments cause EV release from iHBECs using conventional transmission electron microscopy (TEM), nanoparticle tracking analysis (NTA), and Exo-Check exosome antibody arrays. iHBECs were treated with or without CSE (3%), poly (I:C) 10µg/ml, or CSE + poly (I:C) for 24 hours in T75 flasks in order to obtain enough supernatant for EV isolation. EV fractions (~500 µl) were isolated by size exclusion chromatography and concentrated from fractions 1-6 of 0.5 ml of iHBECs supernatant. Transmission electron microscopy (TEM) at two magnifications 100 and 200 nm showed that there were particles that had a

characteristic cup-shaped morphology consistent with the morphology of EVs in all treatment groups. The mean particle diameter for the control group was 8 nm, and the mean frequency distribution of EV diameters showed a peak around 10 ± 8 nm (Figure 4.11A). The mean particle diameter and frequency distribution of EV diameters for CSE, poly (I:C), and CSE + poly (I:C) were 16 nm, 22 ± 19 (Figure 4.10B), 15 nm, 24 ± 17 (Figure 4.11C), and 13 nm, 18 ± 14 (Figure 4.11D), respectively, suggesting that CSE, poly (I:C) and a combination of them may increase both the average size and variability of released EVs. In addition, Gaussian distributions of all treatment groups showed a greater concentration of small EVs in the CSE + poly (I:C) group (Figure 4.11E).

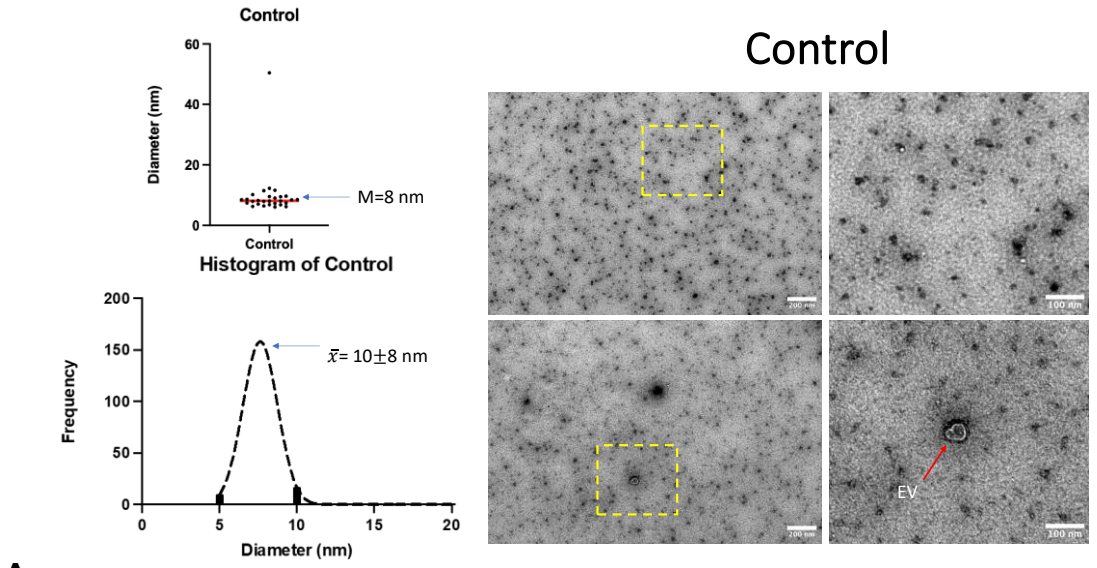
Control
Diameter (nm)
M=8 nm
Control
Histogram of Control
Frequency
$\bar{x}$= 10±8 nm
Diameter (nm)
Control
EV

A.

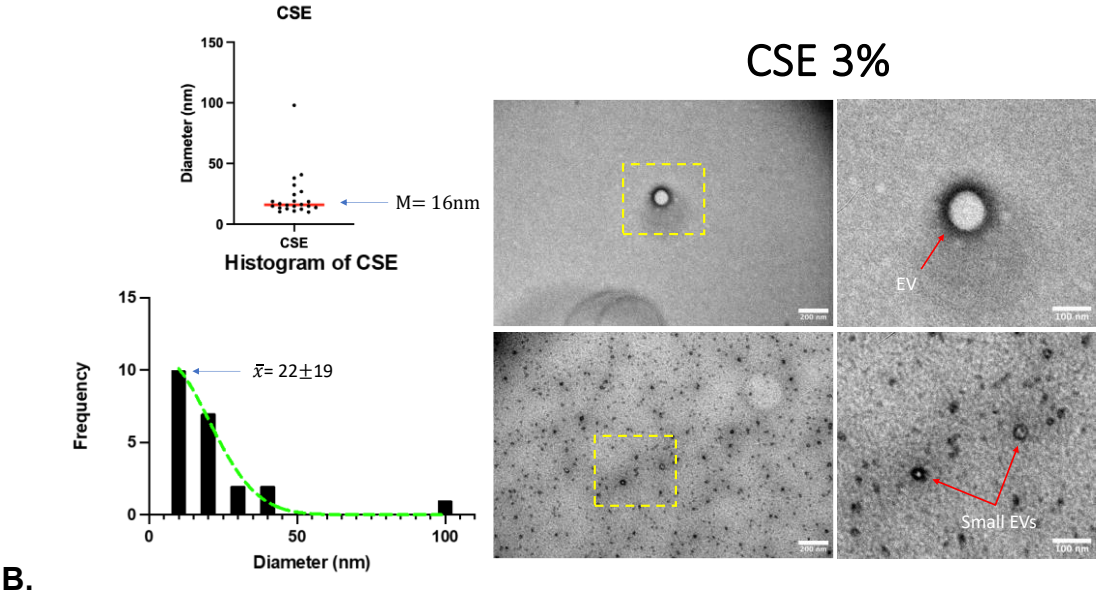
CSE
Diameter (nm)
M= 16nm
CSE
Histogram of CSE
Frequency
$\bar{x}$= 22±19
Diameter (nm)
CSE 3%
EV
Small EVs

B.

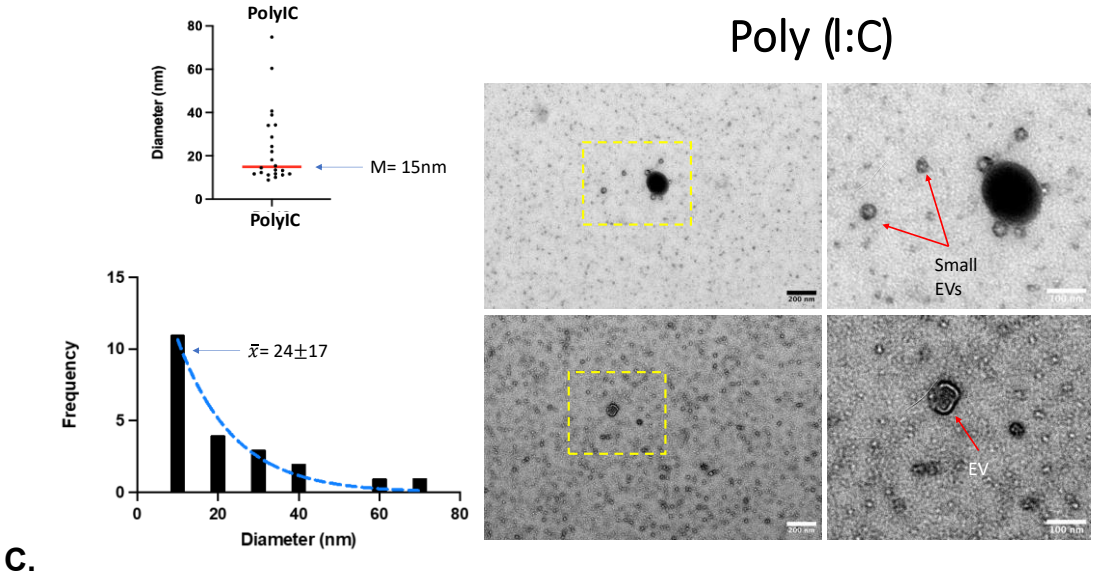
PolyIC
Diameter (nm)
M= 15nm
PolyIC
Frequency
$\bar{x}$= 24±17
Diameter (nm)
Poly (I:C)
Small
EVs
EV

C.

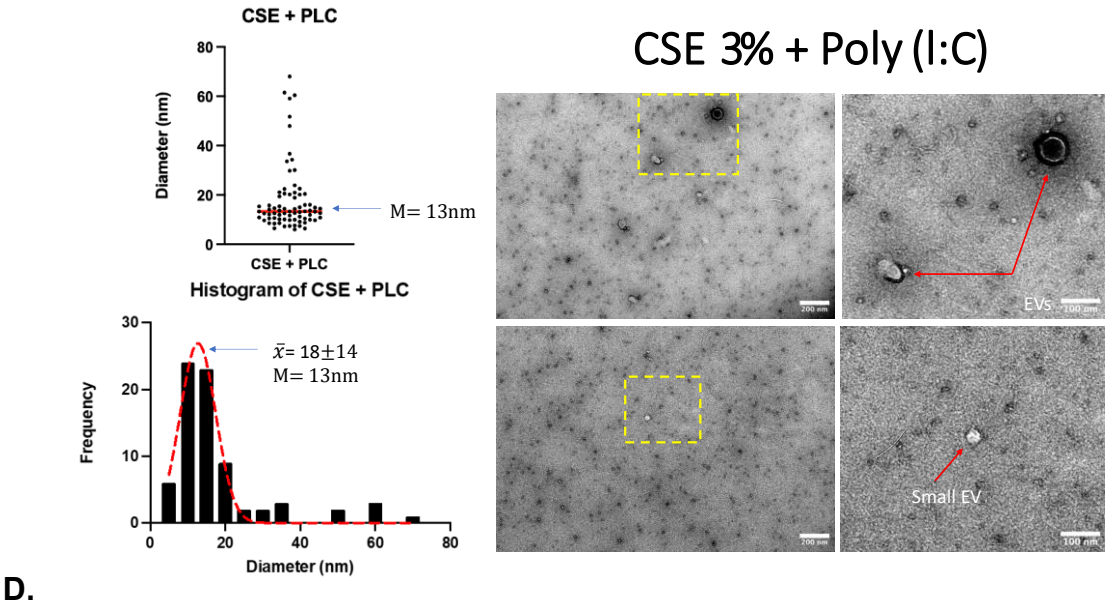

D.

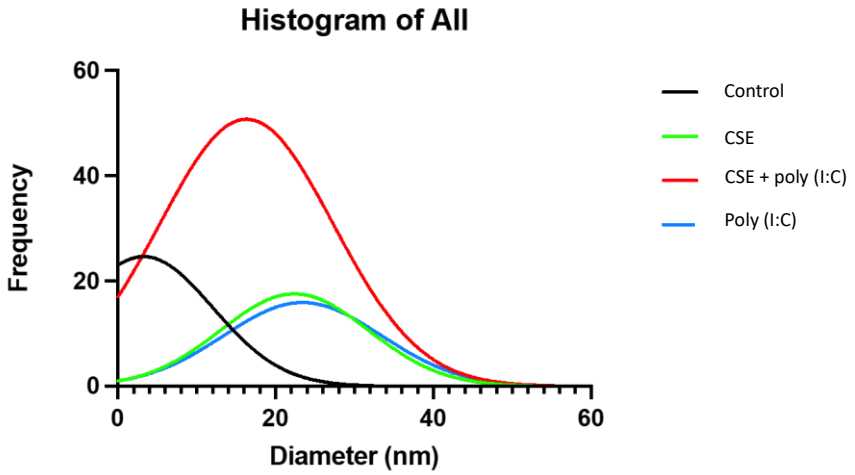

E.

Figure 4.11 EVs characterization by TEM

iHBECs were treated with or without CSE (3%), poly (I:C) 10µg/ml, or CSE + poly (I:C) for 24 hours in T75 flasks. The supernatants were collected, and EVs were isolated by size exclusion chromatography. TEM was performed using Technai T12 (nmRC) to image particles for fractions 1-6 of 0.5ml isolated EVs in conditioned samples of iHBECs from one experiment. Figure A-D, the top left (dot plot) shows individual EV diameters measured from TEM images, the bottom left (histogram) shows the frequency distribution of EV diameters, and the right panels represent TEM micrographs at two magnifications, 100 and 200 nm. Figure F shows Gaussian distributions of individual diameter and the frequency distribution of EVs.

The concentration of particles and particle size released in response to CSE, Poly IC and CSE+ Poly IC stimulation were also assessed by nanoparticle tracking analysis (NTA). The mean concentration of particles for the control group was 3.9 × 10^8 particles/ml. The mean concentration of particles for CSE, poly (I:C), and CSE + poly (I:C) were 7.03 × 10^8, 2.23 × 10^8, and 3.73 × 10^8, respectively, indicating a variation in particle concentration among the treatment groups (Figure 4.12A). The NTA also showed that most particles were between 100-200 nm in size for control and all treatment groups (Figure 4.12B).

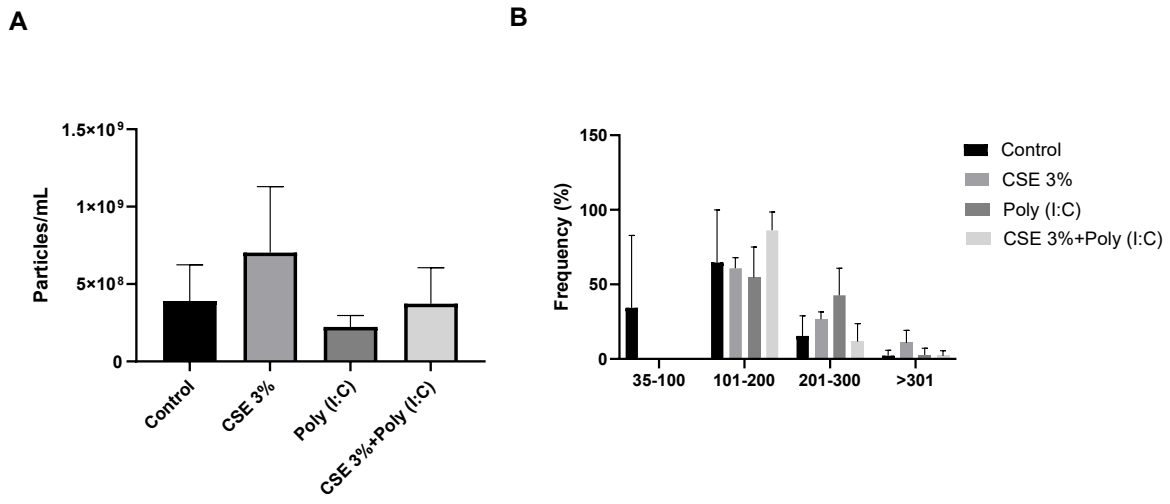

Figure 4.12 EVs characterization by NTA

iHBECs were treated with or without CSE (3%), poly (I:C) 10µg/ml, or CSE + poly (I:C) for 24 hours in T75 flasks. The supernatants were collected, and EVs were isolated by size exclusion chromatography. NTA was performed using a ZataView® Particle Tracking Analyzer to determine EV concentration and particle sizes of conditioned samples of iHBECs. (**A)** Concentration of paticles (EVs/ml) for fractions 1-6 of 0.5 ml of three individual experiments. **(B)** Mean size of particles for fractions 1-6 of 0.5 ml of three individual experiments.

To confirm the released EVs, an Exosome array was used to measure eight known exosome markers including tetraspanin (CD63) and (CD81) which are typical markers of EVs, Programmed cell death 6 interacting protein (ALIX) to confirm the vesicles are exosomes, not a random cellular debris, Flotillin-1 (FLOT1) membrane-associated protein used for exosome identification, Intercellular adhesion molecule 1 (ICAM1) used as a disease- or immune-related exosome marker, epithelial cell adhesion molecule (EpCam) for exosomes derived from epithelial cell, Annexin A5 (ANXA5) to distinguish vesicles based on surface lipid markers, and tumor susceptibility gene 101 (TSG101) as a marker for the purification of EVs. The results of this analysis revealed that the positive control markers showed high expression in all tested sample, confirming that the HRP detection was functioning well in this assay. In addition, GM130 marker was used to detect any cellular contamination in the EV samples, which showed a low expression in all tested samples, suggesting that EV samples had a good purity (Figure 4.13). The array results for the EV markers showed expression of the tested markers among treatment groups. The typical EV marker CD63 and CD 81 were expressed in all treatment groups (Figure 4.13). ICAM marker was also expressed in all treatment groups, suggesting that epithelial-derived EVs in these samples. The remaining markers showed no change in expression across all the treatment groups (Figure 4.13).

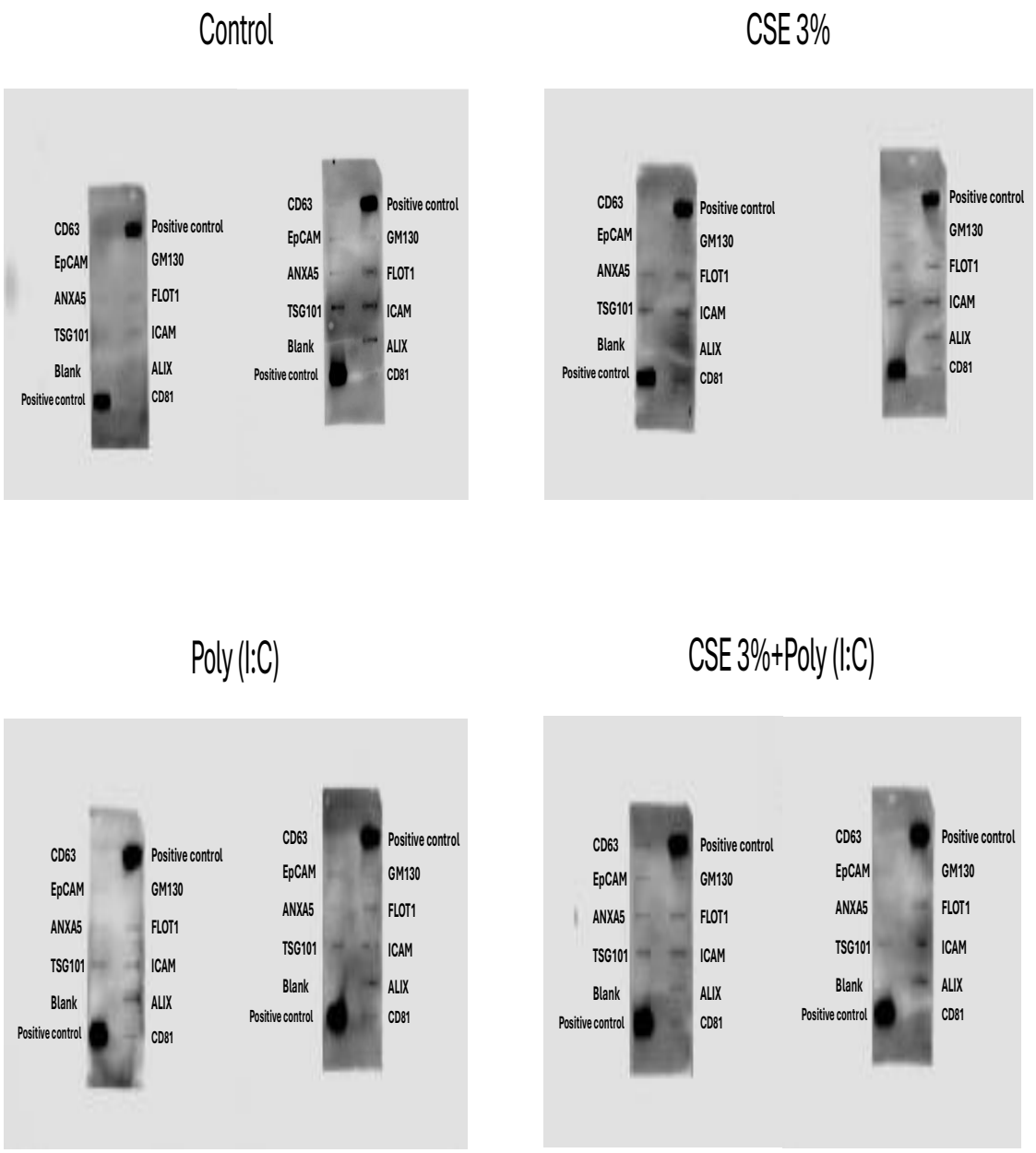

Figure 4.13 Characterisation of EVs protein using Exo-Check exosome antibody arrays

iHBECs were treated with or without CSE (3%), poly (I:C) 10µg/ml, or CSE + poly (I:C) for 24 hours in T75 flasks. The supernatants were collected, and EVs were isolated by size exclusion chromatography. 50 µl of isolated EVs was assessed for EVs-associated protein expression in conditioned samples of iHBECs by Exo-Check exosome antibody arrays. Each spot represents a different marker of known exosomal markers including CD63, EpCAM, ANXA5, TSG101, blank, 2 positive controls, GM130, FLOT1, ICAM, ALIX, and CD81. Data obtained from two individual experiments.

4.4.9 Effect of the oxidative stress inhibitor GSH on CSE-induced IL-8 production and cfDNA release from iHBECs

Oxidative stress plays an important role in the development of airway inflammation and disease progression in asthmatic smokers by increasing reactive oxygen species (ROS) production [345, 346]. The effects of CSE-induced IL-8 production in HAMSCs can be inhibited by the oxidative stress inhibitor glutathione (GSH) [308]. I therefore sought to assess the effect of GSH on IL-8 production and cfDNA release from iHBECs. GSH significantly inhibited CSE-induced and CSE + Poly (I:C)-induced IL-8 release in iHBECs by 49% (*p<0.05) and 42% (*p<0.05), respectively (Figure 4.14 A). CSE alone did not release cfDNA, therefore, the use of GSH had no effect on the release of CSE on iHBECs. However, the co-stimulation of iHBECs with CSE and poly (I:C) significantly increases the release of cfDNA from iHBECs, which was inhibited by GSH by 55% (***p<0.001) compared to CSE + poly (I:C) (Figure 4.14 B). These findings suggest that oxidative stress may play a role in CSE-induced IL8 production and cfDNA release in iHBECs.

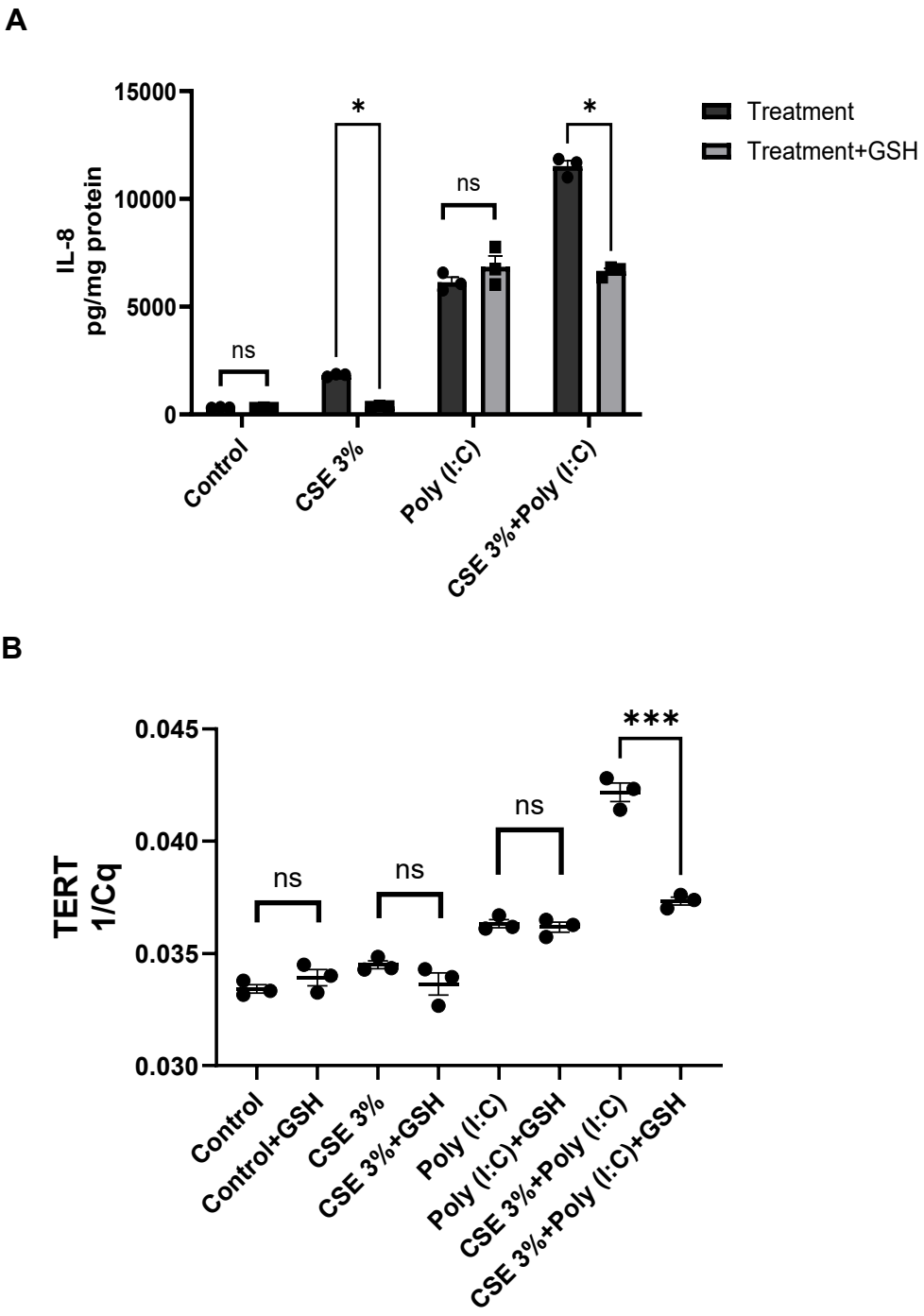

Figure 4.14 Effect of oxidative stress inhibitor GSH on CSE-induced production of IL-8 and cfDNA release from iHBECs

iHBECs were pre-treated with GSH (100 μM) for 1h, followed by treatment with or without CSE (3%), poly (I:C) 10μg/ml, or CSE + poly (I:C) for 24 hours. **(A)** The concentration of IL-8 in cell supernatants was measured by ELISA. Data were normalised to total protein and presented as pg/mg protein. **(B)** DNA was isolated and qPCR targeting TERT gene was used to quantify cfDNA from iHBECs samples using Ariamax Real-Time PCR System (Agilent®). Data were presented as 1/Cq. Each data point represents mean ± SEM of three individual experiments carried out in triplicate samples. *p<0.05 and ***p<0.001 compared with treatment conditions.

4.5 Discussion

This chapter aimed to assess the effect of CSE on the inflammatory responses and the release of cfDNA from iHBECs in response to viral infection. Respiratory viral infections are a major trigger of asthma and the most common cause of asthma exacerbation in children and adults [194, 317]. HBECs respond to viral infection by releasing alarmins that promote Th2 inflammatory responses in asthma [347]. CSE may impair the immune responses of HBECs to viral infection, leading to a switch in inflammatory endotype [213]. Understanding the impact of CSE on viral response in HBECS could provide valuable insights for improving asthma management and could open the door for identifying therapeutic targets.

In this study, I used the viral mimic Polyinosinic:polycytidylic acid **(**poly (I:C)) in combination with CSE to understand how CSE influences viral responses in iHBECs. Poly (I:C) is a synthetic double-stranded RNA that mimics viral RNA, leading to activation of Toll-like receptors (TLRs), causing a trigger to the innate immune response of the cells [320, 348]. Poly (I:C) induces mRNA and protein expression of TSLP in primary nasal epithelial cells of polyposis pathogenesis [349], and can induce non-T2 cytokines production, including IL-6 and IL-8 in primary HBECs [350].

The main findings within this chapter are that CSE inhibited the production of alarmins (IL-25, IL-33 and TSLP), eosinophil chemokines (Eotaxin, IP-10, and RANTES), pleiotropic cytokine (IL-6), but induced the production of neutrophilic chemokine (IL-8) in response to poly (I:C) in iHBECs. In addition, CSE induced the production of Th2 cytokine (IL-4) at an early exposure after 24 hours but had no effect on the other Th2 cytokines, including IL-5 and IL-13. However, in the later exposure, at 48 hours, CSE inhibited the production of IL-4 and IL-5 but had no

effect on IL-13 in response to poly (I:C). Similarly to IL-4 and IL-5, CSE inhibited the production of IL-8 in the later exposure at 48 hours in response to poly (I:C), suggesting a different signaling cascade at 48 hours or a possible reduction in cell viability of iHBECs after 48 hours which was not experimentally assessed as 24 hours experiments' cell viability and the protein concentration, shown previously in figure 4.1. The 24 hours' time point was chosen for further experimental work in this study. Moreover, cell-free DNA (cfDNA) release was also assessed in response to CSE and poly (I:C) in iHBECs, which showed that cfDNA was released in response to poly (I:C) but not CSE. Interestingly, co-stimulation of CSE and poly (I:C) significantly increased the concentration of released cfDNA relative to poly (I:C) alone, suggesting that CSE may exacerbate epithelial damage during viral infections.

As discussed in section 1.5.1, HBECs are the first line of defence against inhaled insults and are capable of mounting innate immune and other biological responses. HBECs releases a variety of cytokines termed alarmins, including IL-25, IL-33, and TSLP. Alarmins promote innate immune and adaptive types 2 responses [102]. Respiratory viral infection induces significant inflammatory responses in HBECs through imbalance of a Th1/Th2 responses and releasing of inflammatory mediators such as alarmins (IL-25, IL-33, TSLP), and other cytokines including IL-6 and IL-8 [351-353]. Here I show that poly (I:C) stimulation of iHBECs exacerbates alarmin release, including IL-25, IL-33, and TSLP at early (24 hours) and late (48 hours) exposure. In line with this, alarmin responses from primary HBECs have been studied in response to poly (I:C). Poly (I:C) induced the production of TSLP, which was associated with severe eosinophilic inflammation, and IL-33, associated with mild steroid-naïve disease [354-356]. These studies, together with the findings

presented in this thesis, provide strong evidence that poly (I:C) induced the production of alarmin responses in iHBECs.

Eosinophil chemokines, including eotaxin IP-10, and RANTES play a key role in the Th2 immune responses, mediating eosinophil activation and recruitment [357]. Poly (I:C) has been shown to influence eosinophilic chemokine release from a variety of cells. For example, poly (I:C) upregulates eotaxin release from cultured human corneal fibroblasts [358] and increased RANTES in spleen homogenates in response to pre-treatment with poly (I:C) in a mice infected with Escherichia coli [359]. In airway cells, poly (I:C) induces IP-10 production in primary human nasal and bronchial epithelial cells [360]. Supporting this, here I showed that poly (I:C) significantly induced the production of all eosinophil chemokines (Eotaxin, IP-10, and RANTES) in iHBECs.

Th2 cytokine-mediated allergic responses are largely driven by eosinophil chemokines [361]. In this study, I found that poly (I:C) significantly induced the IL-4 production at early exposure, followed by inducing the production of all Th2 cytokines (IL-4, IL-5, and IL-13) at later exposure (48 hours). Th2 cytokines particularly IL-4 and IL-13 impaired innate immune responses through inhibition of TLR3 expression to RV-16 infection in HBECs [362]. Evidence indicates that HBECs are relatively unresponsive to direct modulation by Th2-associated cytokines such as IL-4 and IL-13 [363]. These findings suggest that HBECs might not inherently release Th2 cytokines but might be integral in modulating immune responses related to these cytokines, which might explain the findings on our study that IL-5 and IL-13 had no significant production in response to poly (I:C) at early exposure.

I also investigated the response of non-T2 cytokines including IL-8 and IL-6 to poly (I:C). Both IL-6 and IL-8 showed a significant production in response to poly

(I:C). These findings were in line with the other studies found in the literature indicated that poly (I:C) induced IL-6 and IL-8 production in HBECs [364, 365]. Our results indicate that poly(I:C) may upregulate alarmin responses in iHBECs and promote the release of eosinophil- and neutrophil-associated cytokines and chemokines, while exerting minimal effect on Th2 cytokine production.

It was of interest to investigate the effect of CSE on the production of alarmins, Th2 cytokines, eosinophil chemokines, and non-T2 cytokines in iHBECs, given the central role of epithelial cells in orchestrating immune responses to environmental insults and the impact of CSE in exacerbating airway inflammation, particularly in the context of asthma. The results of our study on the effect of CSE on the alarmin responses revealed that CSE increased the production of IL-25 at an early exposure (24 hours) and IL-33 at a later exposure (48 hours) but had no effect on TSLP. It has been shown that the mRNA expression of IL-25 was significantly increased in the nasal epithelium in smokers compared to non-smokers [366]. The literature's findings on the effect of CSE on IL-25 production, particularly in HBECs, were still limited. Based on available literature, the data presented here provide evidence for the first time that CSE can enhance the production of IL-25 in iHBECs, suggesting that cigarette smoke may directly prime bronchial epithelial cells to promote alarmin response through the production of IL-25. For IL-33, treatment with 20% CSE for 24 hours decreased the release of IL-33, but increased IL-33 mRNA levels as measured by real-time PCR, and also increased intracellular IL-33 expression in HBECs, as confirmed by flow cytometry [367]. *In vivo,* CS triggers IL-33-associated inflammation in a mice model of late-stage COPD [368], suggesting that CS-induced IL-33 can influence airway inflammation in vivo, which may have important implications for the pathogenesis of asthma, another inflammatory airways

disease. In line with this, our study showed that CSE enhanced the production of IL-33 but at a later exposure, suggesting that CSE may induce IL-33 production with prolonged exposure. Our study also showed that CSE alone had no effect on the production of TSLP, yet previous research has shown that CSE-induced TSLP mRNA and protein expression in mouse lung, leading to Th2 immune responses [369]. This discrepancy could potentially be explained by the difference in organisms or the fact that this study was performed *in vitro*, whereas the previous research was performed *in vivo*.

Our results showed that CSE induced the production of IL-4 and IL-5 from iHBECs in the early exposure and IL-4 and IL-13 in the late exposure, which supports previous research in other model systems and suggests a role for CS in modulating Th2 responses in the asthmatic airway. For example, CSE stimulation of dendritic cells can lead to increased IL-4 expression in CD4+ T cells [370], and exposure of rats to tobacco smoke leads to increase IL-13 levels in lung tissue [371]. Moreover, in a clinical study, tobacco smoking is associated with increased IL-5 levels in the BAL of acute eosinophilic pneumonia patients [372]. On the contrary, our group previously showed in HASMCs that CSE inhibited the release of Th2 cytokines including IL-4 and IL-13 but not IL-5 (unpublished study), which might highlight the different responses of airway structural cells to CSE.

The data presented in this thesis shows that CSE increased the production of eotaxin in iHBECs. This observation was in line with other studies indicating that CS influences the expression of eotaxin, particularly eotaxin-1 and eotaxin-2, and increases the count of immunoreactive cells in asthmatic smokers [373, 374]. However, in opposite directions, CSE (5-30%) inhibited TNFα-induced release of eotaxin and RANTES from HASMCs [308], which was also supported by the findings

of our group that CSE inhibited the production of eotaxin, IP-10, and RANTES in HASMCs (unpublished study). Previous *in vitro* findings showed that chronic CSE resulted in overexpression of IP-10 in BALF and upregulation of IP-10 mRNA in the lung parenchyma [375], while CSE significantly decreased TNFα-induced RANTES production in HASMC [308]. Our results from iHBECs investigation showed that CSE had no effect on IP-10 or RANTES production, suggesting that iHBECs may be less responsive to CSE-induced changes in IP-10 or RANTES compared to other cells, such as HASMCs or lung parenchymal cells.

An increase in neutrophilic inflammation, marked by the release of non-T2 inflammatory mediators such as neutrophil-attracting chemokines IL-8 in response to CSE, suggests a shift toward a neutrophilic asthma phenotype, which is likely more severe and less responsive to corticosteroid treatment [308]. CSE has previously been shown to increase IL-8 levels in several cell types, including HBECs [308, 376, 377], which is supported by the data presented in this thesis showing that CSE increases IL-8 release from iHBECs and the data from our group showing that CSE increased the production of IL-8 in HASMCs (manuscript in preparation) [153]. In addition, elevated IL-6 in adult-onset asthma is associated with higher blood neutrophils [378]. The data presented in this chapter showed that CSE had no effect on the production of IL-6, another non-T2 mediator, in iHBECs. Contrary to this finding, exposure to 10% CSE for 24 hours led to an increase in IL-6 production of HBECs (BEAS-2B) [379], suggesting that CSE-induced IL-6 production is cell-line dependent and that HBECs may differ in their inflammatory responsiveness to CSE. Taken together, our findings highlight the pro-inflammatory effects of CSE on HBECs, particularly for non-T2 inflammation and cell-type-specific responses.

This study is the first to investigate the effect of co-stimulation of CSE and

poly (I:C) on the production of alarmins (IL-25, IL-33, and TSLP), Th2 cytokines (IL-4, IL-5, and IL-13), eosinophil chemokines (Eotaxin, IP-10, and RANTES), and non-T2 cytokine IL-6 and IL-8 in iHBECs. The interesting results revealed that CSE inhibited poly (I:C)-induced alarmin responses in iHBECs, suggesting that CSE may suppress epithelial-derived alarmin responses to viral infection. Given that alarmins play a key role in amplifying type 2 airway inflammation, this effect could mean that smoking asthmatics who are infected with respiratory viruses have a skewed inflammatory response. Previous i*n vitro* studies have shown that CS can decrease innate immune responses/cytokine production in HBECs during viral infection [327, 380], suggesting a dampened antiviral defense. On the contrary, however, CS can increase IL-33 expression and exacerbate the effects of viral infection in an *in vivo* mouse model [328], and nasal epithelial cells (NECs) derived from smokers expressed significantly higher levels of TSLP in response to influenza A virus compared to non-smokers [326]. Taken together, these findings highlight the complex role of cigarette smoke in impairing protective antiviral responses and amplifying pro-inflammatory alarmin expression, which may contribute to increased susceptibility and severity of virus-induced asthma exacerbations.

The results of our study also show that CSE inhibited the production of eosinophil chemokines in response to poly (I:C) stimulation, suggesting that CSE may impair antiviral-induced eosinophilic inflammation in the HBECs. CSE inhibited Lipopolysaccharide (LPS)-induced IP-10 production in (16-HBE) cell line [306] and CS reduces eosinophils in BAL fluid of OVA-challenged mice [381]. This was also supported by the findings of our group on HASMCs that CSE inhibited the production of eosinophil chemokines (Eotaxin, RANTES, and IP-10) after stimulation with TNFα (manuscript in preparation). The data collectively suggest that CSE may dampen

antiviral eosinophilic defences and suppress eosinophil-associated chemokine production in airway structural cells, including HBECs and HASMCs, which might contribute to a shift in asthma phenotype from eosinophil to non-eosinophil, often neutrophil inflammation in asthmatic smokers.

In addition to the observed inhibitory effects of CSE on eosinophil chemokines, I found that the production of IL-6 in response to poly (I:C) was also inhibited by CSE. IL-6 is a pleiotropic cytokine that has a function in both pro-inflammatory and anti-inflammatory processes in asthma and other respiratory diseases [382]. A supporting *in vitro* study of small airway epithelial cells (SAEC) showed that prior smoking exposure of the cells significantly inhibited the production of IL-6 and IP-10 in response to 0.5 μg/ml of poly (I:C) [383]. In addition to IL-6, our results showed that CSE enhances the production of neutrophilic chemokine (IL-8) in response to poly (I:C), suggesting that CSE may amplify virus-induced neutrophilic inflammation in iHBECs. Supporting this, CSE enhances IL-8 production in response to HRV infection in HBECs [384]. Collectively, these findings suggest that CSE may amplify virus-induced neutrophilic inflammation in HBECs, leading to a shift from T2 eosinophil-immune response to non-T2 neutrophil-immune response, a more severe and steroid-resistant asthma.

cfDNA concentrations are often associated with the extent of tissue damage and inflammation in various pathologies [385]. cfDNA has been widely used as a novel biomarker that offers a non-invasive screening tool for different inflammatory respiratory diseases, including COPD [386] and pulmonary infection [387]. cfDNA concentrations are increased following viral infection [244, 337] and a former PhD student in our group, showed that poly (I:C) significantly increased the release of cfDNA in primary HBECs [338]. Furthermore, cfDNA is increased in smoke inhalation

injury, and is increased by CSE in human endothelial cells [242], providing a potential marker of tissue damage and inflammation [241]. The studies on the effect of CSE on viral infection, particularly in HBECs, are still limited, and based on available literature, this study is the first to investigate the effect of co-stimulation of CSE and poly (I:C) on the release of cfDNA.

The novel data in this thesis revealed that cfDNA was released in response to poly (I:C) but not CSE, and that the combination of CSE and poly (I:C) significantly increased the concentration of released cfDNA relative to poly (I:C) alone. This suggests that cigarette smoke could exacerbate virus-induced epithelial damage, leading to worsening airway inflammation and asthma pathogenesis in virally infected patients.

Most cells generate lipid bilayer-enclosed subcellular bodies known as extracellular vesicles (EVs). The most well-known EV
classes are microvesicles and exosomes, which are both produced by healthy cells, in addition to ApoEVs, which are EVs produced by cells undergoing regulated apoptosis [388]. ApoEVs typically have a relatively large size of 1-5 μm in diameter but can be larger or smaller [389]. In our study, I found that the cfDNA release in response to poly (I:C) and co-stimulation of CSE and poly (I:C) were larger than 1000 bp bases in length, suggesting that the cfDNA might be associated and released as a part of EVs. The EVs were assessed, and I identified particles with a characteristic cup-shaped morphology consistent with the morphology of EVs in all treatment groups. These observations are based on preliminary data and were not replicated with sufficient biological replicates (e.g. n=3). Although changes in cfDNA size were found following stimulation with poly (I:C) and co-stimulation with CSE and poly (I:C), there were no alterations in EV characteristics, such as size or

morphology, across the treatment groups. The results from these observations might suggest that the cfDNA release may not be directly associated with EVs, or alternatively, that the EV cargo composition may have varied between treatment groups. Further studies utilizing extracellular vesicle formation inhibitors, such as manumycin A and Y27632, could provide insight and clarify the findings into whether the release of cfDNA from iHBECs is mediated via EV-associated pathways [390].

Oxidative stress plays an important role in the development of airway inflammation and disease progression in asthmatic smokers by increasing reactive oxygen species (ROS) production [345, 346]. In this study, I found that the use of oxidative stress inhibitor (GSH) significantly inhibited the effect of CSE-induced IL-8 production and cfDNA concentration from iHBECs, highlighting the role of oxidative stress in mediating these responses. Supporting this, the findings of our group and a previous study showed that oxidative stress inhibitor (GSH) significantly inhibits CSE-induced IL-8 production in HASMCs [308]. These findings provide insight that the inhibitory effect of CSE on poly (I:C)-induced production of alarmins and eosinophilic chemokines may be mediated by oxidative stress, potentially dampening the normal epithelial alarmin response to viral infection. Moreover, Direct measurement of oxidative stress in response to CSE stimulation, using different methods of direct measurement of oxidative stress such as DCFH-DA fluorescence for total ROS would help validate these findings [391].

In summary, the results in this chapter show important findings that CSE modulates the response of iHBECs to viruses through altering inflammatory responses, suppressing epithelial-derived alarmin and eosinophil responses and inducing neutrophilic responses, and causeing enhanced release of cfDNA, both of which contribute to pathogenesis of asthma. In the next chapter, I will investigate the

functional effect of cfDNA released from iHBECs on airway structural cells particularly HASMCs.

Chapter 5. The biological impact of the cfDNA released from iHBECs on the proliferation, contraction, and gene expression of HASMCs

5.1 Introduction

In Chapter 4, I showed that cfDNA was released from iHBECs in response to poly (I:C), but not CSE. Interestingly, when CSE was combined with poly (I:C), there was a significant increase in cfDNA release compared to poly (I:C) alone. However, the biological function of iHBEC cfDNA release, particularly in the context of asthma pathogenesis, was not well investigated. cfDNA plays a crucial role as an active molecule that stimulates proinflammatory cytokine synthesis, enhances oxidative stress, and contributes to inflammation in several diseases [334, 335].

HBECs and HASMCs are key contributors to asthma pathogenesis. Their interaction, including direct cell-to-cell communication, promotes hallmark features of asthma such as inflammation, AHR, airway remodeling, and mucus hypersecretion [131]. Mediators released by airway epithelial cells including cytokines, chemokines, growth factors, and extracellular matrix proteins can influence HASMC inflammatory responses, contractility, and proliferation, thereby contributing to asthma pathogenesis [131]. Whether cfDNA plays a role in facilitating HBEC-HASMC crosstalk in asthma is unclear, but our group has previously demonstrated that poly (I:C) can induce the release of cfDNA from HBECs, which subsequently upregulated IL-8 secretion from HASMCs, suggesting a possible role of cfDNA in airway inflammation [338].

HASMCs play a key role in asthma pathogenesis through enhancing airway contraction and proliferation in response to stimuli, which may lead to airway narrowing and remodeling. Evidence indicated that HASMCs hypertrophy may correlate with the severity of asthma [392], and HASMCs are the primary effectors of airway constriction in asthma, leading to airway obstruction and AHR [393].

Assessing HASMCs contraction and proliferation are crucial methods to understand asthma pathophysiology. These processes are essential for AHR and remodelling, which are characteristic hallmarks of asthma progression. In addition, understanding the functional outputs on the effect of release cfDNA from HBECs on HASMCs, and how crosstalk between these cells could contribute to asthma progression may identify potential therapeutic targets for asthma management.

Studying gene expression profiles is an essential tool for understanding how genes are regulated under numerous conditions and how these conditions can affect biological processes [394]. Transcription, as related to genomics, is the process by which DNA sequences are copied into Ribonucleic acid (RNA) molecules, or transcripts, to carry out these genetic instructions. Messenger RNA (mRNA), among RNA, is an essential RNA type for protein production. Genes are copied into complimentary mRNA during transcription, which is then delivered to ribosomes in the cell's cytoplasm. The mRNA sequence is subsequently translated into proteins by ribosomes, which assemble amino acids together in accordance with the instructions encoded in the mRNA [395]. Several factors can influence the transcriptome, such as the cell cycle, exposure to chemical or physical agents, and diseases [396]. The transcriptome can indicate which genes are active in a certain cell type or under certain conditions, allowing us to gain insight into how genes respond to environmental changes [397]. RNA sequencing (RNA-Seq) has been widely used in respiratory research to provide quantitative data on the transcriptome response in airway cells and tissue. A nasal epithelial transcriptomic profile and asthma endotypes study in youth identified 2516 differentially expressed genes for the T2 high profile associated with IL-13 signalling pathways, and 2494 genes for T17 high profiles associated with IL-17 and neutrophil signalling pathways [398].

Another study showed that gene expression biomarkers evaluated in normal-appearing airway epithelium offer a chance to take advantage of lung cancer-associated molecular changes in this tissue for early identification of lung cancer [399]. Furthermore, an RNA-Seq study found that 243 genes were altered after CSE exposure through reactive oxygen species, NF-κB signaling, and proteasome degradation pathways in primary HBECs [400].

Profiling gene expression, cell proliferation and cell contraction in response to cfDNA might help to understand the cellular functional and biological processes it triggers, which may provide a mechanistic link between HBECs injury and asthma-associated response in HASMCs and could lead to potential therapeutic targets.

5.2 Hypothesis and Aims

I hypothesized that poly (I:C) and co-stimulation of CSE and poly (I:C)-induced iHBECs cfDNA modulates the remodeling process and alters gene expression in HASMCs

This chapter aimed to investigate the biological impact of cfDNA released from iHBECs on HASMCs.

The specific aims for this chapter were:

- To investigate whether CSE and poly (I:C)-induced iHBECs cfDNA release stimulates HASMCs proliferation.
- To investigate whether CSE and poly (I:C) induced iHBECs cfDNA release alters HASMCs contraction.
- To identify whether CSE and poly (I:C) induced iHBECs cfDNA release changes gene expression profiles in HASMCs.

5.3 Methods

5.3.1 iHBECs experiment

To generate sufficient cfDNA from iHBECs for functional HASMC assays, further CSE and poly (I:C) experiments were conducted in 6 well-plates. qPCR for TERT and ELISA for IL-8 production (Appendix, section 7.11) were performed on all experiments prior to further analysis to confirm the earlier findings prior to undertaking the functional assays. The final volume of 1000 µl cfDNA from iHBECs was then used for HASMCs experiments.

5.3.2 cfDNA isolation

cfDNA was isolated from iHBECs supernatants using QIAamp®DNA Blood Mini Kit as previously described (General methods and materials, section 2.9).

5.3.3 Cell proliferation

HASMCs proliferation was assessed using two methods as previously explained: the BrdU Cell Proliferation ELISA (General methods and materials, section 2.16.1) and PrestoBlue™ Cell Viability Reagent (General methods and materials, section 2.16.2). In both experiments, HASMCs were stimulated with 33.33 µl of cfDNA released from iHBECs. This was calculated as the final volume of 1000 µl cfDNA generated from iHBECs experiments were carried out in 6 well-plate with a surface area of 9.6 cm^2, and the surface area of the HASMCs 96 well-plate for the proliferation assay was 0.32 cm^2. The following calculation was used to mimic the iHBECs and HASMCs being in direct contact at the surface area level: 9.6/0.32 = 30, then the final volume of 1000 µl cfDNA/ 30 = 33.3 µl cfDNA per well of 96 well-plate (Figure 5.1).

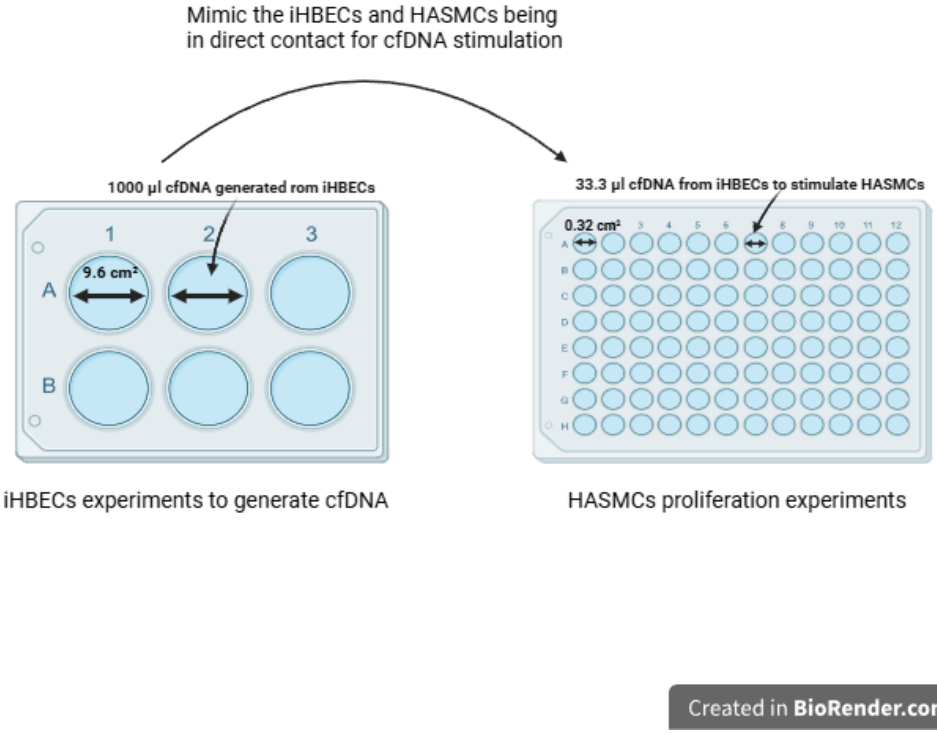

Figure 5.1 Schematic illustration of cfDNA transfer from iHBECs to HASMCs to mimic direct contact stimulation

cfDNA was generated from iHBECs cultured in 6-well plates (surface area: 9.6 cm² per well) and applied to HASMCs seeded in 96-well plates (surface area: 0.32 cm² per well). To simulate direct cell-to-cell surface contact, the cfDNA volume was proportionally scaled down, with 33.3 µl of cfDNA per well used for HASMCs stimulation based on the surface area ratio (9.6/0.32 = 33.3).

TGF-β1 was used in both experiments as a positive control, which was known to promote cell proliferation [401]. In addition, two types of control were used to ensure the validity of the experiments, including blank, in which cell culture medium but no HASMC cells were present in the wells, and background, in which HASMC cells were present within the wells but with no BrdU or PrestoBlue reagents added. A FLUOstar Omega microplate reader (BMG LABTECH) was used to measure optical density for BrdU Cell Proliferation ELISA at a wavelength of 450 nm, and fluorescence for PrestoBlue™ Cell Viability with a dual wavelength of 560/590 nm.

5.3.4 Cell contraction

HASMCs contraction was assessed using a Cell Collagen-based Contraction Assay kit as previously explained (General methods and materials, section 2.17). HASMCs were stimulated with 197.92 µl of cfDNA released from iHBECs. This was calculated as the final volume of 1000 µl cfDNA generated from iHBECs experiments were carried out in 6 well-plate with a surface area of 9.6 cm^2, and the surface area of the HASMCs 24 well-plate for the Collagen-based Contraction assay was 1.9 cm^2, following the same calculation of cfDNA stimulation of direct cell-to-cell surface contact as previously described (Section 5.3.3). Methacholine is known to induce HASMCs contraction [402], and used in this study as a positive control. In addition, 1M 2,3-Butanedione Monoxime (BDM), a cell contraction inhibitor, was added to methacholine and served as a negative control. Images of each gel were captured at zero hours and 24 hours after cfDNA stimulation using EVOS Cell Imaging System (Appendix 7.9). The gel size in each image (zero and 24 hours) was measured using the free-hand drawing function in ImageJ software to measure the gel area. The gel contraction was measured at the baseline (zero hour) and after incubation with cfDNA (24 hours), and the difference between the baseline and 24 hours was expressed as a percentage of gel contraction. The following calculation was used to express the percentage of gel contraction: (Gel area at 24 hours /Gel area at 0 hour x100), followed by subtracting the number generated from 100 to present the percentage of gel contraction.

5.3.5 RNA-Seq

HASMCs were stimulated with 364.58 µl cfDNA released from iHBECs for 24 hours. This was calculated as the final volume of 1000 µl cfDNA generated from iHBECs experiments were carried out in 6 well-plate with a surface area of 9.6 cm^2, and the

surface area of the HASMC 12 well-plate was 3.5 cm^2. The following calculation was used to mimic the iHBECs and HASMCs being in direct contact at the surface area level: 9.6/3.5 = 2.743, then the final volume of 1000 µl cfDNA/ 2.743 = 364.58 µl cfDNA per well of 12 well-plate. The supernatants were collected for further use, and 300 µl of RLT + β-mercaptoethanol (10 µl/ml) buffer was added to each well as previously described (General methods and materials, section 2.11). DNA and RNA isolation was performed using AllPrep DNA/RNA Mini Kit (Appendix 7.7). DNA was stored for future analyses not included in this thesis and RNA was sequenced as detailed below.

5.3.5.2 Samples quality control

After isolation, the quality of RNA samples was initially assessed using a TapeStation (Agilent). The RNA integrity number equivalent (RINe) minimum score of 8 was used as cut off for inclusion in additional processing, which indicated highly intact RNA (Table 5.1). RNA concentrations were measured using the Qubit Fluorometer and the Qubit RNA BR Assay Kit (Appendix 7.7). Twenty RNA samples from four healthy donors (Table 2.1), each stimulated with CSE, poly (I:C), and CSE + poly (I:C) were processed for RNA sequencing.

Table 5.1Quality control of RNA samples assessed by TapeStation

Sample	Cell line	Concentration (pg/µl)	Volume (µl)	RINe	Total RNA (pg)
Control	AZAC05	2090	28	9.4	58520
CSE	AZAC05	3300	28	9.6	92400
Poly (I:C)	AZAC05	10400	28	9.5	291200
CSE+Poly (I:C)	AZAC05	6180	28	9.4	173040
Elution Buffer	AZAC05	4770	28	9.6	133560
Control	AZAC11	7540	28	9.6	211120
CSE	AZAC11	2560	28	9.5	71680
Poly (I:C)	AZAC11	6070	28	9.6	169960
CSE+Poly (I:C)	AZAC11	8480	28	9.5	237440
Elution Buffer	AZAC11	2340	28	9.7	65520
Control	AZAC12	2570	28	9.5	71960
CSE	AZAC12	2300	28	9.5	64400
Poly (I:C)	AZAC12	2380	28	9.6	66640
CSE+Poly (I:C)	AZAC12	3370	28	9.4	94360
Elution Buffer	AZAC12	9830	28	9.4	275240
Control	159	15400	28	9.5	431200
CSE	159	5620	28	9.7	157360
Poly (I:C)	159	32300	28	9.4	904400
CSE+Poly (I:C)	159	36300	28	9.2	1016400
Elution Buffer	159	17300	28	9.4	484400

5.3.5.3 Library preparation and sequencing

Complementary DNA (cDNA) was generated from 10ng of total RNA for all samples using the QuantSeq 3’mA-Seq library prep kit for Illumina. Indexed sequencing libraries were then prepared using the Lexogen i7 6nt Index Set. For all

samples, 17 cycles of PCR were performed. Libraries were quantified using the Qubit Fluorometer and the Qubit dsDNA HS Kit. Library fragment-length distributions were analyzed using the Agilent TapeStation 4200 and the Agilent High Sensitivity D1000 ScreenTape Assay. Library pool sequenced on the Element Biosciences Aviti platform, using an Aviti 2x75 Sequencing Kit - Cloudbreak FS Medium Output to generate approximately 5 million 150bp single-end reads per sample. Per sample, read counts ranged from 2.74 million to 11.8 million (median: 10.10 million). All the RNA-Seq processes were previously described (General methods and materials, section 2.18).

5.3.5.4 Gene Ontology (GO) and Kyoto Encyclopedia of Genes and Genomes (KEGG) pathway analysis

Significantly, differentially expressed genes (DEGs) (adjusted $p < 0.05$ and log2FoldChange of +/- > 0.5) were selected for gene ontology (GO) analysis. The "enrich GO" function of the R package 'clusterProfiler' [269, 270] was used to assign enrichment GO categories for each set of genes, using the R package 'org.Hs.eg.db' [265] as the source of annotations. Biological process, molecular function, and cellular component sub-ontologies were calculated for each set. Gene sets were selected for each contrast and sub-ontology based on those with significant adjusted *p*-values (P value cut off is 0). In addition, biological pathway analysis was performed using KEGG analysis.

5.4 Results

5.4.1 cfDNA released from poly (I:C)- and CSE + poly (I:C)-stimulated iHBECs did not affect HASMCs proliferation

To assess the effect of cfDNA released from poly (I:C) and CSE + poly (I:C) induced iHBECs on HASMCs proliferation, three independent experiments using three different donor cell lines of HASMCs were stimulated with cfDNA from iHBECs. Using BrdU Cell Proliferation ELISA, Poly (I:C), and CSE + poly (I:C) caused no significant change in HASMCs proliferation when compared with control (Figure 5.2 A). In agreement with the BrdU ELISA assay, the PrestoBlue™ assay demonstrated no significant changes over the control in HASMCs proliferation across the treatments tested (Figure 5.2 B). Nevertheless, TGF-β1 significantly increased the proliferation of HASMCs in both BrdU Cell Proliferation ELISA and PrestoBlue™ Cell Viability Reagent (% change 216.2 ± 28.49, ***P<0.001 and 114 ± 4.10, **P<0.01, respectively). These findings suggest that cfDNA released from poly (I:C) and CSE + poly (I:C) induced iHBECs had no effect on HASMCs proliferation.

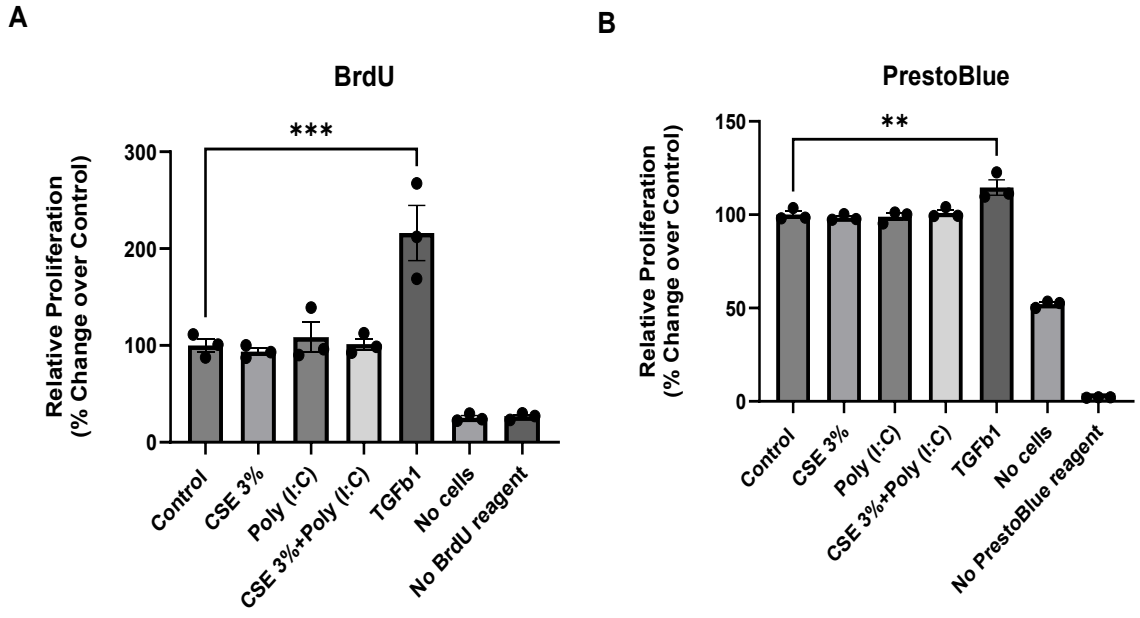

Figure 5.2 Measurement of HASMCs proliferation stimulated with different conditions of cfDNA released from iHBECs using BrdU ELISA and PrestoBlue reagent

A,The absorbance was read at 450 nm to assess cell proliferation by BrdU Cell Proliferation ELISA. **B,** The fluorescence was read at 560/590 nm to assess cell proliferation by PrestoBlue™ Cell Viability Reagent. Data were expressed as relative proliferation (% change over control). Each data point represents mean ± SEM of three independent experiments using three different cell lines, each performed with triplicate samples. ***P*<0.01 and ****P*<0.001 compared with control.

5.4.2 cfDNA released from poly (I:C)- and CSE + poly (I:C)-stimulated iHBECs did not affect HASMCs contraction

In addition to HASMCs proliferation, I investigated the effect of cfDNA released from poly (I:C) and CSE+poly (I:C) induced iHBECs on HASMCs contraction, which is a key feature of asthma contributing to airway narrowing and AHR. In the control group, which was stimulated with cfDNA from the iHBECs control group, basal gel contraction was measured at 55.77 ± 11.40% at 24 hours (Figure 5.3 A). CSE, poly (I:C) and CSE+poly (I:C) caused no change in gel contraction relative to the control group (Figure 5.3 A). In addition, positive control

(Methacholine) and negative control (Methacholine + Cell Contraction Inhibitor) did not significantly cause a change in the gel contraction relative to the control group. The validity of this experiment is limited, as neither the positive control nor the negative control produced the expected effects, indicating a potential failure with this assay. Captured pictures at 0 hours and 24 hours by EVOS Cell Imaging System demonstrating the changes in the collagen gel size are shown in (Figure 5.3 B).

A

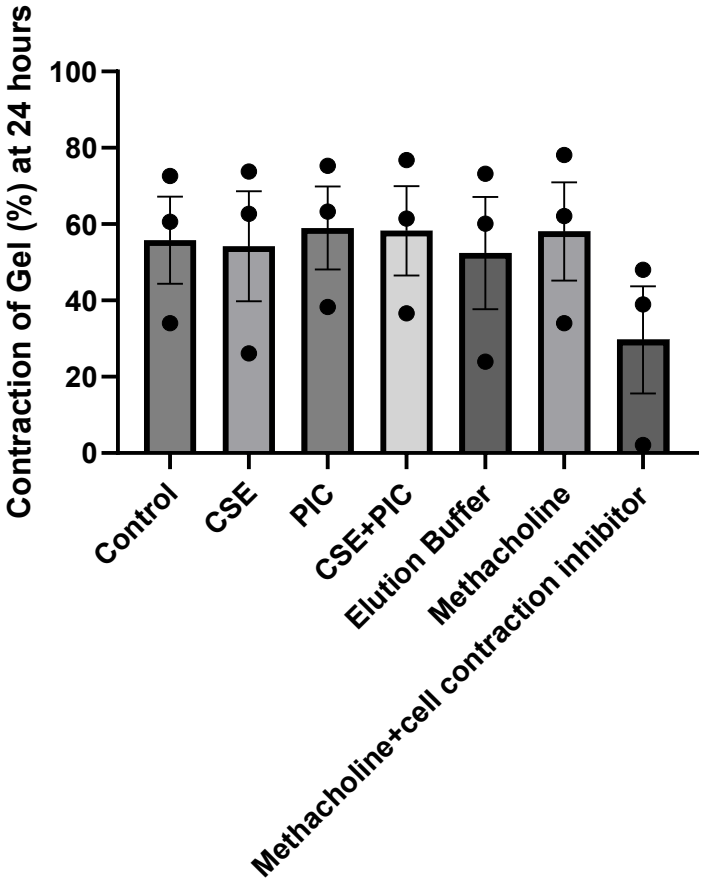

B

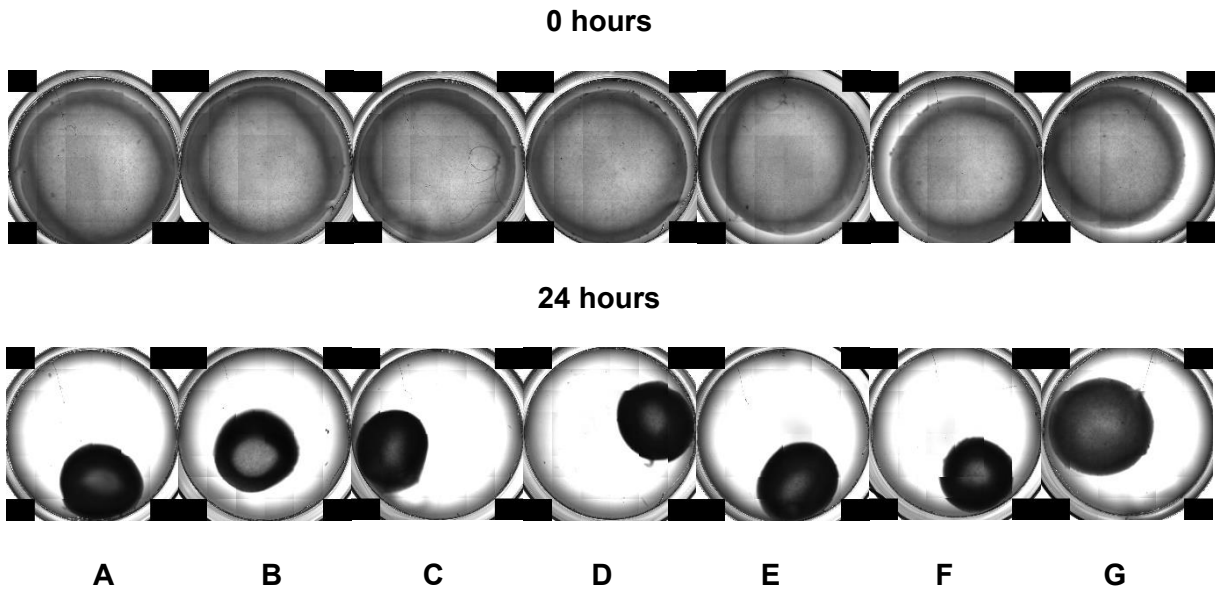

Figure 5.3 Measurement of HASMCs contraction stimulated with different conditions of cfDNA released from iHBECs using Cell Contraction Assay

The diameter of the gel was captured at 0 and 24 hours using EVOS Cell Image System. **A**, Data were expressed as a percentage of gel contraction. Each data point represents mean ± SEM of three independent experiments compared with control. **B,** The change in gel size (diameter) for one of the cell lines of HASMCs at zero and 24 hours. These images represent **A**, Control (cfDNA from iHBECs control group) **B**, CSE **C**, Poly (I:C) **D**, CSE+Poly (I:C) **E**, Elution Buffer **F**, Methacholine **G**, Methacholine+Cell Contraction Inhibitor.

5.4.3 cfDNA released from CSE- and poly (I:C)-stimulated iHBECs induced changes in HASMCs gene expression profiles

5.4.3.1 Data quality control

All samples were processed for RNA sequencing. All primary bioinformatics processing of sequence data was performed using the Lexogen QuantSeq workflow; a pipeline developed specifically for data generated from the family of QuantSeq 3' mRNA-Seq library prep kits for Illumina (including AVITI). During the Lexogen QuantSeq workflow, raw reads were trimmed of poly-A tails and Illumina NextSeq adapters using Cutadapt [264], and resulting fragments of <20bp were removed.

Trimmed reads were aligned to the human reference genome (*Homo sapiens* GRCh38_ensembl_release_107_ERCC_SIRV) using the STAR aligner [265]. Aligned reads were passed to 'featureCounts' [266] in order to classify and count each alignment against the reference, using the appropriate annotation data.

The quality control of the sequencing was performed on the data for all 20 treated samples from four cell lines of HASMCs including (AZAC05, AZAC11, AZAC12, and 159). The extent of clustering of replicates and separation of treatments was presented using principal component analysis (PCA) plots (Figure 5.4), which showed that the genes related to the AZAC12 cell line clustered separately from the other cell lines. Upon further investigation by the DeepSeq team, they established that this cell line was mapped poorly to the human genome (Figure 5.4 A), and most genes mapped were to mycoplasma genes, indicative of a mycoplasma infection in these cells. In addition, the five samples related to AZAC12 cell line were shown to be lower than usual mapping rates and mapping rate % (Table 5.2). Therefore, the samples from this cell line were excluded from all subsequent analyses in this chapter. RNA-seq was therefore carried out using three cell lines (AZAC05, AZAC11, and 159) to eliminate potential mycoplasma effects that have been associated with the cell line AZAC12 (Table 5.2). The PCA plots also showed that the variability of the data and clustering changed when treatments with poly(I:C)- and CSE + poly (I:C)-stimulated iHBECs were added to HASMCs, indicating changes in gene expression in these treatment groups (Figure 5.4 B). Quality scores were shown to be good throughout the length of the reads, with minimal drop-off in quality towards the 3' ends. The total number of gene count analysis of filtered data revealed **13,224** genes were expressed in HASMCs at the basal level.

A

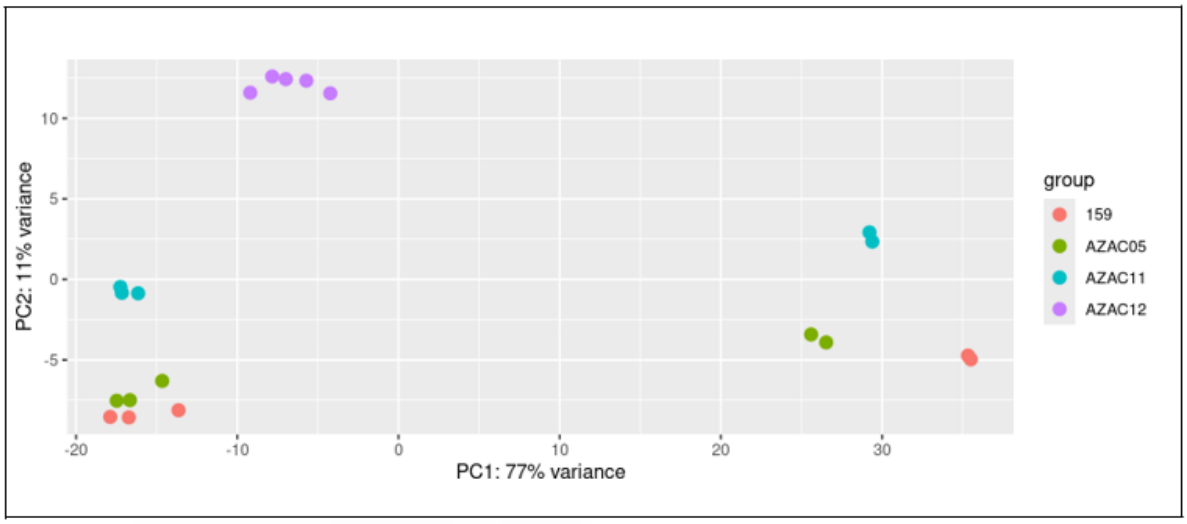

B

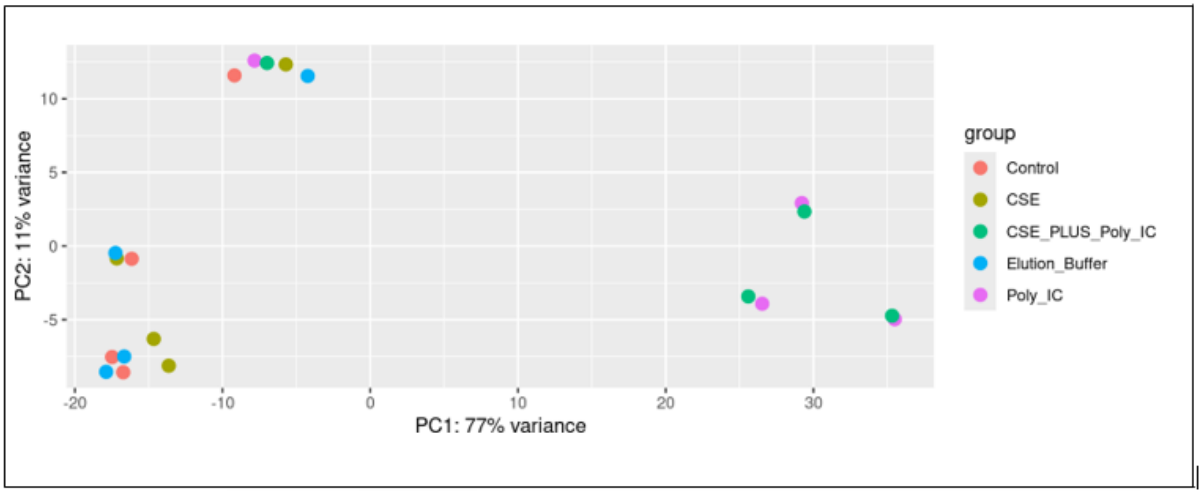

Figure 5.4 PCA plot showing the extent of clustering of A, different cell lines, and B, different treatments

Table 5.2 Statistics relating to the mapping of quality filtered input reads to the reference genome. Five samples related to AZAC12 cell line with lower than usual mapping rates, suggesting mycoplasma contamination, are highlighted in grey.

Sample	Cell line	Uniquely mapped	Uniquely mapped (%)	Average length
1	AZAC05	6693070	62.6	105
2	AZAC05	1615122	59.01	104
3	AZAC05	5026235	51.56	106
4	AZAC05	4831405	48.32	105
5	AZAC05	4575199	47.6	105
6	AZAC11	5878769	56.61	100
7	AZAC11	5808185	54.61	102
8	AZAC11	4219063	41.67	103
9	AZAC11	3804422	41.07	103
10	AZAC11	5309717	47.03	98
11	AZAC12	2444536	22.32	98
12	AZAC12	2081906	17.99	101
13	AZAC12	2572537	21.98	98
14	AZAC12	2305746	19.54	99
15	AZAC12	1396504	15.18	101
16	159	5690346	55.61	103
17	159	5069139	53.59	102
18	159	4944058	49.11	102
19	159	4778323	48.11	100
20	159	5312570	54.25	103

5.4.3.2 Elution buffer as vehicle control had minimal effect on HASMC gene expression compared to iHBECs cfDNA from the control group

cfDNA of iHBECs was isolated using elution buffer, serving as the vehicle control for all treatment groups, prior to HASMCs stimulation. Therefore, it was important to determine whether cfDNA released from iHBECs with no stimulation

affects HASMC gene expression. A differential expression analysis between HASMCs stimulated with elution buffer and HASMCs stimulated with iHBECs cfDNA from the control group, which had no treatment and referred as (control) in this study identified only two upregulated genes (Table 5.3/5.4, Figure 5.5) and no downregulated genes, confirming minimal effect of elution buffer alone on HASMC gene expression. The elution buffer condition was then used as the reference condition for all further comparisons.

Table 5.3 Summary of differential expression analysis for elution buffer vs. control

Gene Expression	*Gene Count*	*% of Total*	*Comment*
Total	13,224	100%	nonzero total read count
LFC >0 (up)	2	0.015%	adjusted *p*-value < 0.05
LFC <0 (down)	0	0%	adjusted *p*-value < 0.05
Outliers	6	0.45%	
Low counts	0	0	Mean count < 1

Table 5.4 UP-regulated genes, in contrast, Elution buffer vs. Control (significantly changed only, sorted by log fold change (LFC)).

Gene ID	Gene Name	baseMean	log2FoldChange	Adjusted P value
ENSG00000107262	BAG1	35.290	2.529	4.04E-07
ENSG00000099622	CIRBP	175.146	1.286	4.36E-02

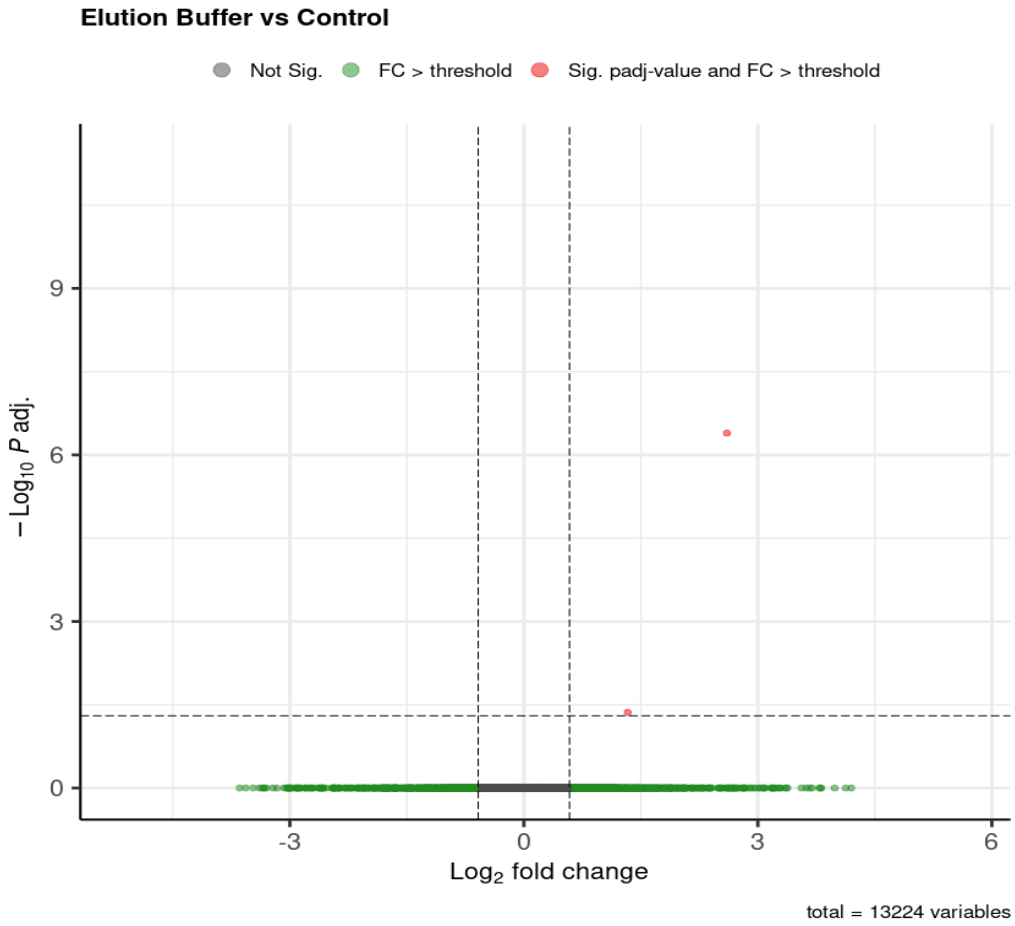

Figure 5.5 Volcano plot shows differentially expressed genes of HASMCs stimulated with elution buffer compared to cfDNA from a control group of iHBECs.

Plot of the total 13,224 genes expressed in HASMCs. The x-axis shows the $\log_2$ fold change, indicating the magnitude of expression difference, while the y-axis shows the $-\log_{10}$ adjusted p-value, reflecting statistical significance. Green dots represent variables with a fold change exceeding the defined threshold but not statistically significant (adjusted p-value). Red dots indicate variables that are both statistically significant (adjusted p-value) and meet the fold change threshold. Grey dots mark variables that did not meet significance or fold change cutoffs.

5.4.3.3 cfDNA of CSE-stimulated iHBECs had minimal effect on HASMC gene expression

cfDNA from CSE-simulated iHBECs significantly changed the expression of only a single gene in HASMCs (Table 5.5/6, Figure 5.6). BAG1

was the only gene that showed down-regulation when HASMCs were stimulated with cfDNA from CSE-stimulated iHBECs. Human BAG proteins include six BAG family members (BAG1- BAG6) known to be involved in various receptor signaling, such as growth factor and TNF receptor, as well as transcription activity, which play a role in regulating apoptosis [403]. In these results, the BAG1 gene was significantly reduced by 2.10-fold relative to the elution buffer.

Table 5.5 Summary of differential expression analysis for CSE vs. elution buffer

Gene Expression	*Gene Count*	*% of Total*	*Comment*
Total	13,224	100%	nonzero total read count
LFC >0 (up)	0	0%	adjusted *p*-value < 0.05
LFC <0 (down)	1	0.0076%	adjusted *p*-value < 0.05
Outliers	6	0.045%	
Low counts	0	0	Mean count < 1

Table 5.6 Top DOWN-regulated genes, in contrast, CSE vs. elution buffer (significantly changed only, sorted by LFC).

Gene ID	Gene Name	baseMean	log2FoldChange	Adjusted P value
ENSG00000107262	BAG1	35.290	-2.107	1.12E-03

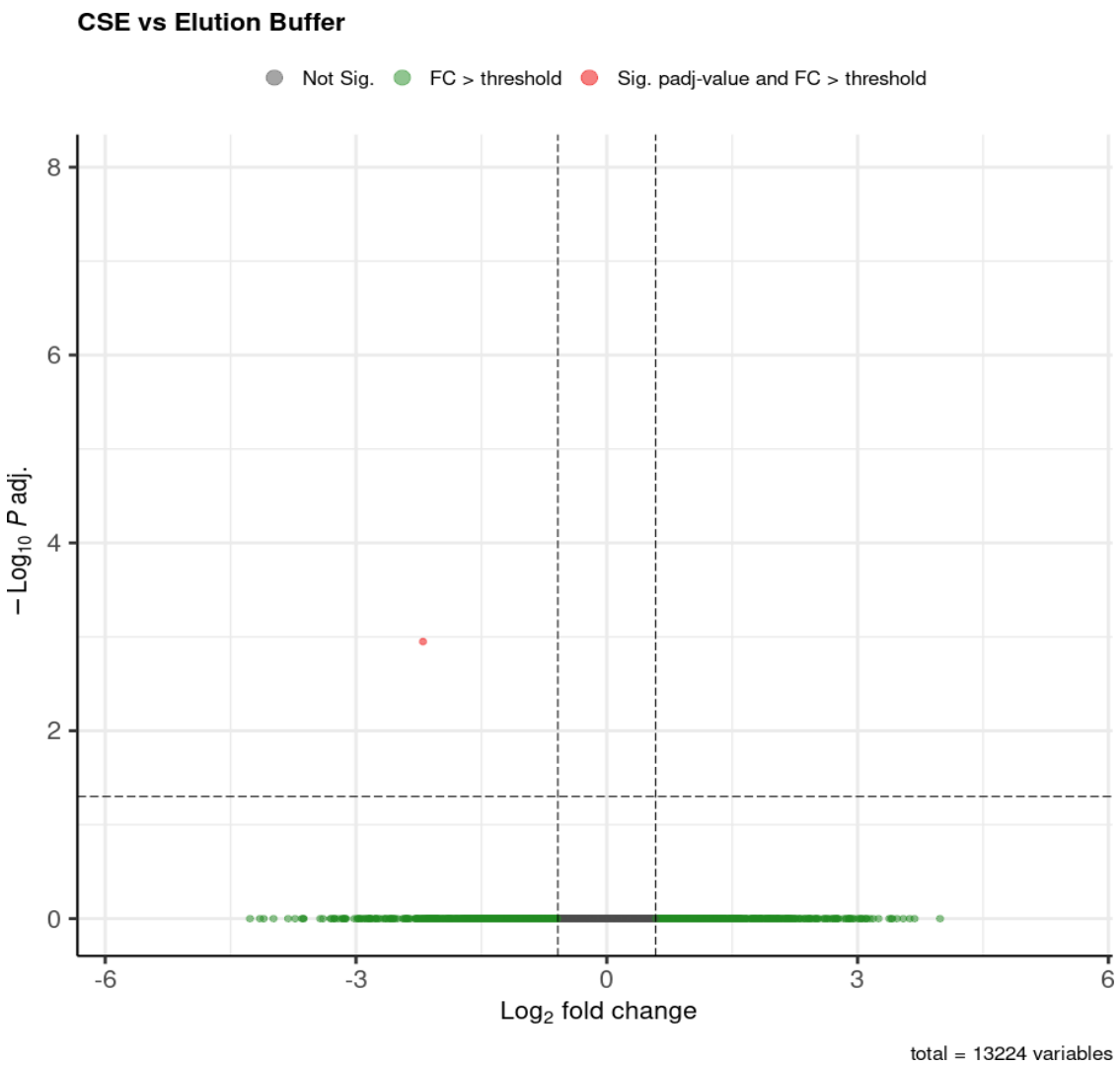

Figure 5.6 Volcano plot shows differentially expressed genes of HASMCs stimulated with cfDNA from CSE-stimulated iHBECs compared to elution buffer group.

Plot of the total 13,224 genes expressed in HASMCs. The x-axis shows the $\log_2$ fold change, indicating the magnitude of expression difference, while the y-axis shows the $-\log_{10}$ adjusted p-value, reflecting statistical significance. Green dots represent variables with a fold change exceeding the defined threshold but not statistically significant (adjusted p-value). Red dots indicate variables that are both statistically significant (adjusted p-value) and meet the fold change threshold. Grey dots mark variables that did not meet significance or fold change cutoffs.

5.4.3.4 cfDNA of poly (I:C)-stimulated iHBECs had a significant effect on HASMC gene expression

cfDNA from poly (I:C)-simulated iHBECs caused significant differential expression of 915 genes (3 HASMCs donor, adjusted p value<0.05, and fold change cut off is 0) (Table 5.7). 698 genes were significantly upregulated and 217 downregulated (Figure 5.7). The top 20 most significant by largest fold change for upregulated and downregulated genes are shown in Table 5.8 and Table 5.9 (full gene lists are available in (Appendix 7.13.1)). The maximum fold change in the upregulated genes was 12.345 for gene CXCL9. CXCL9 plays a key role in antitumor immunity through recruiting and proliferating immune cells [404]. CXCL9, which is considered a Th1-type chemokine, increases significantly in eosinophilic and severe asthma, and its expression is enhanced by IL-27 and IL-13 interactions. Increased serum levels of CXCL9 are related with AHR, acute exacerbations, and disease severity, suggesting a role not just in Type 1 inflammation but also in the complex inflammatory mechanisms underlying asthma pathogenesis [405, 406]. The Guanylate-Binding Protein 5 gene (GBP5) was also found among the top upregulated gene. GBP5 gene is member of the guanylate-binding protein (GBP) family, which are interferon-inducible GTPases involved in host defense and immune responses. GBP5 expression was markedly increased in influenza A virus-infected HBECs A549 cell line, and in patients with influenza, highlighting its role in antiviral defense and its potential significance in lung immune responses during viral infection [407]The maximum fold change for downregulated genes was -5.797 for gene Cystin-1 known as (CYS1), which involved in driving allergic inflammation and the progression of allergic respiratory diseases [408], and contributes in driving nasal epithelial cell recruitment in individuals with chronic eosinophilic rhinosinusitis [409].

Table 5.7 Summary of differential expression analysis for Poly (I:C) vs. elution buffer

Gene Expression	Gene Count	% of Total	Comment
Total	13,224	100%	nonzero total read count
LFC >0 (up)	698	5.3%	adjusted *p*-value < 0.05
LFC <0 (down)	217	1.6%	adjusted *p*-value < 0.05
Outliers	6	0.045%	
Low counts	2,051	16%	Mean count < 1

Table 5.8 Top 20 UP-regulated genes, in contrast, Poly(I:C) vs. elution buffer (significantly changed only, sorted by LFC).

Gene ID	Gene Name	baseMean	log2FoldChange	Adjusted P value
ENSG00000138755	CXCL9	190.832	12.345	3.52E-08
ENSG00000154451	GBP5	114.655	11.803	8.11E-15
ENSG00000134321	RSAD2	1344.951	11.369	1.50E-16
ENSG00000271503	CCL5	1155.738	11.269	3.38E-42
ENSG00000131203	IDO1	83.824	11.250	9.11E-09
ENSG00000169248	CXCL11	1157.170	10.648	2.14E-11
ENSG00000169245	CXCL10	1402.034	10.485	1.75E-13
ENSG00000133328	PLAAT2	38.102	10.157	1.79E-11
ENSG00000183486	MX2	232.015	9.973	2.93E-18
ENSG00000134326	CMPK2	199.388	9.765	1.22E-17
ENSG00000135114	OASL	287.201	9.489	1.12E-15
ENSG00000168389	MFSD2A	19.776	9.141	1.58E-08
ENSG00000171860	C3AR1	17.280	9.018	1.42E-07
ENSG00000104951	IL4I1	54.833	8.699	1.83E-10
ENSG00000081041	CXCL2	14.045	8.673	1.72E-06
ENSG00000162654	GBP4	395.585	8.604	7.88E-39
ENSG00000131979	GCH1	150.707	8.385	7.89E-21
ENSG00000169429	CXCL8	76.023	8.367	7.23E-10
ENSG00000163734	CXCL3	51.919	8.272	3.07E-06
ENSG00000089127	OAS1	227.735	8.194	1.94E-34

Table 5.9 Top 20 DOWN-regulated genes, in contrast, Poly(I:C) vs. elution buffer (significantly changed only, sorted by LFC).

Gene ID	Gene Name	baseMean	log2FoldChange	Adjusted P value
ENSG00000205795	CYS1	8.201	-5.797	9.53E-04
ENSG00000148541	FAM13C	7.008	-4.184	7.30E-03
ENSG00000105048	TNNT1	4.496	-4.016	4.68E-02
ENSG00000138160	KIF11	7.600	-3.884	1.32E-02
ENSG00000120693	SMAD9	27.501	-3.600	2.07E-07
ENSG00000064655	EYA2	6.990	-3.432	4.74E-02
ENSG00000160345	PIERCE1	5.370	-3.354	3.89E-02
ENSG00000126861	OMG	61.558	-3.343	1.13E-09
ENSG00000172346	CSDC2	10.610	-3.289	7.08E-03
ENSG00000276600	RAB7B	16.040	-3.277	3.80E-04
ENSG00000105784	RUNDC3B	20.627	-3.273	1.32E-03
ENSG00000170899	GSTA4	42.864	-3.272	3.15E-06
ENSG00000196932	TMEM26	14.74	-3.255	6.52E-03
ENSG00000154102	C16orf74	7.950	-3.232	2.82E-02
ENSG00000147655	RSPO2	13.472	-3.096	2.39E-02
ENSG00000128602	SMO	13.576	-2.960	9.39E-03
ENSG00000103034	NDRG4	11.498	-2.833	6.03E-03
ENSG00000243244	STON1	28.554	-2.699	4.53E-05
ENSG00000144199	FAHD2B	7.107	-2.679	3.93E-02
ENSG00000216775	ENSG00000216775	6.090	-2.629	2.91E-02

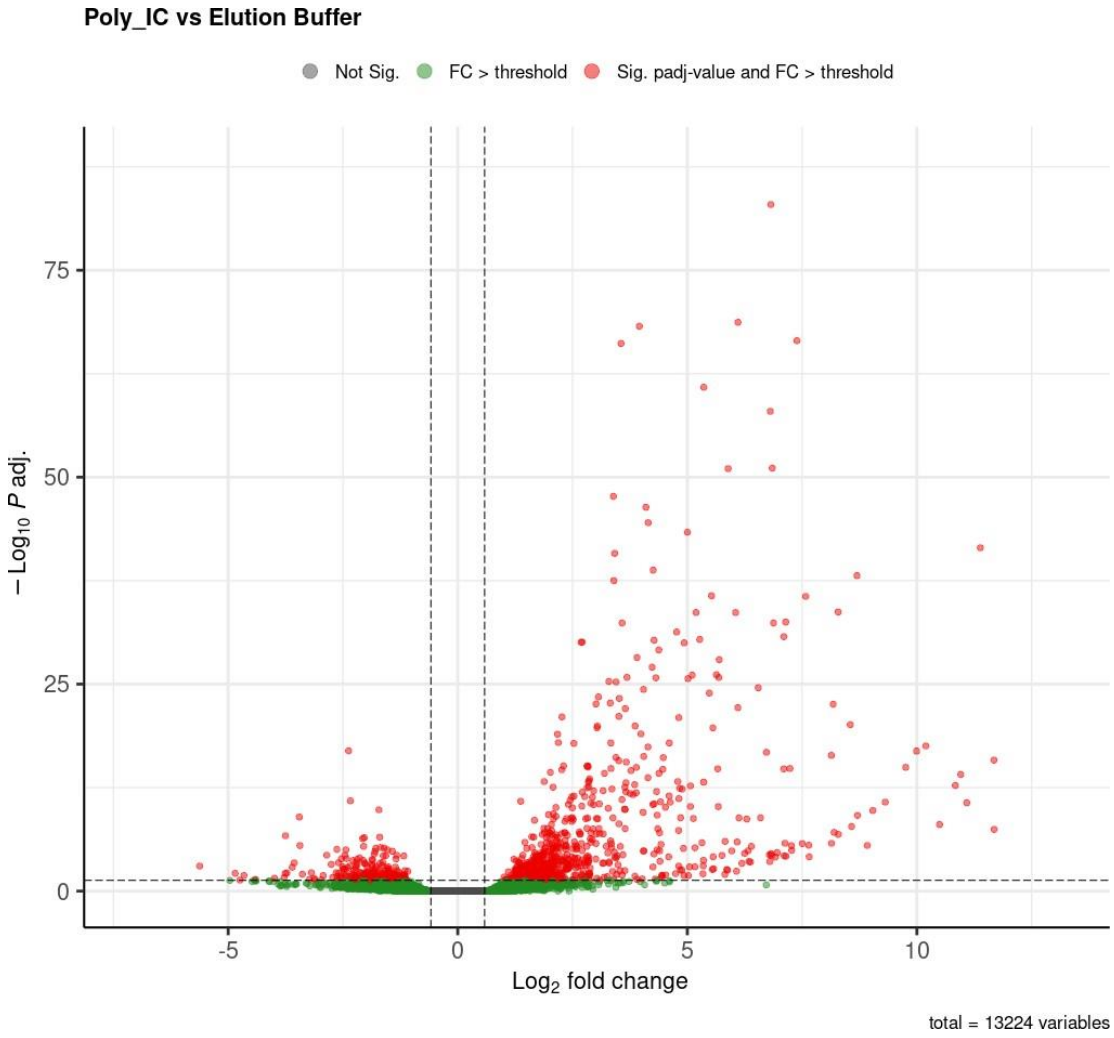

Figure 5 7 Volcano plot shows differentially expressed genes of HASMCs stimulated with cfDNA from poly (I:C)-stimulated iHBECs compared to elution buffer group.

Plot of the total 13,224 genes expressed in HASMCs. The x-axis shows the $\log_2$ fold change, indicating the magnitude of expression difference, while the y-axis shows the $-\log_{10}$ adjusted p-value, reflecting statistical significance. Green dots represent variables with a fold change exceeding the defined threshold but not statistically significant (adjusted p-value). Red dots indicate variables that are both statistically significant (adjusted p-value) and meet the fold change threshold, including 698 upregulated and 217 downregulated genes. Grey dots mark variables that did not meet significance or fold change cutoffs.

Separate pathway analysis of the significantly upregulated and downregulated genes was used to identify overarching potential biological functionality of differentially expressed genes. For upregulated genes pathways grouped by

biological process (Figure 5.8 A), molecular function (Figure 5.8 B), cellular component (Figure 5.8 C) and KEGG pathways (Figure 5.8 D) identified defence response to virus among 816 pathways, double-stranded RNA binding among 40 pathways, cytoplasmic ribonucleoprotein granule among 16 pathways, and TNF signaling pathway among 57 pathways, as the most significant pathways sorted by adjusted P value for upregulated pathways respectively. While, for downregulated genes pathways grouped by biological process (Figure 5.9 A), molecular function (Figure 5.9 B), cellular component (Figure 5.9 C) and KEGG pathways (Figure 5.9 D) identified regulation of mRNA splicing among 10 pathways, rRNA binding among 2 pathways, peroxisome among 14 pathways, and purine metabolism as the most significant downregulated pathways respectively.

Defence response to virus was the most significant pathway for biological process suggesting that HASMCs activated antiviral immune mechanisms for mounting an innate and adaptive immune response to cfDNA of poly (I:C)-induced iHBECs aimed to recognizing and clearing viral infection. Among these pathways, double stranded RNA binding pathway was seen as the most significant molecular function pathway for upregulated genes which suggests an important role of dsRNA binding in viral defense and innate immune responses. TNF signaling pathway was also enriched among the KEGG pathways for upregulated genes which might indicate the role of TNF in inflammatory signaling and apoptotic responses that contribute to asthma pathogenesis. TNF-α has a pivotal role in asthma, which is released during allergic responses, especially in the presence of IgE. It promotes airway inflammation by increasing the expression of adhesion molecules, thereby facilitating the migration of neutrophils and eosinophils into the airway wall [410, 411].

On the other hand, peroxisome coordinates with other organelles to modulate lipid metabolism and oxidative stress signaling, thereby affecting diverse cellular processes [412]. Peroxisome in our study was the most significant downregulated pathway for cellular components suggesting that HASMCs might have a reduced capacity for lipid metabolism and antioxidant defense in response to cfDNA of poly (I:C)-induced iHBECs which might lead to impaired lipid handling, or weakened antioxidant defence, all of which could contribute to airway inflammation. Purine metabolism was found to be associated with downregulated pathway in KEGG pathway. Purine metabolism was the most significantly influenced in ovalbumin-induced asthma in mice [413]. All of these suggest a potential involvement of different pathways in regulated gene expressions of HASMCs in response to cfDNA of poly (I:C)-induced iHBECs.

A

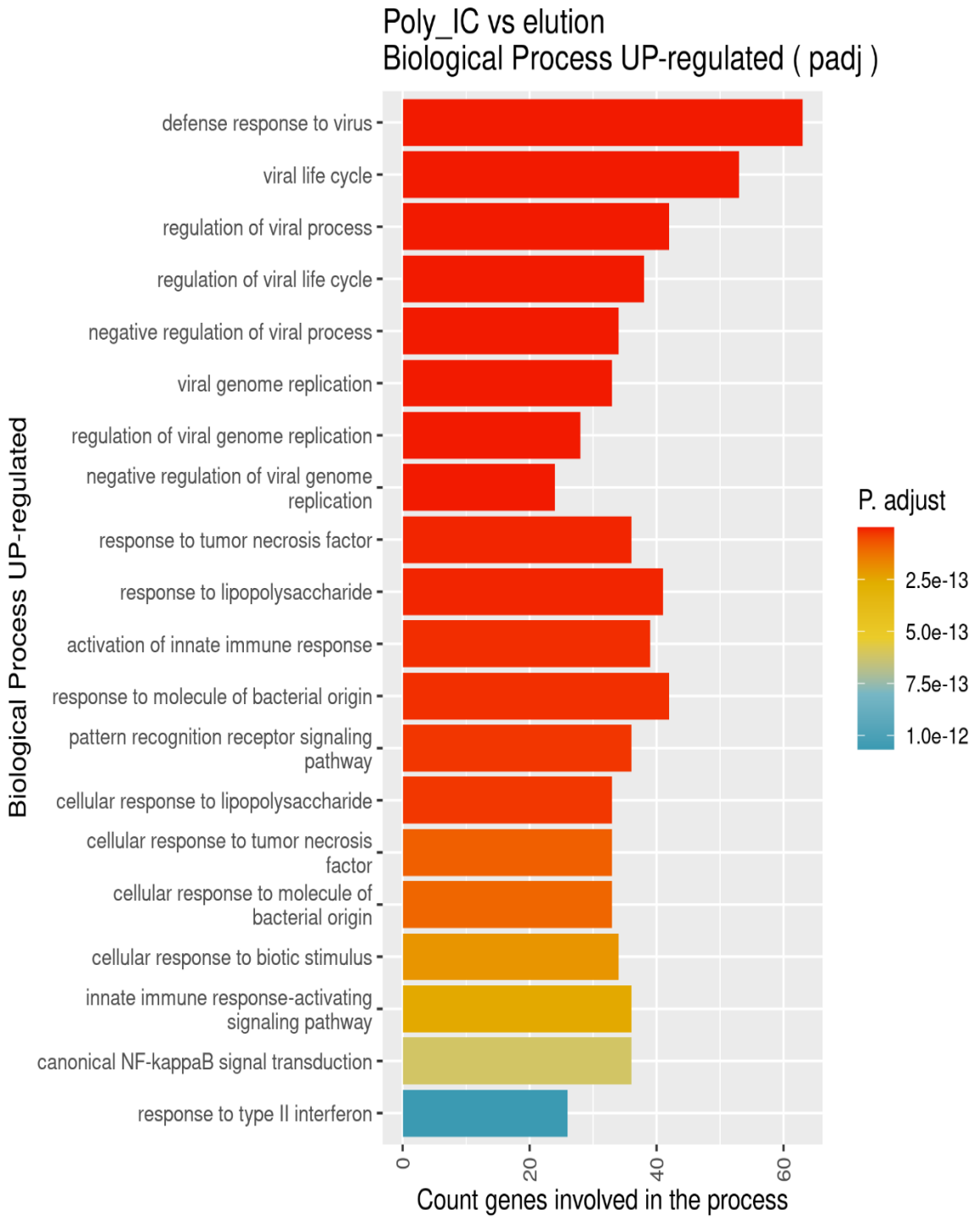
Poly_IC vs elution
Biological Process UP-regulated (padj)
defense response to virus
viral life cycle
regulation of viral process
regulation of viral life cycle
negative regulation of viral process
viral genome replication
regulation of viral genome replication
negative regulation of viral genome replication
response to tumor necrosis factor
response to lipopolysaccharide
activation of innate immune response
response to molecule of bacterial origin
pattern recognition receptor signaling pathway
cellular response to lipopolysaccharide
cellular response to tumor necrosis factor
cellular response to molecule of bacterial origin
cellular response to biotic stimulus
innate immune response-activating signaling pathway
canonical NF-kappaB signal transduction
response to type II interferon
Biological Process UP-regulated
0
20
40
60
Count genes involved in the process
P. adjust
2.5e-13
5.0e-13
7.5e-13
1.0e-12

B

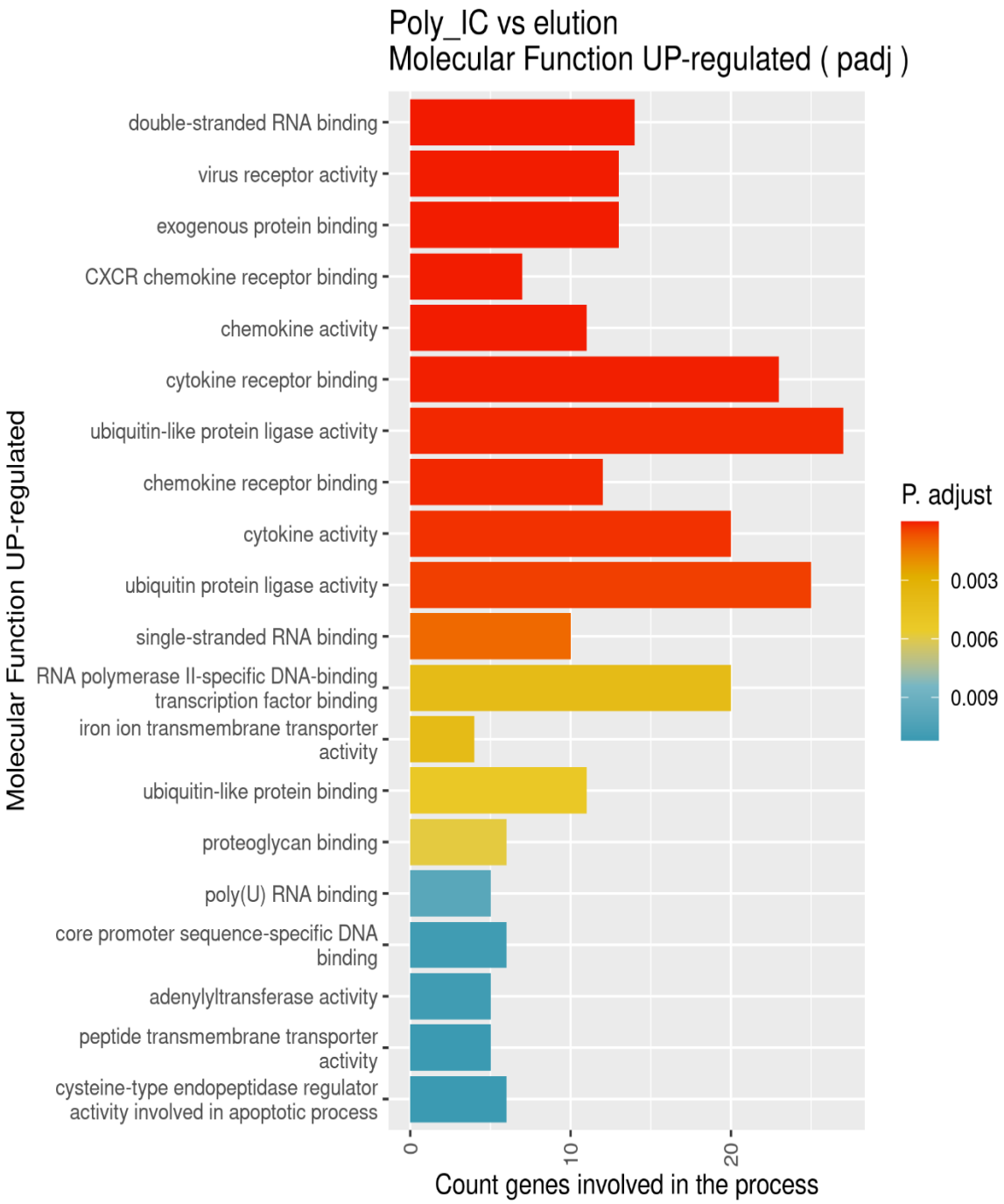
Poly_IC vs elution
Molecular Function UP-regulated (padj)
Molecular Function UP-regulated
double-stranded RNA binding
virus receptor activity
exogenous protein binding
CXCR chemokine receptor binding
chemokine activity
cytokine receptor binding
ubiquitin-like protein ligase activity
chemokine receptor binding
cytokine activity
ubiquitin protein ligase activity
single-stranded RNA binding
RNA polymerase II-specific DNA-binding transcription factor binding
iron ion transmembrane transporter activity
ubiquitin-like protein binding
proteoglycan binding
poly(U) RNA binding
core promoter sequence-specific DNA binding
adenylyltransferase activity
peptide transmembrane transporter activity
cysteine-type endopeptidase regulator activity involved in apoptotic process
0
10
20
Count genes involved in the process
P. adjust
0.003
0.006
0.009

c

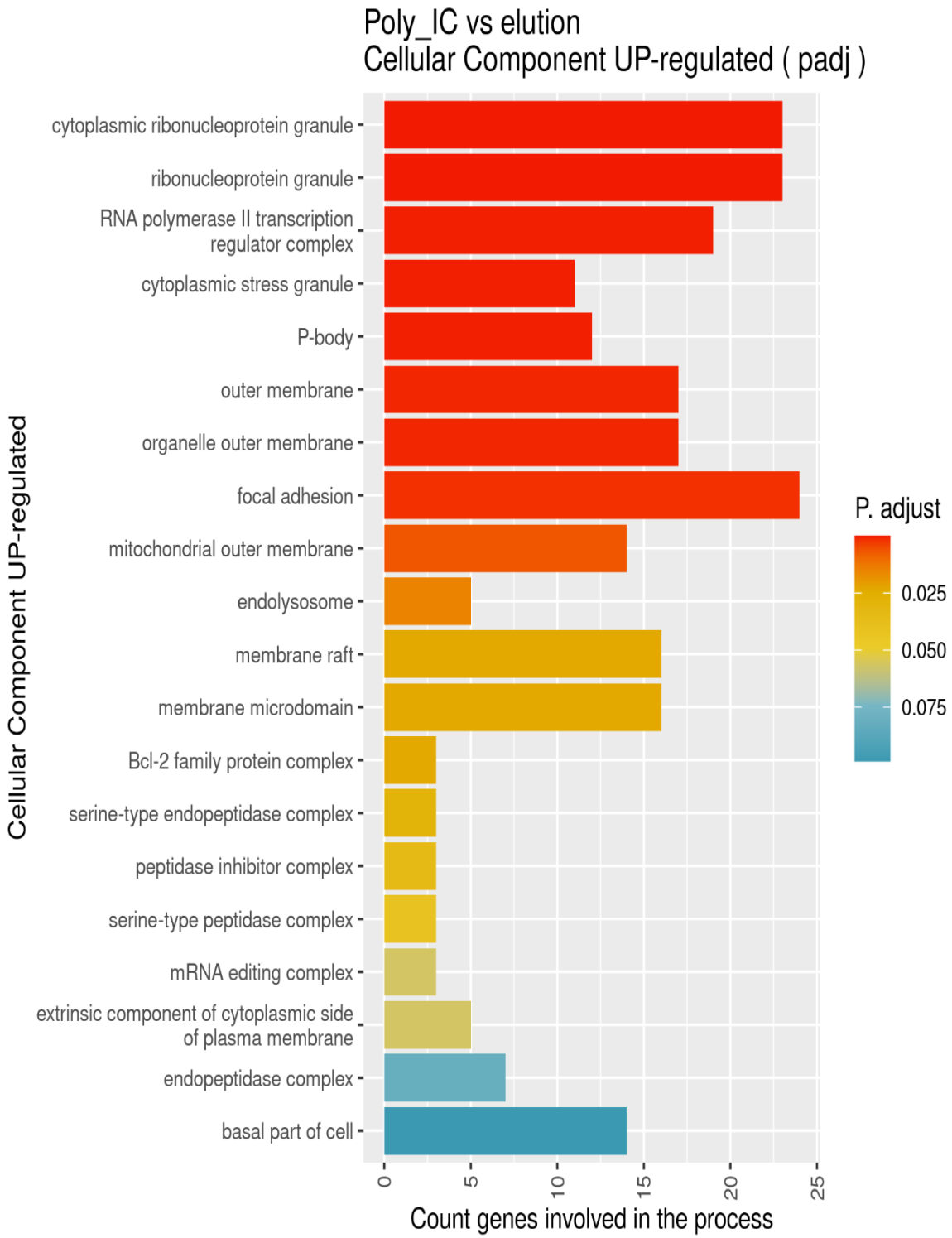
Poly_IC vs elution
Cellular Component UP-regulated (padj)
cytoplasmic ribonucleoprotein granule
ribonucleoprotein granule
RNA polymerase II transcription regulator complex
cytoplasmic stress granule
P-body
outer membrane
organelle outer membrane
focal adhesion
mitochondrial outer membrane
endolysosome
membrane raft
membrane microdomain
Bcl-2 family protein complex
serine-type endopeptidase complex
peptidase inhibitor complex
serine-type peptidase complex
mRNA editing complex
extrinsic component of cytoplasmic side of plasma membrane
endopeptidase complex
basal part of cell
Cellular Component UP-regulated
0
5
10
15
20
25
Count genes involved in the process
P. adjust
0.025
0.050
0.075

D

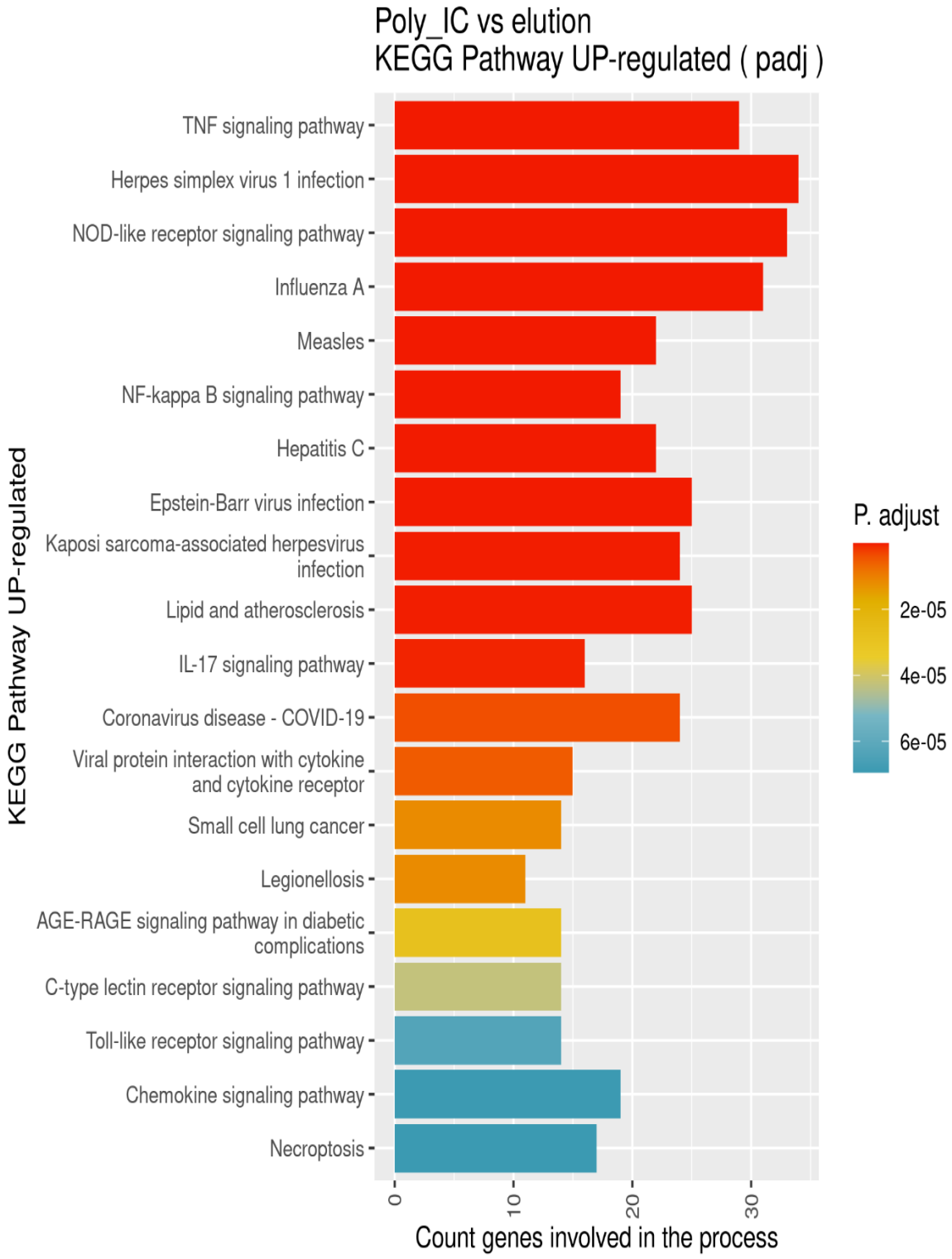

Figure 5.8 Counts of significantly UP-REGULATED genes involved in (A) BIOLOGICAL PROCESS, (B) MOLECULAR FUNCTION, (C) CELLULAR COMPONENT, and (D) KEGG PATHWAY in the contrast Poly (I:C) vs. elution buffer.

Genes were selected for GO and KEGG analysis based on significant differential expression (p.adj < 0.05).

A

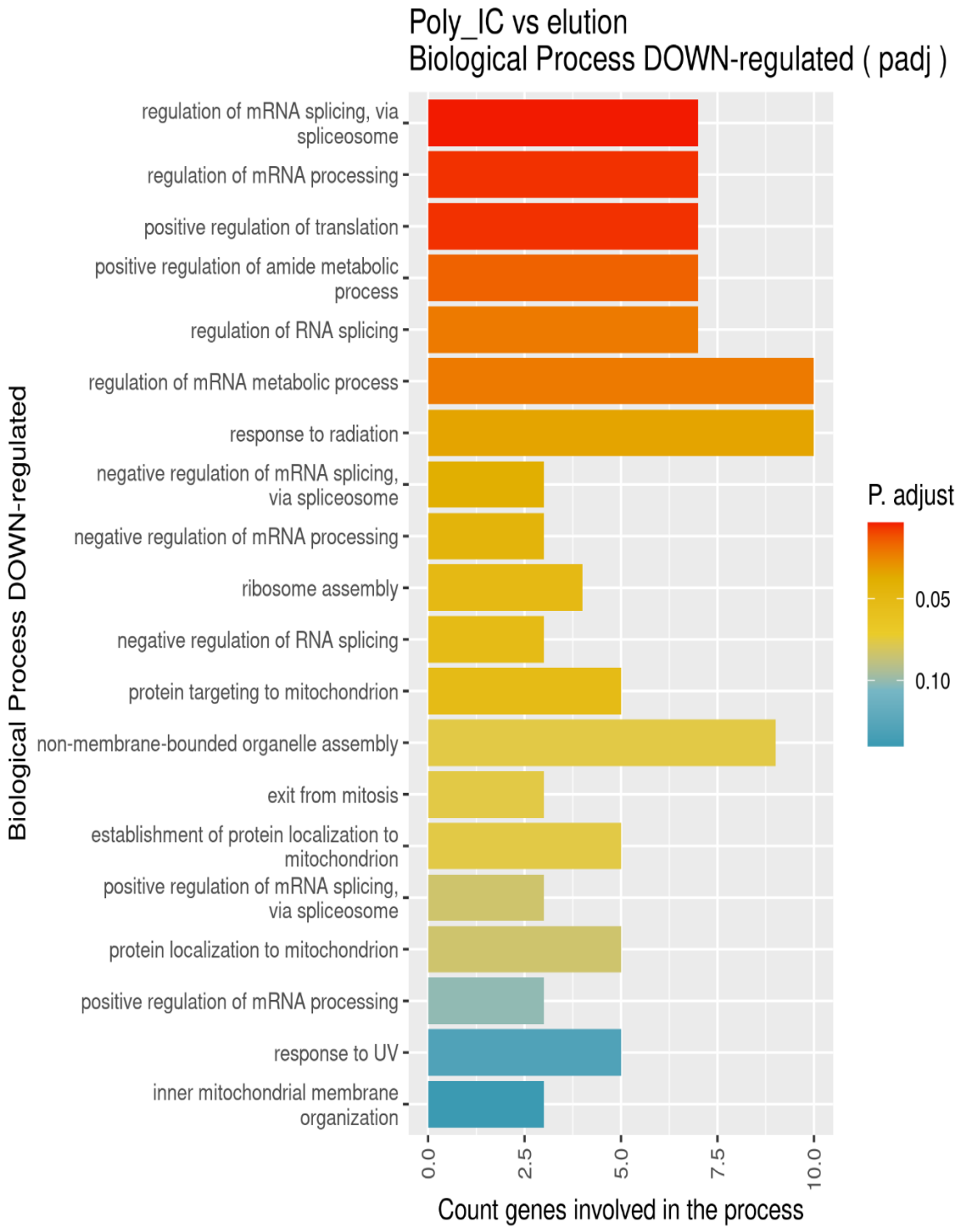
Poly_IC vs elution
Biological Process DOWN-regulated (padj)
Biological Process DOWN-regulated
regulation of mRNA splicing, via spliceosome
regulation of mRNA processing
positive regulation of translation
positive regulation of amide metabolic process
regulation of RNA splicing
regulation of mRNA metabolic process
response to radiation
negative regulation of mRNA splicing, via spliceosome
negative regulation of mRNA processing
ribosome assembly
negative regulation of RNA splicing
protein targeting to mitochondrion
non-membrane-bounded organelle assembly
exit from mitosis
establishment of protein localization to mitochondrion
positive regulation of mRNA splicing, via spliceosome
protein localization to mitochondrion
positive regulation of mRNA processing
response to UV
inner mitochondrial membrane organization
0.0
2.5
5.0
7.5
10.0
Count genes involved in the process
P. adjust
0.05
0.10

B

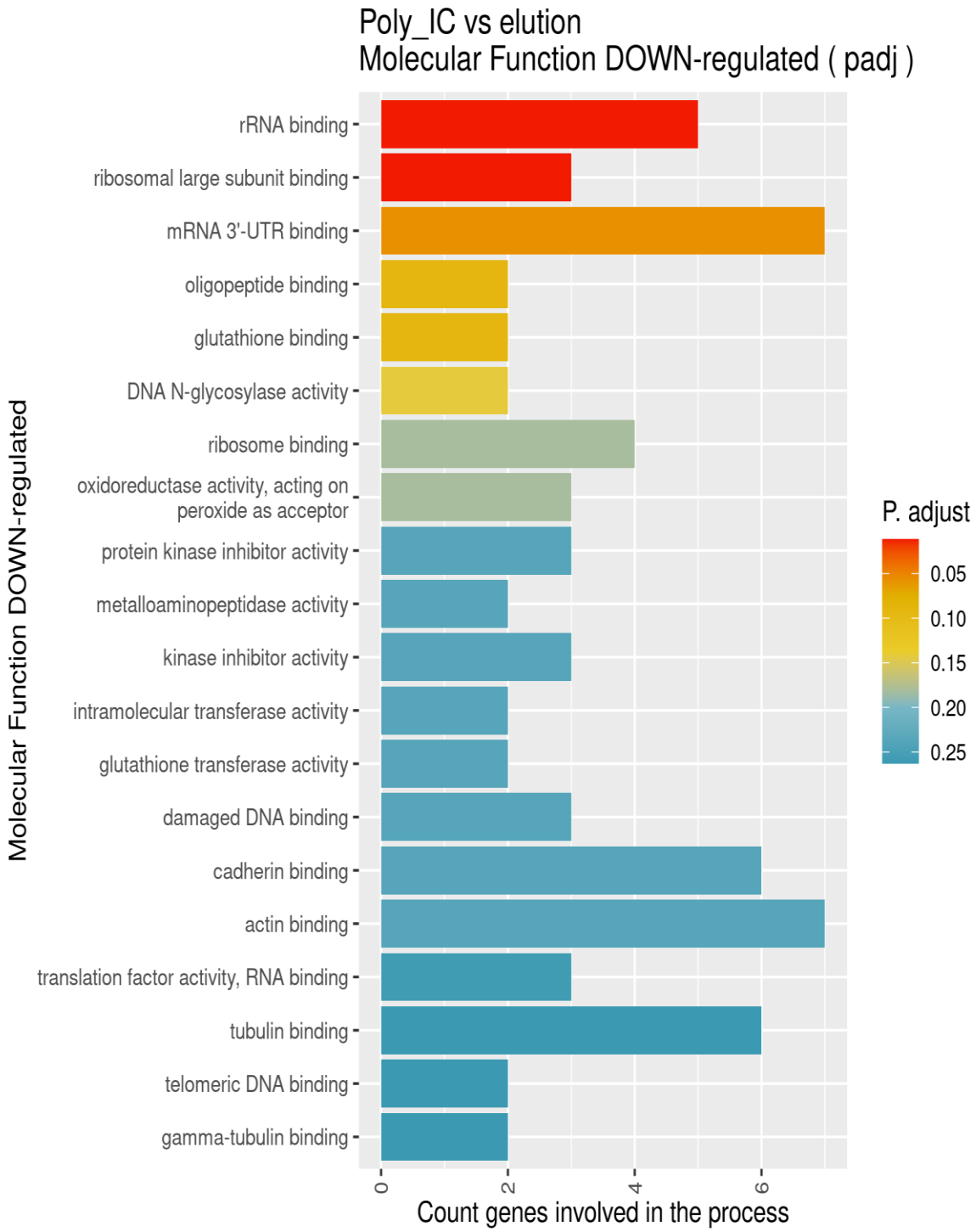
Poly_IC vs elution
Molecular Function DOWN-regulated (padj)
Molecular Function DOWN-regulated
rRNA binding
ribosomal large subunit binding
mRNA 3'-UTR binding
oligopeptide binding
glutathione binding
DNA N-glycosylase activity
ribosome binding
oxidoreductase activity, acting on peroxide as acceptor
protein kinase inhibitor activity
metalloaminopeptidase activity
kinase inhibitor activity
intramolecular transferase activity
glutathione transferase activity
damaged DNA binding
cadherin binding
actin binding
translation factor activity, RNA binding
tubulin binding
telomeric DNA binding
gamma-tubulin binding
0
2
4
6
Count genes involved in the process
P. adjust
0.05
0.10
0.15
0.20
0.25

c

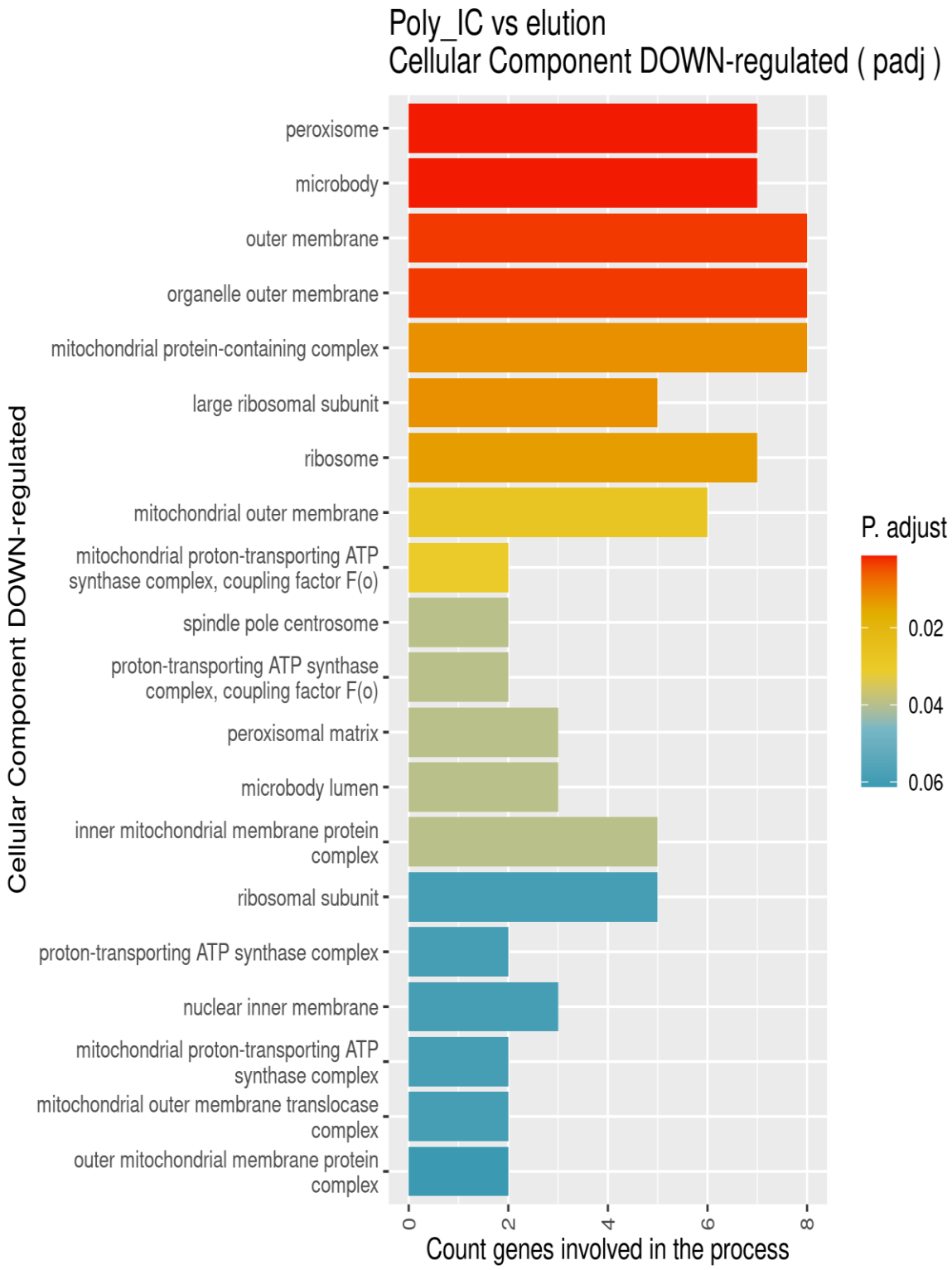
Poly_IC vs elution
Cellular Component DOWN-regulated (padj)
Cellular Component DOWN-regulated
peroxisome
microbody
outer membrane
organelle outer membrane
mitochondrial protein-containing complex
large ribosomal subunit
ribosome
mitochondrial outer membrane
mitochondrial proton-transporting ATP synthase complex, coupling factor F(o)
spindle pole centrosome
proton-transporting ATP synthase complex, coupling factor F(o)
peroxisomal matrix
microbody lumen
inner mitochondrial membrane protein complex
ribosomal subunit
proton-transporting ATP synthase complex
nuclear inner membrane
mitochondrial proton-transporting ATP synthase complex
mitochondrial outer membrane translocase complex
outer mitochondrial membrane protein complex
0
2
4
6
8
Count genes involved in the process
P. adjust
0.02
0.04
0.06

D

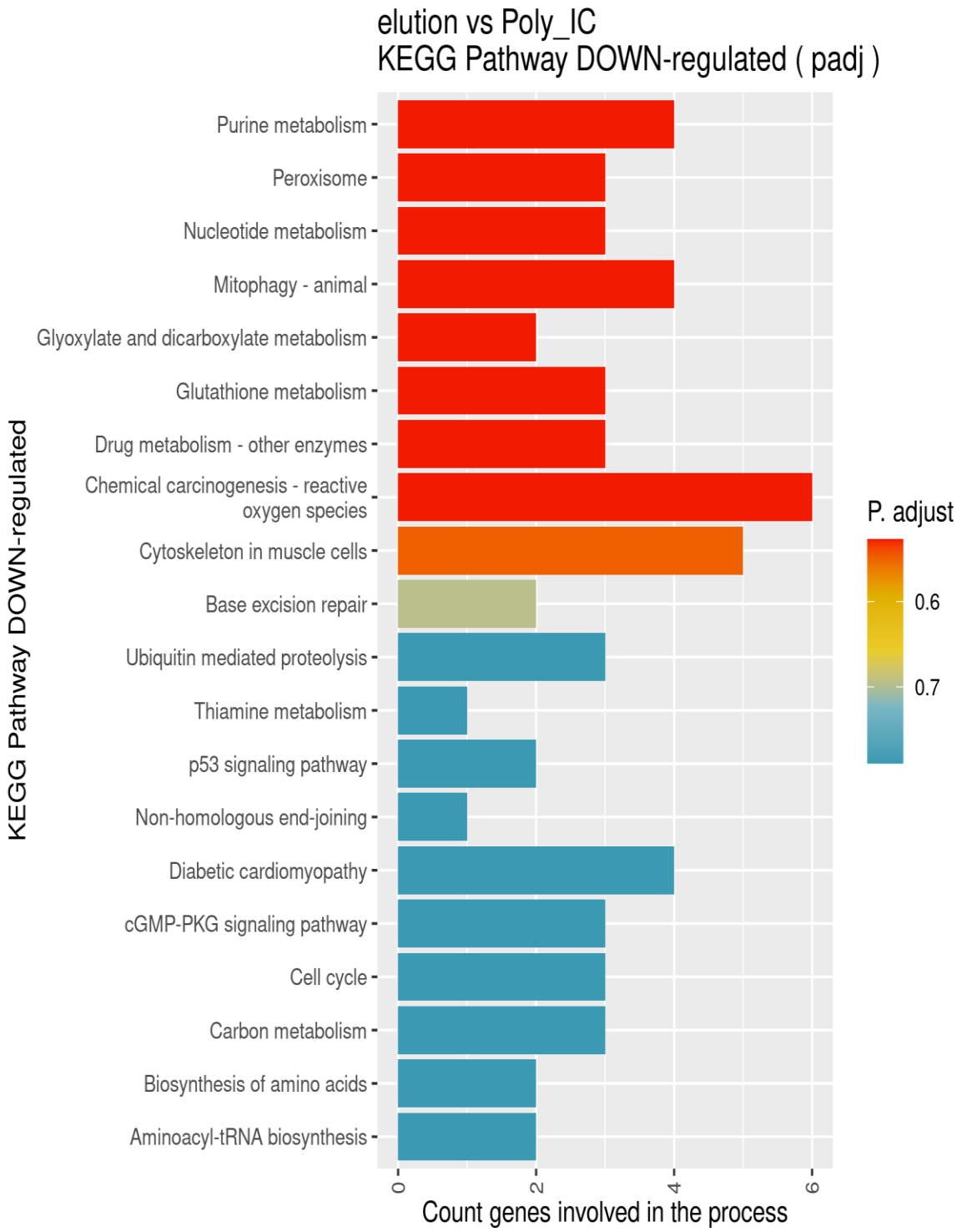

Figure 5.9 Counts of significantly DOWN-REGULATED genes involved in (A) BIOLOGICAL PROCESS, (B) MOLECULAR FUNCTION, (C) CELLULAR COMPONENT, and (D) KEGG PATHWAY in the contrast Poly (I:C) vs. elution buffer.

Genes were selected for GO and KEGG analysis based on significant differential expression (p.adj < 0.05).

5.4.3.5 cfDNA of CSE + poly (I:C)-stimulated iHBECs induced distinct transcriptional changes in HASMC gene expression

cfDNA isolated from CSE+poly (I:C)-simulated iHBECs also caused significant differential expression of 833 genes (3 HASMCs donor, adjusted p value<0.05, and fold change cut off is 0) (Table 5.10), relative to cfDNA from elution buffer-stimulated iHBECs. 652 genes were significantly upregulated and 181 downregulated (Figure 5.10). The top 20 most significant by largest fold change for upregulated and downregulated genes are shown in (Table 5.11 and Table 5.12), (full gene lists are available in (Appendix 7.13.2)). The maximum fold change in the upregulated genes was 12.359, for gene CXCL9, which was the same gene that was shown previously for cfDNA of poly (I:C)-stimulated iHBECs group (Section 5.4.3.4). C-C motif chemokine ligand 5 (CCL5) gene, also known as RANTES was among the top upregulated genes of HASMCs stimulated with cfDNA of CSE +poly (I:C)-stimulated iHBECs. The CCL5 gene plays a role in type 1 (T1) inflammation in asthma, as demonstrated by its strong association with T1 chemokines such as CXCL9 and CXCL10, and has a role in the inflammatory processes occurring in the lungs of asthmatic patients [414] and during COPD exacerbation, contributing to inflammation and airway remodeling [415]. The maximum fold change for down regulated genes was -4.569 for gene SMCO3, which refers to single-pass membrane protein with coiled coil domain 3 [416]. This gene was not well investigated in the available literature. However, it's the most significant downregulation gene in our study, making it a potential target for future research, which could offer novel insights into the molecular mechanisms underlying HASMCs' responses to HBECs injury and cfDNA-mediated signalling.

Table 5.10 Summary of differential expression analysis for CSE + Poly (I:C) vs. elution buffer

Gene Expression	Gene Count	% of Total	Comment
Total	13,224	100%	nonzero total read count
LFC >0 (up)	652	4.9%	adjusted *p*-value < 0.05
LFC <0 (down)	181	1.4%	adjusted *p*-value < 0.05
Outliers	6	0.045%	
Low counts	770	5.8%	Mean count < 1

Table 5.11 Top 20 UP-regulated genes, in contrast, CSE + poly (I:C) vs. elution buffer (significantly changed only, sorted by LFC).

Gene ID	Gene Name	baseMean	log2FoldChange	Adjusted P value
ENSG00000138755	CXCL9	190.832	12.359	3.84E-08
ENSG00000154451	GBP5	114.655	11.815	9.08E-15
ENSG00000271503	CCL5	1155.738	11.461	1.17E-43
ENSG00000134321	RSAD2	1344.951	11.387	1.49E-16
ENSG00000131203	IDO1	83.824	11.272	9.61E-09
ENSG00000169248	CXCL11	1157.170	10.664	2.24E-11
ENSG00000169245	CXCL10	1402.034	10.565	1.29E-13
ENSG00000133328	PLAAT2	38.102	10.282	1.04E-11
ENSG00000183486	MX2	232.015	9.886	6.68E-18
ENSG00000134326	CMPK2	199.388	9.704	2.37E-17
ENSG00000135114	OASL	287.201	9.518	9.63E-16
ENSG00000171860	C3AR1	17.280	8.901	2.54E-07

ENSG00000168389	MFSD2A	19.776	8.697	1.06E-07
ENSG00000162654	GBP4	395.585	8.665	2.28E-39
ENSG00000104951	IL4I1	54.833	8.420	9.20E-10
ENSG00000131979	GCH1	150.707	8.328	1.55E-20
ENSG00000089127	OAS1	227.735	8.292	2.38E-35
ENSG00000204642	HLA-F	38.774	8.197	1.27E-08
ENSG00000169429	CXCL8	76.023	8.174	2.15E-09
ENSG00000163734	CXCL3	51.919	8.071	6.20E-06

Table 5.12 Top 20 DOWN-regulated genes, in contrast, CSE + poly (I:C) vs. elution buffer (significantly changed only, sorted by LFC).

Gene ID	Gene Name	baseMean	log2FoldChange	Adjusted P value
ENSG00000179256	SMCO3	4.089	-4.569	1.34E-02
ENSG00000126861	OMG	61.558	-3.889	1.75E-11
ENSG00000186310	NAP1L3	6.557	-3.793	1.74E-02
ENSG00000150756	ATPSCKMT	5.647	-3.328	4.28E-02
ENSG00000176909	MAMSTR	3.727	-3.315	4.85E-02
ENSG00000243244	STON1	28.554	-3.110	3.47E-06
ENSG00000103034	NDRG4	11.498	-2.963	3.73E-03
ENSG00000147655	RSPO2	13.472	-2.922	3.18E-02
ENSG00000183496	MEX3B	13.317	-2.798	7.28E-03
ENSG00000180354	MTURN	45.195	-2.746	8.49E-07
ENSG00000148541	FAM13C	7.008	-2.718	2.41E-02
ENSG00000113391	FAM172A	104.647	-2.639	1.49E-15
ENSG00000204856	FAM216A	13.416	-2.633	2.57E-03
ENSG00000126785	RHOJ	21.090	-2.591	4.18E-04
ENSG00000159685	CHCHD6	9.713	-2.567	2.91E-02
ENSG00000084693	AGBL5	28.651	-2.564	2.94E-05
ENSG00000168268	NT5DC2	18.880	-2.556	2.36E-03
ENSG00000172346	CSDC2	10.610	-2.554	1.55E-02
ENSG00000216775	ENSG00000216775	6.090	-2.477	3.42E-02
ENSG00000206052	DOK6	14.435	-2.457	6.03E-03

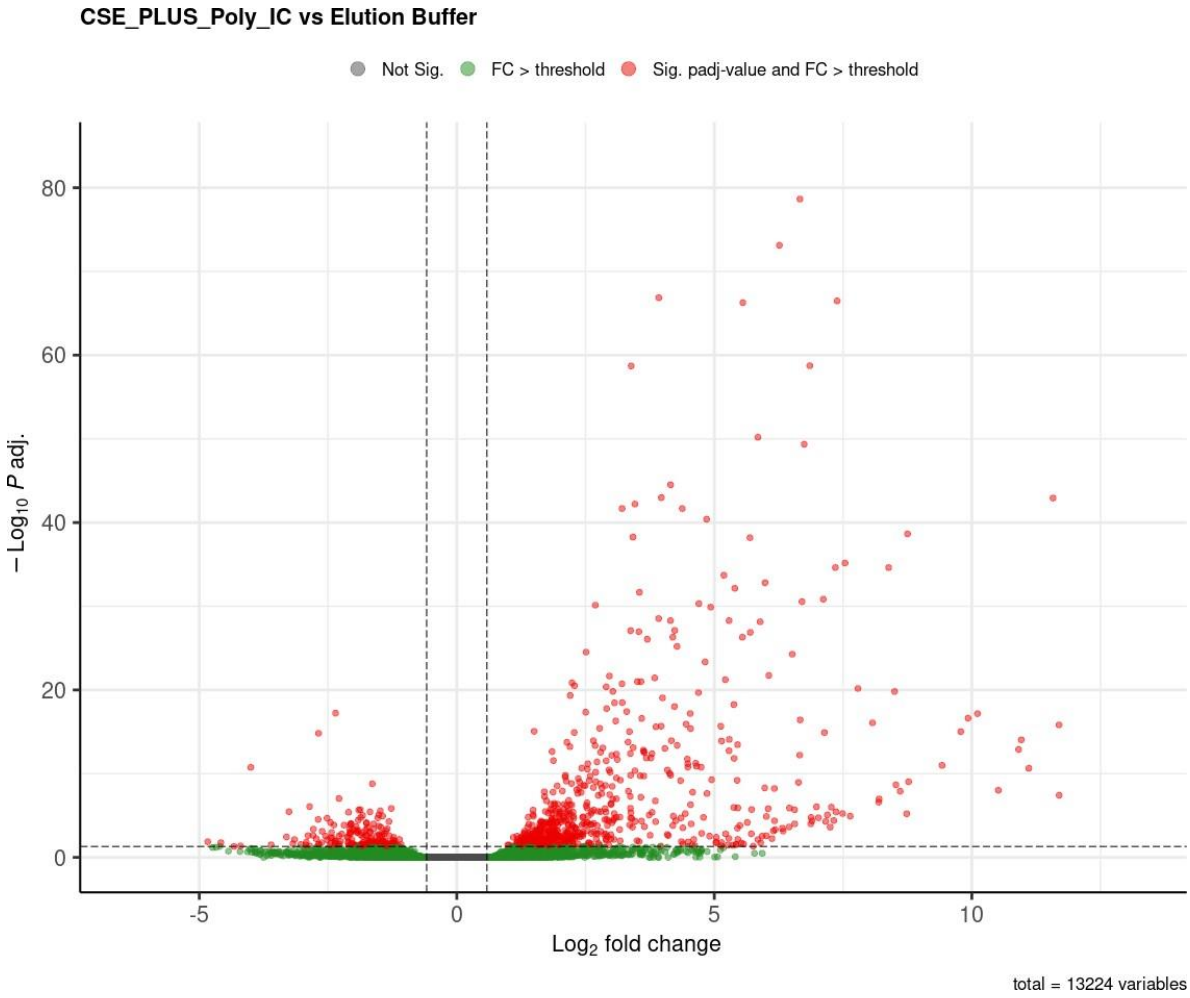

Figure 5.10 Volcano plot shows differentially expressed genes of HASMCs stimulated with cfDNA from CSE+poly (I:C)-stimulated iHBECs compared to elution buffer group.

Plot of the total 13,224 genes expressed in HASMCs. The x-axis shows the $\log_2$ fold change, indicating the magnitude of expression difference, while the y-axis shows the $-\log_{10}$ adjusted p-value, reflecting statistical significance. Green dots represent variables with a fold change exceeding the defined threshold but not statistically significant (adjusted p-value). Red dots indicate variables that are both statistically significant (adjusted p-value) and meet the fold change threshold, including 652 upregulated and 181 downregulated genes. Grey dots mark variables that did not meet significance or fold change cutoffs.

As for section 5.4.3.4, separate pathway analysis of the significantly upregulated and downregulated genes was used to identify the overarching potential biological functionality of differentially expressed genes. For upregulated genes pathways grouped by biological process (Figure 5.11 A), molecular function (Figure

5.11 B), cellular component (Figure 5.11 C) and KEGG pathways (Figure 5.11 D) identified defense response to virus among 805 pathways, double-stranded RNA binding among 37 pathways, cytoplasmic ribonucleoprotein granule among 11 pathways, and TNF signaling pathway among 61 pathways, as the most significant pathways sorted by adjusted P value for upregulated pathways respectively. For downregulated genes pathways grouped by biological process (Figure 5.12 A), molecular function (Figure 5.12 B), cellular component (Figure 5.12 C) and KEGG pathways (Figure 5.12 D) identified positive regulation of translation among 5 pathways, ribosomal large subunit binding, large ribosomal subunit among 3 pathways, and thiamine metabolism as the most significant downregulated pathways respectively.

The upregulated pathways involved in CSE+poly (I:C)-induced iHBECs group were similar to those in cfDNA of poly (I:C)-stimulated iHBECs group including the most significant pathways such as defense response to virus, double-stranded RNA binding, cytoplasmic ribonucleoprotein granule, and TNF signaling pathway and other pathways such as regulation of viral process, chemokine activity, and outer membrane which might suggest that the effect of HASMCs gene expression was largely mediated by poly (I:C). However, the findings of this study revealed that the most significant downregulated pathways were different than those with cfDNA of poly (I:C)-stimulated iHBECs group. Among these pathways, thiamine metabolism was found to be enriched as the most downregulated in KEGG pathway. Thiamine deficiency has been found to be associated with pulmonary hypertension, which might complicate asthma pathogenesis [417], suggesting the impact of CSE on the involvement of this pathway. Ubiquitin protein ligase binding was also found to be associated with downregulated pathways in molecular function in CSE+poly (I:C)-

stimulated iHBECs group but not in poly (I:C)-stimulated iHBECs group. Ubiquitylation is a posttranslational alteration in which ubiquitin molecules are linked to target proteins, either individually or in chains. These various ubiquitin patterns form a type of "code" that affects specific cellular outcomes. This mechanism controls almost all cellular processes by affecting protein destiny, shape, and function [418]. The findings in our study showed that ubiquitin protein ligase binding was among the most significant pathways in cfDNA of CSE+poly (I:C)-stimulated iHBECs group, suggesting a potential disruption in protein degradation and cellular signaling processes caused by CSE.

A

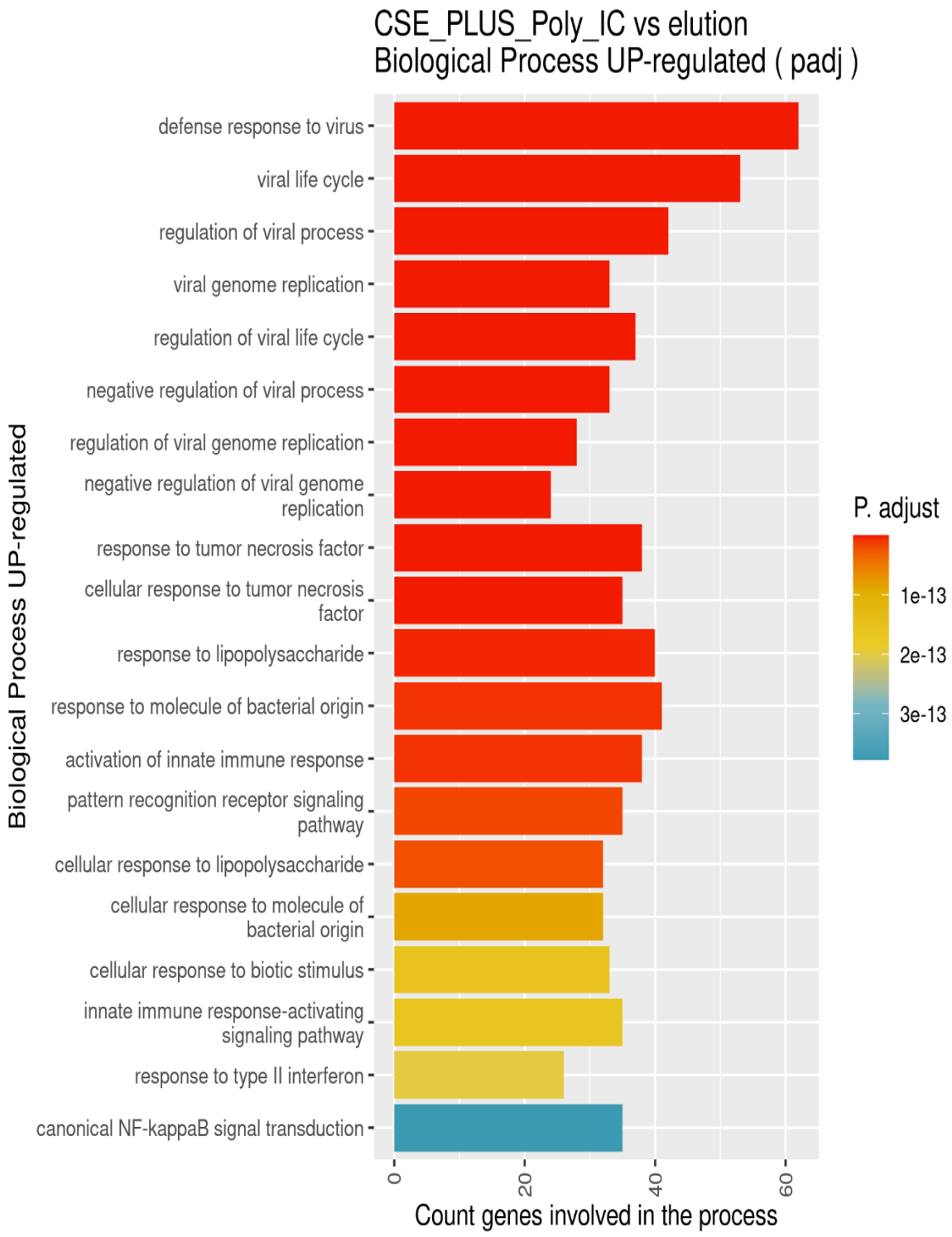
CSE_PLUS_Poly_IC vs elution
Biological Process UP-regulated (padj)
defense response to virus
viral life cycle
regulation of viral process
viral genome replication
regulation of viral life cycle
negative regulation of viral process
regulation of viral genome replication
negative regulation of viral genome replication
response to tumor necrosis factor
cellular response to tumor necrosis factor
response to lipopolysaccharide
response to molecule of bacterial origin
activation of innate immune response
pattern recognition receptor signaling pathway
cellular response to lipopolysaccharide
cellular response to molecule of bacterial origin
cellular response to biotic stimulus
innate immune response-activating signaling pathway
response to type II interferon
canonical NF-kappaB signal transduction
Biological Process UP-regulated
0
20
40
60
Count genes involved in the process
P. adjust
1e-13
2e-13
3e-13

B

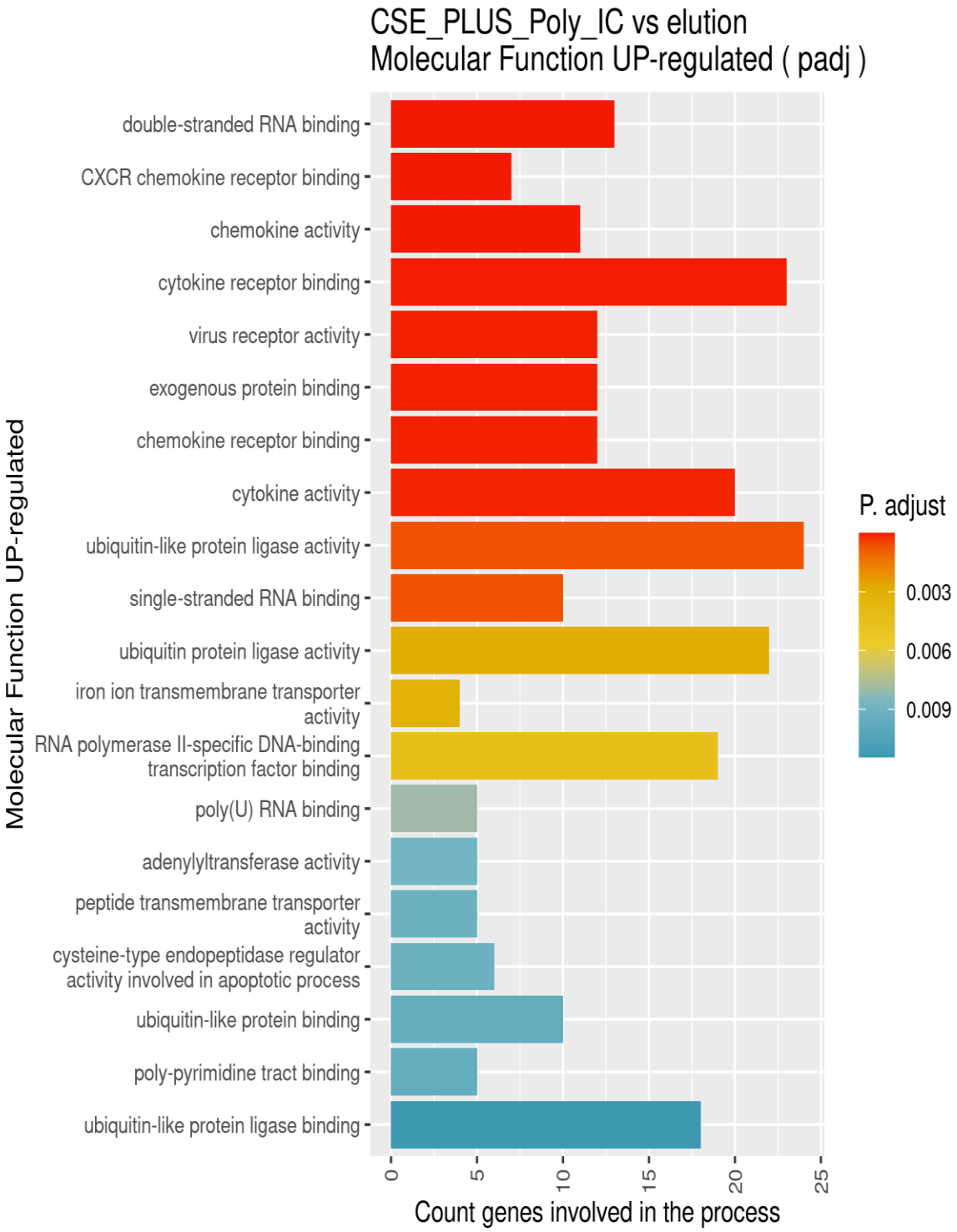
CSE_PLUS_Poly_IC vs elution
Molecular Function UP-regulated (padj)
Molecular Function UP-regulated
double-stranded RNA binding
CXCR chemokine receptor binding
chemokine activity
cytokine receptor binding
virus receptor activity
exogenous protein binding
chemokine receptor binding
cytokine activity
ubiquitin-like protein ligase activity
single-stranded RNA binding
ubiquitin protein ligase activity
iron ion transmembrane transporter activity
RNA polymerase II-specific DNA-binding transcription factor binding
poly(U) RNA binding
adenylyltransferase activity
peptide transmembrane transporter activity
cysteine-type endopeptidase regulator activity involved in apoptotic process
ubiquitin-like protein binding
poly-pyrimidine tract binding
ubiquitin-like protein ligase binding
0
5
10
15
20
25
Count genes involved in the process
P. adjust
0.003
0.006
0.009

c

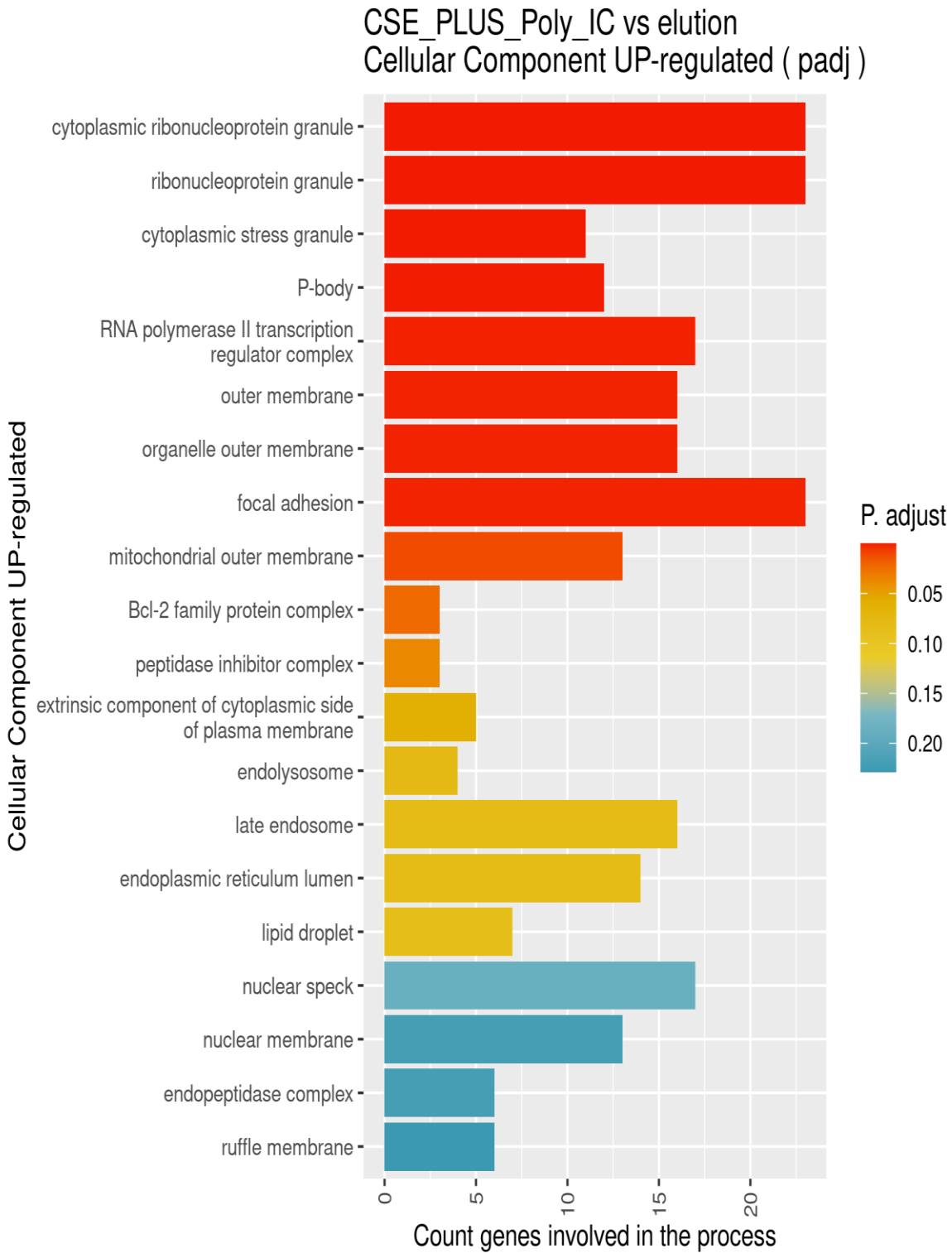
CSE_PLUS_Poly_IC vs elution
Cellular Component UP-regulated (padj)
cytoplasmic ribonucleoprotein granule
ribonucleoprotein granule
cytoplasmic stress granule
P-body
RNA polymerase II transcription regulator complex
outer membrane
organelle outer membrane
focal adhesion
mitochondrial outer membrane
Bcl-2 family protein complex
peptidase inhibitor complex
extrinsic component of cytoplasmic side of plasma membrane
endolysosome
late endosome
endoplasmic reticulum lumen
lipid droplet
nuclear speck
nuclear membrane
endopeptidase complex
ruffle membrane
Cellular Component UP-regulated
0
5
10
15
20
Count genes involved in the process
P. adjust
0.05
0.10
0.15
0.20

D

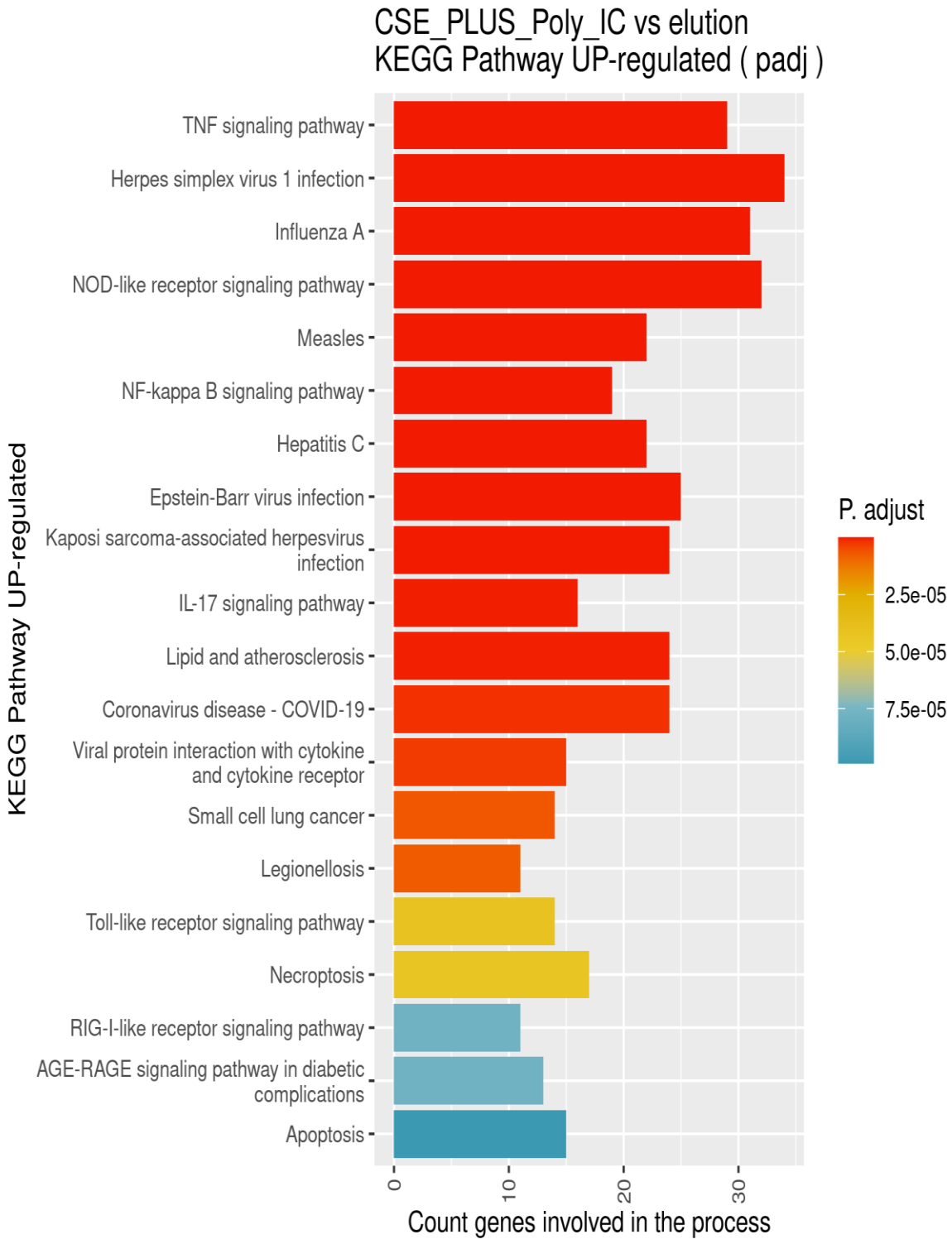

Figure 5.11 Counts of significantly UP-REGULATED genes involved in (A) BIOLOGICAL PROCESS, (B) MOLECULAR FUNCTION, (C) CELLULAR COMPONENT, and (D) KEGG PATHWAY in the contrast CSE + Poly (I:C) vs. elution buffer.

Genes were selected for GO and KEGG analysis based on significant differential expression (p.adj < 0.05).

A

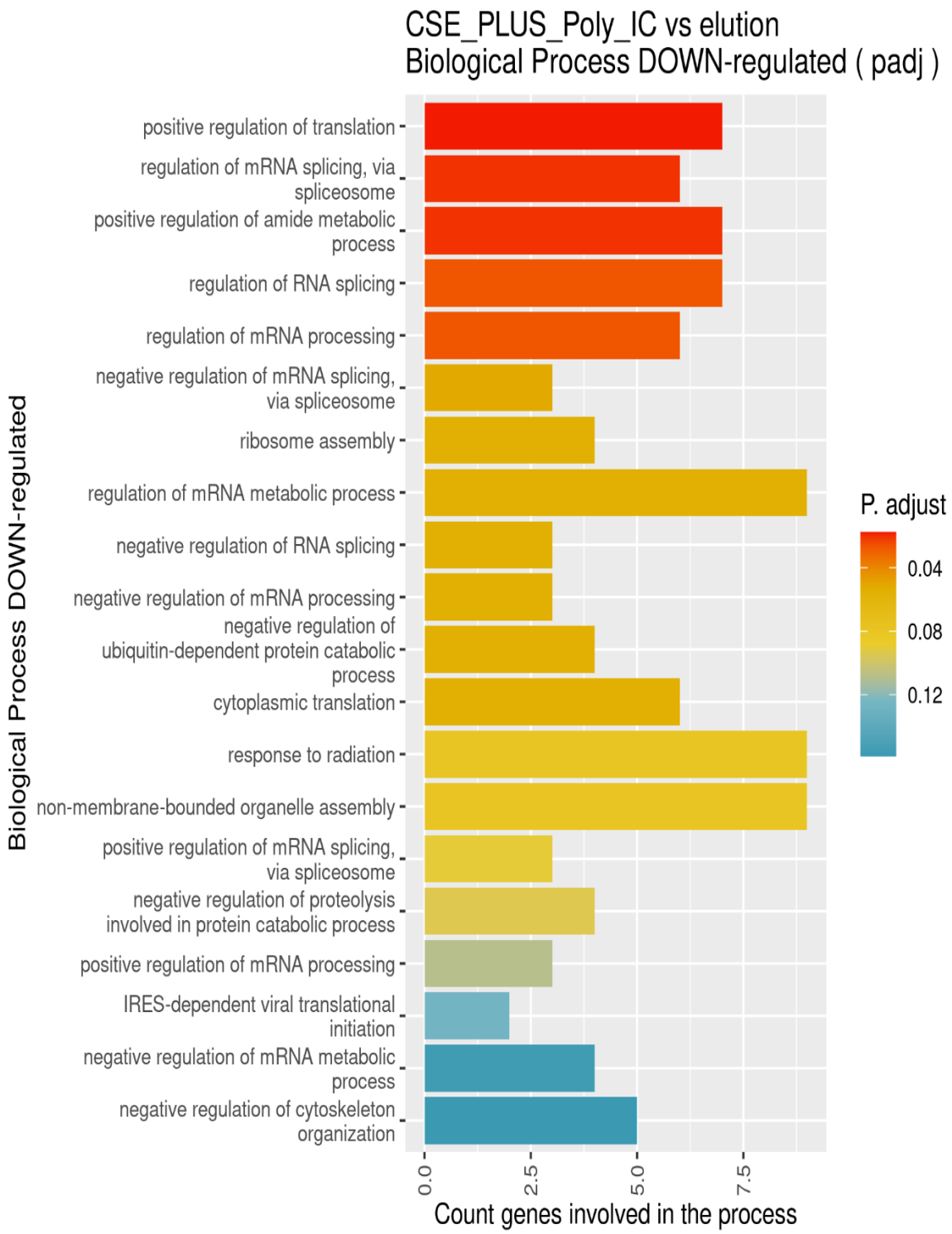
CSE_PLUS_Poly_IC vs elution
Biological Process DOWN-regulated (padj)
positive regulation of translation
regulation of mRNA splicing, via spliceosome
positive regulation of amide metabolic process
regulation of RNA splicing
regulation of mRNA processing
negative regulation of mRNA splicing, via spliceosome
ribosome assembly
regulation of mRNA metabolic process
negative regulation of RNA splicing
negative regulation of mRNA processing
negative regulation of ubiquitin-dependent protein catabolic process
cytoplasmic translation
response to radiation
non-membrane-bounded organelle assembly
positive regulation of mRNA splicing, via spliceosome
negative regulation of proteolysis involved in protein catabolic process
positive regulation of mRNA processing
IRES-dependent viral translational initiation
negative regulation of mRNA metabolic process
negative regulation of cytoskeleton organization
Biological Process DOWN-regulated
0.0
2.5
5.0
7.5
Count genes involved in the process
P. adjust
0.04
0.08
0.12

B

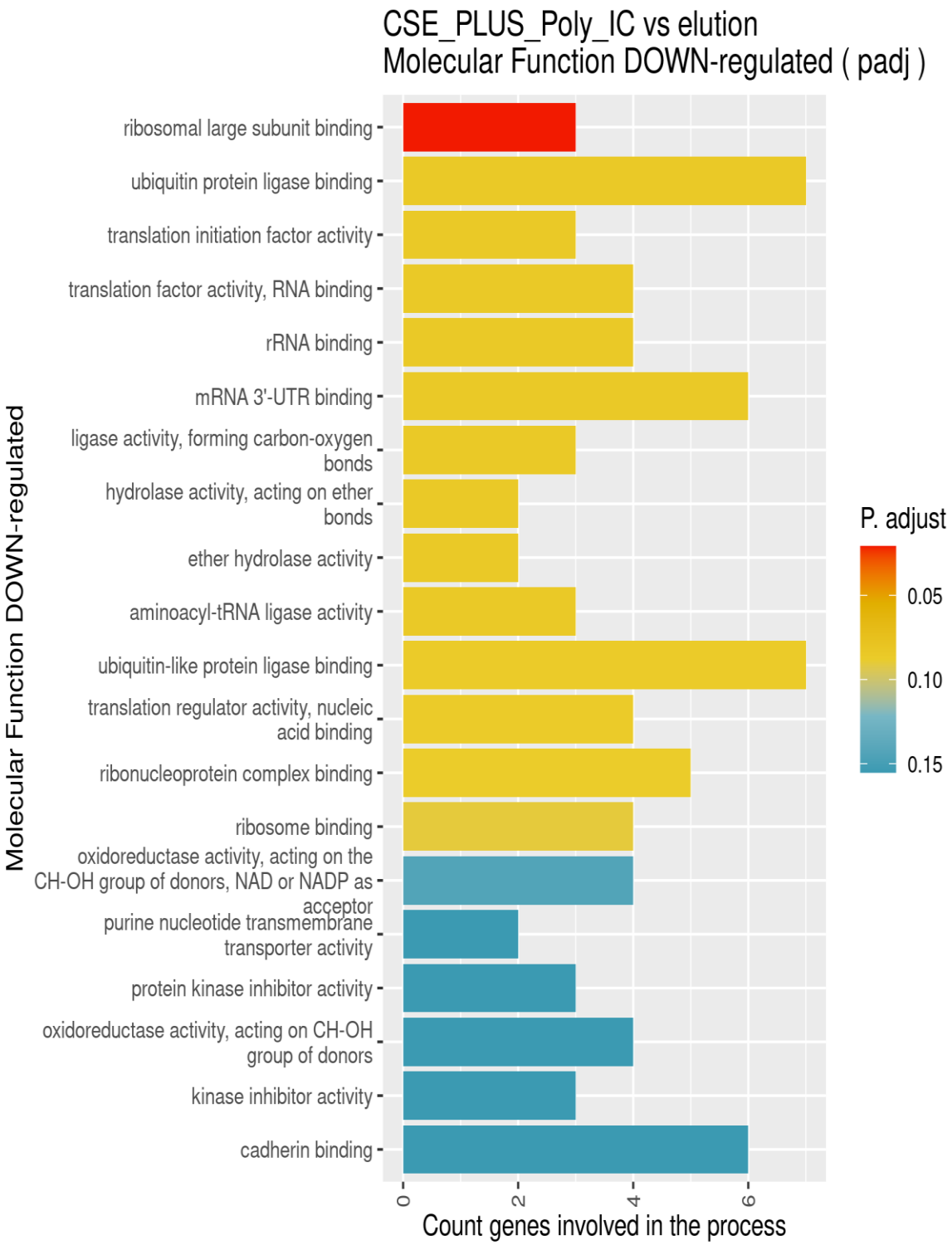
CSE_PLUS_Poly_IC vs elution
Molecular Function DOWN-regulated (padj)
Molecular Function DOWN-regulated
ribosomal large subunit binding
ubiquitin protein ligase binding
translation initiation factor activity
translation factor activity, RNA binding
rRNA binding
mRNA 3'-UTR binding
ligase activity, forming carbon-oxygen bonds
hydrolase activity, acting on ether bonds
ether hydrolase activity
aminoacyl-tRNA ligase activity
ubiquitin-like protein ligase binding
translation regulator activity, nucleic acid binding
ribonucleoprotein complex binding
ribosome binding
oxidoreductase activity, acting on the CH-OH group of donors, NAD or NADP as acceptor
purine nucleotide transmembrane transporter activity
protein kinase inhibitor activity
oxidoreductase activity, acting on CH-OH group of donors
kinase inhibitor activity
cadherin binding
0
2
4
6
Count genes involved in the process
P. adjust
0.05
0.10
0.15

c

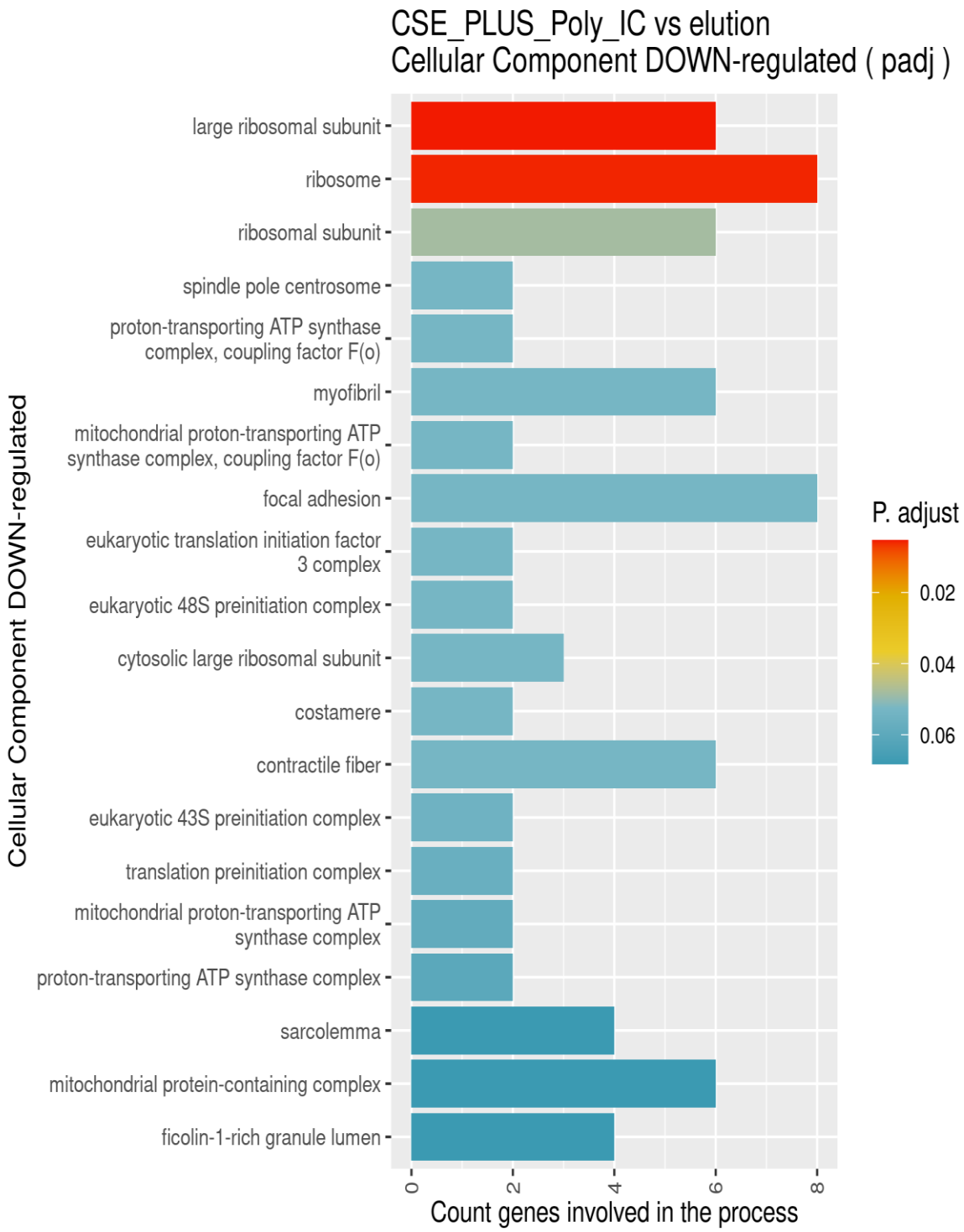
CSE_PLUS_Poly_IC vs elution
Cellular Component DOWN-regulated (padj)
Cellular Component DOWN-regulated
large ribosomal subunit
ribosome
ribosomal subunit
spindle pole centrosome
proton-transporting ATP synthase complex, coupling factor F(o)
myofibril
mitochondrial proton-transporting ATP synthase complex, coupling factor F(o)
focal adhesion
eukaryotic translation initiation factor 3 complex
eukaryotic 48S preinitiation complex
cytosolic large ribosomal subunit
costamere
contractile fiber
eukaryotic 43S preinitiation complex
translation preinitiation complex
mitochondrial proton-transporting ATP synthase complex
proton-transporting ATP synthase complex
sarcolemma
mitochondrial protein-containing complex
ficolin-1-rich granule lumen
0
2
4
6
8
Count genes involved in the process
P. adjust
0.02
0.04
0.06

D

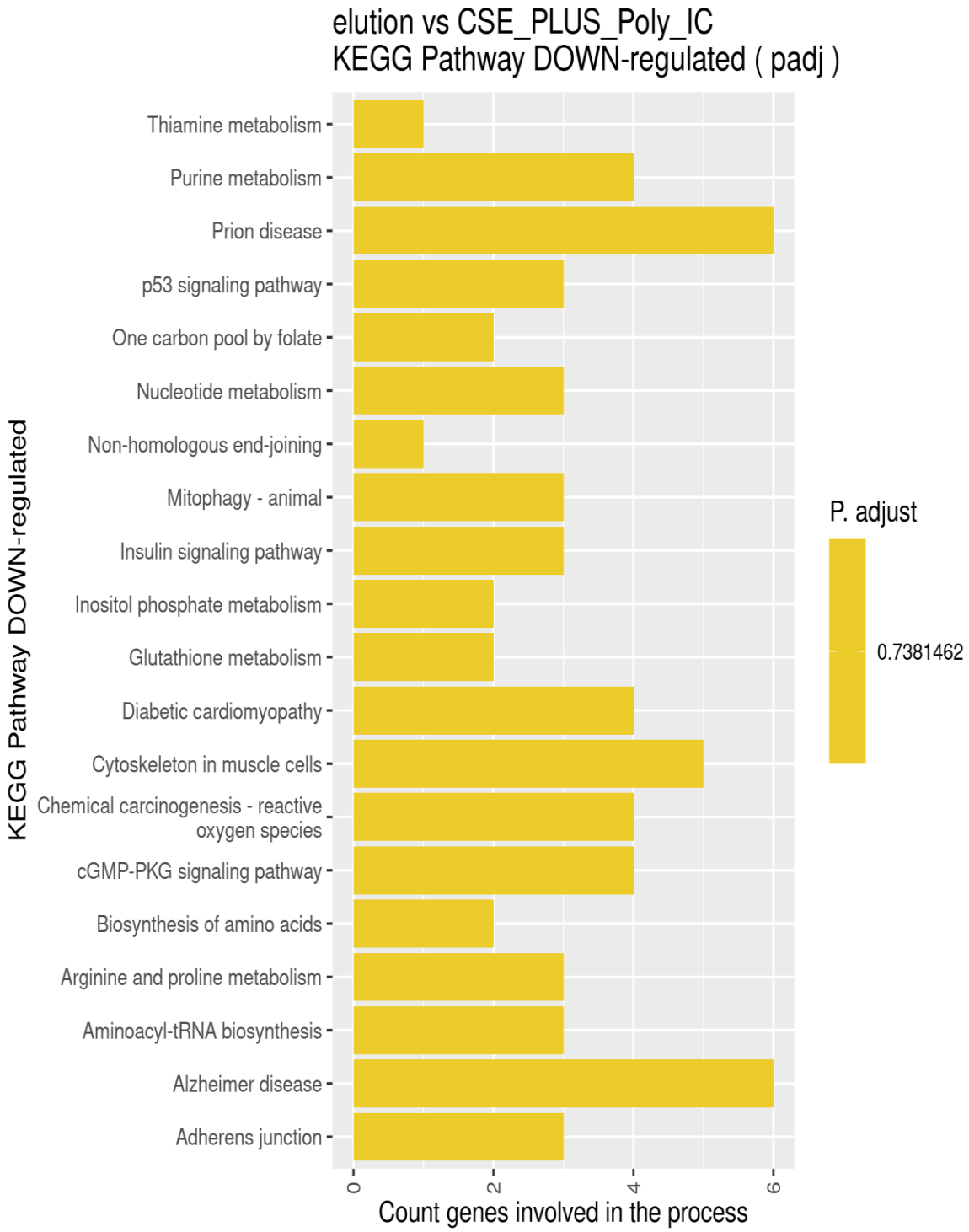

Figure 5.12 Counts of significantly DOWN-REGULATED genes involved in (A) BIOLOGICAL PROCESS, (B) MOLECULAR FUNCTION, (C) CELLULAR COMPONENT, and (D) KEGG PATHWAY in the contrast CSE + Poly (I:C) vs. elution buffer.

Genes were selected for GO and KEGG analysis based on significant differential expression (p.adj < 0.05).

5.4.3.6 cfDNA of CSE + poly (I:C)-stimulated iHBECs induced distinct gene expression change in HASMCs compared to CSE-stimulated iHBECs

cfDNA of CSE+poly (I:C)-simulated iHBECs compared to cfDNA of CSE-stimulated iHBECS caused significant differential expression of 678 genes (3 HASMCs donor, adjusted p value<0.05, and fold change cut off is 0) (Table 5.13). 556 genes were significantly upregulated and 122 downregulated (Figure 5.13). The top 20 most significant by largest fold changes for upregulated and downregulated genes are shown in Table (5.14 and Table 5.15), (full gene lists are available in (Appendix 7.13.3)). The maximum fold change in the upregulated genes was 9.109986, for gene TNF superfamily-15 (TNFSF15), which is known to modulate vascular homeostasis and inflammation and can stimulate T cell activation and increase Th1 cytokine production [419]. The maximum fold change for down regulated genes was -5.066296 for gene SMCO3 similar to the previous comparisons (Section 4.5.3.5).

Table 5.13 Summary of differential expression analysis for CSE + Poly (I:C) vs. CSE

Gene Expression	Gene Count	% of Total	Comment
Total	13,224	100%	nonzero total read count
LFC >0 (up)	556	4.2%	adjusted *p*-value < 0.05
LFC <0 (down)	122	0.92%	adjusted *p*-value < 0.05
Outliers	6	0.045%	
Low counts	1,026	7.8%	Mean count < 1

Table 5.14 Top 20 UP-regulated genes, in contrast, CSE + poly (I:C) vs. CSE (significantly changed only, sorted by LFC).

Gene ID	Gene Name	baseMean	log2FoldChange	Adjusted P value
ENSG00000181634	TNFSF15	32.538	9.109	1.82E-05
ENSG00000271503	CCL5	1155.738	9.055	2.12E-84
ENSG00000131203	IDO1	83.824	8.832	1.02E-06
ENSG00000171860	C3AR1	17.280	8.624	9.52E-07
ENSG00000134321	RSAD2	1344.951	8.426	2.94E-12
ENSG00000134326	CMPK2	199.388	8.243	2.02E-27
ENSG00000154451	GBP5	114.655	8.140	1.93E-14
ENSG00000133328	PLAAT2	38.102	7.929	1.01E-08
ENSG00000135114	OASL	287.201	7.928	5.52E-16
ENSG00000162654	GBP4	395.585	7.888	1.21E-39
ENSG00000089127	OAS1	227.735	7.866	7.06E-35
ENSG00000169245	CXCL10	1402.034	7.822	1.23E-08
ENSG00000226025	LGALS17A	9.911	7.658	1.25E-05
ENSG00000138755	CXCL9	190.832	7.577	2.03E-05
ENSG00000169248	CXCL11	1157.170	7.552	7.56E-07
ENSG00000108688	CCL7	377.048	7.480	2.25E-33
ENSG00000110944	IL23A	8.708	7.424	4.90E-05
ENSG00000104951	IL4I1	54.833	7.372	5.71E-10
ENSG00000169429	CXCL8	76.023	7.349	1.13E-09
ENSG00000158457	TSPAN33	9.189	7.301	2.03E-05

Table 5.15 Top 20 DOWN-regulated genes, in contrast, CSE + poly (I:C) vs. CSE (significantly changed only, sorted by LFC).

Gene ID	Gene Name	baseMean	log2FoldChange	Adjusted P value
ENSG00000179256	SMCO3	4.089	-5.066	6.66E-03
ENSG00000184564	SLITRK6	3.492	-4.244	3.95E-02
ENSG00000126861	OMG	61.558	-4.082	1.11E-12
ENSG00000186310	NAP1L3	6.557	-3.870	1.74E-02
ENSG00000150756	ATPSCKMT	5.647	-3.710	2.59E-02
ENSG00000183496	MEX3B	13.317	-2.951	4.81E-03
ENSG00000274070	CASTOR2	35.727	-2.922	2.85E-05
ENSG00000243244	STON1	28.554	-2.780	7.75E-05
ENSG00000242697	RPL5P12	6.677	-2.767	4.45E-02
ENSG00000168268	NT5DC2	18.880	-2.741	9.21E-04
ENSG00000180354	MTURN	45.1953	-2.532	1.54E-05
ENSG00000103034	NDRG4	11.498	-2.451	2.86E-02
ENSG00000168952	STXBP6	25.318	-2.446	1.14E-03
ENSG00000113391	FAM172A	104.647	-2.412	3.60E-12
ENSG00000122547	EEPD1	14.773	-2.368	5.74E-03
ENSG00000144730	IL17RD	20.061	-2.296	6.99E-03
ENSG00000149823	VPS51	44.551	-2.262	1.68E-04
ENSG00000136044	APPL2	43.085	-2.229	5.54E-04
ENSG00000084693	AGBL5	28.651	-2.206	1.03E-03
ENSG00000122406	RPL5	1259.139	-2.195	2.12E-10

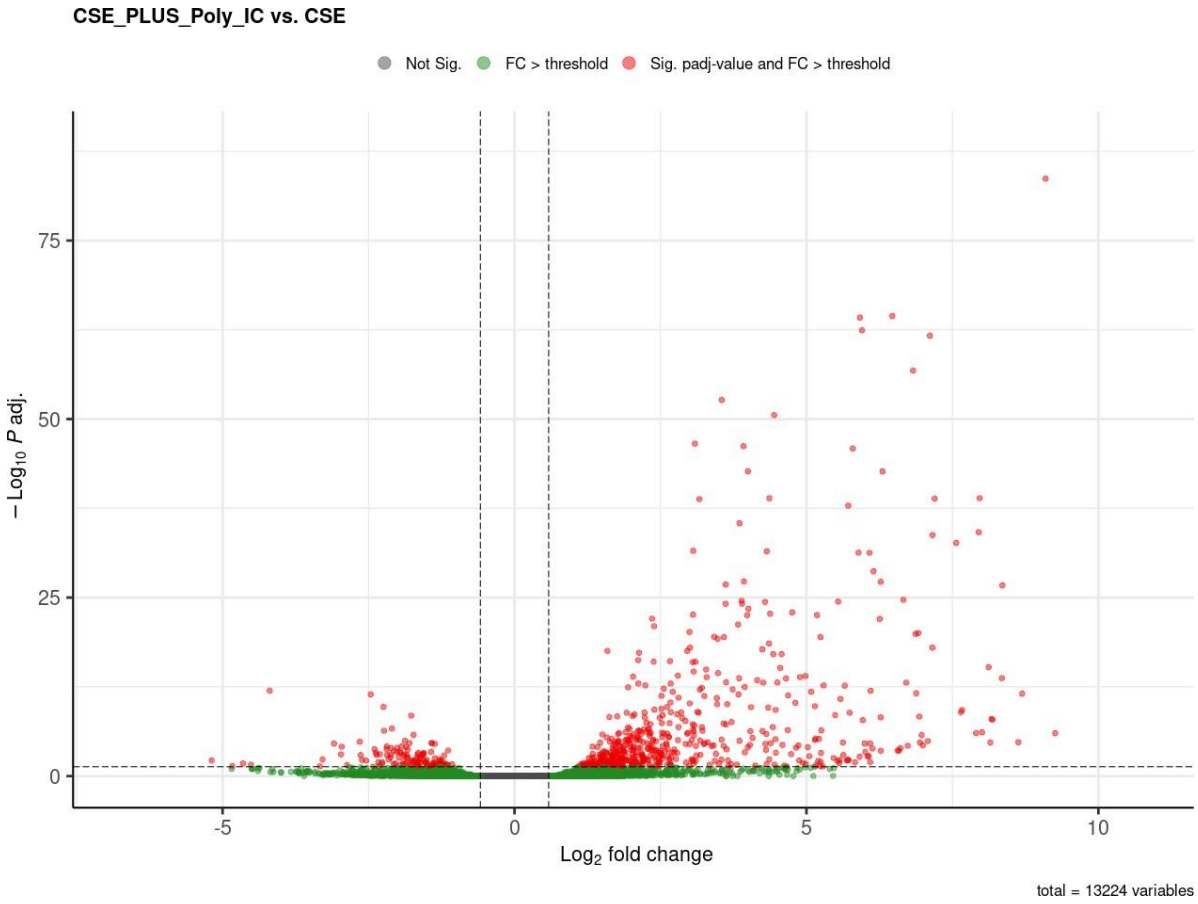

Figure 5.13 Volcano plot shows differentially expressed genes of HASMCs stimulated with cfDNA from CSE+poly (I:C)-stimulated iHBECs compared to cfDNA from CSE-stimulated iHBECs.

Plot of the total 13,224 genes expressed in HASMCs. The x-axis shows the $\log_2$ fold change, indicating the magnitude of expression difference, while the y-axis shows the $-\log_{10}$ adjusted p-value, reflecting statistical significance. Green dots represent variables with a fold change exceeding the defined threshold but not statistically significant (adjusted p-value). Red dots indicate variables that are both statistically significant (adjusted p-value) and meet the fold change threshold, including 556 upregulated and 122 downregulated genes. Grey dots mark variables that did not meet significance or fold change cutoffs.

Pathway analysis was also performed separately for significantly upregulated and downregulated genes to uncover the broader biological functions associated with the observed differential gene expression. Defence response to virus among 645 pathways, chemokine activity among 23 pathways, cytoplasmic

ribonucleoprotein granule among 9 pathways, and 23 Herpes simplex virus 1 infection among 58 pathways, were the most significant upregulated pathways grouped by biological process (Figure 5.14 A), molecular function (Figure 5.14 B), cellular component (Figure 5.14 C) and KEGG pathways (Figure 5.14 D), respectively. On the contrary, positive response to radiation among 4 pathways, rRNA binding among 7 pathways, ribosome among 25 pathways, and purine metabolism were the most significant downregulated pathways grouped by biological process (Figure 5.15 A), molecular function (Figure 5.15 B), cellular component (Figure 5.15 C) and KEGG pathways (Figure 5.15 D), respectively.

In Chapter 4, I showed that CSE alone did not cause a release of cfDNA from iHBECs, which was also confirmed by gene expression analysis showing that cfDNA of CSE-stimulated iHBECs had minimal effect on gene expression. I therefore expected the comparison of CSE + Poly (I:C) vs. CSE to yield comparable results to the Poly (I:C) vs. elution buffer comparison. However, I observed a reduced number of gene expression changes (678 genes) and the pathways were also slightly altered, with chemokine activity and Herpes simplex virus 1 infection among the most significant pathways for molecular function and KEGG pathways. The exact reason for this is unclear. However, it could indicate that CSE induces a low level of cfDNA that was not measurable by qPCR or TapeStation or insufficient to cause a genomewide significant change in gene expression. However, the low levels of cfDNA might have been sufficient to cause non-significant levels of gene expression change in the HASMCs compared to the elution buffer group, which then impacted the CSE+poly (I:C) versus CSE comparison.

A

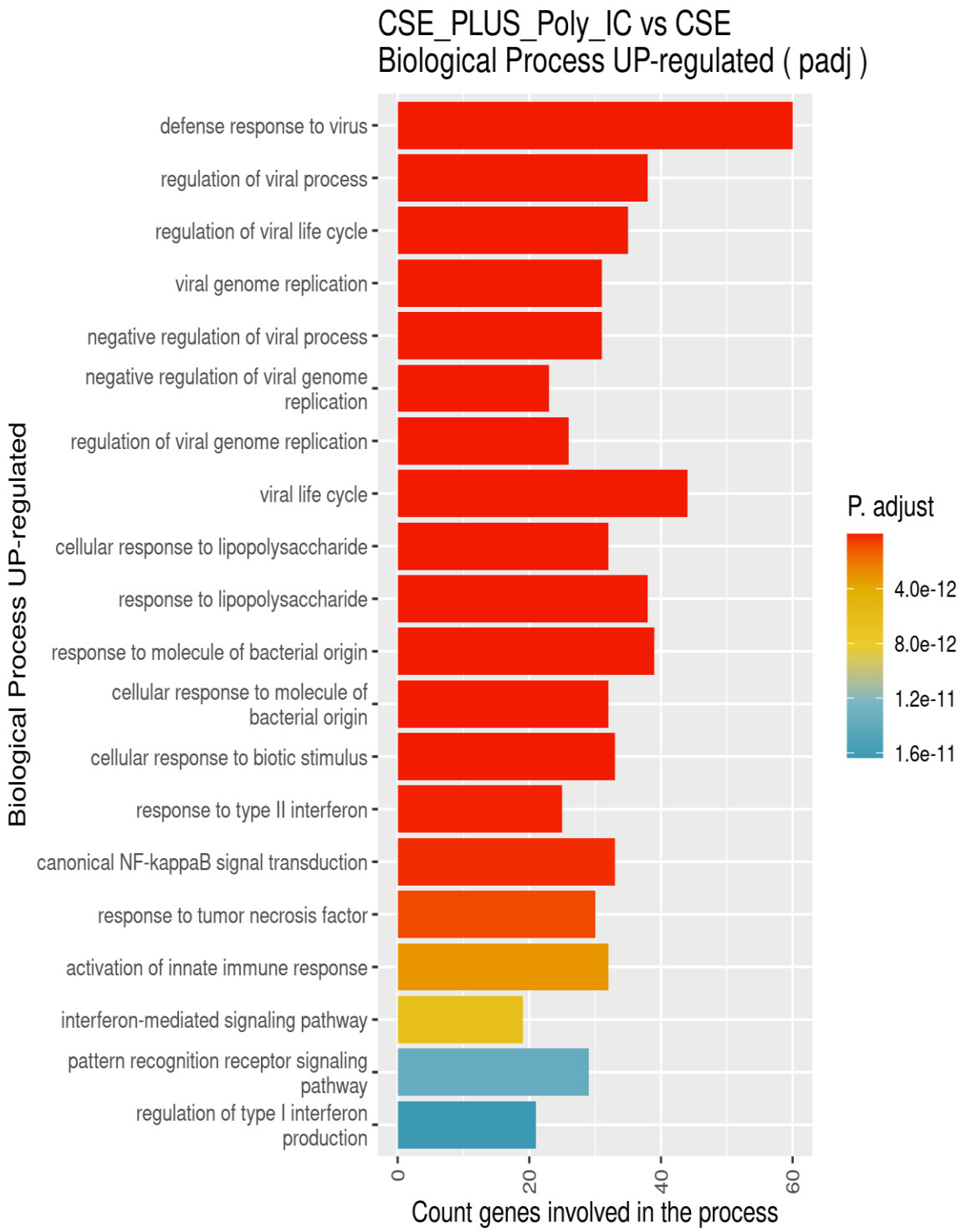
CSE_PLUS_Poly_IC vs CSE
Biological Process UP-regulated (padj)
Biological Process UP-regulated
defense response to virus
regulation of viral process
regulation of viral life cycle
viral genome replication
negative regulation of viral process
negative regulation of viral genome replication
regulation of viral genome replication
viral life cycle
cellular response to lipopolysaccharide
response to lipopolysaccharide
response to molecule of bacterial origin
cellular response to molecule of bacterial origin
cellular response to biotic stimulus
response to type II interferon
canonical NF-kappaB signal transduction
response to tumor necrosis factor
activation of innate immune response
interferon-mediated signaling pathway
pattern recognition receptor signaling pathway
regulation of type I interferon production
0
20
40
60
Count genes involved in the process
P. adjust
4.0e-12
8.0e-12
1.2e-11
1.6e-11

B

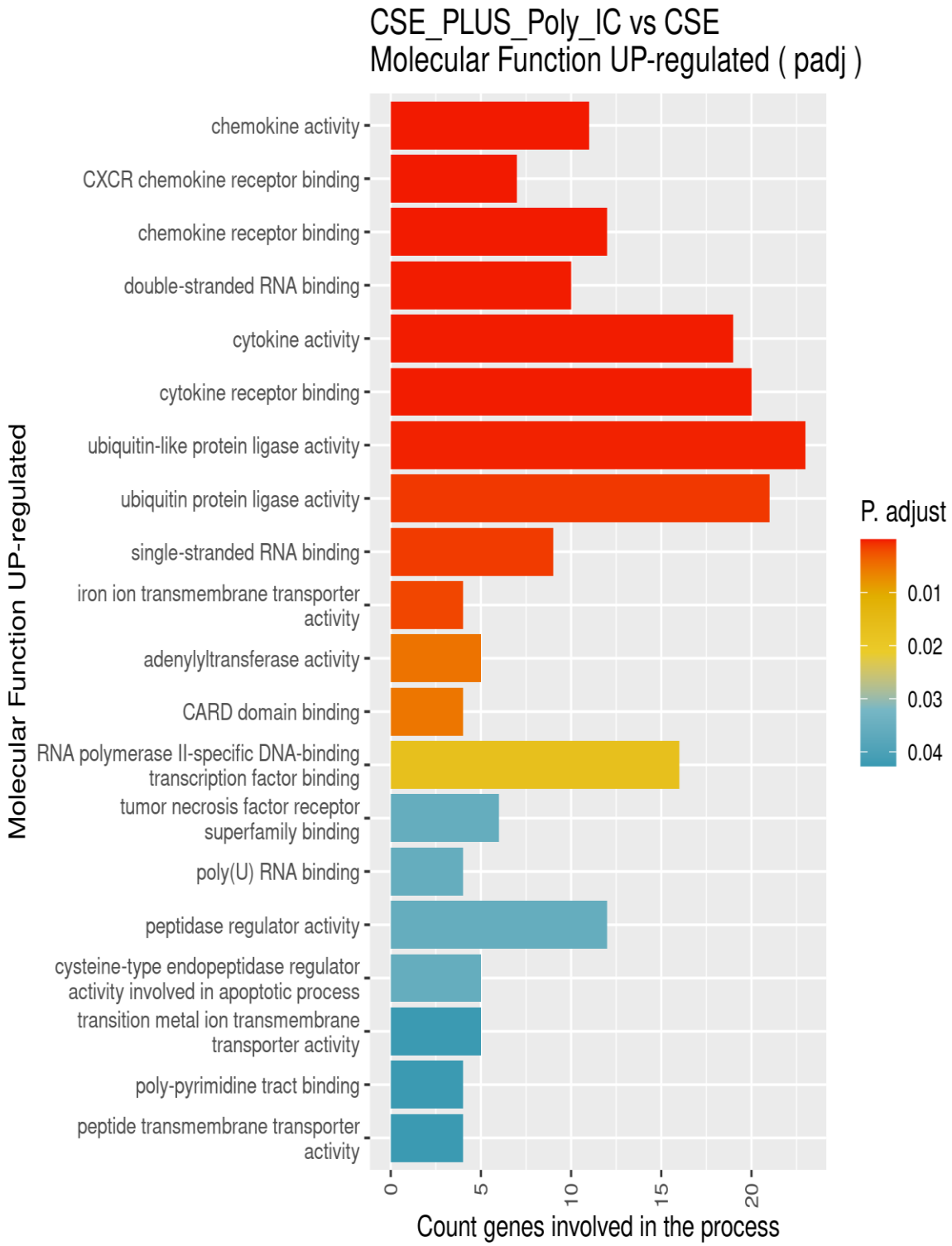
CSE_PLUS_Poly_IC vs CSE
Molecular Function UP-regulated (padj)
Molecular Function UP-regulated
chemokine activity
CXCR chemokine receptor binding
chemokine receptor binding
double-stranded RNA binding
cytokine activity
cytokine receptor binding
ubiquitin-like protein ligase activity
ubiquitin protein ligase activity
single-stranded RNA binding
iron ion transmembrane transporter activity
adenylyltransferase activity
CARD domain binding
RNA polymerase II-specific DNA-binding transcription factor binding
tumor necrosis factor receptor superfamily binding
poly(U) RNA binding
peptidase regulator activity
cysteine-type endopeptidase regulator activity involved in apoptotic process
transition metal ion transmembrane transporter activity
poly-pyrimidine tract binding
peptide transmembrane transporter activity
0
5
10
15
20
Count genes involved in the process
P. adjust
0.01
0.02
0.03
0.04

c

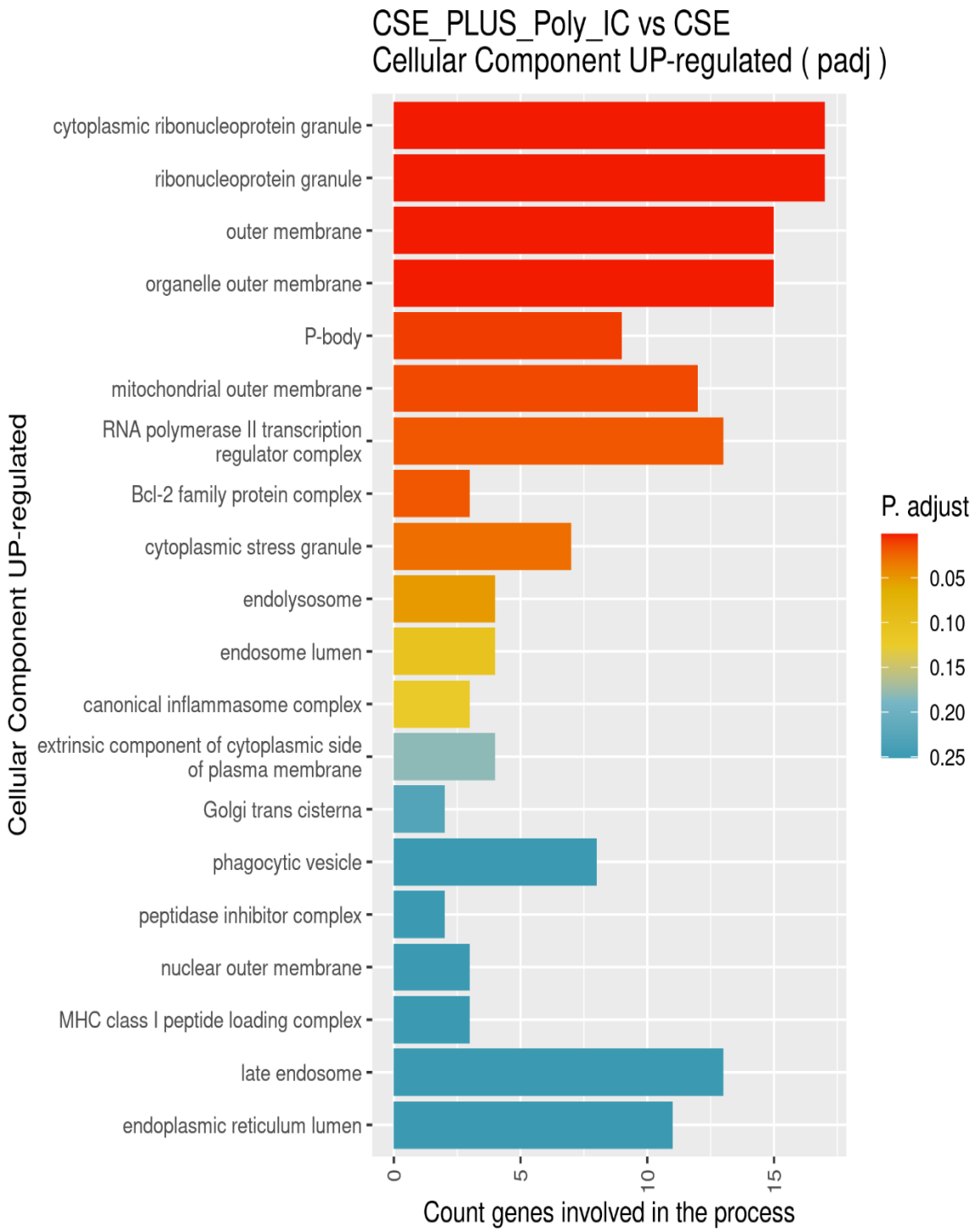
CSE_PLUS_Poly_IC vs CSE
Cellular Component UP-regulated (padj)
cytoplasmic ribonucleoprotein granule
ribonucleoprotein granule
outer membrane
organelle outer membrane
P-body
mitochondrial outer membrane
RNA polymerase II transcription regulator complex
Bcl-2 family protein complex
cytoplasmic stress granule
endolysosome
endosome lumen
canonical inflammasome complex
extrinsic component of cytoplasmic side of plasma membrane
Golgi trans cisterna
phagocytic vesicle
peptidase inhibitor complex
nuclear outer membrane
MHC class I peptide loading complex
late endosome
endoplasmic reticulum lumen
Cellular Component UP-regulated
0
5
10
15
Count genes involved in the process
P. adjust
0.05
0.10
0.15
0.20
0.25

D

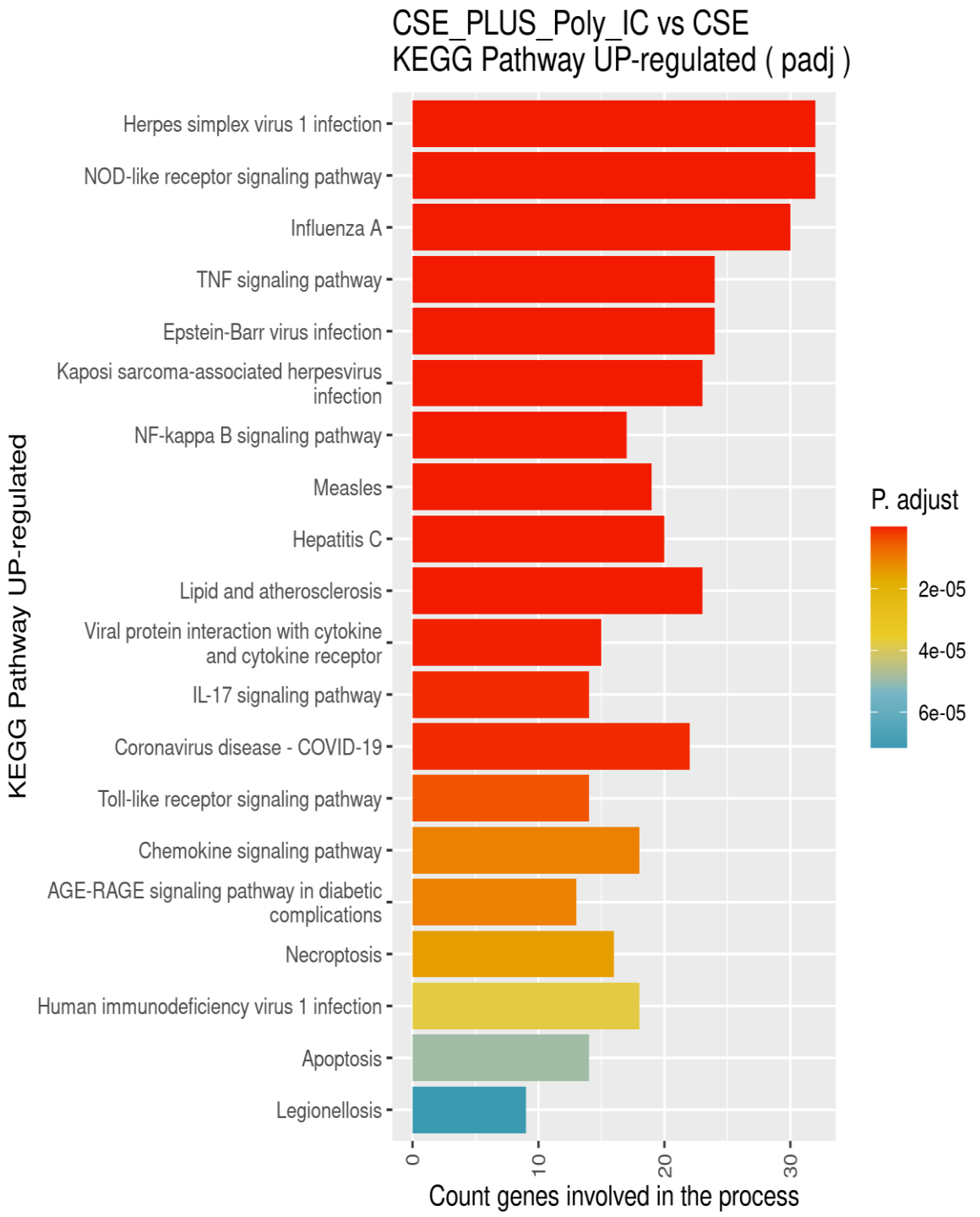

Figure 5.14 Counts of significantly UP-REGULATED genes involved in (A) BIOLOGICAL PROCESS, (B) MOLECULAR FUNCTION, (C) CELLULAR COMPONENT, and (D) KEGG PATHWAY in the contrast CSE + Poly (I:C) vs. CSE.

Genes were selected for GO and KEGG analysis based on significant differential expression (p.adj < 0.05).

A

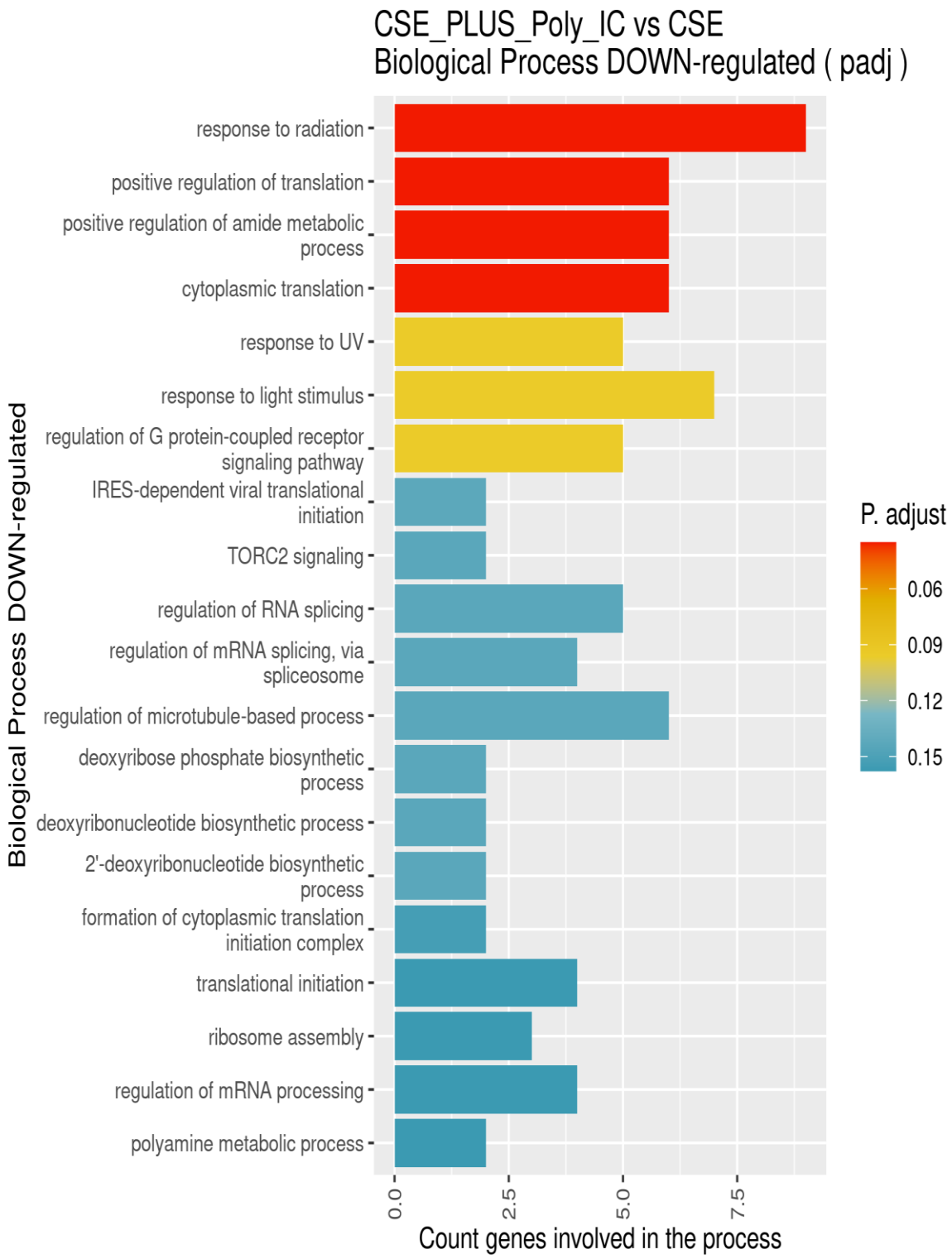
CSE_PLUS_Poly_IC vs CSE
Biological Process DOWN-regulated (padj)
response to radiation
positive regulation of translation
positive regulation of amide metabolic process
cytoplasmic translation
response to UV
response to light stimulus
regulation of G protein-coupled receptor signaling pathway
IRES-dependent viral translational initiation
TORC2 signaling
regulation of RNA splicing
regulation of mRNA splicing, via spliceosome
regulation of microtubule-based process
deoxyribose phosphate biosynthetic process
deoxyribonucleotide biosynthetic process
2'-deoxyribonucleotide biosynthetic process
formation of cytoplasmic translation initiation complex
translational initiation
ribosome assembly
regulation of mRNA processing
polyamine metabolic process
Biological Process DOWN-regulated
0.0
2.5
5.0
7.5
Count genes involved in the process
P. adjust
0.06
0.09
0.12
0.15

B

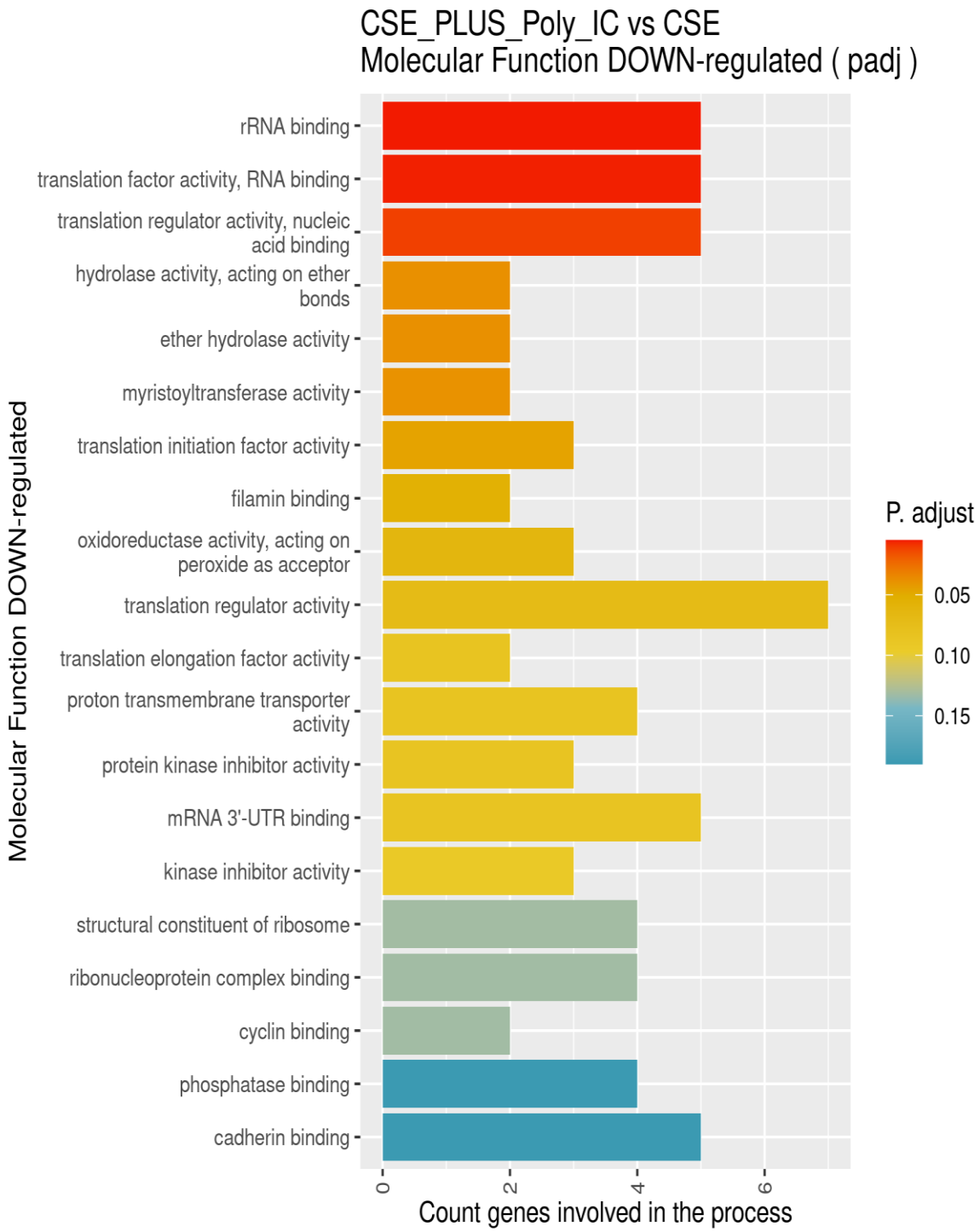
CSE_PLUS_Poly_IC vs CSE
Molecular Function DOWN-regulated (padj)
rRNA binding
translation factor activity, RNA binding
translation regulator activity, nucleic acid binding
hydrolase activity, acting on ether bonds
ether hydrolase activity
myristoyltransferase activity
translation initiation factor activity
filamin binding
oxidoreductase activity, acting on peroxide as acceptor
translation regulator activity
translation elongation factor activity
proton transmembrane transporter activity
protein kinase inhibitor activity
mRNA 3'-UTR binding
kinase inhibitor activity
structural constituent of ribosome
ribonucleoprotein complex binding
cyclin binding
phosphatase binding
cadherin binding
Molecular Function DOWN-regulated
0
2
4
6
Count genes involved in the process
P. adjust
0.05
0.10
0.15

c

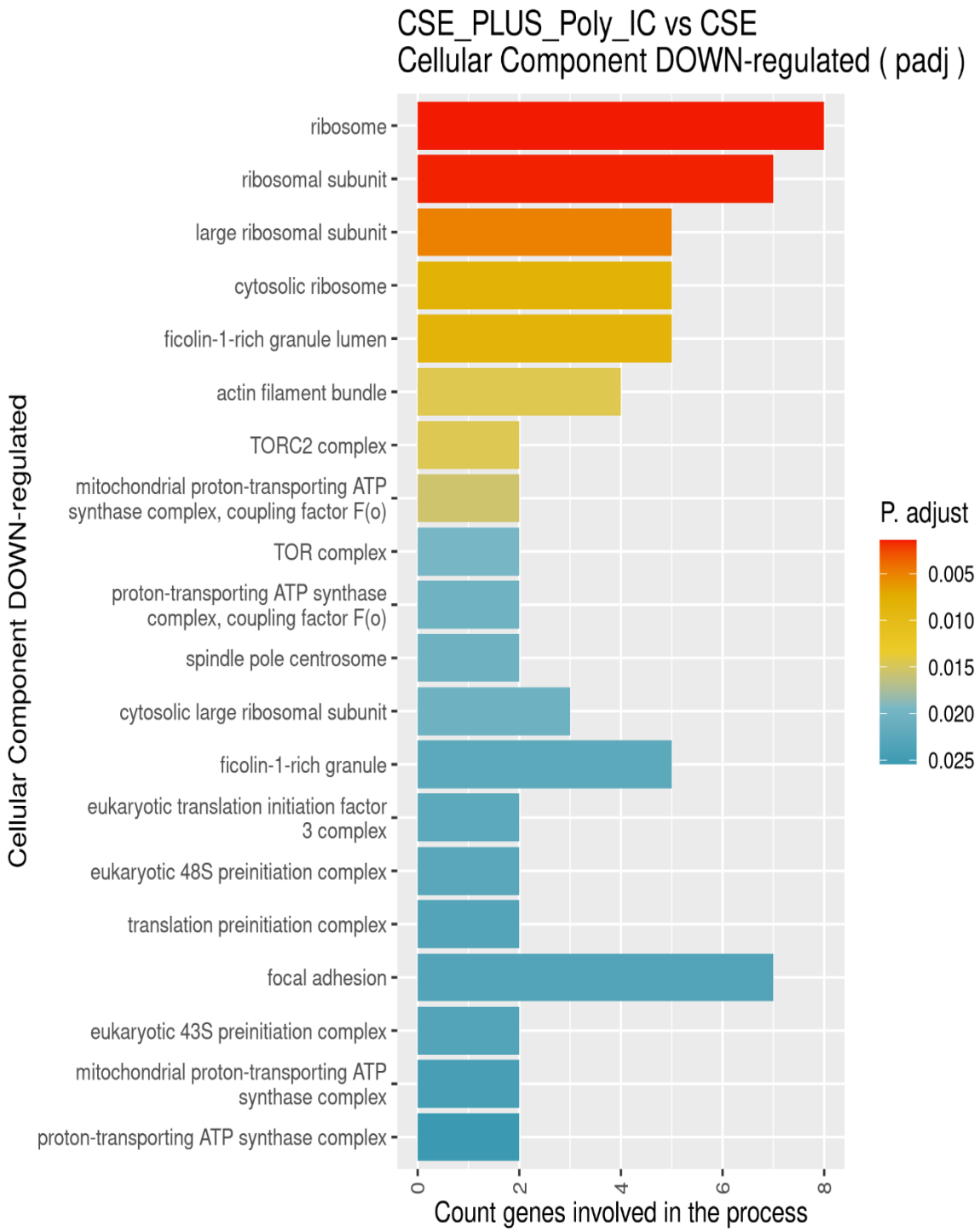
CSE_PLUS_Poly_IC vs CSE
Cellular Component DOWN-regulated (padj)
Cellular Component DOWN-regulated
ribosome
ribosomal subunit
large ribosomal subunit
cytosolic ribosome
ficolin-1-rich granule lumen
actin filament bundle
TORC2 complex
mitochondrial proton-transporting ATP synthase complex, coupling factor F(o)
TOR complex
proton-transporting ATP synthase complex, coupling factor F(o)
spindle pole centrosome
cytosolic large ribosomal subunit
ficolin-1-rich granule
eukaryotic translation initiation factor 3 complex
eukaryotic 48S preinitiation complex
translation preinitiation complex
focal adhesion
eukaryotic 43S preinitiation complex
mitochondrial proton-transporting ATP synthase complex
proton-transporting ATP synthase complex
0
2
4
6
8
Count genes involved in the process
P. adjust
0.005
0.010
0.015
0.020
0.025

D

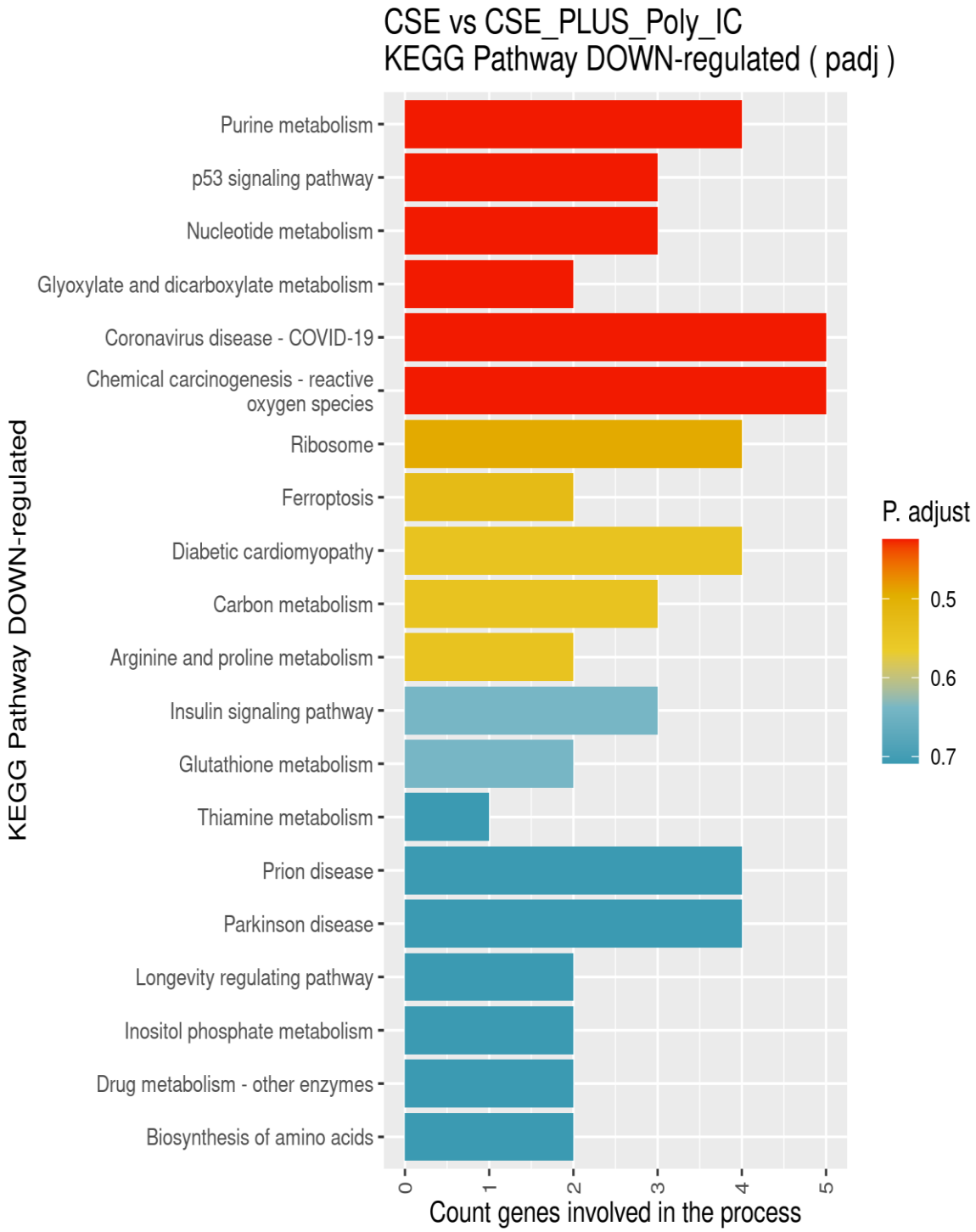

Figure 5.15 Counts of significantly DOWN-REGULATED genes involved in (A) BIOLOGICAL PROCESS, (B) MOLECULAR FUNCTION, (C) CELLULAR COMPONENT, and (D) KEGG PATHWAY in the contrast CSE + Poly (I:C) vs. CSE.

Genes were selected for GO and KEGG analysis based on significant differential expression (p.adj < 0.05).

5.4.3.7 cfDNA of CSE+poly (I:C)-stimulated iHBECs had minimal effect on HASMC gene expression compared to cfDNA of poly (I:C)-stimulated iHBECs

The contrast between cfDNA of CSE+poly (I:C)-stimulated iHBECs and poly (I:C)-stimulated iHBECs on HASMCs gene expression revealed no differentially expressed genes. However, the findings in chapter 4 revealed that co-stimulation of CSE and Poly (I:C) significantly increased the concentration of released cfDNA relative to Poly (I:C) alone in iHBECs. Therefore, I hypothesized that there would be differential effects of cfDNA from CSE+poly (I:C)-induced iHBECs on HASMC gene expression versus Poly (I:C)-induced iHBECs group. Therefore, further investigation was conducted to assess whether cfDNA of CSE+poly (I:C)-stimulated iHBEC altered gene expression differently compared to cfDNA of poly(I:C)-stimulated iHBECs or changed the expression of distinct genes. Comparison of the relative effect size change in differentially expressed genes for poly (I:C)-induced iHBECs vs. elution buffer group and CSE+poly (I:C)-induced iHBECs vs. elution buffer group comparison indicated a higher proportion of smaller fold changes in poly(I:C)-stimulated iHBECs induced HASMCs gene expression, compared to CSE+Poly(I:C)-stimulated iHBECs induced expression (Figure 5.16). However, there were no significant shifts in the overall effect size distribution between the two groups (Figure 5.17), suggesting that the changes in effect size are, therefore, likely to be gene-specific. Furthermore, upon visualization of the 50 most differentially expressed genes in the poly (I:C)-induced iHBECs vs. elution buffer group and CSE+poly (I:C)-induced iHBECs vs. elution buffer group contrasts (Figure 5.18 and 5.19), there were clear occurrences of gene-specific differences in expression magnitude (e.g. CSF3, DLL4, and RPLP0) and direction (e.g. IFT80, GSTZ1, and RGS10). In addition, the fold changes in gene expression between the two comparisons also showed slight

differences. Therefore, the difference in iHBECs cfDNA release between poly (I:C) and CSE + poly (I:C) might explain the gene-specific differences and the slight differences between the fold change of the expressed genes in HASMCs gene expression.

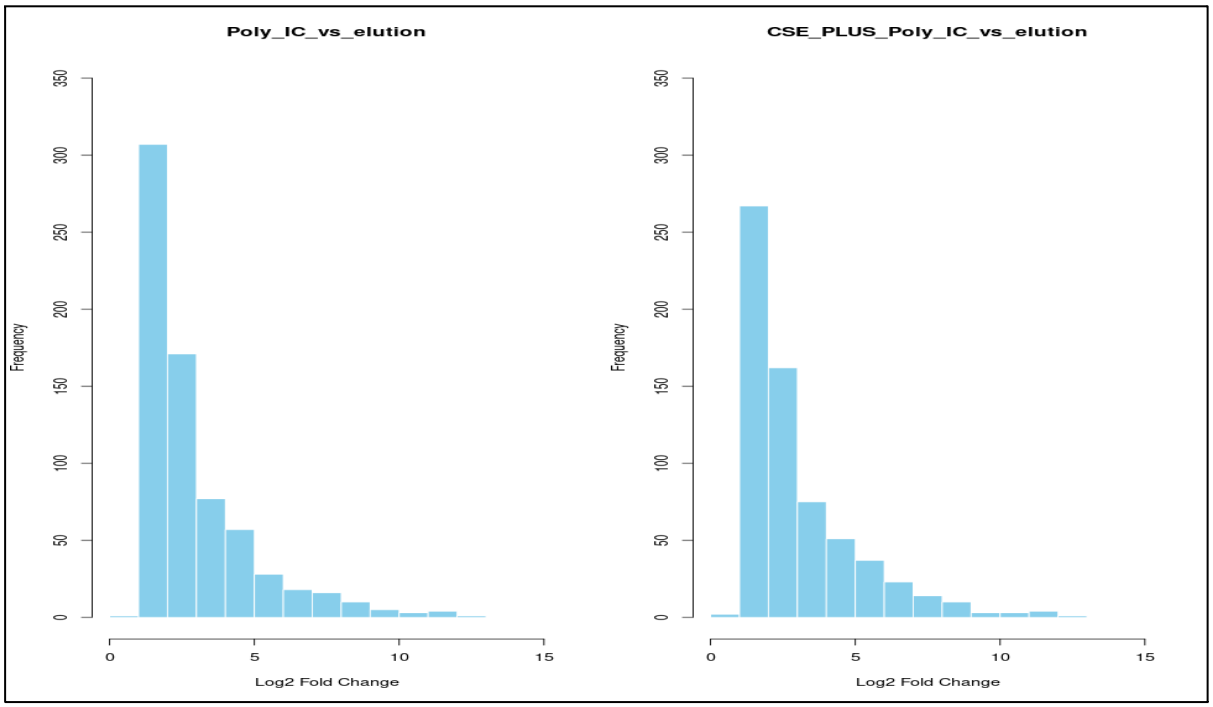

Figure 5.16 Histograms showing the relative effect size in poly (I:C) vs. elution buffer group and CSE + Poly (I:C) vs. elution buffer group.

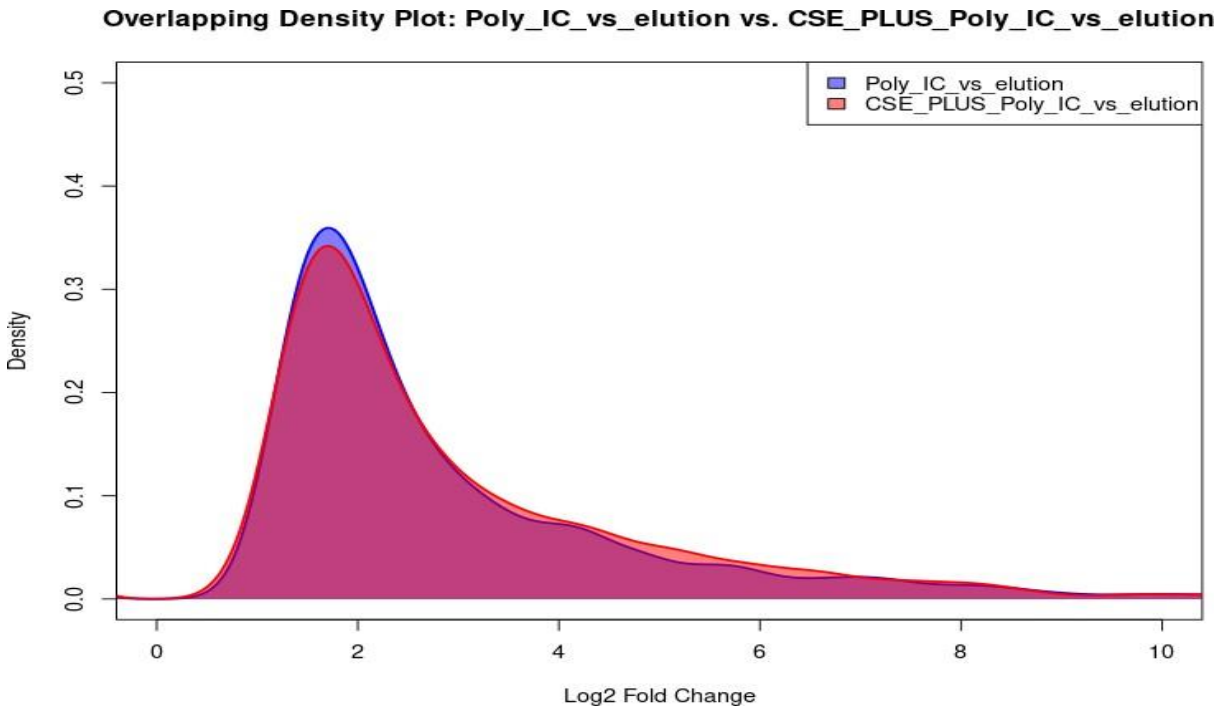

Figure 5.17 Overlapping density plot showing the relative effect size in poly (I:C) vs. elution buffer group and CSE+Poly (I:C) vs. elution buffer group.

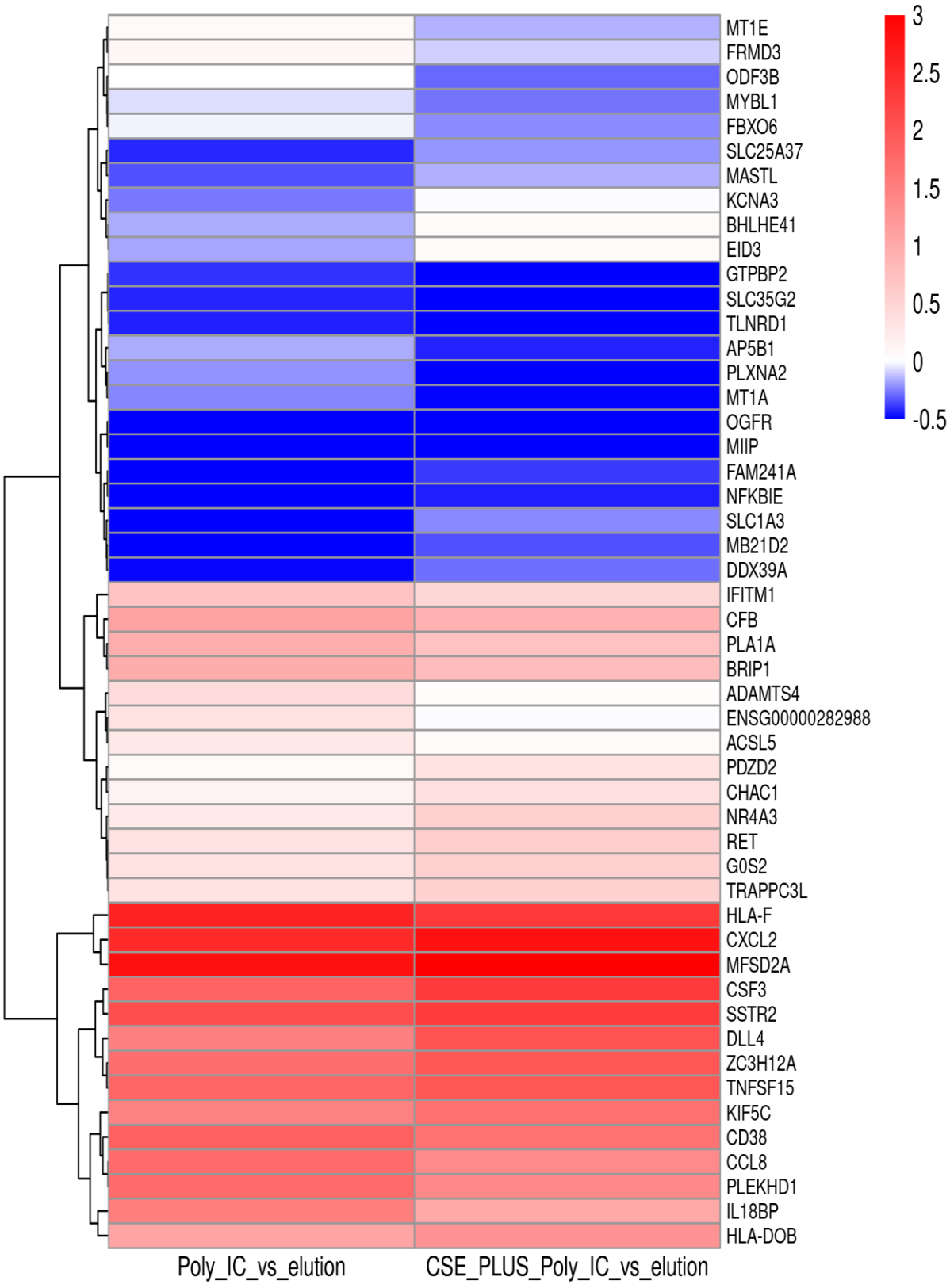

Figure 5.18 Heatmap contrasting significantly differentially UP-regulated genes in poly (I:C) vs. elution buffer against CSE + poly (I:C) vs. elution buffer.

Data are z-scored shrunken log2 fold changes, colour coded by log2 fold change.

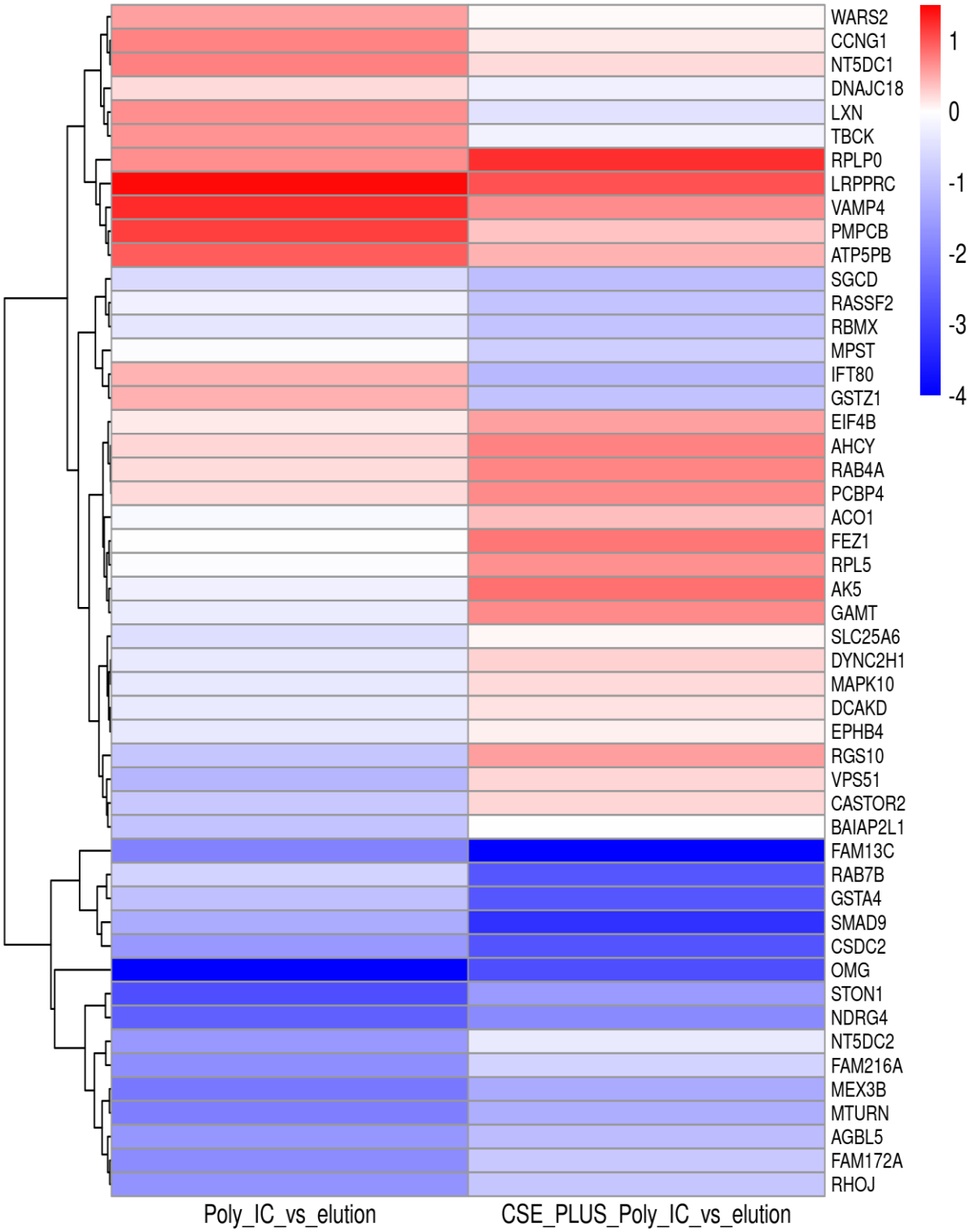

Figure 5.19 Heatmap contrasting significantly differentially DOWN-regulated genes in poly (I:C) vs. elution buffer against CSE + poly (I:C) vs. elution buffer.

Data are z-scored shrunken log2 fold changes, colour coded by log2 fold change.

I next investigated whether distinct genes were being altered by poly (I:C) + CSE versus poly (I:C) alone. There were 605 genes significantly upregulated genes shared between the two comparisons (Figure 5.20 A), while 93 genes were significantly upregulated in response to poly (I:C) compared to elution buffer group and 47 genes were significantly upregulated in response to CSE + poly (I:C) compared to elution buffer group (Figure 5.20 A), including Human Leukocyte Antigen - DR Beta 1 (HLA-DRB1) and Polo-like kinase 3 (PLK3) genes (Lists of distinct upregulated genes are available in (Appendix 7.13.4)). For downregulated gene, 130 genes shared significantly downregulated genes between the two comparisons (Figure 5.20 B), while 87 genes were significantly downregulated in response to poly (I:C) compared to elution buffer and 51 genes were significantly downregulated in response to CSE + poly (I:C) compared to elution buffer group (Figure 5.20 B), such as RNA Binding Motif Protein X-Linked 2 (RBMX2) and Ethanolamine Kinase 2 (ETNK2) genes (Lists of distinct downregulated genes are available in (Appendix 7.13.5)). Taken together, the results suggest that although there was no statistical change between cfDNA of CSE+poly (I:C)-stimulated iHBEC induced HASMCs gene expression compared to cfDNA of poly(I:C)-stimulated iHBECs induced HASMCs gene expression group (potentially due to increased variability in the reference compared to using elution buffer samples as the reference), there were changes in the magnitude of the gene expression changes and in the individual genes identified in the independent comparisons to elution buffer.

A

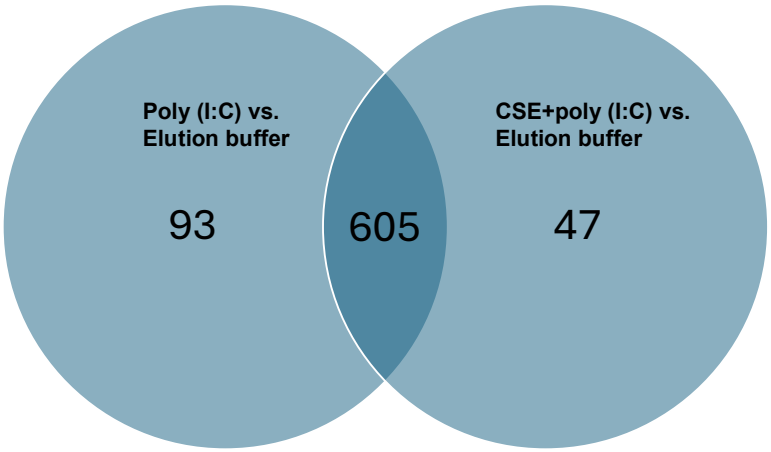

B

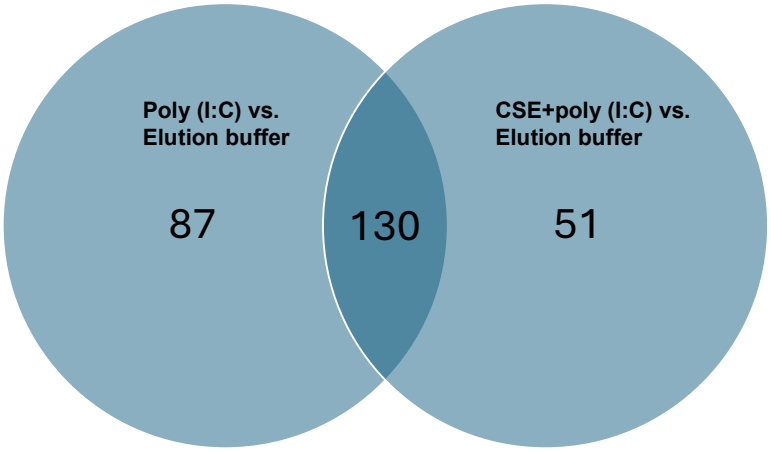

Figure 5.20 Venn diagram showing (A) UP-regulated and (B) DOWN-regulated DEGs between poly (I:C) vs. elution buffer and CSE + poly (I:C) vs. elution buffer contrasts

5.4.3.8 Gene validation

From the RNA-Seq analysis, the IL-8 gene was found to be expressed in response to poly (I:C) and CSE + poly (I:C) from HASMCs (Figure 5.21 A). To validate this, ELISA was performed to assess IL-8 concentrations in the HASMCs supernatants collected from these experiments. Compared to elution buffer, which was used as the control group in HASMCs gene expression analysis, cfDNA from poly (I:C)-induced iHBECs and cfDNA from CSE + poly (I:C)-induced iHBECs significantly increased IL-8 concentrations in HASMCs conditioned media (695.2 ± 146.2 pg/ml, ****P*<0.001 and 669.7 ± 116.4 pg/ml, ****P*<0.001, respectively). Results from ELISA for IL-8 production and RNA-Seq for IL-8 gene expression showed the same pattern of response (Figure 5.21 B).

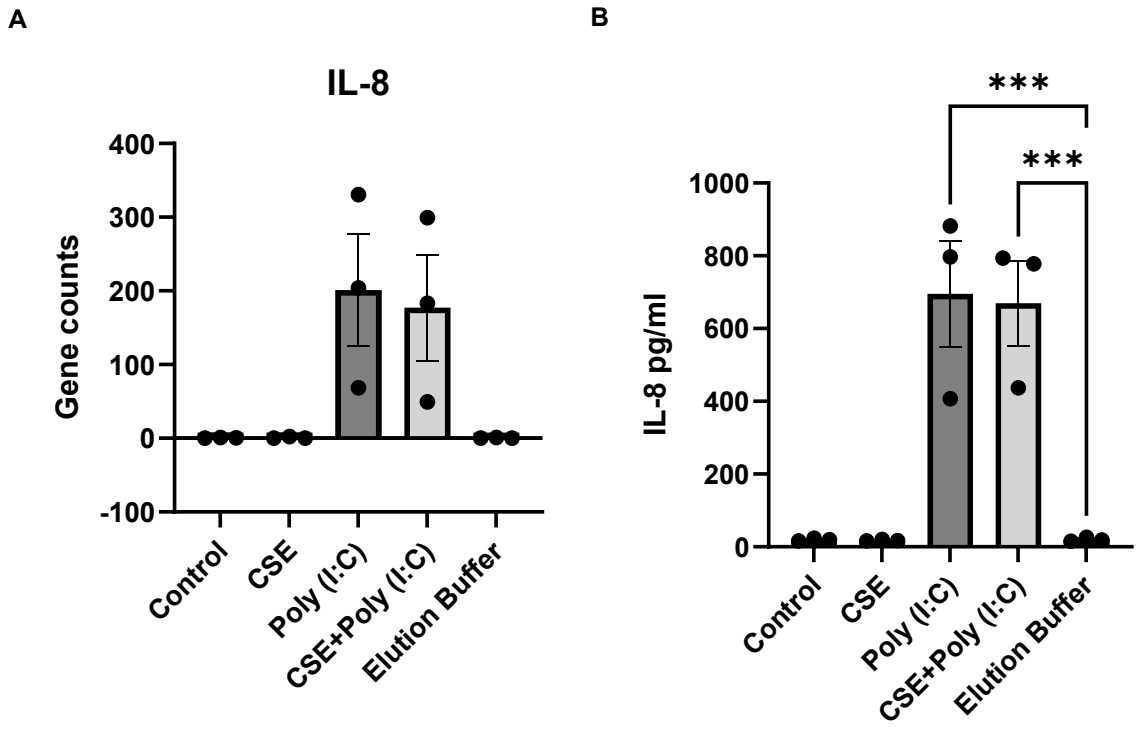

Figure 5.21 Effect of poly (I:C) and CSE on the gene expression and the production of IL-8 in HASMCs

HASMCs were stimulated with 33.33 µl of cfDNA released from iHBECs for 24 hours. RNA was isolated, and the gene expression was assessed by RNA-Seq. **A,** represents the gene count of IL-8 found by RNA-Seq data. **B,** the concentration of IL-8 in cell supernatants measured by ELISA, presented as pg/ml. Each data point represents mean ± SEM of three independent experiments using cells from three different donors. ****P*<0.001, compared with control (Elution buffer).

5.5 Discussion

HASMCs and HBECs play a crucial role in the pathogenesis of chronic lung diseases like asthma through initiating immune responses against stimuli, inducing pro-inflammatory cytokines and chemokines, and contributing to inflammation and structural changes in the airway. The interaction between them is critical in maintaining normal airway function and in the pathophysiology of airway diseases [131]. Cell-to-cell communication is essential in coordinating cell function, lung homeostasis, and the extensive structural cell changes in lung diseases [420]. cfDNA has emerged as a bioactive molecule that can stimulate proinflammatory cytokine synthesis, enhance oxidative stress, and contribute to inflammation in several diseases [334, 335]. In Chapter 4, the release of cfDNA from iHBECs was assessed in response to CSE and poly (I:C) individually or in combination, and I found that cfDNA was released in response to Poly (I:C) but not CSE. Interestingly, co-stimulation of CSE with Poly (I:C) significantly increased the concentration of released cfDNA, relative to Poly (I:C) alone.

HASMCs play a significant role in asthma pathogenesis and constitute an important target for treatment by controlling muscle tone as well as secreting cytokines, chemokines, and growth factors [113]. In addition, HASMCs participate in the airway hyperresponsiveness, inflammation, and remodeling process observed in asthmatic individuals [114]. Several studies have utilized transcriptome profiling of airway cells, including HASMCs and HBECs, to investigate the pathophysiology of asthma by analyzing differential gene expression [421, 422]. However, no studies have investigated the effect of cfDNA released from HBECs on HASMCs' proliferation, contraction, and differential gene expression, processes which may drive asthma progression and influence treatment responses. This chapter aims to

assess whether the cfDNA released from iHBECs can alter the proliferation and contraction of HASMCs and regulate HASMC gene expression.

To the best of my knowledge, this is the first study investigating the role of cfDNA released from iHBECs on HASMCs proliferation and contraction. I used two methods of assessing cell proliferation and one method to assess cell contraction. Furthermore, transcriptome profiling using RNA-Seq technology was used to investigate how cfDNA released from iHBECs can modulate gene expression of HASMCs [397, 423].

HASMCs' proliferation is an important aspect of asthmatic airway remodelling that can affect airway calibre, leading to alteration of contractile force, airway thickening, hyperresponsiveness, and decreased lung function [118, 424]. As cfDNA was released from iHBECs in response to Poly (I:C), and co-stimulation with CSE and Poly (I:C) significantly increased the concentration of released cfDNA, it was hypothesised that cfDNA isolated from iHBECs would increase HASMCs proliferation. The data presented here showed that cfDNA from CSE- and Poly (I:C)-stimulated iHBECs had no effect on HASMCs proliferation over 24 hours. A previous study investigated HASMCs proliferation by BrdU assay using co-culture model of HASMCs with HBECs (BEAS2B cell line) for 24 hours revealed that HBECs induced a proliferative phenotype in HASMCs relative to control (not in co-culture with HBECs) through micro-RNA 210 (miR-210) targeting tumor suppressor max binding protein (Mnt) [425]. A longer co-culture of scrape-injured HBECs with HASMCs for 8 days led to a greater increase in HASMCs proliferation than uninjured HBECs (1.7-fold), and the effect was dependent on matrix metalloproteinases (MMP-9) [133]. Furthermore, cfDNA in the soluble fraction induces cell proliferation and cell transformation in murine embryonic fibroblast cells, suggesting a role of cfDNA in

modulating proliferation, which was offset by enzyme treatment of DNAse I and proteinase K [426].

In our study, to assess the effect of cfDNA released from iHBECs on HASMCs proliferation, two methods of cell proliferation were used, BrdU ELISA and PrestoBlue, which have been widely used in assessing cell proliferation in lung pathophysiology [427-430]. In the BrdU assay, cells are exposed to BrdU, a synthetic analogue of thymidine, which is absorbed into cellular DNA during replication. An ELISA is used to detect the analogue incorporation using labelled anti-BrdU antibodies. BrdU thus serves as a direct cell proliferation measurement. Conversely, PrestoBlue is a resazurin-based cell viability assay that determines the metabolic activity of cells and is therefore an indirect measure of cell proliferation. Using these methods our data showed no difference in HASMC proliferation when the cells were treated with cfDNA collected from HBECs stimulated with either CSE, Poly I:C or CSE+ Poly I:C. TGFb1 was used as a positive control in both methods, as it is known to induce HASMCs proliferation [431, 432]. TGFb1 significantly increased HASMCs proliferation, demonstrating that both methods were working as expected, leading to the conclusion that cfDNA-stimulated iHBECs does not affect HASMCs proliferation. While our investigation provides insight into the effects of cfDNA-stimulated iHBECs on HASMC proliferation, it is limited by a single 24-hour time point. Extending the proliferation assay analysis to 48 or 72 hours may have provided better separation for assay of cell number and strengthened the interpretation of proliferative effects of iHBECs' cfDNA on HASMCs. A previous study demonstrated that HASMC proliferation can occur over a longer period of 8 days [133]. Therefore, future investigations should include long time-course

experiments such as 48 and 72 hours to better understand whether the effects of cfDNA from iHBECs on HASMCs proliferation evolve beyond 24 hours.

HASMC contraction is another key factor in the pathophysiology of airway diseases such as asthma. It regulates the diameter and resistance of the airway and is responsible for bronchoconstriction, a hallmark feature of asthma [125]. The epithelium plays a pivotal role in influencing HASMCs contraction, migration, and proliferation, which may contribute to airway remodelling [131]. Ruptured small airway epithelial cells *in vivo* and primary HBECs *in vitro* induce rapid HASMCs contraction through the release of soluble mediators and subsequent Ca^{2+} dependent mechanisms, and might contribute to airway AHR in asthma [132]. I investigated whether cfDNA might be a mechanism of communication between the airway epithelium and the underlying HASMCs layer to drive HASMCs contraction.

The collagen gel contraction assay is one of the methods useful for evaluating cell contraction within collagen gel matrices by measuring changes in gel size. Sakota et al. demonstrated that the collagen gel contraction assay was useful for evaluating the effect of formoterol on histamine-induced contraction and that fluticasone amplifies the inhibitory effect of formoterol on human bronchial smooth muscle cells [433]. In their study, gel size was assessed at an interval of 10 min for 60 min following the addition of a stimulant. I used in our study the 3D collagen gel contraction assay to assess HASMCs contraction after stimulation with iHBECs cfDNA. I assessed the HASMCs' contraction by a single 24-hour time point, and I used a positive control (Methacholine) and a negative control (Methacholine+Cell Contraction Inhibitor). Methacholine, known to induce cell contraction, induces gel

contraction in primary cultured mouse bronchial smooth muscle cells [434], and HASMCs [435]. However, I found that positive and negative controls did not significantly cause a change in the gel contraction relative to the control group, suggesting a potential failure with this assay. In addition, I found a large amount of baseline contraction in all treatment groups, making differences potentially more difficult to detect. The findings in our study could be attributed to differences in contractility between assay systems or a potential loss of contractility in HASMCs. Combined with the large amount of baseline contraction observed in my study and the use of a single 24-hour time point, these factors may have missed transient or earlier changes in gel contraction, limiting the ability to detect treatment-specific effects. Therefore, measuring gel size frequently at different time points (e.g., 0, 2, 4, 8 and 24 h) until active cell-driven contraction plateaus and before matrix compaction or degradation dominates would better capture true contractile dynamics of the gel. The differences between the chosen contraction assays could also potentially impact cell contraction responses. Ramis et al. showed a difference between asthmatic and healthy HASMCs contraction when assessed by collagen gel contraction assay, but no difference was seen in the same cell lines when the contraction was assessed by traction force microscopy [435]. This could be explained as the collagen gel contraction assay evaluates macroscopic, collective contraction of the cells embedded in a 3D matrix over time by measuring gel size reduction, while traction force microscopy measures microscopic, real-time forces that individual cells exert on a 2D substrate using displacement of fluorescent beads that might provide high-resolution, cell-specific force results. Therefore, further investigation using different contraction assays such as wrinkle assay or traction force microscopy and different time-course experiments could be alternative methods that provide a more precise

measurement for assessing the effect of cfDNA-stimulated iHBECs on HASMCs contractility.

Transcriptome profiling was used to investigate how cfDNA released from iHBECs can modulate gene expression of HASMCs. To ensure whether cfDNA released from iHBECs with no stimulation affects HASMC gene expression, cfDNA from elution buffer-stimulated iHBECs was compared to cfDNA from control-stimulated iHBECs on HASMCs gene expression. Only two genes, BAG1 and cold-inducible RNA-binding protein (CIRBP), were upregulated in this comparison. BAG1 is involved in apoptosis, autophagy, and protein homeostasis, while CIRBP responds to cellular stress and is linked to cancer progression [436-438]. Based on these results, the elution buffer-stimulated iHBECs group was used as the reference control for all subsequent analyses

The findings of the transcriptome profiles showed that cfDNA isolated from both poly (I:C) and CSE+poly (I:C)-stimulated iHBECs had a significant effect on HASMC gene expression, while cfDNA from CSE-stimulated iHBECs had a minimal impact on HASMCs gene expression compared to elution buffer. In chapter four, the result of qPCR for cfDNA release indicated that treatment of iHBECs with CSE alone did not cause the release cfDNA from iHBECs. The transcriptome profile data therefore support this, as there were no upregulated genes, and only one downregulated gene, from HASMCs stimulated with cfDNA of CSE-stimulated iHBECs. I therefore expected the comparison of CSE+Poly (I:C) vs. CSE to yield comparable results to the Poly (I:C) vs. elution buffer comparison. I found fewer gene expression changes (678 genes), as well as minor modifications to the pathways. The precise explanation for this is unclear. It is possible that CSE causes a low level of cfDNA that was not detectable by qPCR or TapeStation, or that the amount was

insufficient to cause a major change in gene expression across the genome. However, the low level of cfDNA may have been sufficient to cause no significant changes in gene expression in HASMCs compared to the elution buffer group, which could have impacted the CSE + poly (I:C) versus CSE comparison.

Among all the 13,224 gene counts mapped by RNA-Seq, cfDNA from poly (I:C)-simulated iHBECs caused significant differential expression of 915 genes, and that 698 of these genes were significantly upregulated. Some genes play a role in the inflammatory responses associated with viral infection. For example, cfDNA of poly (I:C)-stimulated iHBECs significantly upregulated pro-inflammatory and immune-related HASMC genes such as CXCL9, CXCL10, CXCL11, CCL5 (RANTES), and GBP5. Pro-inflammatory chemokine CXCL9, along with CXCL10 and CXCL11 were upregulated following SARS-Cov-2 infection, and the use of AKT inhibitor GSK690693 markedly reduced the effects in human lung epithelial cells [439]. A recent study also found that CXCL11 signalling was significantly elevated in HASMCs in response to infant RSV bronchiolitis [440]. Furthermore, RANTES and GBP5 are upregulated during respiratory viral infections, with RANTES linked to RSV infection and GBP5 shown to increase in response to influenza A virus via the NF-κB pathway in HBECs (A549) cell line [407, 441]. Together with these findings, our findings suggest that cfDNA released from poly (I:C)-stimulated iHBECs can activate pro-inflammatory pathways in HASMCs, similar to responses seen during real viral infections like SARS-CoV-2, RSV, and influenza which could influence HASMCs behaviour and promote inflammatory responses, potentially contributing to asthma progression and exacerbation.

The data presented here showed that 217 genes were significantly downregulated in HASMCs in response to cfDNA isolated from poly (I:C)-stimulated

iHBECs. Among these downregulated genes were SMAD9, EYA2, and GSTA4. SMAD9 belongs to the SMAD family, which is involved in the bone morphogenetic protein (BMP) signalling pathway and has a role in cell growth and tissue homeostasis [442]. EYA2 gene plays a key role in lung cancer, influencing cell proliferation and stimulating tumor cell growth [443, 444]. GSTA4, among the downregulated genes, has also been reported to be associated with an oxidative stress response [445]. The studies on these genes in the context of asthma are still limited. However, the transcriptional findings suggest that cfDNA from poly (I:C)-stimulated iHBECs may suppress genes in HASMCs that are typically involved in cell signalling and proliferation, and protection against oxidative stress, potentially contributing to the airway inflammation and impaired tissue repair mechanisms, which are all characteristics of asthma. Therefore, studying the involvement of these genes in *in vitro* and *in vivo* models of asthma could be an approach for discovering novel molecular mechanisms driving airway remodelling and inflammation in asthma.

The GO enrichment analysis of upregulated genes by cfDNA from poly (I:C)-stimulated iHBECs showed several enriched terms related to biological process and molecular function, which include defence response to virus, regulation to viral process, viral genome replication, and virus receptor activity. These findings suggest that viral recognition, viral replication detection, and antiviral defence mechanisms are significantly active upon cfDNA stimulation. Several enriched terms were also found to be related to cellular components, including cytoplasmic ribonucleoprotein granule and cytoplasmic stress granule. This suggests that HASMCs upon stimulation with cfDNA from poly (I:C)-stimulated iHBECs may activate distinct cytoplasmic structures and defence mechanisms crucial for managing stress, particularly during viral infections. Stress granules (SGs) activated following infection

with certain DNA and RNA viruses and are an important aspect of the antiviral response [446]. It has been reported that SARS-CoV-2 infection can influence SG formation via pathways such as PKR-eIF2α pathway, and that potential antiviral drugs targeting SGs could provide new insights into developing SG-targeted antiviral treatments, particularly against SARS-CoV-2 [447]. Viral infections are a major cause of asthma exacerbation. Dysfunctional stress granule formation could impair cells' ability to regulate viral replication efficiently. Therefore, potential antiviral drugs targeting SGs could provide new insight into asthma management. Moreover, the pathway analysis of upregulated genes by cfDNA of poly (I:C)-stimulated iHBECs revealed several enriched pathways in KEGG analysis such as TNF signaling pathway and influenza A. The dysregulation of TNF-α and its receptors (TNFR1, TNFR2) is a component of the TNF signalling pathway in asthma. The recruitment of airway monocytes is correlated with elevated soluble TNF receptors in neutrophilic asthma, which contributes to the altered inflammatory environment [448]. In addition, Influenza A can trigger a variety of mechanisms in asthma, including apoptosis, autophagy, and endoplasmic reticulum stress. These pathways can either promote or inhibit viral replication, influencing asthma exacerbations and underlining their potential as targets for therapy in asthma management [449]. Together, these findings suggest that TNF signalling and Influenza A-related pathways illustrate how viral infection can exacerbate airway inflammation in asthma, and targeting these mechanisms could improve therapeutic intervention and asthma management.

The downregulated genes of cfDNA from poly (I:C)-stimulated iHBECs were also enriched in several GO and KEGG terms and pathways. The biological process and molecular function were enriched with numerous terms related to RNA and mRNA, including regulation of mRNA processing and regulation of mRNA metabolic

process, and rRNA binding. This suggests that the ability of HASMCs to properly process and regulate RNA, particularly mRNA, which contains the instructions for protein production, might be disturbed or inhibited. Furthermore, the binding of ribosomal RNA (rRNA) is an important part of ribosome activity and protein synthesis, controlling protein production and interactions with other molecules [450]. This could lead to defective production of protein for HASMCs necessary for survival, repair, and immune response, ultimately contributing to dysregulated inflammatory responses and impaired antiviral defences, all of which are key features of asthma pathogenesis. The cellular component also showed some enriched terms such as peroxisome, microbody, and outer membrane. Peroxisomes, formerly known as microbodies, are small organelles vital for maintaining cellular function in lipid metabolism, oxidative balance, and intracellular signalling [451]. The outer membrane composition is influenced by protein-lipid interactions, and the integrity of the outer membranes and peroxisomes is essential for appropriate cellular function, maintaining peroxisomal function, and promoting membrane dynamics [452]. Disruption in peroxisome and outer membrane function may compromise HASMCs ability to manage oxidative stress and lipid metabolism, both of which are critical in regulating inflammation and immune responses Furthermore, the downregulated genes by cfDNA from poly (I:C)-stimulated iHBECs involved in KEGG included but were not limited to chemical carcinogenesis-reactive oxygen species, nucleotide metabolism, and drug metabolism. These pathways suggest that HASMCs may have a decreased capacity to control oxidative stress and repair or synthesize nucleotides, which are essential for DNA replication and for RNA production [453]. In addition, it may affect how HASMCs respond to treatments, thereby lowering the efficacy of

anti-inflammatory medicines such as corticosteroids, which are often used for treating asthma.

In terms of co-stimulation of CSE and poly (I:C), our data showed that cfDNA from CSE+poly (I:C)-simulated iHBECs caused significant differential expression of 833 genes in HASMCs. The findings of transcriptome profiles data indicated that poly (I:C) induced cfDNA largely mediated the expression of most of the genes, even when CSE was combined with poly (I:C). In Chapter 4, I found that co-stimulation of CSE and poly (I:C) significantly increased the concentration of released cfDNA relative to poly (I:C) alone in iHBECs, suggesting a differential response to the co-simulation induced cfDNA may be observed in HASMC gene expression. Therefore, I investigated differential gene expressions in terms of cfDNA of CSE and poly (I:C)-stimulated iHBECs induced HASMCs gene expression compared to poly (I:C) alone-stimulated iHBECs induced HASMCs gene expression group. Most of the differentially expressed genes were similar between the two treatment groups with slight differences in the fold changes of these genes, suggesting that poly (I:C) might mediate the expression for most of the genes even when CSE was combined with poly (I:C). The GO enrichment analyses for biological processes, molecular function, and cellular components, as well as KEGG pathway analysis, also shared the same enriched terms. In addition, there were no significant shifts in the overall effect size between the two groups, suggesting that the changes in effect size might be gene-specific.

Interestingly, I found 47 genes were significantly upregulated and 51 were downregulated, distinctly for cfDNA of CSE+poly (I:C)-simulated iHBECs treatment group compared to cfDNA of poly (I:C)-alone stimulated iHBECs (Appendix 7.13.4/5). Among the 47 genes that were upregulated with CSE+poly (I:C) group, the

Human Leukocyte Antigen - DR Beta 1 (HLA-DRB1) gene encoded the beta chain of the HLA-DR protein, which is necessary for peptide activation of CD4+ T helper cells in the immune system. This gene was found in the literature associated with asthma. A meta-analysis study found that HLA-DRB1 gene, with specific alleles such as DRB1 03 was positively associated with asthma risk and play a key role in regulating immune responses of asthma pathogenesis [454]. Another study of the same gene found that HLA-DRB03 plays an important role in inducing Th2-predominant immune response to HDM and Th2 inflammation, which leads to elevated eosinophil counts in mice model [455]. Polo-like kinase 3 (PLK3), which is involved in stress response pathways and cell cycle regulation, was found among the distinct upregulated genes for the CSE+poly (I:C)-stimulated iHBECs group. Transcriptome studies have identified PLK3 among genes differentially expressed in therapy-resistant asthma in children, indicating a role in disease severity [456]. I found also absent in melanoma 2 (AIM2), which is a gene that encodes a protein that functions in the innate immune response, mainly by recognising cytosolic double-stranded DNA and activating the inflammasome. An *in vivo* study found that AIM2 contributes to epithelial barrier dysfunction in response to allergens such as HDM and ovalbumin (OVA). Eliminating AIM2 in this experimental model decreased inflammatory cytokine levels and improved epithelial cell viability in infant mice, suggesting that AIM2 could be a promising target for paediatric allergic asthma therapy regimens [457].

For the other genes found in the CSE+poly (I:C)-stimulated iHBECs group, there was a limitation in the current research linking these genes to asthma to the best of our knowledge. However, some of these genes were found to be involved in the inflammatory and biological processes. Several genes were found to be associated with the inflammatory process and immune response in various

inflammatory diseases such as GPR84 and TRIM36 [458-460]. In addition, ZNF710 has been reported to be associated with gene expression and DNA binding [461]. Several genes were also found to be associated with the development of cancer including TGIF1 and CSRNP2 [462, 463]. The distinct genes that were found to be associated with CSE+poly (I:C)-stimulated iHBECs induced HASMCs gene expression could be involved in mediating the effect of co-stimulation of CSE and poly (I:C). Therefore, further studies exploring the roles of these genes and their associated pathways are essential to deepen our understanding of how CSE affects viral responses in airway structural cells, potentially uncovering new therapeutic targets for asthma management.

In conclusion, this chapter identified cfDNA released from iHBECs, particularly following poly (I:C) and CSE+poly (I:C) stimulation, as a potent modulator of HASMCs transcriptomic responses. Although cfDNA from stimulated iHBECs did not significantly impact HASMCs proliferation within 24 hours, the transcriptional shifts observed suggest that iHBECs' cfDNA following poly (I:C) and CSE+poly (I:C) stimulation may prime HASMCs for altered function over time via inducing gene expression change. Studying the role of these genes is crucial for understanding how CSE modulates viral responses and alters cellular functions in airway structural cells. In addition, these findings advance our understanding of cfDNA as a novel intercellular signal in the airway cellular environment and provide the groundwork for future investigations into its contributions to the asthma pathogenesis.

Chapter 6. General discussion and conclusions

6.1 General discussion

The overall aims of this thesis were to investigate how CSE modulates bronchial epithelial cell responses to allergen and viruses, with a focus on the production and the release of inflammatory mediators such as alarmins, Th2 cytokines, eosinophilic chemokines, and neutrophilic chemokines, as well as the release of cfDNA. Additionally, I explored the downstream effects of cfDNA released from iHBECs on remodelling processes and gene expression in human airway smooth muscle cells (HASMCs).

The key findings of this thesis were that CSE did not modulate the inflammatory mediator response of bronchial epithelial cells to house dust mite (HDM) allergen (*Der P1*) but did have profound effects on the inflammatory response to the viral mimic poly (I:C). Notably, my results showed that CSE modulates the response of iHBECs to viruses through altering inflammatory responses, suppressing epithelial-derived alarmin and eosinophil responses, and inducing neutrophilic responses. Additionally, my results demonstrated that cfDNA release from iHBECs was significantly enhanced following stimulation with poly (I:C) and co-stimulation of CSE and poly (I:C) but that CSE alone did not lead to cfDNA release. Functional studies from iHBECs cfDNA revealed that cfDNA significantly modulated gene expression in HASMCs but did not affect their proliferative response.

HBECs serve as the primary barrier against inhaled environmental insults and play a pivotal role in the development and progression of asthma [98]. HBECs are a key source of alarmin cytokines, which are released upon exposure to environmental triggers such as allergens and viral infections. These alarmins activate innate immune responses, driving T2-high inflammation and eosinophilic

airway inflammation [214]. HDM is one of the most common environmental allergens linked to asthma development, contributing to persistent eosinophilic airway inflammation, frequent exacerbations, and poor asthma control [75, 276-278]. Cigarette smoke can exacerbate allergen-induced asthma by altering inflammatory responses, increasing bronchial hyperactivity, and enhancing the production of pro-inflammatory cytokines, ultimately contributing to corticosteroid resistance and more severe asthma symptoms [144]. CS induces the production of IL-33 and TSLP, leading to a Th2 immune response and contributing to airway inflammation *in vivo* [369]. The interaction between CSE and HDM has been studied, showing that CSE may enhance damage to and permeability of HBECs, lower the threshold of allergen sensitisation, and inhibit eosinophilia induced by HDM [189, 464, 465]. The limited number of studies investigating the combined effects of CSE and HDM on HBECs highlights a significant gap in our understanding of how cigarette smoke and allergens interact at the airway epithelial level, particularly regarding their impact on the production of epithelial-derived alarmins, Th2 cytokines, eosinophil chemokines, and neutrophil chemokines.

In our study, I used *Der P1*, a cysteine protease and a major HDM allergen, and I assessed the impact of CSE on the effect of *Der P1* on HBECs. The findings in this thesis revealed that there was no interaction between CSE and HDM on the release of alarmins, Th2 cytokines, and eosinophil chemokines from HBECs. However, CSE in our study has been shown to significantly increase the production of neutrophilic chemoattractant (IL-8). Supporting this, both *Der P1* and CSE induced concentration- and time-dependent increases in IL-8 release from primary HBECs and the HBECs (BEAS-2B) cell line, with CSE-induced IL-8 production further correlating with neutrophil counts in BAL fluid [159, 180]. Taken together, this

suggests that CSE may not modify HDM-induced eosinophilic inflammation in HBECs and may drive a shift toward a neutrophilic asthma phenotype, particularly in the presence of allergen exposure, leading to more severe and less responsive asthma to corticosteroids. Immortalized HBECs have been used in this study and are widely used in respiratory research because they have many normal features of primary airway epithelial cells, including inflammatory responses and the ability to differentiate which can provide a stable and reproducible in vitro model of the airway epithelium [256]. Primary HBECs, while physiologically relevant, are limited by donor variability, finite lifespan, and difficulty in maintenance. iHBECs overcome these limitations, making them ideal for mechanistic studies. In addition, iHBECs in our experimental model were cultured under submerged conditions which might not replicate the overall airway's physiological barrier functions. Therefore, while our study provides valuable insights using immortalised HBECs in submerged culture condition which the cells may not be fully differentiated, further validation is required in primary HBECs and using different culture condition such as air-liquid interface (ALI) culture which allow the cells to differentiate into different airway epithelial cell types that make more physiologically relevant model of the airway and closer to *in vivo* airway tissue as well as in vivo models, such as animal studies, and using chronic exposure of allergen to verify whether the observed effects of CSE and allergen exposure on airway inflammation are consistent across different biological systems.

In addition to investigating allergen, I also aimed to investigate the impact of CSE on inflammatory responses in iHBECs following viral infection using the viral mimic polyinosinic:polycytidylic acid (poly (I:C)). Poly (I:C) is a synthetic double-stranded RNA (dsRNA) that mimics viral RNA, which induces inflammatory

responses in the cells [320]. An expanding body of evidence indicates that cigarette smoke increases susceptibility and risk for viral infection [323-325]. CSE significantly inhibited the production of IL-6, IL-8, IP-10, and interferons, and altered endocytic pathways by enhancing caveolin-mediated uptake while inhibiting clathrin-mediated uptake in small airway epithelial cells (SAECs) in response to poly (I:C) and influenza A virus [325, 383]. This study is the first to assess the impact of CSE in response to poly (I:C) stimulation on the release of epithelial-derived alarmins, key initiators of Type 2 immune responses, and their downstream mediators, including Th2 cytokines and eosinophilic chemokines, as well as non-T2 cytokines in HBECs, aiming to identify whether CSE promotes a shift from eosinophilic (Type 2) to neutrophilic (Non-T2) inflammation. The findings within this thesis revealed that CSE significantly inhibited the production of all alarmin responses to poly (I:C) from iHBECs, which suggests that CSE may suppress epithelial-derived alarmin responses. In addition, CSE significantly inhibited the production of eosinophil chemokines but had a minimal effect on Th2 cytokines in response to poly (I:C) stimulation in iHBECs. This suggests that CSE may impair the early innate immune signaling from HBECs to allergen by suppressing alarmin production, which in turn could attenuate downstream eosinophilic inflammation. Also, the observation in our study revealed that there was minimal effect of CSE on Th2 cytokines in response to poly (I:C) in iHBECs. Evidence indicates that HBECs are relatively unresponsive to direct modulation by Th2-associated cytokines such as IL-4 and IL-13 [363]. These findings suggest that HBECs might not inherently release Th2 cytokines but might be integral in modulating immune responses related to these cytokines, which might explain the findings in our study that Th2 cytokines, particularly IL-5 and IL-13 had minimal effect in response to poly (I:C). On the other hand, CSE enhances the

production of neutrophilic chemokine (IL-8) in response to poly (I:C), which showed an additive effect on IL-8 production. This observation was seen previously in our group's study on the impact of CSE on HASMCs, showing that CSE might shift the inflammation from eosinophilic to neutrophilic inflammation through inhibiting of Th2 cytokines and inducing neutrophilic chemokine (IL-8) in HASMCs (manuscript in preparation) [153]. The overall findings in our study provide novel insights into how CSE could impair antiviral defence mechanisms through suppressing the production of epithelial-derived alarmins, suppressing eosinophils, and promoting neutrophilic inflammation in HBECs in response to allergen stimulation. The shift from eosinophil to neutrophil inflammation highlights the important role of HBECs in regulating immune responses and shows the impact of cigarette smoke on asthma pathogenesis. This could lead to identifying potential targets for therapeutic targets in asthmatic smokers.

Besides investigating inflammatory mediators, this study reported for the first time the effect of CSE on the release of cfDNA from iHBECs in response to poly (I:C). cfDNA refers to non-encapsulated DNA present in the bloodstream or other bodily fluids, with its concentration often reflecting the extent of tissue damage and inflammation across a range of pathological conditions [329]. It has been reported that cfDNA concentration increases following COVID-19 and influenza A infection [244, 337]. A former PhD student in our group demonstrated that poly (I:C) significantly increased cfDNA release in primary HBECs [338]. In our study, consistent with the findings of a former PhD student, I found that poly (I:C) caused a significant release of cfDNA. Interestingly, I found that CSE alone did not cause a release of cfDNA from iHBECs, but co-stimulation of CSE and Poly (I:C) significantly increased the concentration of released cfDNA, relative to poly (I:C) alone,

suggesting a possible synergistic or priming effect of CSE in enhancing cfDNA release in the context of viral stimulation. This may contribute to epithelial damage, leading to worsening airway inflammation and increased epithelial tissue damage, both of which contribute to the pathogenesis of asthma, particularly in virally infected asthmatic smokers.

During this research, I noticed that the cfDNA fragment sizes of the tested samples in response to Poly (I:C) and co-stimulation of CSE and Poly (I:C) were relatively large in size, which might indicate the DNA is packaged as part of extracellular vesicles (EVs). EVs are an important cell-to-cell communicator, contributing to both normal physiological functions and pathological conditions, and hold promise as potential diagnostic biomarkers and therapeutic targets [466].

EVs play a crucial role in carrying cfDNA, and a large proportion of cfDNA in human blood plasma is found within EVs [330]. Airway structural and immune cells secrete EVs containing cfDNA, along with various lipids, proteins, and nucleic acids, that can alter normal airway function and initiate respiratory disease processes [331-333]. EVs released during viral infections, including RSV, have been shown to influence immune responses by stimulating epithelial cells to produce cytokines and chemokines such as IP-10, RANTES, and TNF-α [467]. Therefore, I assessed the release of EVs in the tested samples, but I found that there were no significant alterations in EV characteristics, such as size or morphology, across the treatment groups, suggesting that the cfDNA release may not be directly associated with EVs or the EV cargo composition may have varied between treatment groups. It is important to acknowledge that the current EV-related observations in this study are preliminary and based on limited data. Therefore, additional studies using EV formation inhibitors, or isolating EVs from iHBECs and using them to directly

stimulate HASMCs, could help determine whether cfDNA release from iHBECs occurs through EV-associated mechanisms.

Cigarette smoke contributes to increased oxidative stress, leading to macromolecular damage and inflammation in the lung [468]. The effects of cigarette smoke on lung inflammation may result from the enhancement of COX-2 expression in the airway [167]. CSE induces COX-2 expression in many cells [290], including HASMCs [291] and HBECs [292]. In this study, I assessed the roles of oxidative stress and COX-2 expression in mediating the effect of CSE in iHBECs. I found that oxidative stress inhibitor (GSH) significantly inhibited the effect of CSE on the release of IL-8 production and cfDNA concentration. In addition, CSE significantly induced COX-2 protein expression, raising the possibility that the effect of CSE on iHBECs might be mediated by COX2 upregulation via oxidative stress. Consistent with this finding, our group has previously demonstrated that CSE promotes a shift in HASMCs from eosinophilic to neutrophilic inflammation by suppressing T2 cytokine production and enhancing IL-8 (a non-T2 cytokine) expression through the COX-2/mPGES-1/PGE2/EP2/EP4/cAMP signaling pathway, mediated by oxidative stress (manuscript in preparation) [153]. It is possible that this mechanism drives the effect of CSE in iHBECs but further research is needed to confirm this.

Having shown that poly (I:C) stimulation of iHBECs led to increased cfDNA release, it was important to investigate whether the released cfDNA had any functional effect on airway structural cells, particularly HASMCs, as both cell types play key roles in airway inflammation and remodelling processes in asthma. Their crosstalk contributes significantly to asthma pathogenesis through several mechanisms, including direct cell-to-cell contact, which drives features of asthma such as inflammation, AHR, airway remodeling, and mucus hypersecretion [131].

The release of various epithelial cell mediators, including cytokines, chemokines, growth factors, and extracellular matrix proteins, can modulate HASMCs inflammatory responses, contraction, and proliferation [131]. Since cfDNA plays a crucial role in stimulating proinflammatory cytokine synthesis, enhances oxidative stress, and contributes to inflammation in several diseases [334, 335], I investigated the effect of iHBECs' cfDNA on HASMCs' contraction, proliferation, and gene expression to understand whether it might play a pathogenic role in asthma. To the best of my knowledge, this study is the first to report the downstream effects of cfDNA-stimulated iHBECs on HASMCs remodelling processes and gene expression. The findings in this study showed that cfDNA from CSE- and Poly I:C-stimulated iHBECs had no effect on HASMCs proliferation. HASMC proliferation was assessed using two independent methods, both of which yielded consistent results and supported the validity of the findings, as evidenced by the appropriate response in the positive control group. Unfortunately, the 3D collagen gel contraction assay, which was used to assess the contraction of HASMCs, yield inconclusive results due to the lack of effect of both positive and negative controls. It would be important, therefore, to investigate further whether epithelial-derived cfDNA can modulate HASMC contraction in other model systems. Such systems could include using traction force microscopy or the Wrinkle assay, which have been previously used to study cellular contraction *in vitro* [435, 469].

The novel findings in this thesis demonstrated that cfDNA from poly (I:C) and CSE + poly (I:C)-stimulated iHBECs had a significant effect on HASMCs gene expression. cfDNA from iHBECs caused a significant differential expression of 915 genes in response to poly (I:C)-stimulated iHBECs group and 833 genes in response to co-stimulation of CSE and poly (I:C)-stimulated iHBECs, but had no effect on gene

expression in response to cfDNA from CSE alone-stimulated iHBECs group. The findings of transcriptome profiles results indicated most of the differentially expressed genes were similar between the two treatment groups such as CXCL9, CCL5, and CXCL10 with slight differences in the fold changes of these genes, suggesting that poly (I:C) might mediate the expression for most of the genes even when CSE was combined with poly (I:C). In addition, there were no significant shifts in the overall effect size between the two groups, suggesting that the changes in effect size might be gene-specific.

Interestingly, I found 47 genes were significantly upregulated and 51 were downregulated, distinct for cfDNA of CSE+poly (I:C)-simulated iHBECs treatment group compared to cfDNA of poly (I:C)-alone stimulated iHBECs, suggesting that CSE may contribute and modulate the gene expression profile of HASMCs when combined with poly (I:C), potentially altering downstream inflammatory or structural responses. Upon navigating these distinct genes related to co-stimulation of CSE and poly (I:C)-stimulated iHBECs group, studies on these specific genes in the context of asthma were still limited in the current research. However, I found limited studies on some of these genes associated with asthma pathogenesis. For example, the Human Leukocyte Antigen - DR Beta 1 (HLA-DRB1) found in the literature associated with asthma risk and played a key role in regulating immune responses of asthma pathogenesis as well as inducing Th2-predominant immune response to HDM and Th2 inflammation [454, 455]. Furthermore, Polo-like kinase 3 (PLK3), involved in stress response pathways and cell cycle regulation, and transcriptome studies have identified PLK3 among genes differentially expressed in therapy-resistant asthma in children, indicating a role in disease severity [456]. It is highly important to conduct further studies on these specific genes to identify novel

biomarkers and explore epigenetics or signaling pathways, which could provide insight into our understanding of the effect of CSE on airway structural cells and may represent potential therapeutic targets for asthma.

Clinically, asthma patients exhibiting neutrophilic airway inflammation tend to respond poorly to corticosteroid treatment [470]. Crucially, neutrophilic airway inflammation is driven by ongoing smoke inhalation since a clinical study showed that quitting smoking for 6 weeks caused a decrease in sputum neutrophil count and improved lung function [273]. Furthermore, ex-smokers showed a greater increase in eosinophil blood count compared to smokers [471]. The findings of our study, along with other findings, highlighted the importance of smoking cessation as a therapeutic intervention that might control the airway inflammation, reducing the neutrophilic inflammation, which is known to be insensitive to corticosteroid therapy, the main treatment to control asthma [33].

6.2 Conclusion

Airway inflammation is a primary characteristic of asthma, and the endotypes of asthma are classified into two main types based on inflammatory profiles, namely Type 2-high allergic asthma (T2-high) and non-Type 2 asthma (Non-T2). Cigarette smoke combined with asthmatic inflammation may induce important changes in the asthma inflammatory endotype. HBECs are the first line of defence against inhaled insults, including cigarette smoke, viruses, and allergens such as HDM, and are an important source of a group of cytokines termed alarmins. The findings outlined in this thesis show that while CSE did not modulate inflammatory responses of iHBECs to *Der P1* allergens, it was capable of modulating the inflammatory response to a viral mimic poly (I:C). Such modulation included inhibiting alarmins and eosinophilic chemokine production while inducing the neutrophilic chemokine IL-8 and enhances the release of cfDNA. Furthermore, released cfDNA of poly (I:C) and co-stimulation of CSE and poly (I:C) did not affect HASMCs proliferation but had a significant effect on HASMCs gene expression.

6.3 Future direction

All experiments in this study were conducted using in vitro models with immortalised HBECs and healthy donor-derived HASMCs. To enhance physiological relevance, future studies should replicate these findings using primary HBECs and HASMCs from asthmatic and compare them with non-asthmatic patients, including both smokers and non-smokers, and assess the potential mechanisms. Additionally, validating the observed effects of CSE using *in vivo* animal models would help confirm these findings. cfDNA stimulation of HASMCs was based on the calculation of the amount of cfDNA from the surface area of the well-plate used in iHBECs experiments to the HASMCs experiment' plates, trying to mimic the iHBECs and HASMCs being in direct contact at a surface area level. Therefore, using co-culture models of HBECs and HASMCs could provide more accurate insights into cell-cell communication and validate these results. Future studies needed to assess the release of EVs from HBECs and characterize their cargos, including proteins and microRNAs, to better understand their potential role in intercellular signaling and disease processes. To further investigate whether cfDNA release from iHBECs is associated with EVs, future studies could involve clinical research by recruiting individuals with respiratory viral infections. EVs could be isolated from bronchoalveolar lavage (BAL) samples of these patients to assess the functional impact of EV on HASMCs *in vitro*. A comparative analysis between EVs from asthmatic patients experiencing viral infections and those from asthmatic individuals without viral infections could provide insights into viral infection-specific EV profiles and their potential role in airway inflammation in asthma. Moreover, further investigation of the genes differentially expressed in HASMCs in response to cfDNA-stimulated iHBECs is crucial for identifying novel biomarkers and signalling pathways

involved in smoke- and virus-induced asthma, which could ultimately contribute to more effective asthma management and therapeutic strategies.

Chapter 7. Appendix

7.1 Tables of Materials

7.1.1 Materials for cells culture

Keratinocyte serum-free-medium (KSFM)	Thermo Fisher Scientific
Dulbecco's Modified Eagle's Medium (DMEM)	Sigma Aldrich
Bovine pituitary extra (BPE) 25 mg, protein concentration 16.0 mg/ml, for the culture of human keratinocytes	Thermo Fisher Scientific
Epithelial growth factor (EGF) human recombinant 2.5*µg, protein concentration 0.0382 µg/µl,* for culture of human keratinocyte	Thermo Fisher Scientific
Penicillin/streptomycin 5000 units of penicillin and 5 mg of streptomycin/ml, sterile-filtered, BioReagent suitable for cell culture	Sigma Aldrich
G418 sulfate 712.00 *µg/mg, for cell culture*	Sigma Aldrich
Puromycin dihydrochloserum-free mediumride 10 mg/ml in H_2O, for cell culture	Sigma Aldrich
Foetal bovine serum (FBS)	Thermo Fisher Scientific
L-glutamine solution, sterile-filtered, 200 mM solution.	Sigma Aldrich
Amphotericin-B sterile-filtered, 250 mg/ml in deionized water	Sigma Aldrich
Trypsin–Ethylenediamine Tetraacetic Acid (EDTA) solution, 0.25%, sterile-filtered, BioReagent suitable for cell culture, 2.5g porcine trypsin and 0.2g EDTA 4Na per litre of Hanks' Balanced Salt Solution with phenol red	Sigma Aldrich
Dimethyl sulfoxide (DMSO)	Sigma Aldrich
Trypan blue solution	Sigma Aldrich

7.1.2 Cell culture medium recipes

KSFM+	500ml supplemented with 25µg/ml bovine pituitary extract, 0.2ng/ml recombinant epithelial growth factor, 250ng/ml puromycin, 25µg/ml G418, and 10 ml penicillin/streptomycin.
KSFM-	500 ml supplemented with 10 ml penicillin/streptomycin.
DMEM+	500 ml supplemented with 10% FBS, 0.02% (4nM) L-glutamine, 0.02%(100unit/ml) penicillin, (0.1 mg/ml) streptomycin, respectively, and 0.01% (250 mg/ml) amphotericin-B.
DMEM-	500 ml supplemented with 0.02% (4nM) L-glutamine, 0.02% (100unit/ml) penicillin, (0.1 mg/ml) streptomycin, respectively, and 0.01% (250 mg/ml) amphotericin-B.

7.1.3 Cigarette smoke extract (CSE) materials

3R4F research-grade cigarettes, one cigarette contains 9.4mg of tar, 0.7mg of nicotine, 12mg of carbon monoxide	Kentucky Tobacco Research and Development Centre, University of Kentucky, USA
DA7C Pump	Charles Austen Pumps

7.2 Der P1 preparation

Dermatophagoides pteronyssinus1 (*Der P1*) purified 732 µg (BCA) / vial Molecular weight 25 kDa (10 mg) To make the original stock of the final concentration of 25 µg/ml, 732/2500 X 1000 µl = 292.8 µl of unsupplemented KSFM- medium were added to the original vial.	Citeq Biologics

7.3 Poly (I:C) preparation

Polyinosinic-polycytidylic acid sodium salt (Poly (I:C)) purified 10 mg/ vial	Tocris bioscience

To make the original stock of the final concentration of 1 mg/ml, 10 ml of distilled water was added to the original vial. Then, 10 µg/ml was used in each experiment.	

7.4 L-Glutathione (GSH) preparation

L-Glutathione (GSH). Mass: 10 mg. Molecular weight: 307.32. The drug was dissolved in 650.6 µL of water to make the original stock of 0.05 M.	Sigma Aldrich

7.5 TERT primers

Forward primer (TERTF): 5'-CCTCACATAAATGCTACCAAACGA-3' Mass: 424.6 µg 584 µL of nuclease-free water was added to make an original stock of 100 µM Reverse Primer (TERTR) 5'-TTCCAAGAAGGAGGCCATAGTC-3 Mass: 232.0 µg 342 µL of nuclease-free water was added to make an original stock of 100 µM -The original stock for forward and reverse primers were diluted in a 1:10 ratio to make the final concentration of 10 µM, which was used in each experiment.	Sigma Aldrich

7.6 Buffers and reagents

Phosphate-buffered saline (PBS)	Thermo Fisher Scientific
Bovine serum albumin (BSA)	Thermo Fisher Scientific
Tween 20	Sigma Aldrich
Tris-buffered saline (TBS) 20 mM Trizma hydrochloride (Tris-HCl) 150 mM NaCl	Sigma Aldrich
Reagent diluent for IL-8/CXCL8 DuoSet ELISA 0.1% BSA, 0.05% tween 20 in TBS (pH 7.2-7.4) Filtered by 0.2 µm pore syringe filter	
Block buffer for IL-8/CXCL8 DuoSet ELISA 1% BSA in PBS (pH 7.2-7.4) Filtered by 0.2 µm pore syringe filter	
Wash buffer for IL-8/CXCL8 DuoSet ELISA 0.05% (1ml) Tween 20 and 5 PBS tablets in every 1000 ml of distilled water (pH 7.2-7.4)	
Substrate solution 1:1 mixture of Substrate Reagent A Hydrogen Peroxide (H_2O_2) and Substrate Reagent B (Tetramethylbenzidine)	Thermo Fisher Scientific
Radioimmunoprecipitation assay (RIPA) buffer • 50mM Tris-HCL, pH8.0 • 0.5% Sodium Deoxycholate • 150mM Sodium Chloride • 0.1% Sodium Dodecyl Sulphate (SDS) The following contents were added after RIPA buffer preparation for the protein collection: • 2mM Phenylmethylsulphonyl Fluoride (PMSF) • 1mM Protease Inhibitor Cocktail (PIC) • 1mM Sodium Orthovanadate	
Proteinase K Mass: 20 mg	Qiagen

To make original stock, 5.5 ml of protease solvent was added to the original vial.	
β-mercaptoethanol	Sigma Aldrich
PerfeCTa® SYBR® Green FastMix	Avantor®
4% formaldehyde	Thermo Fisher Scientific
TEM carbon film 200 mesh copper grids	Agar Scientific
10x TBS-T buffer: 1000 ml of dH2O, 87.6 g NaCL, 0.2 M tris base, 10 Tween 20 (pH 7.4-7.6). To make 1x TBS-T: 900 ml of dH2O + 100 ml of 10x TBS-T buffer.	
Blocking buffer for Western Blotting. 5% of non-fat dry milk in TBS-T (Tris-Buffered Saline with 0.1% Tween 20)	
20x Bolt MOPS SDS running buffer	Thermo Fisher Scientific
Bolt Transfer Buffer (20x)	Thermo Fisher Scientific
Bolt Antioxidant	Thermo Fisher Scientific
4x Bolt LDS Sample Buffer	Thermo Fisher Scientific
MagicMark XP Western Protein Standard	Thermo Fisher Scientific
Spectra Multicolor Broad Range Protein Ladder	Thermo Fisher Scientific
10x Bolt Sample Reducing Agent	Thermo Fisher Scientific
Running buffer: 50 ml of 20x MOPS SDS running buffer + 950 ml of dH2O.	

Transfer buffer: 50 ml of 20x Transfer buffer with 100 ml methanol, 1 ml of Antioxidant + 849 ml of dH2O.	
Clarity and clarity Max ECL Western Blotting Substrates	Bio-Rad Laboratories
Blot 4 to 12%, Bis-Tris, 1.0 mm Mini Protein Gel	Thermo Fisher Scientific
Non-fat dry milk	Santa Cruz Biotechnology, USA
Phosphate-buffered saline tablets	Sigma Aldrich
Protease inhibitor cocktails	Sigma Aldrich
Sodium chloride	Sigma Aldrich
Trizma® hydrochloride	Sigma Aldrich
Thiazolyl Blue Tetrazolium Bromide	Sigma Aldrich
Ponceau S Staining Solution	Thermo Fisher Scientific
Ethanol	Sigma Aldrich
Methanol	Sigma Aldrich

7.7 kits

Human IL-8/CXCL8 DuoSet ELISA; DY208-05	R&D systems

DuoSet ELISA Ancillary Reagent Kit; DY008B	R&D systems
Human Premixed Multi-Analyte Kit, Luminex® Discovery Assay; LXSAHM	R&D system
QIAamp®DNA Blood Mini Kit	Qiagen
AllPrep DNA/RNA Mini Kit	Qiagen
cfDNA Tapestation kit	Agilent
Exo-Check™ Exosome Antibody Arrays kit (EXORAY210B-8)	System Biosciences
BCA Protein Assay Kit	Thermo Fisher Scientific
BrdU Cell Proliferation ELISA Kit; ab126556	Abcam
PrestoBlue™ Cell Viability Reagent; A13261	Thermo Fisher Scientific
Cell Collagen-based Contraction Assay	Cell Biolabs
Qubit RNA broad range Assay Kit; Q10211	Thermo Fisher Scientific
Qubit dsDNA HS Kit; Q32854	ThermoFisher Scientific
QuantSeq 3' mRNA-Seq library prep kit for Illumina (FWD); 015.96	Lexogen
The Lexogen i7 6nt Index Set; P04496	Lexogen
The Agilent High Sensitivity D1000 ScreenTape Assay; 5067-5584 and 5067-5585	Agilent
KAPA Library Quantification Kit; KK4824	Roche
Aviti 2x75 Sequencing Kit - Cloudbreak FS Medium Output; 860-00014	Element Biosciences

7.8 Antibodies

Mouse anti-human COX-2 monoclonal antibody (12C10)	Cayman Chemical
Goat Anti-Mouse Immunoglobulins/HRP (P0447)	Dako
Goat Anti-Rabbit Immunoglobulins/HRP (P0449)	Dako

7.9 Instruments and materials

FLUOstar Omega microplate reader	BMG LABTECH
NuPAGE mini gel tank system	Invitrogen
Bio-Plex™ 200 System	Bio-Rad
Agilent 4200 TapeStation system	Agilent
Ariamx Real-Time PCR System	Agilent
Odyssey® XF Imaging System	LICORbio
ZataView® Particle Tracking Analyzer	Particle Metrix
EVOS Cell Imaging System	Thermo Fisher Scientific
Vivaspin 20 centrifugal concentrator	Sigma-Mereck
qEV original 35 columns	IZON
Mr. Frosty Freezing Container	Thermo Fisher Scientific
Nunc Biobanking and cell culture cryogenic tubes	Thermo Fisher Scientific

7.10 Testing Poly (I:C) without cells

Poly (I:C) is a synthetic double-stranded RNA (dsRNA) that mimics viral RNA, which induces inflammatory responses in the cells [320]. In this study, Poly (I:C) was used to stimulate iHBECs as a viral mimic. Poly(I:C) can occasionally cause artifacts in gene expression analysis by interfering with RNA extraction or cDNA synthesis.

To ensure that the responses of the cfDNA measured by qPCR and TapeStation were truly due to iHBECs responses rather than artifact of the RNA, samples without cells were tested included control group (only medium without any treatment) and poly (I:C) negative control (only medium with poly (I:C)). QPCR targeting TERT gene was used to quantify the level of cfDNA and TapeStation was used to analyze the quantity and quality of cfDNA. The results showed no Cq was detected in these two groups (Figure 7.1 A) and no change in the cfDNA concentration that assessed by TapeStation (Figure 7.1 B). These findings confirmed that the cfDNA release was due to iHBECs response to viral mimic (poly (I:C) stimulation.

A

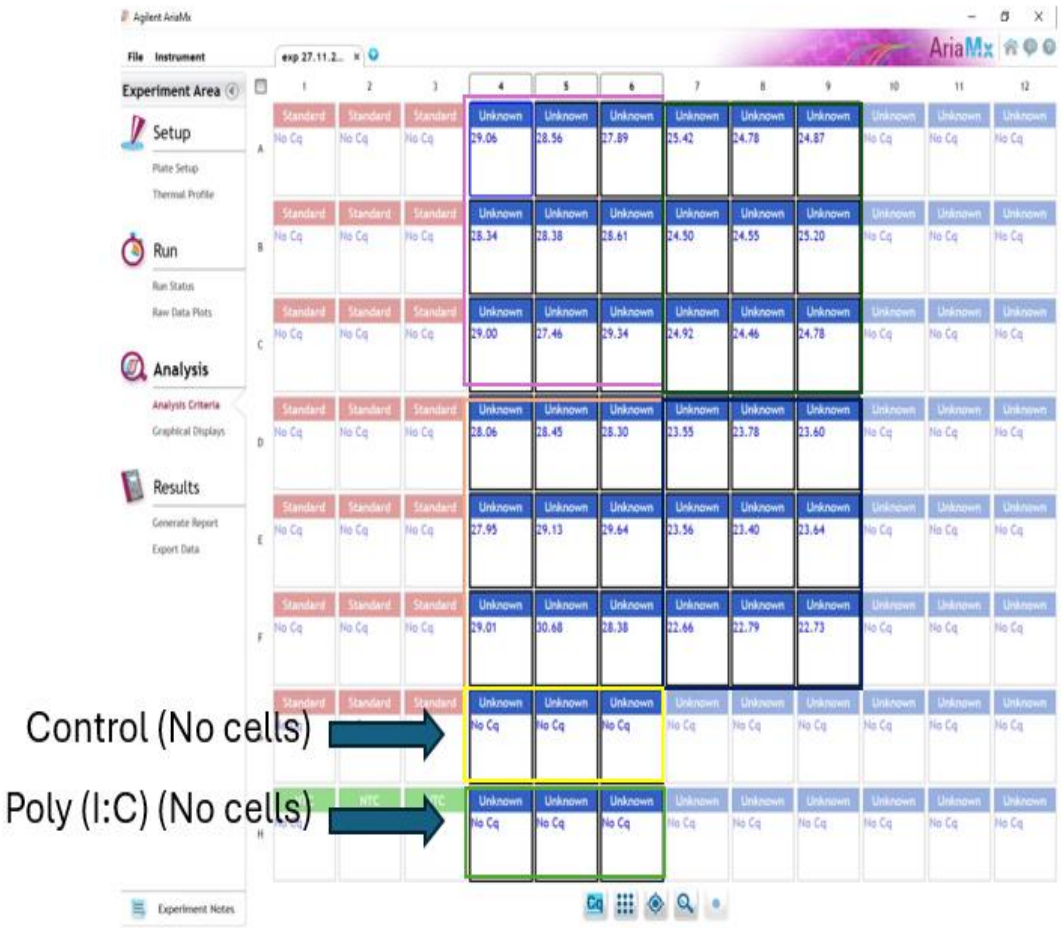
Agilent AriaMx
File Instrument
exp 27.11.2...
AriaMx
Experiment Area
Setup
Plate Setup
Thermal Profile
Run
Run Status
Raw Data Plots
Analysis
Analysis Criteria
Graphical Displays
Results
Generate Report
Export Data
Experiment Notes
Control (No cells)
Poly (I:C) (No cells)

B

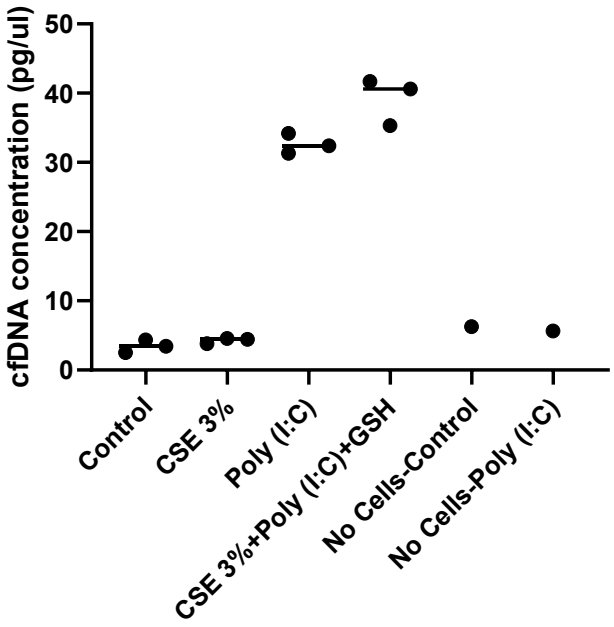

Figure 7.1 Testing the effect of poly (I:C) without cells

A) qPCR targeting TERT gene was used to quantify cfDNA from iHBECs samples and samples without cells **(B)** the concentration of released cfDNA from from iHBECs samples and samples without cells was measured using Agilent 4200 TapeStation system.

7.11 Effect of CSE and poly (I:C) on the production of IL-8 and cfDNA release from iHBECs using 6-well plate

6-well plates were used to isolate more cfDNA from iHBECs in order to stimulate HASMCs. To ensure the expected responses of iHBECs on 24 well-plates were seen prior to undertaking the functional assays, ELISA for IL-8 production and qPCR for TERT were used to assess the responses of iHBECs experiments from 6 well-plate experiments. IL-8 was basally produced by iHBECs at 24 hours (242.3 ± 33.55 pg/mg protein) (Figure 7.1 A). CSE, poly (I:C), and CSE+poly (I:C) significantly increased the production of IL-8 at 24 hours (1447 ± 121.9 pg/mg protein, $^{**}P<0.01$, 2502 ± 174 pg/mg protein, $^{****}P<0.0001$, and 20910 ± 292 pg/mg protein, $^{****}P<0.0001$ pg/mg protein, respectively) (Figure 4.1 A) compared with control. In addition, the findings of qPCR investigation revealed that cfDNA secretions were released basally at 24 hours (0.03489 Cq) (Figure 7.2 B). cfDNA was significantly released in response to poly (I:C) and co-stimulation of CSE and poly (I:C) at 24 hours, as signified by a higher quantification cycle (0.04013 Cq, $^{****}p<0.0001$ and 0.04331 Cq, $^{****}p<0.0001$, respectively) compared to control (Figure 7.2 B). These results showed the same effect of CSE and poly (I:C) on IL-8 production and the release of cfDNA from iHBECs found in 24-well plate experiments.

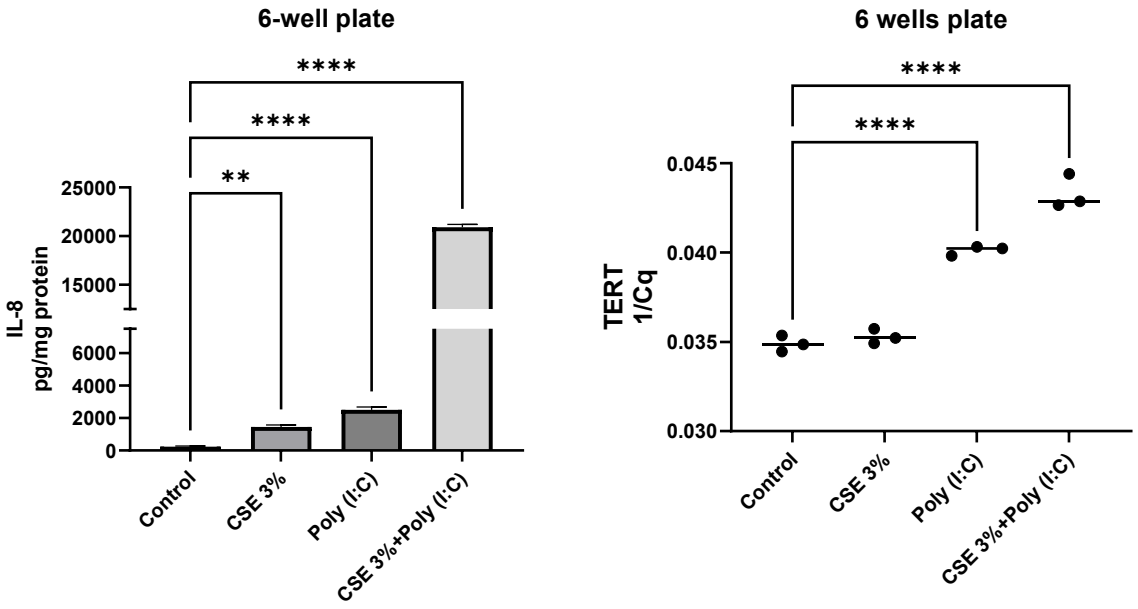

Figure 7.2 Effect of CSE and poly (I:C) on the production of non-T2 inflammatory cytokines

iHBECs were treated with or without CSE (3%), poly (I:C) (10 µg/ml), or CSE + poly (I:C) for 24 hours. **(A)** The concentration of IL-8 in cell supernatants was measured by ELISA. Data were normalised with total protein and presented as pg/mg protein. . **(B)** qPCR targeting TERT gene was used to quantify cfDNA from iHBECs samples using Ariamax Real-Time PCR System (Agilent®). Data were presented as 1/Raw quantification cycle (1/Cq). Each data point represents mean ± SEM of one experiments carried out in triplicate samples. ***P*<0.01 and *****P*<0.0001 compared with untreated cells (control).

7.12 The quality of RNA samples

The quality of RNA samples after RNA isolation was assessed using a TapeStation (Agilent). The RNA integrity number equivalent (RINe) minimum score of 8 was used as cut off for inclusion which indicated highly intact RNA. Twenty samples of HASMCs from 4 donors each stimulated with CSE, poly (I:C), and CSE+poly (I:C) were assessed and showed RINe ranged between 9.2 and 9.7. The results are showed in (Figure 7.3).

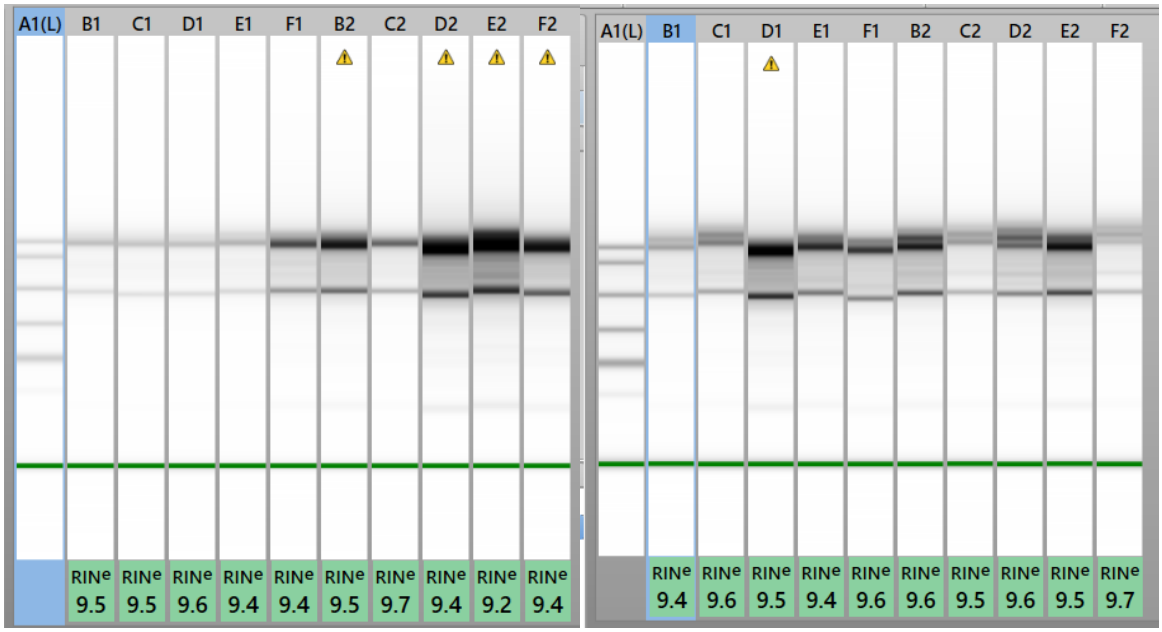

Figure 7.3 The quality of RNA samples assessed by a TapeStation (Agilent)

7.13 RNAseq supplementary Tables

Table 7.13.1 Lists of all significantly expressed genes from cfDNA of poly (I:C)-stimulated iHBECs induced HASMCs gene expression compered to control

Gene_ID	Gene_name	baseMean	log2FoldChange	Adjusted P value
ENSG00000100577	GSTZ1	36.995	-2.459	0.00010
ENSG00000243742	RPLP0P2	10.817	5.755	0.00011
ENSG00000164181	ELOVL7	6.628	6.834	0.00011
ENSG00000164237	CMBL	144.019	-1.568	0.00011
ENSG00000124098	FAM210B	364.043	-1.623	0.00011
ENSG00000089692	LAG3	8.062	7.108	0.00012
ENSG00000120910	PPP3CC	70.315	1.801	0.00012
ENSG00000206190	ATP10A	15.265	3.471	0.00012
ENSG00000067798	NAV3	53.533	2.831	0.00012
ENSG00000181163	NPM1	885.439	-1.175	0.00012
ENSG00000181649	PHLDA2	177.230	1.718	0.00012
ENSG00000115009	CCL20	8.631	7.148	0.00013
ENSG00000181634	TNFSF15	32.539	7.653	0.00015
ENSG00000196850	PPTC7	46.739	2.143	0.00015
ENSG00000137496	IL18BP	14.171	5.563	0.00015
ENSG00000163735	CXCL5	50.329	4.595	0.00016
ENSG00000145860	RNF145	98.585	1.651	0.00016
ENSG00000204516	MICB	48.246	2.483	0.00016
ENSG00000121274	TENT4B	111.326	1.827	0.00016
ENSG00000133392	MYH11	6.784	6.919	0.00017
ENSG00000184014	DENND5A	80.563	1.707	0.00017
ENSG00000179021	C3orf38	109.604	1.827	0.00017
ENSG00000197142	ACSL5	14.796	3.422	0.00018
ENSG00000147454	SLC25A37	103.846	2.851	0.00018
ENSG00000160888	IER2	100.466	2.332	0.00018
ENSG00000163661	PTX3	167.236	2.800	0.00018
ENSG00000042286	AIFM2	75.996	2.036	0.00020
ENSG00000116514	RNF19B	42.163	2.546	0.00021

ENSG00000123095	BHLHE41	59.732	3.447	0.00021
ENSG00000130939	UBE4B	53.149	-2.137	0.00021
ENSG00000065060	UHRF1BP1	18.849	2.617	0.00022
ENSG00000157227	MMP14	763.955	1.392	0.00024
ENSG00000125844	RRBP1	273.240	2.174	0.00025
ENSG00000159110	IFNAR2	50.158	2.117	0.00025
ENSG00000188343	CIBAR1	75.331	-2.426	0.00025
ENSG00000084693	AGBL5	28.652	-2.536	0.00027
ENSG00000090621	PABPC4	506.482	-1.346	0.00028
ENSG00000101665	SMAD7	25.649	3.007	0.00029
ENSG00000056972	TRAF3IP2	66.620	1.866	0.00029
ENSG00000122417	ODF2L	83.123	2.409	0.00029
ENSG00000127666	TICAM1	26.574	2.560	0.00029
ENSG00000145907	G3BP1	282.077	1.223	0.00030
ENSG00000185722	ANKFY1	131.046	1.663	0.00031
ENSG00000100647	SUSD6	53.387	1.924	0.00032
ENSG00000178035	IMPDH2	132.468	-2.194	0.00032
ENSG00000169100	SLC25A6	768.781	-1.865	0.00032
ENSG00000072121	ZFYVE26	29.268	2.274	0.00033
ENSG00000087245	MMP2	645.970	1.774	0.00034
ENSG00000185697	MYBL1	32.793	2.714	0.00035
ENSG00000166889	PATL1	67.724	2.056	0.00038
ENSG00000149131	SERPING1	179.552	2.060	0.00038
ENSG00000115159	GPD2	131.109	2.414	0.00039
ENSG00000161091	MFSD12	87.836	2.288	0.00040
ENSG00000165475	CRYL1	65.623	-1.856	0.00040
ENSG00000138135	CH25H	14.643	5.352	0.00041
ENSG00000205364	MT1M	23.666	2.846	0.00041
ENSG00000153048	CARHSP1	60.775	-2.059	0.00042
ENSG00000149212	SESN3	129.724	-2.282	0.00043
ENSG00000026950	BTN3A1	73.115	1.600	0.00046
ENSG00000101745	ANKRD12	146.391	2.283	0.00046
ENSG00000155506	LARP1	346.356	1.274	0.00049

ENSG00000115977	AAK1	114.287	1.684	0.00051
ENSG00000198814	GK	36.117	2.173	0.00053
ENSG00000155363	MOV10	70.350	1.802	0.00054
ENSG00000158457	TSPAN33	9.189	4.404	0.00054
ENSG00000101236	RNF24	163.527	1.677	0.00055
ENSG00000158417	EIF5B	328.946	1.628	0.00055
ENSG00000164211	STARD4	36.129	2.849	0.00057
ENSG00000197063	MAFG	97.654	1.678	0.00057
ENSG00000128917	DLL4	5.138	6.797	0.00057
ENSG00000167550	RHEBL1	4.608	6.340	0.00057
ENSG00000171621	SPSB1	41.016	2.004	0.00061
ENSG00000070814	TCOF1	11.370	3.296	0.00062
ENSG00000152749	GPR180	53.112	2.255	0.00063
ENSG00000213928	IRF9	28.017	2.092	0.00063
ENSG00000237276	ANO7L1	4.726	6.376	0.00063
ENSG00000178685	PARP10	16.268	2.772	0.00063
ENSG00000157654	PALM2AKAP2	772.381	2.110	0.00065
ENSG00000103855	CD276	157.156	1.327	0.00066
ENSG00000116663	FBXO6	15.601	2.833	0.00067
ENSG00000146232	NFKBIE	25.606	2.353	0.00069
ENSG00000064666	CNN2	216.758	-1.632	0.00072
ENSG00000146648	EGFR	265.737	1.503	0.00075
ENSG00000008130	NADK	17.516	2.515	0.00075
ENSG00000095951	HIVEP1	31.429	2.648	0.00080
ENSG00000068885	IFT80	28.286	-2.598	0.00081
ENSG00000276600	RAB7B	16.041	-3.559	0.00081
ENSG00000166165	CKB	159.921	1.588	0.00082
ENSG00000043143	JADE2	58.226	1.854	0.00085
ENSG00000274180	NATD1	41.909	-2.210	0.00085
ENSG00000150510	FAM124A	13.132	3.179	0.00086
ENSG00000138756	BMP2K	84.639	1.780	0.00086
ENSG00000248527	MTATP6P1	92.637	1.858	0.00089
ENSG00000172159	FRMD3	19.936	3.154	0.00090

ENSG00000104321	TRPA1	388.874	3.299	0.00090
ENSG00000125826	RBCK1	168.541	1.352	0.00090
ENSG00000145348	TBCK	44.141	-2.035	0.00091
ENSG00000105819	PMPCB	62.295	-1.693	0.00092
ENSG00000110944	IL23A	8.709	6.187	0.00095
ENSG00000091073	DTX2	29.893	2.350	0.00097
ENSG00000102921	N4BP1	64.684	1.662	0.00098
ENSG00000086061	DNAJA1	550.498	1.348	0.00099
ENSG00000128274	A4GALT	46.306	1.797	0.00099
ENSG00000064932	SBNO2	34.895	1.944	0.00104
ENSG00000124151	NCOA3	110.483	2.043	0.00104
ENSG00000187957	DNER	22.348	2.386	0.00104
ENSG00000185561	TLCD2	50.784	2.759	0.00108
ENSG00000172053	QARS1	100.781	-2.005	0.00108
ENSG00000120526	NUDCD1	28.029	2.452	0.00110
ENSG00000173575	CHD2	118.441	1.508	0.00110
ENSG00000041353	RAB27B	44.003	2.580	0.00113
ENSG00000138685	FGF2	293.777	1.931	0.00114
ENSG00000110042	DTX4	54.086	1.728	0.00118
ENSG00000106346	USP42	36.358	2.192	0.00118
ENSG00000111052	LIN7A	21.314	-2.755	0.00125
ENSG00000107262	BAG1	35.291	-1.874	0.00131
ENSG00000079257	LXN	47.227	-2.191	0.00139
ENSG00000170852	KBTBD2	42.967	1.755	0.00143
ENSG00000116406	EDEM3	88.453	1.527	0.00144
ENSG00000255150	EID3	9.230	3.490	0.00145
ENSG00000006327	TNFRSF12A	51.369	1.865	0.00150
ENSG00000174749	FAM241A	18.161	2.488	0.00150
ENSG00000197646	PDCD1LG2	28.083	2.191	0.00150
ENSG00000204264	PSMB8	97.652	1.532	0.00155
ENSG00000168310	IRF2	65.975	1.985	0.00158
ENSG00000161921	CXCL16	21.562	2.796	0.00162
ENSG00000110911	SLC11A2	167.689	2.008	0.00165

ENSG00000174720	LARP7	158.616	1.483	0.00165
ENSG00000138821	SLC39A8	33.588	2.674	0.00169
ENSG00000204389	HSPA1A	249.506	1.373	0.00169
ENSG00000171310	CHST11	26.836	2.388	0.00175
ENSG00000182670	TTC3	502.553	-1.647	0.00181
ENSG00000128590	DNAJB9	91.234	1.671	0.00183
ENSG00000138760	SCARB2	656.282	1.487	0.00184
ENSG00000124831	LRRFIP1	177.150	1.602	0.00184
ENSG00000196411	EPHB4	54.497	-1.862	0.00191
ENSG00000174808	BTC	8.391	5.348	0.00192
ENSG00000116691	MIIP	23.005	2.090	0.00193
ENSG00000124882	EREG	36.035	4.813	0.00201
ENSG00000136044	APPL2	43.086	-2.349	0.00201
ENSG00000188786	MTF1	55.563	1.871	0.00201
ENSG00000117523	PRRC2C	207.899	1.984	0.00201
ENSG00000205795	CYS1	8.201	-5.622	0.00201
ENSG00000182093	GET1	44.568	-1.975	0.00217
ENSG00000196776	CD47	390.584	1.393	0.00219
ENSG00000178425	NT5DC1	49.173	-1.780	0.00228
ENSG00000013374	NUB1	193.544	2.071	0.00234
ENSG00000101265	RASSF2	88.435	-2.507	0.00237
ENSG00000066084	DIP2B	57.641	1.604	0.00238
ENSG00000159314	ARHGAP27	6.948	5.165	0.00242
ENSG00000118257	NRP2	176.745	2.426	0.00249
ENSG00000122406	RPL5	1259.139	-1.514	0.00249
ENSG00000144837	PLA1A	8.236	5.049	0.00256
ENSG00000170581	STAT2	266.382	1.292	0.00256
ENSG00000180611	MB21D2	14.946	2.616	0.00256
ENSG00000077782	FGFR1	811.869	1.364	0.00258
ENSG00000149218	ENDOD1	132.279	2.046	0.00258
ENSG00000198130	HIBCH	27.304	-2.218	0.00259
ENSG00000163347	CLDN1	57.225	4.252	0.00260
ENSG00000161638	ITGA5	102.497	1.468	0.00273

ENSG00000105784	RUNDC3B	20.627	-3.606	0.00281
ENSG00000136048	DRAM1	381.082	1.572	0.00281
ENSG00000141279	NPEPPS	197.207	-1.357	0.00281
ENSG00000131459	GFPT2	42.256	1.966	0.00286
ENSG00000113583	C5orf15	143.166	1.493	0.00303
ENSG00000171425	ZNF581	39.522	-2.399	0.00306
ENSG00000139318	DUSP6	75.443	2.418	0.00307
ENSG00000151694	ADAM17	190.567	1.436	0.00313
ENSG00000141526	SLC16A3	93.809	1.653	0.00329
ENSG00000186470	BTN3A2	69.924	1.469	0.00340
ENSG00000168016	TRANK1	29.800	2.574	0.00340
ENSG00000079215	SLC1A3	17.702	2.885	0.00344
ENSG00000042062	RIPOR3	21.959	2.131	0.00347
ENSG00000169047	IRS1	157.202	1.272	0.00360
ENSG00000167081	PBX3	292.124	-1.552	0.00363
ENSG00000176845	METRNL	182.966	1.343	0.00368
ENSG00000196371	FUT4	18.561	2.363	0.00378
ENSG00000185201	IFITM2	812.603	1.589	0.00381
ENSG00000109339	MAPK10	63.116	-1.789	0.00392
ENSG00000113504	SLC12A7	28.540	2.009	0.00392
ENSG00000067221	STOML1	41.067	1.961	0.00409
ENSG00000170340	B3GNT2	71.653	2.349	0.00413
ENSG00000183137	CEP57L1	30.688	1.939	0.00414
ENSG00000155744	FAM126B	27.100	2.029	0.00420
ENSG00000117533	VAMP4	94.244	-1.506	0.00420
ENSG00000126785	RHOJ	21.091	-2.501	0.00429
ENSG00000174059	CD34	6.183	5.570	0.00432
ENSG00000254470	AP5B1	17.199	2.412	0.00432
ENSG00000069399	BCL3	110.411	1.488	0.00434
ENSG00000074964	ARHGEF10L	47.934	1.564	0.00452
ENSG00000136147	PHF11	101.299	1.579	0.00454
ENSG00000119707	RBM25	199.402	1.454	0.00456
ENSG00000108551	RASD1	22.808	2.365	0.00476

ENSG00000144674	GOLGA4	137.384	2.390	0.00486
ENSG00000110318	CEP126	16.840	-2.477	0.00505
ENSG00000152689	RASGRP3	5.053	5.543	0.00508
ENSG00000164164	OTUD4	58.742	1.697	0.00510
ENSG00000175985	PLEKHD1	4.085	5.860	0.00520
ENSG00000172123	SLFN12	49.374	2.286	0.00526
ENSG00000178860	MSC	50.008	1.943	0.00526
ENSG00000083799	CYLD	125.662	1.855	0.00531
ENSG00000108679	LGALS3BP	99.604	1.808	0.00535
ENSG00000132475	H3-3B	1003.193	1.267	0.00540
ENSG00000096968	JAK2	59.549	1.679	0.00542
ENSG00000128309	MPST	35.227	-2.449	0.00546
ENSG00000026103	FAS	115.782	1.329	0.00558
ENSG00000175550	DRAP1	289.612	1.240	0.00569
ENSG00000141295	SCRN2	26.638	-2.218	0.00582
ENSG00000189337	KAZN	43.493	1.874	0.00582
ENSG00000117155	SSX2IP	75.176	-1.834	0.00585
ENSG00000160767	FAM189B	152.660	1.329	0.00585
ENSG00000056558	TRAF1	22.785	4.880	0.00598
ENSG00000165731	RET	7.671	4.846	0.00601
ENSG00000164327	RICTOR	62.040	1.642	0.00601
ENSG00000138675	FGF5	129.931	1.672	0.00609
ENSG00000122257	RBBP6	81.967	1.866	0.00615
ENSG00000178951	ZBTB7A	223.433	1.359	0.00620
ENSG00000079385	CEACAM1	3.463	5.877	0.00620
ENSG00000103222	ABCC1	95.512	1.787	0.00620
ENSG00000103152	MPG	73.467	-1.702	0.00638
ENSG00000087842	PIR	37.155	-2.262	0.00640
ENSG00000145780	FEM1C	71.198	1.411	0.00655
ENSG00000135148	TRAFD1	48.312	1.607	0.00660
ENSG00000168118	RAB4A	75.208	-1.487	0.00664
ENSG00000109320	NFKB1	116.525	1.475	0.00669
ENSG00000109113	RAB34	182.158	-1.330	0.00686

ENSG00000173120	KDM2A	129.168	1.431	0.00702
ENSG00000148908	RGS10	116.787	-1.574	0.00703
ENSG00000135905	DOCK10	36.955	1.979	0.00719
ENSG00000020577	SAMD4A	74.351	1.745	0.00723
ENSG00000187210	GCNT1	43.489	1.897	0.00726
ENSG00000160013	PTGIR	8.361	3.640	0.00727
ENSG00000158859	ADAMTS4	19.767	3.530	0.00728
ENSG00000143320	CRABP2	297.578	-1.151	0.00728
ENSG00000110330	BIRC2	145.359	1.267	0.00731
ENSG00000116017	ARID3A	42.881	1.713	0.00734
ENSG00000163565	IFI16	550.257	1.566	0.00755
ENSG00000174032	SLC25A30	33.014	1.781	0.00783
ENSG00000163435	ELF3	3.633	6.072	0.00821
ENSG00000137842	TMEM62	11.011	2.734	0.00830
ENSG00000205581	HMGN1	288.469	-1.089	0.00861
ENSG00000052802	MSMO1	113.232	2.133	0.00868
ENSG00000174705	SH3PXD2B	81.613	1.575	0.00868
ENSG00000112149	CD83	29.508	2.063	0.00880
ENSG00000101079	NDRG3	63.254	-1.517	0.00885
ENSG00000136689	IL1RN	16.553	3.371	0.00891
ENSG00000154640	BTG3	111.179	1.254	0.00901
ENSG00000160953	PWWP3A	26.090	-1.987	0.00954
ENSG00000119522	DENND1A	36.854	1.764	0.00958
ENSG00000100219	XBP1	223.243	1.331	0.00964
ENSG00000108179	PPIF	101.222	1.518	0.00969
ENSG00000196968	FUT11	63.978	1.549	0.00980
ENSG00000116874	WARS2	29.359	-1.933	0.00981
ENSG00000107249	GLIS3	34.746	2.149	0.01009
ENSG00000135535	CD164	392.592	1.102	0.01011
ENSG00000138095	LRPPRC	106.579	-1.295	0.01017
ENSG00000184588	PDE4B	26.383	2.227	0.01028
ENSG00000138018	SELENOI	26.551	1.866	0.01039
ENSG00000099290	WASHC2A	112.297	1.347	0.01067

ENSG00000135052	GOLM1	88.868	1.444	0.01076
ENSG00000197818	SLC9A8	20.287	1.919	0.01076
ENSG00000144749	LRIG1	65.328	1.770	0.01114
ENSG00000146966	DENND2A	23.990	-2.128	0.01142
ENSG00000081791	DELE1	31.631	-1.875	0.01142
ENSG00000125779	PANK2	107.375	1.331	0.01142
ENSG00000172992	DCAKD	41.718	-1.844	0.01157
ENSG00000166741	NNMT	258.249	1.524	0.01263
ENSG00000163932	PRKCD	53.070	1.749	0.01266
ENSG00000183010	PYCR1	39.565	-1.820	0.01266
ENSG00000197081	IGF2R	340.460	1.481	0.01266
ENSG00000122729	ACO1	165.939	-1.712	0.01278
ENSG00000137752	CASP1	111.955	1.721	0.01278
ENSG00000103034	NDRG4	11.498	-3.188	0.01287
ENSG00000170624	SGCD	55.836	-2.650	0.01292
ENSG00000108256	NUFIP2	184.904	1.452	0.01295
ENSG00000102317	RBM3	210.671	-1.555	0.01302
ENSG00000111058	ACSS3	24.127	-1.983	0.01358
ENSG00000132670	PTPRA	104.953	1.298	0.01358
ENSG00000176170	SPHK1	14.663	2.873	0.01358
ENSG00000099860	GADD45B	27.506	1.982	0.01369
ENSG00000196932	TMEM26	14.748	-3.721	0.01388
ENSG00000182979	MTA1	33.594	-2.043	0.01422
ENSG00000119938	PPP1R3C	262.169	-1.667	0.01427
ENSG00000140406	TLNRD1	36.587	1.959	0.01427
ENSG00000132122	SPATA6	15.318	-2.596	0.01433
ENSG00000106665	CLIP2	50.950	1.492	0.01435
ENSG00000149557	FEZ1	113.055	-1.438	0.01468
ENSG00000104689	TNFRSF10A	14.004	2.266	0.01495
ENSG00000170464	DNAJC18	24.135	-2.114	0.01495
ENSG00000172346	CSDC2	10.610	-3.756	0.01508
ENSG00000117475	BLZF1	47.751	1.673	0.01510
ENSG00000148541	FAM13C	7.008	-4.849	0.01527

ENSG00000141582	CBX4	76.119	1.516	0.01535
ENSG00000011021	CLCN6	13.724	2.294	0.01578
ENSG00000205659	LIN52	39.292	1.839	0.01589
ENSG00000114450	GNB4	181.713	1.446	0.01599
ENSG00000115365	LANCL1	77.102	-1.402	0.01637
ENSG00000185885	IFITM1	6.156	4.745	0.01664
ENSG00000072210	ALDH3A2	39.655	-1.800	0.01690
ENSG00000182704	TSKU	86.484	1.404	0.01690
ENSG00000198133	TMEM229B	5.426	5.340	0.01690
ENSG00000167658	EEF2	2499.996	-1.501	0.01699
ENSG00000068366	ACSL4	427.945	1.726	0.01746
ENSG00000123136	DDX39A	14.410	2.846	0.01759
ENSG00000134851	TMEM165	90.242	1.379	0.01770
ENSG00000116863	ADPRS	45.804	1.711	0.01777
ENSG00000117713	ARID1A	52.433	1.495	0.01808
ENSG00000066629	EML1	73.826	-1.928	0.01846
ENSG00000090097	PCBP4	84.858	-1.519	0.01854
ENSG00000150630	VEGFC	69.472	1.622	0.01856
ENSG00000188229	TUBB4B	160.143	1.284	0.01856
ENSG00000120053	GOT1	19.438	-2.317	0.01915
ENSG00000152503	TRIM36	2.436	5.356	0.01915
ENSG00000154642	C21orf91	63.430	1.955	0.01915
ENSG00000198888	MT-ND1	1009.654	1.310	0.01915
ENSG00000109654	TRIM2	34.521	-1.998	0.01916
ENSG00000185112	FAM43A	154.198	1.404	0.01935
ENSG00000176994	SMCR8	52.918	1.467	0.01972
ENSG00000132481	TRIM47	21.460	2.695	0.01981
ENSG00000063046	EIF4B	118.764	-1.604	0.01985
ENSG00000105643	ARRDC2	22.026	2.087	0.01999
ENSG00000111266	DUSP16	44.235	1.630	0.01999
ENSG00000128602	SMO	13.577	-3.384	0.01999
ENSG00000241106	HLA-DOB	3.050	5.817	0.01999
ENSG00000087074	PPP1R15A	94.775	1.339	0.02000

ENSG00000173276	ZBTB21	29.102	1.656	0.02004
ENSG00000170271	FAXDC2	24.266	-2.027	0.02005
ENSG00000128849	CGNL1	13.366	2.874	0.02021
ENSG00000197312	DDI2	52.463	1.556	0.02024
ENSG00000152661	GJA1	238.556	1.700	0.02029
ENSG00000067064	IDI1	61.807	1.714	0.02060
ENSG00000165949	IFI27	197.090	3.458	0.02076
ENSG00000104823	ECH1	88.354	-1.380	0.02080
ENSG00000146409	SLC18B1	29.631	1.742	0.02080
ENSG00000163935	SFMBT1	16.603	2.119	0.02080
ENSG00000197632	SERPINB2	43.565	1.979	0.02133
ENSG00000149823	VPS51	44.551	-1.812	0.02137
ENSG00000172915	NBEA	16.025	-2.268	0.02148
ENSG00000163629	PTPN13	75.403	-1.549	0.02165
ENSG00000173114	LRRN3	34.382	1.827	0.02167
ENSG00000171223	JUNB	97.675	1.579	0.02170
ENSG00000197442	MAP3K5	101.799	1.536	0.02173
ENSG00000179051	RCC2	204.155	2.067	0.02179
ENSG00000167325	RRM1	128.227	-1.342	0.02186
ENSG00000178607	ERN1	24.582	1.769	0.02195
ENSG00000196792	STRN3	128.935	1.265	0.02195
ENSG00000100417	PMM1	103.711	-1.390	0.02201
ENSG00000253958	CLDN23	19.195	2.152	0.02207
ENSG00000170961	HAS2	37.411	2.039	0.02217
ENSG00000184988	TMEM106A	20.670	2.001	0.02229
ENSG00000089157	RPLP0	2517.836	-1.169	0.02319
ENSG00000168917	SLC35G2	20.131	1.949	0.02332
ENSG00000144959	NCEH1	94.971	2.870	0.02395
ENSG00000051620	HEBP2	172.610	-1.209	0.02398
ENSG00000065526	SPEN	35.881	2.236	0.02413
ENSG00000108406	DHX40	95.149	-1.356	0.02413
ENSG00000188211	NCR3LG1	5.773	4.528	0.02421
ENSG00000282988	ENSG00000282988	6.619	3.578	0.02421

ENSG00000115919	KYNU	15.467	2.578	0.02454
ENSG00000103257	SLC7A5	28.301	2.177	0.02504
ENSG00000161813	LARP4	68.237	1.411	0.02513
ENSG00000133401	PDZD2	3.974	4.449	0.02553
ENSG00000271900	ENSG00000271900	11.014	2.537	0.02564
ENSG00000204388	HSPA1B	174.713	1.350	0.02576
ENSG00000158615	PPP1R15B	46.565	1.676	0.02581
ENSG00000204856	FAM216A	13.417	-2.448	0.02590
ENSG00000130024	PHF10	35.551	-1.671	0.02601
ENSG00000175390	EIF3F	102.608	-1.583	0.02601
ENSG00000215021	PHB2	192.805	-1.402	0.02601
ENSG00000078304	PPP2R5C	196.645	-1.150	0.02602
ENSG00000278845	MRPL45	93.844	-1.562	0.02652
ENSG00000164086	DUSP7	39.453	1.692	0.02669
ENSG00000175946	KLHL38	4.189	5.023	0.02688
ENSG00000100731	PCNX1	86.247	1.259	0.02751
ENSG00000138160	KIF11	7.601	-4.658	0.02751
ENSG00000210082	MT-RNR2	48053.241	1.161	0.02769
ENSG00000170485	NPAS2	21.265	2.202	0.02787
ENSG00000173626	TRAPPC3L	3.264	4.926	0.02787
ENSG00000183496	MEX3B	13.318	-2.931	0.02809
ENSG00000172716	SLFN11	40.282	1.824	0.02816
ENSG00000156471	PTDSS1	125.072	-1.815	0.02827
ENSG00000221676	RNU6ATAC	4.346	4.448	0.02858
ENSG00000104549	SQLE	71.080	1.866	0.02865
ENSG00000166169	POLL	18.096	-2.136	0.02865
ENSG00000137944	KYAT3	32.975	-1.804	0.02877
ENSG00000197451	HNRNPAB	115.032	1.228	0.02877
ENSG00000112941	TENT4A	30.923	1.801	0.02894
ENSG00000161682	FAM171A2	20.462	-2.532	0.02938
ENSG00000029153	ARNTL2	28.712	2.073	0.02955
ENSG00000121691	CAT	201.482	-1.271	0.02982
ENSG00000137764	MAP2K5	33.667	-1.923	0.02982

ENSG00000168958	MFF	84.456	-1.365	0.03019
ENSG00000107968	MAP3K8	10.372	2.709	0.03080
ENSG00000178234	GALNT11	38.195	-1.680	0.03080
ENSG00000000971	CFH	116.996	1.437	0.03157
ENSG00000102081	FMR1	76.072	1.449	0.03221
ENSG00000166974	MAPRE2	61.117	-1.453	0.03271
ENSG00000003400	CASP10	8.332	2.831	0.03286
ENSG00000082641	NFE2L1	196.300	1.260	0.03309
ENSG00000186907	RTN4RL2	5.253	3.858	0.03324
ENSG00000123146	ADGRE5	81.825	1.537	0.03411
ENSG00000119699	TGFB3	30.325	2.063	0.03412
ENSG00000138078	PREPL	112.658	-1.407	0.03443
ENSG00000163660	CCNL1	44.721	1.980	0.03443
ENSG00000120690	ELF1	60.787	1.443	0.03478
ENSG00000166780	BMERB1	57.789	-1.635	0.03483
ENSG00000100139	MICALL1	19.577	1.836	0.03488
ENSG00000089289	IGBP1	239.547	-1.556	0.03527
ENSG00000119471	HSDL2	147.237	-1.231	0.03527
ENSG00000141338	ABCA8	20.426	-2.454	0.03527
ENSG00000137767	SQOR	337.230	1.277	0.03549
ENSG00000125384	PTGER2	47.760	1.687	0.03579
ENSG00000147251	DOCK11	45.059	-1.723	0.03584
ENSG00000157557	ETS2	234.473	1.415	0.03613
ENSG00000198517	MAFK	48.093	1.595	0.03629
ENSG00000247596	TWF2	115.137	-1.421	0.03632
ENSG00000075415	SLC25A3	680.353	-1.177	0.03691
ENSG00000162599	NFIA	92.076	-2.326	0.03693
ENSG00000168268	NT5DC2	18.880	-2.233	0.03712
ENSG00000175197	DDIT3	101.655	1.347	0.03738
ENSG00000003096	KLHL13	23.811	-1.978	0.03753
ENSG00000144730	IL17RD	20.061	-2.386	0.03759
ENSG00000164305	CASP3	29.515	1.841	0.03759
ENSG00000129682	FGF13	15.769	-2.623	0.03787

ENSG00000089041	P2RX7	17.887	1.943	0.03811
ENSG00000163249	CCNYL1	54.206	1.546	0.03811
ENSG00000146282	RARS2	112.713	-1.545	0.03813
ENSG00000090013	BLVRB	139.941	-1.310	0.03849
ENSG00000138435	CHRNA1	4.860	4.441	0.03849
ENSG00000163545	NUAK2	6.331	3.255	0.03873
ENSG00000162643	DNAI3	18.743	-2.552	0.03993
ENSG00000135837	CEP350	126.131	1.565	0.03995
ENSG00000108669	CYTH1	18.167	2.061	0.04002
ENSG00000170035	UBE2E3	186.751	-1.152	0.04008
ENSG00000173218	VANGL1	46.940	1.499	0.04031
ENSG00000151474	FRMD4A	51.203	1.700	0.04080
ENSG00000169504	CLIC4	835.886	1.008	0.04217
ENSG00000196839	ADA	16.148	-2.231	0.04217
ENSG00000104221	BRF2	15.167	-2.132	0.04229
ENSG00000213694	S1PR3	173.121	1.309	0.04258
ENSG00000019549	SNAI2	169.949	-1.592	0.04363
ENSG00000253729	PRKDC	59.915	-1.493	0.04363
ENSG00000117543	DPH5	62.065	-1.575	0.04405
ENSG00000100347	SAMM50	64.036	-1.517	0.04422
ENSG00000147324	MFHAS1	52.277	1.662	0.04422
ENSG00000128203	ASPHD2	6.614	2.778	0.04511
ENSG00000179431	FJX1	16.814	1.985	0.04516
ENSG00000038219	BOD1L1	87.593	1.472	0.04536
ENSG00000129757	CDKN1C	74.643	-2.213	0.04559
ENSG00000078401	EDN1	5.778	3.189	0.04577
ENSG00000204256	BRD2	195.964	1.189	0.04577
ENSG00000111885	MAN1A1	128.928	1.465	0.04583
ENSG00000184838	PRR16	25.933	2.019	0.04686
ENSG00000075336	TIMM21	26.329	-1.844	0.04723
ENSG00000072952	IRAG1	64.381	-1.617	0.04760
ENSG00000176692	FOXC2	21.616	2.657	0.04838
ENSG00000187240	DYNC2H1	39.589	-1.837	0.04883

ENSG00000116711	PLA2G4A	22.047	2.079	0.04901
ENSG00000136141	LRCH1	50.430	1.400	0.04908
ENSG00000103479	RBL2	36.973	-1.659	0.04947

Table 7.13.2 Lists of all significantly expressed genes from cfDNA of CSE + poly (I:C)-stimulated iHBECs induced HASMCs gene expression compered to control

Gene_ID	Gene_name	baseMean	log2FoldChange	Adjusted P value
ENSG00000120913	PDLIM2	278.148	-1.318	0.00010
ENSG00000160326	SLC2A6	18.796	3.860	0.00011
ENSG00000101966	XIAP	158.038	1.962	0.00011
ENSG00000173039	RELA	142.078	1.635	0.00011
ENSG00000070961	ATP2B1	545.578	2.025	0.00012
ENSG00000105287	PRKD2	52.523	1.931	0.00012
ENSG00000115159	GPD2	131.109	2.526	0.00012
ENSG00000172216	CEBPB	438.745	1.742	0.00012
ENSG00000138135	CH25H	14.643	5.642	0.00013
ENSG00000141526	SLC16A3	93.809	1.869	0.00013
ENSG00000149823	VPS51	44.551	-2.452	0.00013
ENSG00000168118	RAB4A	75.208	-1.757	0.00013
ENSG00000052795	FNIP2	139.275	1.700	0.00013
ENSG00000091073	DTX2	29.893	2.532	0.00013
ENSG00000157657	ZNF618	76.756	1.933	0.00013
ENSG00000062598	ELMO2	89.736	1.650	0.00014
ENSG00000145632	PLK2	160.467	1.813	0.00014
ENSG00000185561	TLCD2	50.784	3.010	0.00014
ENSG00000120910	PPP3CC	70.315	1.777	0.00015
ENSG00000122417	ODF2L	83.123	2.461	0.00016
ENSG00000112773	TENT5A	363.608	1.810	0.00017
ENSG00000137449	CPEB2	43.425	2.656	0.00017
ENSG00000167081	PBX3	292.124	-1.751	0.00017
ENSG00000109339	MAPK10	63.116	-2.057	0.00018
ENSG00000197622	CDC42SE1	76.872	1.799	0.00019
ENSG00000213024	NUP62	105.483	1.612	0.00019
ENSG00000196411	EPHB4	54.497	-2.052	0.00019
ENSG00000133392	MYH11	6.784	6.872	0.00019
ENSG00000168280	KIF5C	12.280	6.561	0.00019
ENSG00000079102	RUNX1T1	127.388	-1.619	0.00019

ENSG00000163735	CXCL5	50.329	4.551	0.00019
ENSG00000184014	DENND5A	80.563	1.690	0.00020
ENSG00000122566	HNRNPA2B1	384.954	1.399	0.00021
ENSG00000120526	NUDCD1	28.029	2.612	0.00023
ENSG00000010818	HIVEP2	99.506	2.161	0.00023
ENSG00000065060	UHRF1BP1	18.849	2.600	0.00023
ENSG00000130939	UBE4B	53.149	-2.074	0.00025
ENSG00000131459	GFPT2	42.256	2.168	0.00025
ENSG00000206190	ATP10A	15.265	3.357	0.00025
ENSG00000120539	MASTL	23.737	2.502	0.00026
ENSG00000113504	SLC12A7	28.540	2.241	0.00026
ENSG00000204516	MICB	48.246	2.433	0.00026
ENSG00000188343	CIBAR1	75.331	-2.388	0.00026
ENSG00000178035	IMPDH2	132.468	-2.190	0.00027
ENSG00000185112	FAM43A	154.198	1.684	0.00028
ENSG00000076108	BAZ2A	81.886	1.957	0.00028
ENSG00000176845	METRNL	182.966	1.468	0.00028
ENSG00000147883	CDKN2B	54.764	1.860	0.00028
ENSG00000243742	RPLP0P2	10.817	5.498	0.00029
ENSG00000164211	STARD4	36.129	2.922	0.00030
ENSG00000158470	B4GALT5	121.533	2.249	0.00030
ENSG00000158859	ADAMTS4	19.767	4.194	0.00030
ENSG00000041353	RAB27B	44.003	2.726	0.00031
ENSG00000135390	ATP5MC2	472.933	-1.510	0.00036
ENSG00000166165	CKB	159.921	1.628	0.00039
ENSG00000107262	BAG1	35.291	-1.952	0.00040
ENSG00000128965	CHAC1	24.686	3.644	0.00041
ENSG00000100647	SUSD6	53.387	1.894	0.00044
ENSG00000108342	CSF3	7.054	6.452	0.00044
ENSG00000181634	TNFSF15	32.539	7.250	0.00046
ENSG00000134851	TMEM165	90.242	1.608	0.00046
ENSG00000104321	TRPA1	388.874	3.412	0.00046
ENSG00000125826	RBCK1	168.541	1.376	0.00047

ENSG00000109113	RAB34	182.158	-1.475	0.00049
ENSG00000182670	TTC3	502.553	-1.731	0.00052
ENSG00000140406	TLNRD1	36.587	2.302	0.00055
ENSG00000158457	TSPAN33	9.189	4.389	0.00056
ENSG00000170385	SLC30A1	156.908	2.287	0.00056
ENSG00000196968	FUT11	63.978	1.748	0.00057
ENSG00000160888	IER2	100.466	2.224	0.00059
ENSG00000144837	PLA1A	8.236	5.451	0.00062
ENSG00000110944	IL23A	8.709	6.322	0.00064
ENSG00000102119	EMD	161.099	-1.350	0.00074
ENSG00000152465	NMT2	78.012	-1.620	0.00074
ENSG00000181649	PHLDA2	177.230	1.612	0.00076
ENSG00000168917	SLC35G2	20.131	2.320	0.00076
ENSG00000116017	ARID3A	42.881	1.890	0.00077
ENSG00000126785	RHOJ	21.091	-2.784	0.00080
ENSG00000147274	RBMX	82.849	-2.084	0.00080
ENSG00000197063	MAFG	97.654	1.650	0.00082
ENSG00000204397	CARD16	120.000	1.859	0.00091
ENSG00000150510	FAM124A	13.132	3.162	0.00092
ENSG00000167550	RHEBL1	4.608	6.185	0.00094
ENSG00000234127	TRIM26	70.871	1.565	0.00095
ENSG00000154027	AK5	53.548	-2.010	0.00096
ENSG00000090097	PCBP4	84.858	-1.768	0.00100
ENSG00000113583	C5orf15	143.166	1.556	0.00106
ENSG00000122729	ACO1	165.939	-1.949	0.00108
ENSG00000121274	TENT4B	111.326	1.702	0.00110
ENSG00000137752	CASP1	111.955	1.945	0.00115
ENSG00000198814	GK	36.117	2.097	0.00115
ENSG00000096968	JAK2	59.549	1.796	0.00116
ENSG00000128274	A4GALT	46.306	1.779	0.00116
ENSG00000139318	DUSP6	75.443	2.540	0.00119
ENSG00000116459	ATP5PB	232.376	-1.376	0.00122
ENSG00000153048	CARHSP1	60.775	-1.912	0.00125

ENSG00000237276	ANO7L1	4.726	6.146	0.00130
ENSG00000185722	ANKFY1	131.046	1.573	0.00138
ENSG00000161091	MFSD12	87.836	2.168	0.00138
ENSG00000186470	BTN3A2	69.924	1.517	0.00138
ENSG00000175985	PLEKHD1	4.085	6.338	0.00139
ENSG00000130513	GDF15	410.737	1.958	0.00139
ENSG00000043143	JADE2	58.226	1.810	0.00141
ENSG00000101236	RNF24	163.527	1.615	0.00141
ENSG00000157227	MMP14	763.955	1.313	0.00142
ENSG00000204264	PSMB8	97.652	1.533	0.00144
ENSG00000101665	SMAD7	25.649	2.791	0.00147
ENSG00000111052	LIN7A	21.314	-2.615	0.00150
ENSG00000172992	DCAKD	41.718	-2.061	0.00164
ENSG00000087245	MMP2	645.970	1.667	0.00171
ENSG00000100219	XBP1	223.243	1.434	0.00171
ENSG00000167658	EEF2	2499.996	-1.690	0.00171
ENSG00000168016	TRANK1	29.800	2.664	0.00174
ENSG00000196371	FUT4	18.561	2.446	0.00179
ENSG00000172053	QARS1	100.781	-1.934	0.00184
ENSG00000106346	USP42	36.358	2.145	0.00185
ENSG00000138685	FGF2	293.777	1.892	0.00188
ENSG00000063046	EIF4B	118.764	-1.823	0.00197
ENSG00000170899	GSTA4	42.865	-2.431	0.00202
ENSG00000149131	SERPING1	179.552	1.919	0.00207
ENSG00000182093	GET1	44.568	-1.936	0.00212
ENSG00000166889	PATL1	67.724	1.911	0.00213
ENSG00000165475	CRYL1	65.623	-1.680	0.00215
ENSG00000152749	GPR180	53.112	2.130	0.00219
ENSG00000008130	NADK	17.516	2.382	0.00229
ENSG00000116514	RNF19B	42.163	2.288	0.00239
ENSG00000187957	DNER	22.348	2.287	0.00249
ENSG00000110330	BIRC2	145.359	1.319	0.00260
ENSG00000124098	FAM210B	364.043	-1.440	0.00260

ENSG00000124882	EREG	36.035	4.754	0.00260
ENSG00000130005	GAMT	38.475	-2.065	0.00260
ENSG00000132475	H3-3B	1003.193	1.307	0.00260
ENSG00000149212	SESN3	129.724	-2.077	0.00260
ENSG00000196776	CD47	390.584	1.385	0.00260
ENSG00000042062	RIPOR3	21.959	2.153	0.00262
ENSG00000123146	ADGRE5	81.825	1.774	0.00264
ENSG00000138821	SLC39A8	33.588	2.612	0.00265
ENSG00000119471	HSDL2	147.237	-1.402	0.00269
ENSG00000164327	RICTOR	62.040	1.697	0.00287
ENSG00000174059	CD34	6.183	5.719	0.00290
ENSG00000137842	TMEM62	11.011	2.892	0.00296
ENSG00000174808	BTC	8.391	5.220	0.00297
ENSG00000006327	TNFRSF12A	51.369	1.803	0.00298
ENSG00000108551	RASD1	22.808	2.420	0.00298
ENSG00000173575	CHD2	118.441	1.448	0.00298
ENSG00000161921	CXCL16	21.562	2.705	0.00299
ENSG00000177272	KCNA3	20.269	2.743	0.00300
ENSG00000136044	APPL2	43.086	-2.235	0.00310
ENSG00000163661	PTX3	167.236	2.448	0.00332
ENSG00000113328	CCNG1	234.917	-1.509	0.00338
ENSG00000170961	HAS2	37.411	2.287	0.00342
ENSG00000115977	AAK1	114.287	1.556	0.00349
ENSG00000282988	ENSG00000282988	6.619	4.088	0.00353
ENSG00000076356	PLXNA2	11.162	2.866	0.00359
ENSG00000161638	ITGA5	102.497	1.447	0.00364
ENSG00000128590	DNAJB9	91.234	1.618	0.00368
ENSG00000182704	TSKU	86.484	1.510	0.00368
ENSG00000196850	PPTC7	46.739	1.873	0.00374
ENSG00000123095	BHLHE41	59.732	2.990	0.00376
ENSG00000171621	SPSB1	41.016	1.846	0.00377
ENSG00000117155	SSX2IP	75.176	-1.865	0.00389
ENSG00000042286	AIFM2	75.996	1.797	0.00393

ENSG00000110911	SLC11A2	167.689	1.924	0.00405
ENSG00000125844	RRBP1	273.240	1.921	0.00411
ENSG00000154642	C21orf91	63.430	2.142	0.00431
ENSG00000160013	PTGIR	8.361	3.753	0.00444
ENSG00000167325	RRM1	128.227	-1.455	0.00453
ENSG00000168268	NT5DC2	18.880	-2.793	0.00453
ENSG00000101079	NDRG3	63.254	-1.554	0.00458
ENSG00000064666	CNN2	216.758	-1.497	0.00459
ENSG00000066084	DIP2B	57.641	1.551	0.00474
ENSG00000183137	CEP57L1	30.688	1.919	0.00474
ENSG00000060491	OGFR	90.727	1.647	0.00478
ENSG00000163347	CLDN1	57.225	4.107	0.00478
ENSG00000118257	NRP2	176.745	2.345	0.00480
ENSG00000175390	EIF3F	102.608	-1.753	0.00485
ENSG00000204856	FAM216A	13.417	-2.888	0.00493
ENSG00000127666	TICAM1	26.574	2.242	0.00494
ENSG00000163931	TKT	631.445	-1.309	0.00494
ENSG00000101444	AHCY	74.732	-1.776	0.00497
ENSG00000128917	DLL4	5.138	6.010	0.00501
ENSG00000119522	DENND1A	36.854	1.819	0.00502
ENSG00000108179	PPIF	101.222	1.565	0.00510
ENSG00000171425	ZNF581	39.522	-2.285	0.00517
ENSG00000112763	BTN2A1	30.127	1.993	0.00520
ENSG00000101745	ANKRD12	146.391	2.033	0.00528
ENSG00000172432	GTPBP2	18.834	2.443	0.00530
ENSG00000079385	CEACAM1	3.463	5.929	0.00545
ENSG00000138760	SCARB2	656.282	1.421	0.00545
ENSG00000110042	DTX4	54.086	1.609	0.00554
ENSG00000159314	ARHGAP27	6.948	4.907	0.00555
ENSG00000175581	MRPL48	19.560	-2.547	0.00561
ENSG00000124151	NCOA3	110.483	1.883	0.00563
ENSG00000155506	LARP1	346.356	1.169	0.00566
ENSG00000253958	CLDN23	19.195	2.334	0.00577

ENSG00000185201	IFITM2	812.603	1.559	0.00583
ENSG00000171310	CHST11	26.836	2.235	0.00599
ENSG00000013374	NUB1	193.544	1.972	0.00604
ENSG00000070814	TCOF1	11.370	2.925	0.00604
ENSG00000136048	DRAM1	381.082	1.518	0.00612
ENSG00000026103	FAS	115.782	1.316	0.00647
ENSG00000166780	BMERB1	57.789	-1.825	0.00660
ENSG00000149218	ENDOD1	132.279	1.949	0.00660
ENSG00000147454	SLC25A37	103.846	2.392	0.00665
ENSG00000086061	DNAJA1	550.498	1.252	0.00682
ENSG00000109654	TRIM2	34.521	-2.133	0.00686
ENSG00000197646	PDCD1LG2	28.083	2.021	0.00711
ENSG00000103034	NDRG4	11.498	-3.308	0.00714
ENSG00000029153	ARNTL2	28.712	2.276	0.00738
ENSG00000178860	MSC	50.008	1.904	0.00740
ENSG00000185885	IFITM1	6.156	5.038	0.00753
ENSG00000172123	SLFN12	49.374	2.238	0.00754
ENSG00000178951	ZBTB7A	223.433	1.346	0.00758
ENSG00000031698	SARS1	153.343	-1.224	0.00774
ENSG00000145907	G3BP1	282.077	1.099	0.00774
ENSG00000157654	PALM2AKAP2	772.381	1.871	0.00774
ENSG00000159110	IFNAR2	50.158	1.812	0.00776
ENSG00000187240	DYNC2H1	39.589	-2.111	0.00804
ENSG00000056972	TRAF3IP2	66.620	1.615	0.00809
ENSG00000173114	LRRN3	34.382	1.938	0.00809
ENSG00000138018	SELENOI	26.551	1.883	0.00816
ENSG00000183726	TMEM50A	235.909	1.261	0.00824
ENSG00000186854	TRABD2A	48.497	2.035	0.00824
ENSG00000072786	STK10	32.742	2.082	0.00840
ENSG00000103222	ABCC1	95.512	1.756	0.00841
ENSG00000141582	CBX4	76.119	1.559	0.00878
ENSG00000105643	ARRDC2	22.026	2.192	0.00889
ENSG00000006453	BAIAP2L1	19.680	-2.443	0.00920

ENSG00000274070	CASTOR2	35.727	-2.415	0.00923
ENSG00000109320	NFKB1	116.525	1.450	0.00928
ENSG00000112576	CCND3	79.833	1.497	0.00956
ENSG00000197818	SLC9A8	20.287	1.922	0.00957
ENSG00000278845	MRPL45	93.844	-1.661	0.00973
ENSG00000170340	B3GNT2	71.653	2.229	0.01009
ENSG00000152689	RASGRP3	5.053	5.284	0.01021
ENSG00000117475	BLZF1	47.751	1.703	0.01058
ENSG00000196092	PAX5	2.978	6.120	0.01072
ENSG00000095951	HIVEP1	31.429	2.293	0.01157
ENSG00000206052	DOK6	14.436	-2.731	0.01157
ENSG00000116863	ADPRS	45.804	1.752	0.01175
ENSG00000069399	BCL3	110.411	1.416	0.01177
ENSG00000128849	CGNL1	13.366	2.988	0.01199
ENSG00000197312	DDI2	52.463	1.600	0.01203
ENSG00000148700	ADD3	815.065	1.552	0.01220
ENSG00000176170	SPHK1	14.663	2.893	0.01225
ENSG00000173120	KDM2A	129.168	1.391	0.01229
ENSG00000160767	FAM189B	152.660	1.282	0.01242
ENSG00000103855	CD276	157.156	1.184	0.01263
ENSG00000115919	KYNU	15.467	2.705	0.01284
ENSG00000100731	PCNX1	86.247	1.307	0.01306
ENSG00000198133	TMEM229B	5.426	5.456	0.01318
ENSG00000137764	MAP2K5	33.667	-2.038	0.01320
ENSG00000111885	MAN1A1	128.928	1.592	0.01322
ENSG00000107249	GLIS3	34.746	2.109	0.01346
ENSG00000146425	DYNLT1	182.061	1.319	0.01355
ENSG00000102921	N4BP1	64.684	1.472	0.01363
ENSG00000119938	PPP1R3C	262.169	-1.669	0.01371
ENSG00000056558	TRAF1	22.785	4.602	0.01372
ENSG00000143320	CRABP2	297.578	-1.114	0.01376
ENSG00000163435	ELF3	3.633	5.848	0.01381
ENSG00000255150	EID3	9.230	3.050	0.01381

ENSG00000183496	MEX3B	13.318	-3.148	0.01393
ENSG00000117523	PRRC2C	207.899	1.789	0.01400
ENSG00000188786	MTF1	55.563	1.687	0.01449
ENSG00000204389	HSPA1A	249.506	1.251	0.01458
ENSG00000179431	FJX1	16.814	2.148	0.01480
ENSG00000064932	SBNO2	34.895	1.700	0.01501
ENSG00000118898	PPL	18.991	-2.515	0.01528
ENSG00000213928	IRF9	28.017	1.784	0.01554
ENSG00000173846	PLK3	29.336	1.862	0.01613
ENSG00000164949	GEM	55.246	1.932	0.01620
ENSG00000119699	TGFB3	30.325	2.180	0.01631
ENSG00000135052	GOLM1	88.868	1.410	0.01631
ENSG00000151694	ADAM17	190.567	1.328	0.01633
ENSG00000075415	SLC25A3	680.353	-1.232	0.01643
ENSG00000074964	ARHGEF10L	47.934	1.459	0.01682
ENSG00000168679	SLC16A4	73.950	1.689	0.01720
ENSG00000103257	SLC7A5	28.301	2.236	0.01738
ENSG00000166037	CEP57	66.828	-1.437	0.01738
ENSG00000077782	FGFR1	811.869	1.252	0.01765
ENSG00000179051	RCC2	204.155	2.106	0.01796
ENSG00000136147	PHF11	101.299	1.468	0.01819
ENSG00000205362	MT1A	9.875	2.899	0.01819
ENSG00000138430	OLA1	87.982	-1.525	0.01823
ENSG00000160285	LSS	98.972	1.491	0.01881
ENSG00000188229	TUBB4B	160.143	1.281	0.01898
ENSG00000165949	IFI27	197.090	3.497	0.01929
ENSG00000100417	PMM1	103.711	-1.392	0.01965
ENSG00000138495	COX17	92.435	1.473	0.02008
ENSG00000171155	C1GALT1C1	42.379	1.583	0.02013
ENSG00000197442	MAP3K5	101.799	1.545	0.02014
ENSG00000183010	PYCR1	39.565	-1.724	0.02016
ENSG00000176697	BDNF	68.094	1.436	0.02019
ENSG00000140280	LYSMD2	21.484	1.791	0.02065

ENSG00000136689	IL1RN	16.553	3.172	0.02087
ENSG00000082641	NFE2L1	196.300	1.295	0.02113
ENSG00000100353	EIF3D	374.876	-1.431	0.02119
ENSG00000197157	SND1	237.586	-1.202	0.02124
ENSG00000146232	NFKBIE	25.606	1.958	0.02171
ENSG00000178425	NT5DC1	49.173	-1.522	0.02196
ENSG00000276600	RAB7B	16.041	-2.359	0.02213
ENSG00000132122	SPATA6	15.318	-2.368	0.02221
ENSG00000103888	CEMIP	146.747	-1.432	0.02259
ENSG00000158615	PPP1R15B	46.565	1.691	0.02259
ENSG00000172716	SLFN11	40.282	1.854	0.02259
ENSG00000173917	HOXB2	26.887	2.244	0.02259
ENSG00000184988	TMEM106A	20.670	1.998	0.02259
ENSG00000173218	VANGL1	46.940	1.554	0.02319
ENSG00000168952	STXBP6	25.318	-2.255	0.02370
ENSG00000169047	IRS1	157.202	1.167	0.02377
ENSG00000170852	KBTBD2	42.967	1.521	0.02385
ENSG00000184588	PDE4B	26.383	2.102	0.02412
ENSG00000105829	BET1	63.102	1.565	0.02436
ENSG00000146409	SLC18B1	29.631	1.721	0.02442
ENSG00000165731	RET	7.671	4.361	0.02463
ENSG00000089289	IGBP1	239.547	-1.598	0.02468
ENSG00000177989	ODF3B	4.863	3.541	0.02490
ENSG00000179256	SMCO3	4.089	-4.836	0.02490
ENSG00000164164	OTUD4	58.742	1.549	0.02524
ENSG00000125741	OPA3	15.404	2.107	0.02573
ENSG00000072210	ALDH3A2	39.655	-1.709	0.02581
ENSG00000138756	BMP2K	84.639	1.502	0.02603
ENSG00000105281	SLC1A5	239.567	-1.676	0.02635
ENSG00000175946	KLHL38	4.189	5.038	0.02714
ENSG00000184838	PRR16	25.933	2.111	0.02722
ENSG00000101265	RASSF2	88.435	-2.103	0.02736
ENSG00000188211	NCR3LG1	5.773	4.491	0.02765

ENSG00000151883	PARP8	22.439	1.757	0.02809
ENSG00000100577	GSTZ1	36.995	-1.691	0.02849
ENSG00000172493	AFF1	31.599	1.604	0.02920
ENSG00000205659	LIN52	39.292	1.763	0.02961
ENSG00000146282	RARS2	112.713	-1.573	0.02968
ENSG00000172346	CSDC2	10.610	-2.923	0.02968
ENSG00000107758	PPP3CB	98.185	-1.234	0.02987
ENSG00000100316	RPL3	920.509	-1.469	0.03004
ENSG00000157557	ETS2	234.473	1.437	0.03028
ENSG00000145348	TBCK	44.141	-1.592	0.03037
ENSG00000099860	GADD45B	27.506	1.875	0.03045
ENSG00000106992	AK1	28.747	-1.817	0.03053
ENSG00000023318	ERP44	164.776	1.179	0.03112
ENSG00000152503	TRIM36	2.436	5.143	0.03127
ENSG00000123975	CKS2	89.026	1.742	0.03145
ENSG00000204256	BRD2	195.964	1.216	0.03203
ENSG00000186310	NAP1L3	6.558	-4.581	0.03254
ENSG00000068366	ACSL4	427.945	1.658	0.03306
ENSG00000103876	FAH	61.185	-1.493	0.03327
ENSG00000061455	PRDM6	18.375	-2.624	0.03329
ENSG00000065526	SPEN	35.881	2.187	0.03329
ENSG00000161682	FAM171A2	20.462	-2.443	0.03333
ENSG00000113658	SMAD5	216.615	-1.252	0.03346
ENSG00000171223	JUNB	97.675	1.535	0.03391
ENSG00000138078	PREPL	112.658	-1.402	0.03425
ENSG00000196126	HLA-DRB1	2.660	5.900	0.03436
ENSG00000212961	HNRNPA1P40	3.088	5.031	0.03440
ENSG00000102317	RBM3	210.671	-1.459	0.03443
ENSG00000107864	CPEB3	11.191	2.559	0.03443
ENSG00000100139	MICALL1	19.577	1.833	0.03467
ENSG00000115758	ODC1	94.110	-1.305	0.03479
ENSG00000146648	EGFR	265.737	1.259	0.03510
ENSG00000132670	PTPRA	104.953	1.230	0.03519

ENSG00000144674	GOLGA4	137.384	2.090	0.03570
ENSG00000132481	TRIM47	21.460	2.571	0.03590
ENSG00000135148	TRAFD1	48.312	1.454	0.03629
ENSG00000241106	HLA-DOB	3.050	5.525	0.03629
ENSG00000151502	VPS26B	52.990	-1.563	0.03631
ENSG00000166741	NNMT	258.249	1.428	0.03704
ENSG00000114450	GNB4	181.713	1.375	0.03711
ENSG00000204388	HSPA1B	174.713	1.322	0.03711
ENSG00000111266	DUSP16	44.235	1.562	0.03712
ENSG00000116584	ARHGEF2	72.577	1.287	0.03724
ENSG00000175197	DDIT3	101.655	1.348	0.03750
ENSG00000070770	CSNK2A2	114.081	-1.235	0.03801
ENSG00000167216	KATNAL2	14.914	-2.110	0.03801
ENSG00000154640	BTG3	111.179	1.163	0.03813
ENSG00000100347	SAMM50	64.036	-1.523	0.03818
ENSG00000213626	LBH	145.399	-1.768	0.03818
ENSG00000150630	VEGFC	69.472	1.543	0.03863
ENSG00000073910	FRY	12.882	-2.357	0.03922
ENSG00000144959	NCEH1	94.971	2.753	0.04071
ENSG00000180611	MB21D2	14.946	2.183	0.04220
ENSG00000182963	GJC1	24.831	1.646	0.04255
ENSG00000117632	STMN1	226.223	-1.201	0.04259
ENSG00000108679	LGALS3BP	99.604	1.590	0.04290
ENSG00000164904	ALDH7A1	72.557	-1.432	0.04358
ENSG00000072952	IRAG1	64.381	-1.621	0.04366
ENSG00000143013	LMO4	302.705	1.257	0.04366
ENSG00000172915	NBEA	16.025	-2.042	0.04371
ENSG00000152661	GJA1	238.556	1.614	0.04396
ENSG00000128309	MPST	35.227	-2.012	0.04409
ENSG00000176678	FOXL1	40.149	1.691	0.04472
ENSG00000140350	ANP32A	63.389	-1.426	0.04491
ENSG00000163121	NEURL3	2.137	5.570	0.04491
ENSG00000163431	LMOD1	55.085	-1.743	0.04491

ENSG00000178234	GALNT11	38.195	-1.605	0.04491
ENSG00000138435	CHRNA1	4.860	4.393	0.04502
ENSG00000144730	IL17RD	20.061	-2.278	0.04581
ENSG00000170624	SGCD	55.836	-2.357	0.04581
ENSG00000108256	NUFIP2	184.904	1.345	0.04581
ENSG00000174749	FAM241A	18.161	2.016	0.04581
ENSG00000148541	FAM13C	7.008	-3.183	0.04597
ENSG00000067221	STOML1	41.067	1.682	0.04707
ENSG00000170464	DNAJC18	24.135	-1.856	0.04739
ENSG00000263934	SNORD3A	9.555	2.350	0.04739
ENSG00000140548	ZNF710	9.258	2.602	0.04748
ENSG00000177426	TGIF1	56.405	1.680	0.04849
ENSG00000050426	LETMD1	40.595	-2.056	0.04849
ENSG00000159216	RUNX1	51.486	1.613	0.04884
ENSG00000143845	ETNK2	13.138	-2.683	0.04914
ENSG00000116874	WARS2	29.359	-1.653	0.04941
ENSG00000122068	FYTTD1	161.904	1.244	0.04953
ENSG00000139572	GPR84	2.249	5.428	0.04957
ENSG00000112941	TENT4A	30.923	1.729	0.04979
ENSG00000105819	PMPCB	62.295	-1.323	0.04979
ENSG00000172667	ZMAT3	664.545	-1.338	0.04980

Table 7.13.3 Lists of all significantly expressed genes from cfDNA of poly (I:C)+CSE-stimulated iHBECs induced HASMCs gene expression compered to cfDNA of CSE-stimulated iHBECs induced HASMCs gene expression

Gene_ID	Gene_name	baseMean	log2FoldChange	Adjusted P value
ENSG00000167207	NOD2	6.916	-6.735	0.00011
ENSG00000070961	ATP2B1	545.578	-2.042	0.00011
ENSG00000122417	ODF2L	83.123	-2.538	0.00011
ENSG00000185561	TLCD2	50.784	-3.107	0.00011
ENSG00000157657	ZNF618	76.756	-1.986	0.00011
ENSG00000197142	ACSL5	14.796	-3.375	0.00011
ENSG00000175197	DDIT3	101.655	-1.799	0.00012
ENSG00000172159	FRMD3	19.936	-3.583	0.00012
ENSG00000158470	B4GALT5	121.533	-2.359	0.00013
ENSG00000148908	RGS10	116.787	1.932	0.00013
ENSG00000154027	AK5	53.548	2.185	0.00013
ENSG00000136147	PHF11	101.299	-1.869	0.00014
ENSG00000182752	PAPPA	957.461	-1.337	0.00014
ENSG00000139921	TMX1	181.485	-1.811	0.00014
ENSG00000243244	STON1	28.555	2.960	0.00015
ENSG00000167658	EEF2	2499.996	1.856	0.00016
ENSG00000135604	STX11	15.418	-5.023	0.00016
ENSG00000170581	STAT2	266.382	-1.423	0.00016
ENSG00000160326	SLC2A6	18.796	-3.995	0.00017
ENSG00000137393	RNF144B	20.773	-4.822	0.00020
ENSG00000063046	EIF4B	118.764	2.010	0.00020
ENSG00000137752	CASP1	111.955	-2.118	0.00020
ENSG00000134802	SLC43A3	270.710	-2.156	0.00020
ENSG00000103966	EHD4	50.848	-2.034	0.00020
ENSG00000166165	CKB	159.921	-1.681	0.00023
ENSG00000164181	ELOVL7	6.628	-6.609	0.00024
ENSG00000172053	QARS1	100.781	2.117	0.00024
ENSG00000114933	INO80D	31.450	-2.297	0.00025
ENSG00000163734	CXCL3	51.919	-6.132	0.00026
ENSG00000048052	HDAC9	51.483	-2.281	0.00028

ENSG00000149823	VPS51	44.551	2.396	0.00032
ENSG00000178035	IMPDH2	132.468	2.192	0.00032
ENSG00000141574	SECTM1	269.987	-2.625	0.00032
ENSG00000135052	GOLM1	88.868	-1.724	0.00034
ENSG00000168404	MLKL	11.488	-3.634	0.00034
ENSG00000067798	NAV3	53.533	-2.736	0.00035
ENSG00000100316	RPL3	920.509	1.826	0.00036
ENSG00000198355	PIM3	177.436	-1.985	0.00038
ENSG00000101745	ANKRD12	146.391	-2.340	0.00039
ENSG00000115159	GPD2	131.109	-2.429	0.00041
ENSG00000187479	C11orf96	168.901	-4.308	0.00042
ENSG00000042286	AIFM2	75.996	-2.035	0.00043
ENSG00000138685	FGF2	293.777	-2.029	0.00045
ENSG00000146859	TMEM140	124.606	-1.697	0.00046
ENSG00000196968	FUT11	63.978	-1.802	0.00046
ENSG00000173114	LRRN3	34.382	-2.341	0.00047
ENSG00000110042	DTX4	54.086	-1.858	0.00048
ENSG00000178607	ERN1	24.582	-2.395	0.00049
ENSG00000185885	IFITM1	6.156	-6.560	0.00050
ENSG00000181163	NPM1	885.439	1.137	0.00051
ENSG00000133392	MYH11	6.784	-6.584	0.00051
ENSG00000168280	KIF5C	12.280	-6.273	0.00054
ENSG00000182093	GET1	44.568	2.067	0.00056
ENSG00000120539	MASTL	23.737	-2.502	0.00058
ENSG00000198604	BAZ1A	107.908	-1.869	0.00060
ENSG00000091073	DTX2	29.893	-2.423	0.00062
ENSG00000170961	HAS2	37.411	-2.577	0.00063
ENSG00000179021	C3orf38	109.604	-1.751	0.00063
ENSG00000174720	LARP7	158.616	-1.546	0.00065
ENSG00000198053	SIRPA	169.526	-1.863	0.00068
ENSG00000130939	UBE4B	53.149	2.011	0.00070
ENSG00000099622	CIRBP	175.146	1.427	0.00077
ENSG00000109339	MAPK10	63.116	1.965	0.00079

ENSG00000185650	ZFP36L1	2004.148	-1.515	0.00079
ENSG00000144837	PLA1A	8.236	-6.006	0.00081
ENSG00000163565	IFI16	550.257	-1.752	0.00083
ENSG00000170525	PFKFB3	94.074	-1.888	0.00083
ENSG00000125844	RRBP1	273.240	-2.091	0.00084
ENSG00000115271	GCA	10.731	-3.944	0.00091
ENSG00000184588	PDE4B	26.383	-2.734	0.00091
ENSG00000116663	FBXO6	15.601	-2.698	0.00092
ENSG00000182704	TSKU	86.484	-1.636	0.00092
ENSG00000138135	CH25H	14.643	-4.476	0.00100
ENSG00000065060	UHRF1BP1	18.849	-2.499	0.00101
ENSG00000153048	CARHSP1	60.775	1.946	0.00101
ENSG00000136044	APPL2	43.086	2.377	0.00104
ENSG00000115758	ODC1	94.110	1.553	0.00108
ENSG00000117152	RGS4	79.366	-2.787	0.00109
ENSG00000168118	RAB4A	75.208	1.650	0.00109
ENSG00000186470	BTN3A2	69.924	-1.566	0.00110
ENSG00000120526	NUDCD1	28.029	-2.478	0.00110
ENSG00000124882	EREG	36.035	-5.250	0.00112
ENSG00000234127	TRIM26	70.871	-1.585	0.00119
ENSG00000076641	PAG1	279.606	-2.176	0.00122
ENSG00000123131	PRDX4	130.396	1.558	0.00144
ENSG00000060491	OGFR	90.727	-1.778	0.00146
ENSG00000086061	DNAJA1	550.498	-1.341	0.00149
ENSG00000128656	CHN1	339.787	-1.834	0.00150
ENSG00000243742	RPLP0P2	10.817	-3.449	0.00150
ENSG00000113328	CCNG1	234.917	1.568	0.00157
ENSG00000082641	NFE2L1	196.300	-1.482	0.00159
ENSG00000135077	HAVCR2	11.331	-4.737	0.00163
ENSG00000102081	FMR1	76.072	-1.756	0.00164
ENSG00000141542	RAB40B	26.786	2.307	0.00165
ENSG00000101444	AHCY	74.732	1.887	0.00167
ENSG00000168268	NT5DC2	18.880	2.971	0.00173

ENSG00000182670	TTC3	502.553	1.660	0.00173
ENSG00000132670	PTPRA	104.953	-1.458	0.00173
ENSG00000158373	H2BC5	54.203	-2.187	0.00175
ENSG00000130005	GAMT	38.475	2.124	0.00176
ENSG00000131459	GFPT2	42.256	-2.022	0.00181
ENSG00000084693	AGBL5	28.652	2.361	0.00193
ENSG00000148700	ADD3	815.065	-1.711	0.00193
ENSG00000104321	TRPA1	388.874	-3.183	0.00207
ENSG00000175390	EIF3F	102.608	1.840	0.00207
ENSG00000120693	SMAD9	27.502	2.185	0.00208
ENSG00000180616	SSTR2	7.947	-5.632	0.00208
ENSG00000134330	IAH1	64.762	1.581	0.00209
ENSG00000168952	STXBP6	25.318	2.636	0.00214
ENSG00000041353	RAB27B	44.003	-2.515	0.00217
ENSG00000023902	PLEKHO1	105.987	-1.656	0.00222
ENSG00000143322	ABL2	141.137	-1.913	0.00231
ENSG00000141526	SLC16A3	93.809	-1.684	0.00239
ENSG00000120913	PDLIM2	278.148	1.207	0.00243
ENSG00000013374	NUB1	193.544	-2.092	0.00246
ENSG00000134070	IRAK2	18.091	-3.117	0.00248
ENSG00000155363	MOV10	70.350	-1.685	0.00249
ENSG00000254470	AP5B1	17.199	-2.400	0.00250
ENSG00000182957	SPATA13	45.464	-2.528	0.00256
ENSG00000019549	SNAI2	169.949	1.894	0.00257
ENSG00000140406	TLNRD1	36.587	-2.173	0.00259
ENSG00000116514	RNF19B	42.163	-2.321	0.00273
ENSG00000166741	NNMT	258.249	-1.667	0.00278
ENSG00000115009	CCL20	8.631	-6.067	0.00291
ENSG00000163661	PTX3	167.236	-2.489	0.00292
ENSG00000081041	CXCL2	14.046	-5.050	0.00303
ENSG00000172432	GTPBP2	18.834	-2.628	0.00321
ENSG00000175985	PLEKHD1	4.085	-6.050	0.00324
ENSG00000185722	ANKFY1	131.046	-1.533	0.00332

ENSG00000186854	TRABD2A	48.497	-2.195	0.00338
ENSG00000042062	RIPOR3	21.959	-2.196	0.00345
ENSG00000163162	RNF149	101.608	-1.512	0.00356
ENSG00000076108	BAZ2A	81.886	-1.772	0.00368
ENSG00000204264	PSMB8	97.652	-1.495	0.00368
ENSG00000089692	LAG3	8.062	-5.910	0.00369
ENSG00000143384	MCL1	550.544	-1.470	0.00392
ENSG00000157693	TMEM268	23.038	-2.053	0.00393
ENSG00000120690	ELF1	60.787	-1.691	0.00412
ENSG00000213928	IRF9	28.017	-2.020	0.00412
ENSG00000122729	ACO1	165.939	1.839	0.00435
ENSG00000188343	CIBAR1	75.331	2.121	0.00435
ENSG00000100422	CERK	42.746	1.983	0.00443
ENSG00000090097	PCBP4	84.858	1.669	0.00456
ENSG00000189114	BLOC1S3	19.433	-2.393	0.00464
ENSG00000096696	DSP	30.389	-2.685	0.00467
ENSG00000135211	TMEM60	126.849	-1.321	0.00485
ENSG00000196776	CD47	390.584	-1.358	0.00497
ENSG00000188786	MTF1	55.563	-1.837	0.00515
ENSG00000165475	CRYL1	65.623	1.629	0.00529
ENSG00000159314	ARHGAP27	6.948	-5.466	0.00547
ENSG00000096968	JAK2	59.549	-1.693	0.00564
ENSG00000132475	H3-3B	1003.193	-1.273	0.00576
ENSG00000149131	SERPING1	179.552	-1.839	0.00578
ENSG00000135390	ATP5MC2	472.933	1.366	0.00578
ENSG00000053371	AKR7A2	154.741	1.830	0.00578
ENSG00000128274	A4GALT	46.306	-1.675	0.00605
ENSG00000138821	SLC39A8	33.588	-2.536	0.00605
ENSG00000168679	SLC16A4	73.950	-1.827	0.00630
ENSG00000187957	DNER	22.348	-2.224	0.00630
ENSG00000010818	HIVEP2	99.506	-1.867	0.00666
ENSG00000197858	GPAA1	63.032	1.559	0.00688
ENSG00000138735	PDE5A	327.280	1.604	0.00689

ENSG00000159208	CIART	16.304	-2.471	0.00753
ENSG00000087245	MMP2	645.970	-1.563	0.00781
ENSG00000173145	NOC3L	66.608	-2.237	0.00786
ENSG00000154175	ABI3BP	29.823	-2.766	0.00797
ENSG00000177272	KCNA3	20.269	-2.648	0.00806
ENSG00000185201	IFITM2	812.603	-1.545	0.00821
ENSG00000116459	ATP5PB	232.376	1.286	0.00823
ENSG00000181649	PHLDA2	177.230	-1.467	0.00831
ENSG00000128965	CHAC1	24.686	-3.033	0.00835
ENSG00000174808	BTC	8.391	-4.363	0.00835
ENSG00000157985	AGAP1	23.108	2.153	0.00895
ENSG00000183496	MEX3B	13.318	3.287	0.00901
ENSG00000101236	RNF24	163.527	-1.497	0.00931
ENSG00000118257	NRP2	176.745	-2.276	0.00931
ENSG00000171621	SPSB1	41.016	-1.796	0.00931
ENSG00000212961	HNRNPA1P40	3.088	-5.708	0.00941
ENSG00000255150	EID3	9.230	-3.544	0.00947
ENSG00000119522	DENND1A	36.854	-1.796	0.00981
ENSG00000146409	SLC18B1	29.631	-1.898	0.00994
ENSG00000043143	JADE2	58.226	-1.667	0.00996
ENSG00000100353	EIF3D	374.876	1.503	0.01016
ENSG00000173762	CD7	3.177	-5.569	0.01052
ENSG00000122547	EEPD1	14.774	2.613	0.01073
ENSG00000171310	CHST11	26.836	-2.211	0.01088
ENSG00000128917	DLL4	5.138	-5.723	0.01106
ENSG00000184988	TMEM106A	20.670	-2.195	0.01115
ENSG00000176170	SPHK1	14.663	-3.049	0.01135
ENSG00000116863	ADPRS	45.804	-1.798	0.01142
ENSG00000075415	SLC25A3	680.353	1.261	0.01185
ENSG00000056558	TRAF1	22.785	-4.875	0.01226
ENSG00000179256	SMCO3	4.089	5.188	0.01229
ENSG00000073331	ALPK1	23.309	-1.965	0.01229
ENSG00000196411	EPHB4	54.497	1.726	0.01229

ENSG00000113645	WWC1	4.074	-5.691	0.01231
ENSG00000198018	ENTPD7	52.633	-1.909	0.01239
ENSG00000101966	XIAP	158.038	-1.608	0.01245
ENSG00000160888	IER2	100.466	-1.917	0.01245
ENSG00000144674	GOLGA4	137.384	-2.293	0.01250
ENSG00000165949	IFI27	197.090	-3.658	0.01272
ENSG00000083097	DOP1A	25.601	-2.429	0.01293
ENSG00000213024	NUP62	105.483	-1.368	0.01300
ENSG00000144730	IL17RD	20.061	2.541	0.01309
ENSG00000176697	BDNF	68.094	-1.504	0.01315
ENSG00000105281	SLC1A5	239.567	1.767	0.01317
ENSG00000198382	UVRAG	55.052	-1.504	0.01321
ENSG00000197646	PDCD1LG2	28.083	-1.995	0.01340
ENSG00000143486	EIF2D	46.401	1.714	0.01341
ENSG00000165731	RET	7.671	-5.531	0.01341
ENSG00000099860	GADD45B	27.506	-2.063	0.01348
ENSG00000160818	GPATCH4	26.175	-2.067	0.01380
ENSG00000108342	CSF3	7.054	-5.200	0.01401
ENSG00000136689	IL1RN	16.553	-3.430	0.01422
ENSG00000149212	SESN3	129.724	1.903	0.01422
ENSG00000002745	WNT16	15.313	-3.102	0.01445
ENSG00000128849	CGNL1	13.366	-3.061	0.01454
ENSG00000139318	DUSP6	75.443	-2.215	0.01463
ENSG00000110911	SLC11A2	167.689	-1.802	0.01493
ENSG00000121274	TENT4B	111.326	-1.512	0.01547
ENSG00000152661	GJA1	238.556	-1.756	0.01547
ENSG00000100647	SUSD6	53.387	-1.607	0.01581
ENSG00000161714	PLCD3	85.391	1.666	0.01609
ENSG00000117632	STMN1	226.223	1.275	0.01715
ENSG00000173626	TRAPPC3L	3.264	-5.243	0.01828
ENSG00000114942	EEF1B2	1183.989	1.220	0.01830
ENSG00000167106	FAM102A	116.334	1.521	0.01920
ENSG00000111885	MAN1A1	128.928	-1.579	0.01925

ENSG00000204287	HLA-DRA	3.660	-6.091	0.01948
ENSG00000135837	CEP350	126.131	-1.686	0.01949
ENSG00000117523	PRRC2C	207.899	-1.771	0.01970
ENSG00000180611	MB21D2	14.946	-2.476	0.02003
ENSG00000120910	PPP3CC	70.315	-1.444	0.02015
ENSG00000171155	C1GALT1C1	42.379	-1.622	0.02016
ENSG00000099290	WASHC2A	112.297	-1.337	0.02021
ENSG00000229119	RPLP0P9	18.130	2.270	0.02030
ENSG00000206190	ATP10A	15.265	-2.471	0.02081
ENSG00000072786	STK10	32.742	-1.999	0.02132
ENSG00000196092	PAX5	2.978	-5.832	0.02147
ENSG00000159110	IFNAR2	50.158	-1.734	0.02172
ENSG00000102921	N4BP1	64.684	-1.461	0.02198
ENSG00000108679	LGALS3BP	99.604	-1.698	0.02198
ENSG00000204397	CARD16	120.000	-1.593	0.02198
ENSG00000026103	FAS	115.782	-1.258	0.02245
ENSG00000006453	BAIAP2L1	19.680	2.333	0.02273
ENSG00000072210	ALDH3A2	39.655	1.747	0.02287
ENSG00000107249	GLIS3	34.746	-2.076	0.02287
ENSG00000151502	VPS26B	52.990	1.634	0.02287
ENSG00000030419	IKZF2	27.494	-2.135	0.02305
ENSG00000115919	KYNU	15.467	-2.660	0.02310
ENSG00000144959	NCEH1	94.971	-2.937	0.02348
ENSG00000137842	TMEM62	11.011	-2.491	0.02411
ENSG00000112763	BTN2A1	30.127	-1.842	0.02471
ENSG00000119938	PPP1R3C	262.169	1.623	0.02473
ENSG00000167550	RHEBL1	4.608	-4.937	0.02520
ENSG00000109113	RAB34	182.158	1.260	0.02580
ENSG00000136048	DRAM1	381.082	-1.416	0.02586
ENSG00000172123	SLFN12	49.374	-2.087	0.02607
ENSG00000153786	ZDHHC7	213.422	1.387	0.02642
ENSG00000106346	USP42	36.358	-1.847	0.02672
ENSG00000105643	ARRDC2	22.026	-2.075	0.02712

ENSG00000163435	ELF3	3.633	-5.561	0.02771
ENSG00000106992	AK1	28.747	1.855	0.02809
ENSG00000173575	CHD2	118.441	-1.309	0.02853
ENSG00000128590	DNAJB9	91.234	-1.463	0.02901
ENSG00000125826	RBCK1	168.541	-1.173	0.02916
ENSG00000135148	TRAFD1	48.312	-1.516	0.02916
ENSG00000152465	NMT2	78.012	1.383	0.02918
ENSG00000072121	ZFYVE26	29.268	-1.731	0.02946
ENSG00000103876	FAH	61.185	1.524	0.02984
ENSG00000150403	TMCO3	72.102	1.501	0.02989
ENSG00000138449	SLC40A1	432.664	1.790	0.02990
ENSG00000166780	BMERB1	57.789	1.686	0.03011
ENSG00000067221	STOML1	41.067	-1.789	0.03066
ENSG00000134851	TMEM165	90.242	-1.337	0.03073
ENSG00000141504	SAT2	68.836	1.520	0.03098
ENSG00000186310	NAP1L3	6.558	4.652	0.03180
ENSG00000185567	AHNAK2	68.080	2.041	0.03237
ENSG00000079102	RUNX1T1	127.388	1.315	0.03260
ENSG00000142583	SLC2A5	6.420	-3.505	0.03269
ENSG00000077782	FGFR1	811.869	-1.221	0.03292
ENSG00000137767	SQOR	337.230	-1.302	0.03295
ENSG00000086062	B4GALT1	415.740	-1.267	0.03320
ENSG00000149809	TM7SF2	19.529	-2.016	0.03323
ENSG00000173120	KDM2A	129.168	-1.332	0.03323
ENSG00000126785	RHOJ	21.091	2.266	0.03368
ENSG00000138435	CHRNA1	4.860	-4.989	0.03448
ENSG00000282988	ENSG00000282988	6.619	-3.068	0.03523
ENSG00000168016	TRANK1	29.800	-2.192	0.03528
ENSG00000204628	RACK1	1541.349	1.374	0.03533
ENSG00000124151	NCOA3	110.483	-1.692	0.03651
ENSG00000119487	MAPKAP1	91.960	1.234	0.03716
ENSG00000173065	FAM222B	34.813	-1.721	0.03815
ENSG00000183688	RFLNB	77.200	1.323	0.03815

ENSG00000198814	GK	36.117	-1.718	0.03815
ENSG00000276141	WHAMMP3	5.869	-3.709	0.03840
ENSG00000101265	RASSF2	88.435	2.070	0.03855
ENSG00000172716	SLFN11	40.282	-1.819	0.03878
ENSG00000149218	ENDOD1	132.279	-1.754	0.03896
ENSG00000078401	EDN1	5.778	-4.317	0.03932
ENSG00000106819	ASPN	39.421	1.914	0.04002
ENSG00000196850	PPTC7	46.739	-1.635	0.04129
ENSG00000170340	B3GNT2	71.653	-2.034	0.04208
ENSG00000197622	CDC42SE1	76.872	-1.398	0.04208
ENSG00000114450	GNB4	181.713	-1.380	0.04327
ENSG00000183010	PYCR1	39.565	1.660	0.04327
ENSG00000128342	LIF	20.460	-2.170	0.04342
ENSG00000121691	CAT	201.482	1.246	0.04364
ENSG00000164327	RICTOR	62.040	-1.469	0.04364
ENSG00000196678	ERI2	8.429	-2.665	0.04373
ENSG00000143320	CRABP2	297.578	1.064	0.04389
ENSG00000122566	HNRNPA2B1	384.954	-1.136	0.04394
ENSG00000116017	ARID3A	42.881	-1.523	0.04444
ENSG00000166974	MAPRE2	61.117	1.419	0.04444
ENSG00000106829	TLE4	128.823	-1.231	0.04563
ENSG00000197157	SND1	237.586	1.164	0.04605
ENSG00000166750	SLFN5	475.988	-1.812	0.04620
ENSG00000177283	FZD8	25.165	-4.455	0.04620
ENSG00000068383	INPP5A	74.639	1.871	0.04659
ENSG00000150756	ATPSCKMT	5.648	4.514	0.04693
ENSG00000174059	CD34	6.183	-3.346	0.04693
ENSG00000102554	KLF5	6.745	-3.806	0.04783
ENSG00000100731	PCNX1	86.247	-1.232	0.04891
ENSG00000157106	SMG1	31.902	-1.615	0.04891
ENSG00000102119	EMD	161.099	1.140	0.04904
ENSG00000148429	USP6NL	14.401	-2.312	0.04970
ENSG00000163249	CCNYL1	54.206	-1.558	0.04970

ENSG00000197442	MAP3K5	101.799	-1.474	0.04970

Table 7.13.4 Lists of distinct significantly upregulated genes from cfDNA of poly (I:C)-stimulated iHBECs vs. elution buffer group compared to cfDNA of CSE+poly (I:C)-stimulated iHBECs vs. elution buffer group

Distinct significantly upregulated genes from cfDNA of poly (I:C) vs. elution buffer group	Distinct significantly upregulated genes from cfDNA of CSE+poly (I:C) vs. elution buffer group
CFH	SLC38A5
KMT2E	ERP44
CLCN6	DICER1
BOD1L1	BET1
SCML1	CSRNP2
LIMA1	ARHGEF2
GPBP1	FYTTD1
JMJD6	KLK10
PPP1R15A	SAT1
P2RX7	GPR84
PRKY	LYSMD2
SQLE	ZNF710
TNFRSF10A	DYNLT1
AVL9	SCLT1
ADAP1	PARP8
CLIP2	TRIM36
VEGFA	LSS
BCL6	MT2P1
PLA2G4A	AIM2
DUSP1	ATXN7
RBBP6	GEM
RUNX2	VPS37C
LRRFIP1	AFF1
PTGER2	MFSD4B
PANK2	PLK3
ASPHD2	FOXL1
RFTN1	TGIF1
DOCK10	ERICH3
SDCBP	GPBAR1

CLSTN3	GJC1
PHLDA1	TMEM50A
RAB20	HLA-DRB1
ARHGAP17	C17orf67
RGL1	PLXNA2
VPS54	GTPBP2
LRIG1	TRABD2A
LYAR	STK10
FEM1C	PAX5
RSPO3	ADD3
ASB6	SLC16A4
AUTS2	MT1A
SPATA2	COX17
AGPAT3	C1GALT1C1
MGAT4B	BDNF
REL	HOXB2
NUAK2	ODF3B
TIPARP	OPA3
CCNL1	
RBM47	
PRKCD	
SFMBT1	
RNF168	
DUSP7	
CASP3	
ABCA1	
ANPEP	
NEMP1	
ZNF146	
ZBTB43	
NPAS2	
KCNS3	
TRIM8	

ZBTB21	
RGMB	
MCTP1	
DRAP1	
FOXC2	
SMCR8	
SP140L	
RTN4RL2	
STRN3	
HNRNPAB	
MAFK	
MT-ND1	
MT-RNR2	
S1PR3	
RNU6ATAC	
MTATP6P1	
ELOVL7	
LAG3	
NAV3	
CCL20	
IL18BP	
RNF145	
C3orf38	
ACSL5	
ZFYVE26	
MYBL1	
MT1M	
BTN3A1	
MOV10	
EIF5B	
PARP10	
FBXO6	
FRMD3	

EDEM3	
IRF2	
LARP7	
MIIP	
STAT2	
SLC1A3	
FAM126B	
AP5B1	
RBM25	
CYLD	
KAZN	
FGF5	
SAMD4A	
GCNT1	
IFI16	
SLC25A30	
MSMO1	
SH3PXD2B	
CD83	
CD164	
WASHC2A	
IGF2R	
DDX39A	
ARID1A	
IDI1	
SERPINB2	
ERN1	
LARP4	
PDZD2	
TRAPPC3L	
MAP3K8	
FMR1	
CASP10	

ELF1 SQOR CCNYL1 CEP350 CYTH1 FRMD4A CLIC4 MFHAS1 EDN1 LRCH1	

Table 7.13.5 Lists of distinct significantly downregulated genes from cfDNA of poly (I:C)-stimulated iHBECs vs. elution buffer group compared to cfDNA of CSE+poly (I:C)-stimulated iHBECs vs. elution buffer group

Distinct significantly downregulated genes from cfDNA of poly (I:C) vs. elution buffer group	Distinct significantly downregulated genes from cfDNA of CSE+poly (I:C) vs. elution buffer group
KLHL13	SARS1
PDK2	CSNK2A2
DNASE1L1	FRY
GLT8D1	CEMIP
CC2D2A	PPP3CB
HEBP2	SMAD5
EYA2	PPL
EML1	ABCC4
TIMM21	BFSP1
SNRPA	RBMX2
PIAS2	POLR1E
PPP2R5C	ANP32A
DELE1	SELENBP1
ULK2	CREB3L4
MGST2	ETNK2
PIR	CHCHD6
KIF9	UBXN1
BLVRB	ERMAP
CRAT	ALDH7A1
MPG	KATNAL2
RBL2	TTC39C
BRF2	ZNF16
ECH1	TNFRSF10D
TNNT1	MRPL48
RUNDC3B	MAMSTR
DHX40	FLRT2
CEP126	DOK6
ACSS3	SELENOH
ASF1A	LBH

DBN1	AK5
LANCL1	GAMT
GOT1	TKT
GLT8D2	AHCY
PLA2G12A	BAIAP2L1
TMTC4	CASTOR2
SMO	CEP57
FGF13	OLA1
PHF10	EIF3D
HNRNPA1	SLC1A5
SCN7A	RPL3
KYAT3	AK1
KIF11	NAP1L3
TCF25	FAH
NPEPPS	VPS26B
SCRN2	STMN1
ABCA8	LMOD1
TMEM91	LETMD1
FAHD2B	
DENND2A	
DOCK11	
DOCK1	
C16orf74	
TOMM70	
PTDSS1	
PIERCE1	
PWWP3A	
FDXR	
NFIA	
DNAI3	
PTPN13	
KLHDC2	
RPUSD4	

SPACA9	
POLL	
MFF	
MRPL1	
UBE2E3	
FAXDC2	
SETMAR	
INSR	
OXTR	
CHRM2	
MTA1	
NIPSNAP1	
SPIN2B	
TMEM120A	
ADA	
TMEM26	
ZNF667	
HIBCH	
HMGN1	
ETFRF1	
CYS1	
PHB2	
NATD1	
CMBL	
NPM1	
AGBL5	
PABPC4	
SLC25A6	
IFT80	
LXN	
RPL5	
VAMP4	
RGS10	

LRPPRC FEZ1 RPLP0 CAT MAPRE2 TWF2 SNAI2 PRKDC DPH5 CDKN1C	

Chapter 8. References

8.1 References

1. Reddel, H.K., et al., *A summary of the new GINA strategy: a roadmap to asthma control.* European Respiratory Journal, 2015. **46**(3): p. 622-639.
2. Mims, J.W., *Asthma: definitions and pathophysiology.* Int Forum Allergy Rhinol, 2015. **5 Suppl 1**: p. S2-6.
3. Calhoun, W.J. and G.L. Chupp, *The new era of add-on asthma treatments: where do we stand?* Allergy, Asthma & Clinical Immunology, 2022. **18**(1): p. 42.
4. Dharmage, S.C., J.L. Perret, and A. Custovic, *Epidemiology of asthma in children and adults.* Frontiers in pediatrics, 2019. **7**: p. 246.
5. Stern, J., J. Pier, and A.A. Litonjua. *Asthma epidemiology and risk factors*. in *Seminars in immunopathology*. 2020. Springer.
6. World Health Organisation. *Asthma Key Facts*. 2021, May 3; Available from: https://www.who.int/news-room/fact-sheets/detail/asthma.
7. Masoli, M., et al., *The global burden of asthma: executive summary of the GINA Dissemination Committee report.* Allergy, 2004. **59**(5): p. 469-478.
8. National Institute for Health and Care Excellence. *What is the prevalence of asthma?* 2021, May; Available from: https://cks.nice.org.uk/topics/asthma/background-information/prevalence/#:~:text=In%20the%20UK%2C%20over%208,people%20are%20receiving%20asthma%20treatment.
9. Mukherjee, M., et al., *The epidemiology, healthcare and societal burden and costs of asthma in the UK and its member nations: analyses of standalone and linked national databases.* BMC medicine, 2016. **14**(1): p. 1-15.
10. Braman, S.S., *The global burden of asthma.* Chest, 2006. **130**(1 Suppl): p. 4s-12s.
11. Bahadori, K., et al., *Economic burden of asthma: a systematic review.* BMC pulmonary medicine, 2009. **9**: p. 1-16.
12. Medic Alert. *Understanding asthma in the UK*. 2021, July 21; Available from: https://www.medicalert.org.uk/news/2021/07/21/understanding-asthma-in-the-uk?gclid=EAIaIQobChMI3LrVucCI9wIVj7rtCh1FBA9XEAAYAyAAEgJFZvD_BwE.
13. Mapp, C.E., *Genetics and the occupational environment.* Current opinion in allergy and clinical immunology, 2005. **5**(2): p. 113-118.
14. Mukherjee, A.B. and Z. Zhang, *Allergic asthma: influence of genetic and environmental factors.* Journal of Biological Chemistry, 2011. **286**(38): p. 32883-32889.
15. Momtazmanesh, S., et al., *Global burden of chronic respiratory diseases and risk factors, 1990–2019: an update from the Global Burden of Disease Study 2019.* EClinicalMedicine, 2023. **59**.
16. Torén, K. and B.A. Hermansson, *Incidence rate of adult-onset asthma in relation to age, sex, atopy and smoking: a Swedish population-based study of 15813 adults.* Int J Tuberc Lung Dis, 1999. **3**(3): p. 192-7.
17. Piipari, R., et al., *Smoking and asthma in adults.* Eur Respir J, 2004. **24**(5): p. 734-9.
18. Shaler, C.R., et al., *Continuous and discontinuous cigarette smoke exposure differentially affects protective Th1 immunity against pulmonary tuberculosis.* PLoS One, 2013. **8**(3): p. e59185.
19. Johnston, S.L., et al., *Community study of role of viral infections in exacerbations of asthma in 9-11 year old children.* Bmj, 1995. **310**(6989): p. 1225-9.
20. Nicholson, K.G., J. Kent, and D.C. Ireland, *Respiratory viruses and exacerbations of asthma in adults.* Bmj, 1993. **307**(6910): p. 982-6.

21. Willemsen, G., et al., *Heritability of self-reported asthma and allergy: a study in adult Dutch twins, siblings and parents.* Twin Res Hum Genet, 2008. **11**(2): p. 132-42.
22. Ober, C. and S. Hoffjan, *Asthma genetics 2006: the long and winding road to gene discovery.* Genes & Immunity, 2006. **7**(2): p. 95-100.
23. Burke, W., et al., *Family history as a predictor of asthma risk.* American journal of preventive medicine, 2003. **24**(2): p. 160-169.
24. Heart, N., Lung, and B.I.N.A.E.P.E.P.o.t.M.o. Asthma, *Guidelines for the diagnosis and management of asthma*. 1991: National Asthma Education Program, Office of Prevention, Education, and ….
25. Brigham, E.P. and N.E. West, *Diagnosis of asthma: diagnostic testing.* Int Forum Allergy Rhinol, 2015. **5 Suppl 1**: p. S27-30.
26. Brigham, E.P. and N.E. West. *Diagnosis of asthma: diagnostic testing*. in *International forum of allergy & rhinology*. 2015. Wiley Online Library.
27. UK, C.E., *Asthma: diagnosis and monitoring of asthma in adults, children and young people.* 2017.
28. Kwah, J.H. and A.T. Peters, *Asthma in adults: Principles of treatment.* Allergy Asthma Proc, 2019. **40**(6): p. 396-402.
29. WebMD. *Asthma treatment: Steroids and other anti-inflammatory drugs*. 2021, August 25; Available from: https://www.webmd.com/asthma/guide/asthma-control-with-anti-inflammatory-drugs.
30. Barnes, P.J., *Inhaled corticosteroids.* Pharmaceuticals, 2010. **3**(3): p. 514-540.
31. Juniper, E.F., et al., *Long-term effects of budesonide on airway responsiveness and clinical asthma severity in inhaled steroid-dependent asthmatics.* Eur Respir J, 1990. **3**(10): p. 1122-7.
32. Fahy, J.V., *Type 2 inflammation in asthma—present in most, absent in many.* Nature Reviews Immunology, 2015. **15**(1): p. 57-65.
33. Barnes, P.J., *Corticosteroid resistance in patients with asthma and chronic obstructive pulmonary disease.* Journal of Allergy and Clinical Immunology, 2013. **131**(3): p. 636-645.
34. Kelly, M.M., et al., *Corticosteroid-induced gene expression in allergen-challenged asthmatic subjects taking inhaled budesonide.* Br J Pharmacol, 2012. **165**(6): p. 1737-1747.
35. Barnes, P.J., *How corticosteroids control inflammation: quintiles prize lecture 2005.* British journal of pharmacology, 2006. **148**(3): p. 245-254.
36. Trevor, J. and J. Deshane, *Refractory asthma: mechanisms, targets, and therapy.* Allergy, 2014. **69**(7): p. 817-827.
37. Adams, N.P., et al., *Fluticasone at different doses for chronic asthma in adults and children.* Cochrane Database of Systematic Reviews, 2005(3).
38. Adams, N.P., J.C. Bestall, and P. Jones, *Budesonide at different doses for chronic asthma.* Cochrane Database of Systematic Reviews, 2000(2).
39. Wen, F.-Q., et al., *TH2 Cytokine-enhanced and TGF-β-enhanced vascular endothelial growth factor production by cultured human airway smooth muscle cells is attenuated by IFN-γ and corticosteroids.* Journal of allergy and clinical immunology, 2003. **111**(6): p. 1307-1318.
40. Bleecker, E.R., et al., *Systematic literature review of systemic corticosteroid use for asthma management.* American journal of respiratory and critical care medicine, 2020. **201**(3): p. 276-293.
41. Rowe, B.H., et al., *Early emergency department treatment of acute asthma with systemic corticosteroids.* Cochrane Database of Systematic Reviews, 2001(1).

42. Barnes, P.J., *Current issues for establishing inhaled corticosteroids as the antiinflammatory agents of choice in asthma.* Journal of allergy and clinical immunology, 1998. **101**(4): p. S427-S433.
43. Tamada, T. and M. Ichinose, *Leukotriene Receptor Antagonists and Antiallergy Drugs.* Handb Exp Pharmacol, 2017. **237**: p. 153-169.
44. Rand, T.H., et al., *Nedocromil sodium and cromolyn (sodium cromoglycate) selectively inhibit antibody-dependent granulocyte-mediated cytotoxicity.* Int Arch Allergy Appl Immunol, 1988. **87**(2): p. 151-8.
45. Murphy, S. and H.W. Kelly, *Cromolyn sodium: a review of mechanisms and clinical use in asthma.* Drug Intell Clin Pharm, 1987. **21**(1 Pt 1): p. 22-35.
46. Brogden, R.N. and E.M. Sorkin, *Nedocromil sodium. An updated review of its pharmacological properties and therapeutic efficacy in asthma.* Drugs, 1993. **45**(5): p. 693-715.
47. Cazzola, M., et al., *Pharmacology and therapeutics of bronchodilators.* Pharmacol Rev, 2012. **64**(3): p. 450-504.
48. Albertson, T.E., M.E. Sutter, and A.L. Chan, *The acute management of asthma.* Clinical reviews in allergy & immunology, 2015. **48**(1): p. 114-125.
49. *Expert Panel Report 3 (EPR-3): Guidelines for the Diagnosis and Management of Asthma-Summary Report 2007.* J Allergy Clin Immunol, 2007. **120**(5 Suppl): p. S94-138.
50. Almadhoun, K. and S. Sharma, *Bronchodilators*, in *StatPearls [Internet]*. 2021, StatPearls Publishing.
51. Guyer, A.C. and A.A. Long, *Long-acting anticholinergics in the treatment of asthma.* Current opinion in allergy and clinical immunology, 2013. **13**(4): p. 392-398.
52. Mazzarella, G., et al., *Th1/Th2 lymphocyte polarization in asthma.* Allergy, 2000. **55**: p. 6-9.
53. Jeffery, P., et al., *Bronchial biopsies in asthma.* Am Rev Respir Dis, 1989. **140**: p. 1745-1753.
54. Agache, I. and C.A. Akdis, *Endotypes of allergic diseases and asthma: an important step in building blocks for the future of precision medicine.* Allergology international, 2016. **65**(3): p. 243-252.
55. Muraro, A., et al., *Precision medicine in allergic disease—food allergy, drug allergy, and anaphylaxis—PRACTALL document of the European Academy of Allergy and Clinical Immunology and the American Academy of Allergy, Asthma and Immunology.* Allergy, 2017. **72**(7): p. 1006-1021.
56. Lockey, R.F., *Asthma phenotypes: an approach to the diagnosis and treatment of asthma.* The Journal of Allergy and Clinical Immunology: In Practice, 2014. **2**(6): p. 682-685.
57. Lambrecht, B.N. and H. Hammad, *The immunology of asthma.* Nature immunology, 2015. **16**(1): p. 45-56.
58. Chung, K. and P. Barnes, *Cytokines in asthma.* Thorax, 1999. **54**(9): p. 825-857.
59. Lukacs, N.W., *Role of chemokines in the pathogenesis of asthma.* Nature Reviews Immunology, 2001. **1**(2): p. 108-116.
60. Cowan, D.C., et al., *Effects of steroid therapy on inflammatory cell subtypes in asthma.* Thorax, 2010. **65**(5): p. 384-390.
61. Barnes, P.J., *Therapeutic approaches to asthma–chronic obstructive pulmonary disease overlap syndromes.* Journal of Allergy and Clinical Immunology, 2015. **136**(3): p. 531-545.

62. Wenzel, S.E., et al., *Evidence that severe asthma can be divided pathologically into two inflammatory subtypes with distinct physiologic and clinical characteristics.* American journal of respiratory and critical care medicine, 1999. **160**(3): p. 1001-1008.
63. Tan, H.-T.T., K. Sugita, and C.A. Akdis, *Novel biologicals for the treatment of allergic diseases and asthma.* Current allergy and asthma reports, 2016. **16**: p. 1-14.
64. Schatz, M. and L. Rosenwasser, *The allergic asthma phenotype.* The Journal of Allergy and Clinical Immunology: In Practice, 2014. **2**(6): p. 645-648.
65. Caminati, M., et al., *Type 2 immunity in asthma.* World Allergy Organization Journal, 2018. **11**(1): p. 1-10.
66. Boonpiyathad, T., et al. *Immunologic mechanisms in asthma*. in *Seminars in immunology*. 2019. Elsevier.
67. Galli, S.J., M. Tsai, and A.M. Piliponsky, *The development of allergic inflammation.* Nature, 2008. **454**(7203): p. 445-454.
68. Valero, A., et al., *Allergic respiratory disease: different allergens, different symptoms.* Allergy, 2017. **72**(9): p. 1306-1316.
69. Ying, S., et al., *Thymic stromal lymphopoietin expression is increased in asthmatic airways and correlates with expression of Th2-attracting chemokines and disease severity.* The Journal of Immunology, 2005. **174**(12): p. 8183-8190.
70. Graziano, F.M., E.B. Cook, and J.L. Stahl. *Cytokines, chemokines, RANTES, and eotaxin*. in *Allergy and Asthma Proceedings*. 1999. OceanSide Publications.
71. Terl, M., et al., *Asthma management: a new phenotype-based approach using presence of eosinophilia and allergy.* Allergy, 2017. **72**(9): p. 1279-1287.
72. Amin, K., *The role of mast cells in allergic inflammation.* Respiratory medicine, 2012. **106**(1): p. 9-14.
73. Matucci, A., et al., *Is IgE or eosinophils the key player in allergic asthma pathogenesis? Are we asking the right question?* Respiratory research, 2018. **19**(1): p. 1-10.
74. Urry, Z., E. Xystrakis, and C.M. Hawrylowicz, *Interleukin-10-secreting regulatory T cells in allergy and asthma.* Current Allergy and Asthma Reports, 2006. **6**(5): p. 363-371.
75. Johnson, J.R., et al., *Continuous exposure to house dust mite elicits chronic airway inflammation and structural remodeling.* American journal of respiratory and critical care medicine, 2004. **169**(3): p. 378-385.
76. Robinson, D., et al., *Revisiting T ype 2-high and T ype 2-low airway inflammation in asthma: current knowledge and therapeutic implications.* Clinical & Experimental Allergy, 2017. **47**(2): p. 161-175.
77. Peters, S.P., *Asthma phenotypes: nonallergic (intrinsic) asthma.* The Journal of Allergy and Clinical Immunology: In Practice, 2014. **2**(6): p. 650-652.
78. Hammad, H. and B.N. Lambrecht, *The basic immunology of asthma.* Cell, 2021. **184**(6): p. 1469-1485.
79. Baggiolini, M., B. Dewald, and B. Moser, *lnterleukin-8 and related chemotactic cytokines—CXC and CC chemokines.* Advances in immunology, 1993. **55**: p. 97-179.
80. Poynter, M.E. and C.G. Irvin, *Interleukin-6 as a biomarker for asthma: hype or is there something else?* 2016, Eur Respiratory Soc. p. 979-981.
81. Al-Ramli, W., et al., *TH17-associated cytokines (IL-17A and IL-17F) in severe asthma.* Journal of Allergy and Clinical Immunology, 2009. **123**(5): p. 1185-1187.
82. Desai, M. and J. Oppenheimer, *Elucidating asthma phenotypes and endotypes: progress towards personalized medicine.* Annals of Allergy, Asthma & Immunology, 2016. **116**(5): p. 394-401.
83. Chiu, C.-J. and M.-T. Huang, *Asthma in the precision medicine era: biologics and probiotics.* International Journal of Molecular Sciences, 2021. **22**(9): p. 4528.

84. Bousquet, J., et al., *Eosinophilic inflammation in asthma.* New England Journal of Medicine, 1990. **323**(15): p. 1033-1039.
85. Sanderson, C.J., *Interleukin-5, eosinophils, and disease.* 1992.
86. Garcia, G., et al., *Anti-interleukin-5 therapy in severe asthma.* European Respiratory Review, 2013. **22**(129): p. 251-257.
87. Liu, A.H., et al., *Advances in asthma 2015: Across the lifespan.* Journal of Allergy and Clinical Immunology, 2016. **138**(2): p. 397-404.
88. Laviolette, M., et al., *Effects of benralizumab on airway eosinophils in asthmatic patients with sputum eosinophilia.* Journal of allergy and clinical immunology, 2013. **132**(5): p. 1086-1096. e5.
89. Licari, A., et al., *Targeted therapy for severe asthma in children and adolescents: current and future perspectives.* Pediatric Drugs, 2019. **21**(4): p. 215-237.
90. Stokes, J.R. and T.B. Casale, *Characterization of asthma endotypes: implications for therapy.* Annals of Allergy, Asthma & Immunology, 2016. **117**(2): p. 121-125.
91. Hanania, N.A., et al., *Lebrikizumab in moderate-to-severe asthma: pooled data from two randomised placebo-controlled studies.* Thorax, 2015. **70**(8): p. 748-756.
92. Harb, H. and T.A. Chatila, *Mechanisms of dupilumab.* Clinical & Experimental Allergy, 2020. **50**(1): p. 5-14.
93. Pfeffer, P., et al., *P18 Real-world experience of dupilumab for the treatment of severe asthma in the United Kingdom: a retrospective study*. 2024, BMJ Publishing Group Ltd.
94. Ballantyne, S.J., et al., *Blocking IL-25 prevents airway hyperresponsiveness in allergic asthma.* Journal of Allergy and Clinical Immunology, 2007. **120**(6): p. 1324-1331.
95. Papathanassiou, E., S. Loukides, and P. Bakakos, *Severe asthma: anti-IgE or anti-IL-5?* European Clinical Respiratory Journal, 2016. **3**(1): p. 31813.
96. Gauvreau, G.M., et al., *Targeting membrane-expressed IgE B cell receptor with an antibody to the M1 prime epitope reduces IgE production.* Science Translational Medicine, 2014. **6**(243): p. 243ra85-243ra85.
97. Frey, A., et al., *More than just a barrier: the immune functions of the airway epithelium in asthma pathogenesis.* Frontiers in immunology, 2020. **11**: p. 761.
98. Lambrecht, B.N. and H. Hammad, *The airway epithelium in asthma.* Nature medicine, 2012. **18**(5): p. 684-692.
99. Hiemstra, P.S., P.B. McCray Jr, and R. Bals, *The innate immune function of airway epithelial cells in inflammatory lung disease.* European respiratory journal, 2015. **45**(4): p. 1150-1162.
100. Vareille, M., et al., *The airway epithelium: soldier in the fight against respiratory viruses.* Clinical microbiology reviews, 2011. **24**(1): p. 210-229.
101. Aghapour, M., et al., *Airway epithelial barrier dysfunction in chronic obstructive pulmonary disease: role of cigarette smoke exposure.* American journal of respiratory cell and molecular biology, 2018. **58**(2): p. 157-169.
102. Bonser, L.R. and D.J. Erle, *The airway epithelium in asthma.* Advances in immunology, 2019. **142**: p. 1-34.
103. Allakhverdi, Z., et al., *Thymic stromal lymphopoietin is released by human epithelial cells in response to microbes, trauma, or inflammation and potently activates mast cells.* The Journal of experimental medicine, 2007. **204**(2): p. 253-258.
104. Kim, B.S., et al., *TSLP elicits IL-33–independent innate lymphoid cell responses to promote skin inflammation.* Science translational medicine, 2013. **5**(170): p. 170ra16-170ra16.
105. Soumelis, V., et al., *Human epithelial cells trigger dendritic cell–mediated allergic inflammation by producing TSLP.* Nature immunology, 2002. **3**(7): p. 673-680.

106. Gerbe, F., et al., *Intestinal epithelial tuft cells initiate type 2 mucosal immunity to helminth parasites.* Nature, 2016. **529**(7585): p. 226-230.
107. Cheng, D., et al., *Epithelial interleukin-25 is a key mediator in Th2-high, corticosteroid-responsive asthma.* American journal of respiratory and critical care medicine, 2014. **190**(6): p. 639-648.
108. Corrigan, C.J., et al., *T-helper cell type 2 (Th2) memory T cell-potentiating cytokine IL-25 has the potential to promote angiogenesis in asthma.* Proceedings of the National Academy of Sciences, 2011. **108**(4): p. 1579-1584.
109. Lefrançais, E., et al., *Central domain of IL-33 is cleaved by mast cell proteases for potent activation of group-2 innate lymphoid cells.* Proceedings of the National Academy of Sciences, 2014. **111**(43): p. 15502-15507.
110. Kearley, J., et al., *Resolution of allergic inflammation and airway hyperreactivity is dependent upon disruption of the T1/ST2–IL-33 pathway.* American journal of respiratory and critical care medicine, 2009. **179**(9): p. 772-781.
111. Sy, C.B. and M.C. Siracusa, *The therapeutic potential of targeting cytokine alarmins to treat allergic airway inflammation.* Frontiers in Physiology, 2016. **7**: p. 214.
112. Glaser, L., et al., *Airway epithelial derived cytokines and chemokines and their role in the immune response to respiratory syncytial virus infection.* Pathogens, 2019. **8**(3): p. 106.
113. Zuyderduyn, S., et al., *Treating asthma means treating airway smooth muscle cells.* European Respiratory Journal, 2008. **32**(2): p. 265-274.
114. Camoretti-Mercado, B. and R.F. Lockey, *Airway smooth muscle pathophysiology in asthma.* Journal of Allergy and Clinical Immunology, 2021. **147**(6): p. 1983-1995.
115. John, A.E., et al., *Human airway smooth muscle cells from asthmatic individuals have CXCL8 hypersecretion due to increased NF-κB p65, C/EBPβ, and RNA polymerase II binding to the CXCL8 promoter.* The Journal of Immunology, 2009. **183**(7): p. 4682-4692.
116. Préfontaine, D., et al., *Increased expression of IL-33 in severe asthma: evidence of expression by airway smooth muscle cells.* The Journal of Immunology, 2009. **183**(8): p. 5094-5103.
117. Moore, P.E., et al., *IL-13 and IL-4 cause eotaxin release in human airway smooth muscle cells: a role for ERK.* American Journal of Physiology-Lung Cellular and Molecular Physiology, 2002. **282**(4): p. L847-L853.
118. Joubert, P. and Q. Hamid, *Role of airway smooth muscle in airway remodeling.* Journal of allergy and clinical immunology, 2005. **116**(3): p. 713-716.
119. Tang, D.D., *Critical role of actin-associated proteins in smooth muscle contraction, cell proliferation, airway hyperresponsiveness and airway remodeling.* Respiratory research, 2015. **16**: p. 1-14.
120. Martin, J., A. Duguet, and D. Eidelman, *The contribution of airway smooth muscle to airway narrowing and airway hyperresponsiveness in disease.* European Respiratory Journal, 2000. **16**(2): p. 349-354.
121. Taylor-Clark, T. and B.J. Undem, *Transduction mechanisms in airway sensory nerves.* Journal of applied physiology, 2006. **101**(3): p. 950-959.
122. Sharopov, B.R., et al., *Contribution of transient receptor potential vanilloid 1 (TRPV1) channel to cholinergic contraction of rat bladder smooth muscle.* The Journal of Physiology, 2024. **602**(15): p. 3693-3713.
123. Phan, T.X., et al., *Trpv1 expressed throughout the arterial circulation enables inflammatory vasoconstriction.* The Journal of physiology, 2020. **598**: p. 5639-5659.
124. Wettschureck, N. and S. Offermanns, *Rho/Rho-kinase mediated signaling in physiology and pathophysiology.* Journal of molecular medicine, 2002. **80**: p. 629-638.

125. Doeing, D.C. and J. Solway, *Airway smooth muscle in the pathophysiology and treatment of asthma.* Journal of applied physiology, 2013. **114**(7): p. 834-843.
126. Vignola, A.M., et al., *Airway remodeling in asthma.* Chest, 2003. **123**(3): p. 417S-422S.
127. Munakata, M., *Airway remodeling and airway smooth muscle in asthma.* Allergology International, 2006. **55**(3): p. 235-243.
128. Howarth, P.H., et al., *Synthetic responses in airway smooth muscle.* Journal of allergy and clinical immunology, 2004. **114**(2): p. S32-S50.
129. Burgess, J.K., et al., *Expression of connective tissue growth factor in asthmatic airway smooth muscle cells.* American journal of respiratory and critical care medicine, 2003. **167**(1): p. 71-77.
130. Johnson, P.R., et al., *Extracellular matrix proteins modulate asthmatic airway smooth muscle cell proliferation via an autocrine mechanism.* Journal of Allergy and Clinical Immunology, 2004. **113**(4): p. 690-696.
131. Abohalaka, R., *Bronchial epithelial and airway smooth muscle cell interactions in health and disease.* Heliyon, 2023.
132. Zhou, J., et al., *Local small airway epithelial injury induces global smooth muscle contraction and airway constriction.* Journal of Applied Physiology, 2012. **112**(4): p. 627-637.
133. Malavia, N.K., et al., *Airway epithelium stimulates smooth muscle proliferation.* American journal of respiratory cell and molecular biology, 2009. **41**(3): p. 297-304.
134. Allard, B., et al., *Asthmatic bronchial smooth muscle increases CCL5-dependent monocyte migration in response to rhinovirus-infected epithelium.* Frontiers in immunology, 2020. **10**: p. 2998.
135. Deacon, K. and A.J. Knox, *Human airway smooth muscle cells secrete amphiregulin via bradykinin/COX-2/PGE2, inducing COX-2, CXCL8, and VEGF expression in airway epithelial cells.* American Journal of Physiology-Lung Cellular and Molecular Physiology, 2015. **309**(3): p. L237-L249.
136. Chalmers, G.W., et al., *Smoking and airway inflammation in patients with mild asthma.* Chest, 2001. **120**(6): p. 1917-1922.
137. Polosa, R. and N.C. Thomson, *Smoking and asthma: dangerous liaisons.* European respiratory journal, 2013. **41**(3): p. 716-726.
138. Broekema, M., et al., *Airway epithelial changes in smokers but not in ex-smokers with asthma.* American journal of respiratory and critical care medicine, 2009. **180**(12): p. 1170-1178.
139. van der Vaart, H., et al., *Acute effects of cigarette smoke on inflammation and oxidative stress: a review.* Thorax, 2004. **59**(8): p. 713-721.
140. Lugade, A.A., et al., *Cigarette smoke exposure exacerbates lung inflammation and compromises immunity to bacterial infection.* The Journal of Immunology, 2014. **192**(11): p. 5226-5235.
141. Feng, Y., et al., *Exposure to cigarette smoke inhibits the pulmonary T-cell response to influenza virus and Mycobacterium tuberculosis.* Infection and immunity, 2011. **79**(1): p. 229-237.
142. Chen, L., et al., *Effects of cigarette smoke extract on human airway smooth muscle cells in COPD.* European Respiratory Journal, 2014. **44**(3): p. 634-646.
143. Tamimi, A., D. Serdarevic, and N.A. Hanania, *The effects of cigarette smoke on airway inflammation in asthma and COPD: therapeutic implications.* Respiratory medicine, 2012. **106**(3): p. 319-328.
144. Thomson, N., R. Chaudhuri, and E. Livingston, *Asthma and cigarette smoking.* European respiratory journal, 2004. **24**(5): p. 822-833.

145. Cao, W., et al., *Effect of cigarette smoke exposure on the expression of CCR7 and levels of Th1/Th2 cytokines in asthmatic rats.* Zhonghua yi xue za zhi, 2018. **98**(28): p. 2264-2268.
146. Kühn, R., K. Rajewsky, and W. Müller, *Generation and analysis of interleukin-4 deficient mice.* Science, 1991. **254**(5032): p. 707-710.
147. McCrea, K.A., et al., *Altered cytokine regulation in the lungs of cigarette smokers.* American journal of respiratory and critical care medicine, 1994. **150**(3): p. 696-703.
148. Drazen, J.M., J.P. Arm, and K.F. Austen, *Sorting out the cytokines of asthma.* The Journal of experimental medicine, 1996. **183**(1): p. 1-5.
149. Zhao, J., et al., *Immunomodulatory effects of cigarette smoke condensate in mouse macrophage cell line.* International Journal of Immunopathology and Pharmacology, 2017. **30**(3): p. 315-321.
150. Nakamura, Y., et al., *Cigarette smoke extract induces thymic stromal lymphopoietin expression, leading to T(H)2-type immune responses and airway inflammation.* J Allergy Clin Immunol, 2008. **122**(6): p. 1208-14.
151. Lloyd, C.M. and S. Saglani, *Epithelial cytokines and pulmonary allergic inflammation.* Curr Opin Immunol, 2015. **34**: p. 52-8.
152. Liu, Y.J., et al., *TSLP: an epithelial cell cytokine that regulates T cell differentiation by conditioning dendritic cell maturation.* Annu Rev Immunol, 2007. **25**: p. 193-219.
153. Alahmari, M., *Effect of cigarette smoke extract on inflammatory cytokine production and corticosteroid insensitivity in human airway smooth muscle cells*. 2022, University of Nottingham.
154. Botelho, F.M., et al., *Cigarette smoke differentially affects eosinophilia and remodeling in a model of house dust mite asthma.* American journal of respiratory cell and molecular biology, 2011. **45**(4): p. 753-760.
155. Thatcher, T.H., et al., *High-dose but not low-dose mainstream cigarette smoke suppresses allergic airway inflammation by inhibiting T cell function.* American Journal of Physiology-Lung Cellular and Molecular Physiology, 2008. **295**(3): p. L412-L421.
156. Siew, L., et al., *Cigarette smoking increases bronchial mucosal IL-17A expression in asthmatics, which acts in concert with environmental aeroallergens to engender neutrophilic inflammation.* Clinical & Experimental Allergy, 2017. **47**(6): p. 740-750.
157. Adesina, A.M., et al., *Bronchiolar inflammation and fibrosis associated with smoking.* Am Rev Respir Dis, 1991. **143**: p. 144-149.
158. Bosken, C.H., et al., *Characterization of the inflammatory reaction in the peripheral airways of cigarette smokers using immunocytochemistry.* American Journal of Respiratory and Critical Care Medicine, 1992. **145**(4): p. 911-917.
159. Mio, T., et al., *Cigarette smoke induces interleukin-8 release from human bronchial epithelial cells.* American journal of respiratory and critical care medicine, 1997. **155**(5): p. 1770-1776.
160. Zhao, Y., et al., *NF-κB-mediated inflammation leading to EMT via miR-200c is involved in cell transformation induced by cigarette smoke extract.* Toxicological Sciences, 2013. **135**(2): p. 265-276.
161. Ermert, L., C. Dierkes, and M. Ermert, *Immunohistochemical expression of cyclooxygenase isoenzymes and downstream enzymes in human lung tumors.* Clinical Cancer Research, 2003. **9**(5): p. 1604-1610.
162. Hawkey, C., *COX-1 and COX-2 inhibitors.* Best Practice & Research Clinical Gastroenterology, 2001. **15**(5): p. 801-820.
163. Smith, W.L., D.L. DeWitt, and R.M. Garavito, *Cyclooxygenases: structural, cellular, and molecular biology.* Annual review of biochemistry, 2000. **69**(1): p. 145-182.

164. Sheng, H., et al., *Induction of Cyclooxygenase-2 by Activated Ha-rasOncogene in Rat-1 Fibroblasts and the Role of Mitogen-activated Protein Kinase Pathway.* Journal of Biological Chemistry, 1998. **273**(34): p. 22120-22127.
165. Murakami, M., et al., *Cellular prostaglandin E2 production by membrane-bound prostaglandin E synthase-2 via both cyclooxygenases-1 and-2.* Journal of Biological Chemistry, 2003. **278**(39): p. 37937-37947.
166. Anto, R.J., et al., *Cigarette smoke condensate activates nuclear transcription factor-κB through phosphorylation and degradation of IκBα: correlation with induction of cyclooxygenase-2.* Carcinogenesis, 2002. **23**(9): p. 1511-1518.
167. Martey, C., et al., *The aryl hydrocarbon receptor is a regulator of cigarette smoke induction of the cyclooxygenase and prostaglandin pathways in human lung fibroblasts.* American Journal of Physiology-Lung Cellular and Molecular Physiology, 2005. **289**(3): p. L391-L399.
168. Martey, C.A., et al., *Cigarette smoke induces cyclooxygenase-2 and microsomal prostaglandin E2 synthase in human lung fibroblasts: implications for lung inflammation and cancer.* American Journal of Physiology-Lung Cellular and Molecular Physiology, 2004. **287**(5): p. L981-L991.
169. Baskoro, H., et al., *Regional heterogeneity in response of airway epithelial cells to cigarette smoke.* BMC pulmonary medicine, 2018. **18**(1): p. 1-11.
170. Ding, S., et al., *Wedelolactone protects human bronchial epithelial cell injury against cigarette smoke extract-induced oxidant stress and inflammation responses through Nrf2 pathway.* International immunopharmacology, 2015. **29**(2): p. 648-655.
171. Nana-Sinkam, S.P., et al., *Prostacyclin prevents pulmonary endothelial cell apoptosis induced by cigarette smoke.* American Journal of Respiratory and Critical Care Medicine, 2007. **175**(7): p. 676-685.
172. Holt, P., et al., *The role of allergy in the development of asthma.* Nature, 1999. **402**(Suppl 6760): p. 12-17.
173. Langley, S.J., et al., *Exposure and sensitization to indoor allergens: association with lung function, bronchial reactivity, and exhaled nitric oxide measures in asthma.* Journal of allergy and clinical immunology, 2003. **112**(2): p. 362-368.
174. Cayrol, C., et al., *Environmental allergens induce allergic inflammation through proteolytic maturation of IL-33.* Nature immunology, 2018. **19**(4): p. 375-385.
175. Reithofer, M. and B. Jahn-Schmid, *Allergens with protease activity from house dust mites.* International journal of molecular sciences, 2017. **18**(7): p. 1368.
176. Thomas, W.R., *Hierarchy and molecular properties of house dust mite allergens.* Allergology International, 2015. **64**(4): p. 304-311.
177. Jacquet, A., *Innate immune responses in house dust mite allergy.* International Scholarly Research Notices, 2013. **2013**.
178. Post, S., et al., *The composition of house dust mite is critical for mucosal barrier dysfunction and allergic sensitisation.* Thorax, 2012. **67**(6): p. 488-95.
179. Hammad, H., et al., *Monocyte-derived dendritic cells induce a house dust mite-specific Th2 allergic inflammation in the lung of humanized SCID mice: involvement of CCR7.* The Journal of Immunology, 2002. **169**(3): p. 1524-1534.
180. King, C., et al., *Dust mite proteolytic allergens induce cytokine release from cultured airway epithelium.* The Journal of Immunology, 1998. **161**(7): p. 3645-3651.
181. van de Pol, M.A., et al., *Increase in allergen-specific IgE and ex vivo Th2 responses after a single bronchial challenge with house dust mite in allergic asthmatics.* Allergy, 2012. **67**(1): p. 67-73.
182. Chiappara, G., et al., *Airway remodelling in the pathogenesis of asthma.* Current opinion in allergy and clinical immunology, 2001. **1**(1): p. 85-93.

183. Mattoli, S., *Allergen-induced generation of mediators in the mucosa.* Environmental health perspectives, 2001. **109**(suppl 4): p. 553-557.
184. Park, S.-Y., et al., *House dust mite allergen Der f 2-induced phospholipase D1 activation is critical for the production of interleukin-13 through activating transcription factor-2 activation in human bronchial epithelial cells.* Journal of Biological Chemistry, 2009. **284**(30): p. 20099-20110.
185. Yasuda, Y., et al., *Group 2 Innate Lymphoid Cells and the House Dust Mite-Induced Asthma Mouse Model.* Cells, 2020. **9**(5).
186. Gerrard, J.W., et al., *Increased nonspecific bronchial reactivity in cigarette smokers with normal lung function.* American review of respiratory disease, 1980. **122**(4): p. 577-581.
187. Vrtala, S., H. Huber, and W.R. Thomas, *Recombinant house dust mite allergens.* Methods, 2014. **66**(1): p. 67-74.
188. Rusznak, C., et al., *Interaction of cigarette smoke and house dust mite allergens on inflammatory mediator release from primary cultures of human bronchial epithelial cells.* Clinical & Experimental Allergy, 2001. **31**(2): p. 226-238.
189. Lanckacker, E.A., et al., *Short cigarette smoke exposure facilitates sensitisation and asthma development in mice.* European Respiratory Journal, 2013. **41**(5): p. 1189-1199.
190. Bao, Z., et al., *Effect of PM2. 5 mediated oxidative stress on the innate immune cellular response of Der p1 treated human bronchial epithelial cells.* Eur. Rev. Med. Pharmacol. Sci, 2017. **21**: p. 2907-2912.
191. Busse, W.W., R.F. Lemanske, and J.E. Gern, *Role of viral respiratory infections in asthma and asthma exacerbations.* The Lancet, 2010. **376**(9743): p. 826-834.
192. Khetsuriani, N., et al., *Prevalence of viral respiratory tract infections in children with asthma.* Journal of Allergy and Clinical Immunology, 2007. **119**(2): p. 314-321.
193. Message, S.D., et al., *Rhinovirus-induced lower respiratory illness is increased in asthma and related to virus load and Th1/2 cytokine and IL-10 production.* Proceedings of the National Academy of Sciences, 2008. **105**(36): p. 13562-13567.
194. Jartti, T. and J.E. Gern, *Role of viral infections in the development and exacerbation of asthma in children.* Journal of allergy and clinical immunology, 2017. **140**(4): p. 895-906.
195. Johnston, S.L., et al., *The relationship between upper respiratory infections and hospital admissions for asthma: a time-trend analysis.* American journal of respiratory and critical care medicine, 1996. **154**(3): p. 654-660.
196. Mallia, P. and S.L. Johnston, *How viral infections cause exacerbation of airway diseases.* Chest, 2006. **130**(4): p. 1203-1210.
197. Zhao, J., et al., *Altered eosinophil levels as a result of viral infection in asthma exacerbation in childhood.* Pediatric allergy and immunology, 2002. **13**(1): p. 47-50.
198. Alexander-Brett, J. and M.J. Holtzman, *Virus infection of airway epithelial cells*, in *Mucosal Immunology*. 2015, Elsevier. p. 1013-1021.
199. Kawai, T. and S. Akira, *The role of pattern-recognition receptors in innate immunity: update on Toll-like receptors.* Nature immunology, 2010. **11**(5): p. 373-384.
200. Takeda, K., T. Kaisho, and S. Akira, *Toll-like receptors.* Annual review of immunology, 2003. **21**(1): p. 335-376.
201. Barton, G.M. and J.C. Kagan, *A cell biological view of Toll-like receptor function: regulation through compartmentalization.* Nature Reviews Immunology, 2009. **9**(8): p. 535-542.
202. Groskreutz, D.J., et al., *Respiratory syncytial virus induces TLR3 protein and protein kinase R, leading to increased double-stranded RNA responsiveness in airway epithelial cells.* The Journal of Immunology, 2006. **176**(3): p. 1733-1740.

203. Hewson, C.A., et al., *Toll-like receptor 3 is induced by and mediates antiviral activity against rhinovirus infection of human bronchial epithelial cells.* Journal of virology, 2005. **79**(19): p. 12273-12279.
204. G Drake, M., et al., *The therapeutic potential of Toll-like receptor 7 stimulation in asthma.* Inflammation & Allergy-Drug Targets (Formerly Current Drug Targets-Inflammation & Allergy)(Discontinued), 2012. **11**(6): p. 484-491.
205. de Marcken, M., et al., *TLR7 and TLR8 activate distinct pathways in monocytes during RNA virus infection.* Science signaling, 2019. **12**(605): p. eaaw1347.
206. Hemmi, H., et al., *A Toll-like receptor recognizes bacterial DNA.* Nature, 2000. **408**(6813): p. 740-745.
207. Blasius, A.L. and B. Beutler, *Intracellular toll-like receptors.* Immunity, 2010. **32**(3): p. 305-315.
208. Marcy, T.W. and W.W. Merrill, *Cigarette smoking and respiratory tract infection.* Clinics in chest medicine, 1987. **8**(3): p. 381-391.
209. Sopori, M., *Effects of cigarette smoke on the immune system.* Nature Reviews Immunology, 2002. **2**(5): p. 372-377.
210. Arcavi, L. and N.L. Benowitz, *Cigarette smoking and infection.* Archives of internal medicine, 2004. **164**(20): p. 2206-2216.
211. Strzelak, A., et al., *Tobacco smoke induces and alters immune responses in the lung triggering inflammation, allergy, asthma and other lung diseases: a mechanistic review.* International journal of environmental research and public health, 2018. **15**(5): p. 1033.
212. Mortaz, E., et al., *Cigarette smoke attenuates the production of cytokines by human plasmacytoid dendritic cells and enhances the release of IL-8 in response to TLR-9 stimulation.* Respiratory research, 2009. **10**: p. 1-9.
213. Eddleston, J., et al., *Cigarette smoke decreases innate responses of epithelial cells to rhinovirus infection.* American journal of respiratory cell and molecular biology, 2011. **44**(1): p. 118-126.
214. Whetstone, C.E., et al., *The role of airway epithelial cell alarmins in asthma.* Cells, 2022. **11**(7): p. 1105.
215. Hatchwell, L., et al., *Toll-like receptor 7 governs interferon and inflammatory responses to rhinovirus and is suppressed by IL-5-induced lung eosinophilia.* Thorax, 2015. **70**(9): p. 854-861.
216. Beeh, K.-M., et al., *The novel TLR-9 agonist QbG10 shows clinical efficacy in persistent allergic asthma.* Journal of Allergy and Clinical Immunology, 2013. **131**(3): p. 866-874.
217. Papaioannou, A.I., et al., *The role of endosomal toll-like receptors in asthma.* European journal of pharmacology, 2017. **808**: p. 14-20.
218. Mandel, P., *Les acides nucleiques du plasma sanguin chez 1 homme.* CR Seances Soc Biol Fil, 1948. **142**: p. 241-243.
219. Garcia-Pardo, M., et al., *Integrating circulating-free DNA (cfDNA) analysis into clinical practice: opportunities and challenges.* British Journal of Cancer, 2022. **127**(4): p. 592-602.
220. Pan, Y., et al., *Dynamic circulating tumor DNA during chemoradiotherapy predicts clinical outcomes for locally advanced non-small cell lung cancer patients.* Cancer Cell, 2023. **41**(10): p. 1763-1773. e4.
221. Palacín-Aliana, I., et al., *Clinical utility of liquid biopsy-based actionable mutations detected via ddPCR.* Biomedicines, 2021. **9**(8): p. 906.

222. Aucamp, J., et al., *The diverse origins of circulating cell-free DNA in the human body: a critical re-evaluation of the literature.* Biological Reviews, 2018. **93**(3): p. 1649-1683.
223. Anani, H.A., et al., *Circulating Cell-Free DNA as Inflammatory Marker in Egyptian Psoriasis Patients.* Psoriasis: Targets and Therapy, 2020: p. 13-21.
224. Chen, X., et al., *Intranasal PAMAM-G3 scavenges cell-free DNA attenuating the allergic airway inflammation.* Cell Death Discovery, 2024. **10**(1): p. 213.
225. Jahr, S., et al., *DNA fragments in the blood plasma of cancer patients: quantitations and evidence for their origin from apoptotic and necrotic cells.* Cancer research, 2001. **61**(4): p. 1659-1665.
226. Norbury, C.J. and B. Zhivotovsky, *DNA damage-induced apoptosis.* Oncogene, 2004. **23**(16): p. 2797-2808.
227. Oberhammer, F., et al., *Apoptotic death in epithelial cells: cleavage of DNA to 300 and/or 50 kb fragments prior to or in the absence of internucleosomal fragmentation.* The EMBO journal, 1993. **12**(9): p. 3679-3684.
228. Holdenrieder, S. and P. Stieber, *Clinical use of circulating nucleosomes.* Critical reviews in clinical laboratory sciences, 2009. **46**(1): p. 1-24.
229. Diehl, F., et al., *Circulating mutant DNA to assess tumor dynamics.* Nature medicine, 2008. **14**(9): p. 985-990.
230. Pietrzak, B., et al., *Circulating microbial cell-free DNA in health and disease.* International Journal of Molecular Sciences, 2023. **24**(3): p. 3051.
231. Lo, Y.D., et al., *Presence of fetal DNA in maternal plasma and serum.* The lancet, 1997. **350**(9076): p. 485-487.
232. Cheng, A.P., et al., *Cell-free DNA in blood reveals significant cell, tissue and organ specific injury and predicts COVID-19 severity.* medRxiv, 2020.
233. Szpechcinski, A., et al., *Cell-free DNA levels in plasma of patients with non-small-cell lung cancer and inflammatory lung disease.* British journal of cancer, 2015. **113**(3): p. 476-483.
234. Pathak, A.K., et al., *Circulating cell-free DNA in plasma/serum of lung cancer patients as a potential screening and prognostic tool.* Clinical chemistry, 2006. **52**(10): p. 1833-1842.
235. Mathios, D., et al., *Detection and characterization of lung cancer using cell-free DNA fragmentomes.* Nature communications, 2021. **12**(1): p. 5060.
236. Toussaint, M., et al., *Host DNA released by NETosis promotes rhinovirus-induced type-2 allergic asthma exacerbation.* Nature medicine, 2017. **23**(6): p. 681-691.
237. Ware, S.A., et al., *Cell-free DNA levels associate with COPD exacerbations and mortality.* Respiratory Research, 2024. **25**(1): p. 42.
238. Magenheim, J., et al., *Universal lung epithelium DNA methylation markers for detection of lung damage in liquid biopsies.* European Respiratory Journal, 2022. **60**(5).
239. A. nker, P., et al., *The role of extracellular DNA in the transfer of information from T to B human lymphocytes in the course of an immune response.* International Journal of Immunogenetics, 1980. **7**(6): p. 475-481.
240. Cañas, J.A., et al., *Exosomes from eosinophils autoregulate and promote eosinophil functions.* Journal of Leucocyte Biology, 2017. **101**(5): p. 1191-1199.
241. Hayun, Y., et al., *Circulating cell-free DNA as a potential marker in smoke inhalation injury.* Medicine, 2019. **98**(12): p. e14863.
242. Ueda, K., et al., *Cigarette smoke induces mitochondrial DNA damage and activates cGAS-STING pathway: application to a biomarker for atherosclerosis.* Clinical Science, 2023. **137**(2): p. 163-180.

243. Tanaka, A., et al., *Increased levels of circulating cell-free DNA in COVID-19 patients with respiratory failure.* Scientific Reports, 2024. **14**(1): p. 17399.
244. Zhu, L., et al., *High level of neutrophil extracellular traps correlates with poor prognosis of severe influenza A infection.* The Journal of infectious diseases, 2018. **217**(3): p. 428-437.
245. Zhou, X., et al., *The function and clinical application of extracellular vesicles in innate immune regulation.* Cellular & molecular immunology, 2020. **17**(4): p. 323-334.
246. El Andaloussi, S., et al., *Extracellular vesicles: biology and emerging therapeutic opportunities.* Nature reviews Drug discovery, 2013. **12**(5): p. 347-357.
247. Raposo, G. and W. Stoorvogel, *Extracellular vesicles: exosomes, microvesicles, and friends.* Journal of Cell Biology, 2013. **200**(4): p. 373-383.
248. Yáñez-Mó, M., et al., *Biological properties of extracellular vesicles and their physiological functions.* Journal of extracellular vesicles, 2015. **4**(1): p. 27066.
249. Buzas, E.I., *The roles of extracellular vesicles in the immune system.* Nature Reviews Immunology, 2023. **23**(4): p. 236-250.
250. Javeed, N. and D. Mukhopadhyay, *Exosomes and their role in the micro-/macro-environment: a comprehensive review.* Journal of biomedical research, 2017. **31**(5): p. 386.
251. Gutiérrez-Vázquez, C., et al., *Transfer of extracellular vesicles during immune cell-cell interactions.* Immunological reviews, 2013. **251**(1): p. 125-142.
252. Lee, J.S., et al., *Liquid biopsy using the supernatant of a pleural effusion for EGFR genotyping in pulmonary adenocarcinoma patients: a comparison between cell-free DNA and extracellular vesicle-derived DNA.* BMC cancer, 2018. **18**: p. 1-8.
253. Elzanowska, J., C. Semira, and B. Costa-Silva, *DNA in extracellular vesicles: biological and clinical aspects.* Molecular Oncology, 2021. **15**(6): p. 1701-1714.
254. Armstrong, E.A., et al., *Exosomes in pancreatic cancer: from early detection to treatment.* Journal of Gastrointestinal Surgery, 2018. **22**(4): p. 737-750.
255. Cai, J., et al., *Extracellular vesicle-mediated transfer of donor genomic DNA to recipient cells is a novel mechanism for genetic influence between cells.* Journal of molecular cell biology, 2013. **5**(4): p. 227-238.
256. Ramirez, R.D., et al., *Immortalization of human bronchial epithelial cells in the absence of viral oncoproteins.* Cancer research, 2004. **64**(24): p. 9027-9034.
257. Choina, M., et al., *Dermatophagoides pteronyssinus proteins and their role in the diagnostics and management of house dust mite allergy: exploring allergenic components.* Advances in Dermatology and Allergology/Postępy Dermatologii i Alergologii, 2024. **41**(1).
258. Alexopoulou, L., et al., *Recognition of double-stranded RNA and activation of NF-κB by Toll-like receptor 3.* Nature, 2001. **413**(6857): p. 732-738.
259. Welinder, C. and L. Ekblad, *Coomassie staining as loading control in Western blot analysis.* Journal of proteome research, 2011. **10**(3): p. 1416-1419.
260. Devonshire, A.S., et al., *Towards standardisation of cell-free DNA measurement in plasma: controls for extraction efficiency, fragment size bias and quantification.* Analytical and bioanalytical chemistry, 2014. **406**: p. 6499-6512.
261. Gardiner, C., et al., *Extracellular vesicle sizing and enumeration by nanoparticle tracking analysis.* Journal of extracellular vesicles, 2013. **2**(1): p. 19671.
262. Mead, T.J. and V. Lefebvre, *Proliferation assays (BrdU and EdU) on skeletal tissue sections.* Skeletal Development and Repair: Methods and Protocols, 2014: p. 233-243.
263. Gratzner, H.G., *Monoclonal antibody to 5-bromo-and 5-iododeoxyuridine: a new reagent for detection of DNA replication.* Science, 1982. **218**(4571): p. 474-475.

264. Martin, M., *Cutadapt removes adapter sequences from high-throughput sequencing reads.* EMBnet. journal, 2011. **17**(1): p. 10-12.
265. Dobin, A., et al., *STAR: ultrafast universal RNA-seq aligner.* Bioinformatics, 2013. **29**(1): p. 15-21.
266. Liao, Y., G.K. Smyth, and W. Shi, *featureCounts: an efficient general purpose program for assigning sequence reads to genomic features.* Bioinformatics, 2014. **30**(7): p. 923-930.
267. Love, M.I., W. Huber, and S. Anders, *Moderated estimation of fold change and dispersion for RNA-seq data with DESeq2.* Genome biology, 2014. **15**: p. 1-21.
268. Team, R.C., *R: A language and environment for statistical computing'*. 2023, R Foundation for Statistical Computing: Vienna, Austria.
269. Yu, G., et al., *clusterProfiler: an R package for comparing biological themes among gene clusters.* Omics: a journal of integrative biology, 2012. **16**(5): p. 284-287.
270. Wu, T., et al., *clusterProfiler 4.0: A universal enrichment tool for interpreting omics data.* The innovation, 2021. **2**(3).
271. Carlson, M., et al., *org. Hs. eg. db: Genome wide annotation for Human.* R package version, 2019. **3**(2): p. 3.
272. Gülşen, A., *Asthma phenotypes and current biological treatments*, in *Recent Advances in Asthma Research and Treatments*. 2021, IntechOpen.
273. Chaudhuri, R., et al., *Effects of smoking cessation on lung function and airway inflammation in smokers with asthma.* American journal of respiratory and critical care medicine, 2006. **174**(2): p. 127-133.
274. Chalmers, G., et al., *Influence of cigarette smoking on inhaled corticosteroid treatment in mild asthma.* Thorax, 2002. **57**(3): p. 226-230.
275. Calderón, M.A., et al., *Respiratory allergy caused by house dust mites: what do we really know?* Journal of Allergy and Clinical Immunology, 2015. **136**(1): p. 38-48.
276. Agache, I., et al., *EAACI Guidelines on Allergen Immunotherapy: House dust mite-driven allergic asthma.* Allergy, 2019. **74**(5): p. 855-873.
277. Miller, J.D., *The role of dust mites in allergy.* Clinical reviews in allergy & immunology, 2019. **57**(3): p. 312-329.
278. Virchow, J.C., et al., *Efficacy of a house dust mite sublingual allergen immunotherapy tablet in adults with allergic asthma: a randomized clinical trial.* Jama, 2016. **315**(16): p. 1715-1725.
279. Bernhard, S., et al., *Interleukin 8 elicits rapid physiological changes in neutrophils that are altered by inflammatory conditions.* Journal of innate immunity, 2021. **13**(4): p. 225-241.
280. Alshehri, M., et al., *P115 Cigarettes smoke extract induces inflammatory gene expression in human bronchial epithelial cells*. 2017, BMJ Publishing Group Ltd.
281. Lee, K.-H., et al., *Cigarette smoke extract enhances IL-17A-induced IL-8 production via up-regulation of IL-17R in human bronchial epithelial cells.* Molecules and cells, 2018. **41**(4): p. 282-289.
282. Waltl, E.E., et al., *Betamethasone prevents human rhinovirus-and cigarette smoke-induced loss of respiratory epithelial barrier function.* Scientific reports, 2018. **8**(1): p. 9688.
283. Janbazacyabar, H., et al., *Prenatal and postnatal cigarette smoke exposure is associated with increased risk of exacerbated allergic airway immune responses: a preclinical mouse model.* Frontiers in Immunology, 2021. **12**: p. 797376.
284. Nedeva, D., et al., *Epithelial alarmins: A new target to treat chronic respiratory diseases.* Expert Review of Respiratory Medicine, 2023. **17**(9): p. 773-786.

285. O'Grady, S.M. and H. Kita, *ATP functions as a primary alarmin in allergen-induced type 2 immunity.* American Journal of Physiology-Cell Physiology, 2023. **325**(5): p. C1369-C1386.
286. Davoine, F. and P. Lacy, *Eosinophil cytokines, chemokines, and growth factors: emerging roles in immunity.* Frontiers in immunology, 2014. **5**: p. 570.
287. Pease, J.E. and I. Sabroe, *The role of interleukin-8 and its receptors in inflammatory lung disease: implications for therapy.* American Journal of Respiratory Medicine, 2002. **1**: p. 19-25.
288. Rincon, M. and C.G. Irvin, *Role of IL-6 in asthma and other inflammatory pulmonary diseases.* International journal of biological sciences, 2012. **8**(9): p. 1281.
289. Chang, H.S., et al., *Neutrophilic inflammation in asthma: mechanisms and therapeutic considerations.* Expert review of respiratory medicine, 2017. **11**(1): p. 29-40.
290. Vassallo, R., et al., *Nicotine and oxidative cigarette smoke constituents induce immune-modulatory and pro-inflammatory dendritic cell responses.* Molecular immunology, 2008. **45**(12): p. 3321-3329.
291. Lin, C.-C., et al., *Induction of COX-2/PGE2/IL-6 is crucial for cigarette smoke extract-induced airway inflammation: role of TLR4-dependent NADPH oxidase activation.* Free Radical Biology and Medicine, 2010. **48**(2): p. 240-254.
292. Zhang, W., Y. Zhang, and Q. Zhu, *Cigarette smoke extract-mediated FABP4 upregulation suppresses viability and induces apoptosis, inflammation and oxidative stress of bronchial epithelial cells by activating p38 MAPK/MK2 signaling pathway.* Journal of Inflammation, 2022. **19**(1): p. 7.
293. Lloyd, C.M. and S. Saglani, *Epithelial cytokines and pulmonary allergic inflammation.* Current opinion in immunology, 2015. **34**: p. 52-58.
294. Duchesne, M., I. Okoye, and P. Lacy, *Epithelial cell alarmin cytokines: Frontline mediators of the asthma inflammatory response.* Frontiers in Immunology, 2022. **13**: p. 975914.
295. Gregory, L.G., et al., *IL-25 drives remodelling in allergic airways disease induced by house dust mite.* Thorax, 2013. **68**(1): p. 82-90.
296. Ramu, S., et al., *Comparing epithelial alarmin responses to different aeroallergens in bronchial epithelial cells from allergic asthma patients*. 2022, Eur Respiratory Soc.
297. Kasakura, K., et al., *Histamine-releasing factor is a novel alarmin induced by house dust mite allergen, cytokines, and cell death.* The Journal of Immunology, 2022. **209**(10): p. 1851-1859.
298. Canbaz, D., et al., *IL-33 promotes the induction of immunoglobulin production after inhalation of house dust mite extract in mice.* Allergy, 2015. **70**(5): p. 522-532.
299. Ouyang, X., et al., *House dust mite allergens induce Ca2+ signalling and alarmin responses in asthma airway epithelial cells.* Biochimica et Biophysica Acta (BBA)-Molecular Basis of Disease, 2024. **1870**(4): p. 167079.
300. Gauvreau, G.M., L. White, and B.E. Davis, *Anti-alarmin approaches entering clinical trials.* Current opinion in pulmonary medicine, 2020. **26**(1): p. 69-76.
301. Abo-Shanab, A.M., et al., *Role of Th2 type cytokines and IgE in asthmatic children.* Biomedical and Pharmacology Journal, 2020. **13**(4): p. 1765-1772.
302. Woo, L., et al., *A 4-week model of house dust mite (HDM) induced allergic airways inflammation with airway remodeling.* Scientific reports, 2018. **8**(1): p. 6925.
303. Kauffman, H.F., et al., *House dust mite major allergens Der p 1 and Der p 5 activate human airway-derived epithelial cells by protease-dependent and protease-independent mechanisms.* Clinical and Molecular Allergy, 2006. **4**: p. 1-8.

304. Shi, J., et al., *Induction of IL-6 and IL-8 by House Dust Mite Allergen Der p1 in Cultured Human Nasal Epithelial Cells Is Associated with PAR/PI3K/NFκB Signaling.* ORL, 2010. **72**(5): p. 256-265.
305. Di Vincenzo, S., et al., *TSLP and oxidative stress: two associated events reflecting airway epithelium injury upon cigarette smoke exposure*. 2023, Eur Respiratory Soc.
306. Pace, E., et al., *Cilomilast counteracts the effects of cigarette smoke in airway epithelial cells.* Cellular Immunology, 2011. **268**(1): p. 47-53.
307. Son, E.S., et al., *Effects of antioxidants on oxidative stress and inflammatory responses of human bronchial epithelial cells exposed to particulate matter and cigarette smoke extract.* Toxicology in Vitro, 2020. **67**: p. 104883.
308. Oltmanns, U., et al., *Cigarette smoke induces IL-8, but inhibits eotaxin and RANTES release from airway smooth muscle.* Respiratory research, 2005. **6**: p. 1-10.
309. Liu, J., et al., *Interplay of IL-33 and IL-35 modulates Th2/Th17 responses in cigarette smoke exposure HDM-induced asthma.* Inflammation, 2024. **47**(1): p. 173-190.
310. Fung, N.H., et al., *Early-life house dust mite aeroallergen exposure augments cigarette smoke-induced myeloid inflammation and emphysema in mice.* Respiratory Research, 2024. **25**(1): p. 161.
311. Mitchell, V.L., L.S. Van Winkle, and L.J. Gershwin, *Environmental tobacco smoke and progesterone alter lung inflammation and mucous metaplasia in a mouse model of allergic airway disease.* Clinical reviews in allergy & immunology, 2012. **43**: p. 57-68.
312. Hillyer, P., et al., *Differential responses by human respiratory epithelial cell lines to respiratory syncytial virus reflect distinct patterns of infection control.* Journal of virology, 2018. **92**(15): p. 10.1128/jvi. 02202-17.
313. Post, S., et al., *The composition of house dust mite is critical for mucosal barrier dysfunction and allergic sensitisation.* Thorax, 2012. **67**(6): p. 488-495.
314. Karaaslan, C., et al., *The expression profile of protease inhibitors in the airway epithelial cells after allergen (Der p 1) stimulation.* International Archives of Allergy and Immunology, 2022. **183**(1): p. 25-33.
315. Baskoro, H., et al., *Regional heterogeneity in response of airway epithelial cells to cigarette smoke.* BMC Pulmonary Medicine, 2018. **18**: p. 1-11.
316. Yang, C.-M., et al., *Cigarette smoke extract induces COX-2 expression via a PKCα/c-Src/EGFR, PDGFR/PI3K/Akt/NF-κB pathway and p300 in tracheal smooth muscle cells.* American Journal of Physiology-Lung Cellular and Molecular Physiology, 2009. **297**(5): p. L892-L902.
317. Jackson, D.J. and S.L. Johnston, *The role of viruses in acute exacerbations of asthma.* Journal of Allergy and Clinical Immunology, 2010. **125**(6): p. 1178-1187.
318. Wark, P.A., et al., *Asthmatic bronchial epithelial cells have a deficient innate immune response to infection with rhinovirus.* The Journal of experimental medicine, 2005. **201**(6): p. 937-947.
319. Nakayama, M., et al., *Quantitative proteomics of differentiated primary bronchial epithelial cells from chronic obstructive pulmonary disease and control identifies potential novel host factors post-influenza A virus infection.* Frontiers in Microbiology, 2023. **13**: p. 957830.
320. Cai, X., et al., *Protective role of activated protein C against viral mimetic poly (I: C)-induced inflammation.* Thrombosis and haemostasis, 2021. **121**(11): p. 1448-1463.
321. Lever, A.R., et al., *Comprehensive evaluation of poly (I: C) induced inflammatory response in an airway epithelial model.* Physiological reports, 2015. **3**(4): p. e12334.
322. Li, Y.-G., et al., *Poly (I: C), an agonist of toll-like receptor-3, inhibits replication of the Chikungunya virus in BEAS-2B cells.* Virology journal, 2012. **9**: p. 1-8.

323. Kark, J.D., M. Lebiush, and L. Rannon, *Cigarette smoking as a risk factor for epidemic a (h1n1) influenza in young men.* New England Journal of Medicine, 1982. **307**(17): p. 1042-1046.
324. Oostwoud, L., et al., *Apocynin and ebselen reduce influenza A virus-induced lung inflammation in cigarette smoke-exposed mice.* Scientific reports, 2016. **6**(1): p. 20983.
325. Duffney, P.F., et al., *Cigarette smoke increases susceptibility to infection in lung epithelial cells by upregulating caveolin-dependent endocytosis.* PloS one, 2020. **15**(5): p. e0232102.
326. Horvath, K.M., et al., *Epithelial cells from smokers modify dendritic cell responses in the context of influenza infection.* American journal of respiratory cell and molecular biology, 2011. **45**(2): p. 237-245.
327. Danov, O., et al., *Cigarette smoke affects dendritic cell populations, epithelial barrier function, and the immune response to viral infection with H1N1.* Frontiers in medicine, 2020. **7**: p. 571003.
328. Kearley, J., et al., *Cigarette smoke silences innate lymphoid cell function and facilitates an exacerbated type I interleukin-33-dependent response to infection.* Immunity, 2015. **42**(3): p. 566-579.
329. Demchenko, E., et al., *Dynamics of cell-free DNA levels in the in vivo LPS-induced inflammation model.* Russian Journal of Immunology, 2022. **25**(4): p. 423-430.
330. Fernando, M.R., et al., *New evidence that a large proportion of human blood plasma cell-free DNA is localized in exosomes.* PloS one, 2017. **12**(8): p. e0183915.
331. Lachowicz-Scroggins, M.E., et al., *Extracellular DNA, neutrophil extracellular traps, and inflammasome activation in severe asthma.* American journal of respiratory and critical care medicine, 2019. **199**(9): p. 1076-1085.
332. Cañas, J., et al., *Eosinophil-derived exosomes contribute to asthma remodelling by activating structural lung cells.* Clinical & Experimental Allergy, 2018. **48**(9): p. 1173-1185.
333. Hough, K.P., et al., *Exosomes in immunoregulation of chronic lung diseases.* Allergy, 2017. **72**(4): p. 534-544.
334. Glebova, K., et al., *Oxidized extracellular DNA as a stress signal that may modify response to anticancer therapy.* Cancer Letters, 2015. **356**(1): p. 22-33.
335. Mittra, I., et al., *Circulating nucleic acids damage DNA of healthy cells by integrating into their genomes.* Journal of biosciences, 2015. **40**: p. 91-111.
336. Nishimoto, S., et al., *Obesity-induced DNA released from adipocytes stimulates chronic adipose tissue inflammation and insulin resistance.* Science advances, 2016. **2**(3): p. e1501332.
337. Andargie, T.E., et al., *Cell-free DNA maps COVID-19 tissue injury and risk of death and can cause tissue injury.* JCI insight, 2021. **6**(7).
338. Thompson, S., et al., *Investigating the Role of Cell-Free DNA (cfDNA) Release from Airway Structural Cells in Asthma Pathogenesis*, in *D110. EPITHELIAL FUNCTION IN HEALTH AND DISEASE*. 2018, American Thoracic Society. p. A7632-A7632.
339. Jing-xi, Z., et al., *Effects of Poly (I: C), LPS and PGN stimulation on the innate immune function of human bronchial epithelium.* Jie Fang Jun Yi Xue Za Zhi, 2013. **38**(7): p. 552.
340. Stanbery, A.G., et al., *TSLP, IL-33, and IL-25: Not just for allergy and helminth infection.* Journal of Allergy and Clinical Immunology, 2022. **150**(6): p. 1302-1313.
341. Kumar, R.K., P.S. Foster, and H.F. Rosenberg, *Respiratory viral infection, epithelial cytokines, and innate lymphoid cells in asthma exacerbations.* Journal of leukocyte biology, 2014. **96**(3): p. 391-396.

342. De Luca, G., et al., *High cell-free DNA is associated with disease progression, inflammasome activation and elevated levels of inflammasome-related cytokine IL-18 in patients with myelofibrosis.* Frontiers in Immunology, 2023. **14**: p. 1161832.
343. Duvvuri, B. and C. Lood, *Cell-free DNA as a biomarker in autoimmune rheumatic diseases.* Frontiers in immunology, 2019. **10**: p. 502.
344. Swarup, N., et al., *Cell-Free DNA: Features and Attributes Shaping the Next Frontier in Liquid Biopsy.* Molecular Diagnosis & Therapy, 2025. **29**(3): p. 277-290.
345. Alsharairi, N.A., *Antioxidant intake and biomarkers of asthma in relation to smoking status—a review.* Current Issues in Molecular Biology, 2023. **45**(6): p. 5099-5117.
346. Emma, R., et al., *Enhanced oxidative stress in smoking and ex-smoking severe asthma in the U-BIOPRED cohort.* PLoS One, 2018. **13**(9): p. e0203874.
347. Rossi, G.A., et al., *Alarmins and innate lymphoid cells 2 activation: A common pathogenetic link connecting respiratory syncytial virus bronchiolitis and later wheezing/asthma?* Pediatric allergy and immunology, 2022. **33**(6): p. e13803.
348. Zhong, N., *Coordinating Poly (I: C) and Aluminum within Liposomal Vesicles for Enhanced Innate Immune Activation.* Highlights in Science, Engineering and Technology, 2023. **74**: p. 577-583.
349. Golebski, K., et al., *Specific induction of TSLP by the viral RNA analogue Poly (I: C) in primary epithelial cells derived from nasal polyps.* PloS one, 2016. **11**(4): p. e0152808.
350. Fujita, A., et al., *Inhibition of PI3Kδ enhances poly I: C-induced antiviral responses and inhibits replication of human metapneumovirus in murine lungs and human bronchial epithelial cells.* Frontiers in immunology, 2020. **11**: p. 432.
351. Guo-Parke, H., et al., *Altered differentiation and inflammation profiles contribute to enhanced innate responses in severe COPD epithelium to rhinovirus infection.* Frontiers in Medicine, 2022. **9**: p. 741989.
352. Valette, K., et al., *Late response of bronchial epithelium to rhinovirus in severe asthma.* Revue des Maladies Respiratoires, 2024. **41**(3): p. 187-188.
353. Noah, T.L. and S. Becker, *Respiratory syncytial virus-induced cytokine production by a human bronchial epithelial cell line.* American Journal of Physiology-Lung Cellular and Molecular Physiology, 1993. **265**(5): p. L472-L478.
354. Frøssing, L., et al., *Clustering of bronchial epithelial immune response to a viral mimic identifies clinically recognizable viral exacerbation profiles*. 2023, Eur Respiratory Soc.
355. Aizawa, H., et al., *Oxidative stress enhances the expression of IL-33 in human airway epithelial cells.* Respiratory research, 2018. **19**: p. 1-12.
356. Harada, M., et al., *Functional analysis of the thymic stromal lymphopoietin variants in human bronchial epithelial cells.* American journal of respiratory cell and molecular biology, 2009. **40**(3): p. 368-374.
357. Amerio, P., et al., *Role of Th2 cytokines, RANTES and eotaxin in AIDS-associated eosinophilic folliculitis.* Acta dermato-venereologica, 2001. **81**(2): p. 92-95.
358. Liu, Y., et al., *Cytokine, chemokine, and adhesion molecule expression mediated by MAPKs in human corneal fibroblasts exposed to poly (I: C).* Investigative ophthalmology & visual science, 2008. **49**(8): p. 3336-3344.
359. Ribes, S., et al., *Pre-treatment with the viral Toll-like receptor 3 agonist poly (I: C) modulates innate immunity and protects neutropenic mice infected intracerebrally with Escherichia coli.* Journal of Neuroinflammation, 2020. **17**: p. 1-10.
360. Alves, M.P., et al., *IP-10 is selectively produced in the airways upon respiratory virus infection*. 2013, European Respiratory Society.

361. MoriA, O., *Th2-cell-mediatedchemokinesynthesisisinvolvedinallergicairway inflammationinmice.* IntArchAllergyImmunol, 2006. **140**: p. 55-58.
362. Contoli, M., et al., *Th2 cytokines impair innate immune responses to rhinovirus in respiratory epithelial cells.* Allergy, 2015. **70**(8): p. 910-920.
363. White, S.R., et al., *Human leukocyte antigen-G expression in differentiated human airway epithelial cells: lack of modulation by Th2-associated cytokines.* Respiratory research, 2013. **14**: p. 1-11.
364. Okuma, N., et al., *Amplification of poly (I: C)-induced interleukin-6 production in human bronchial epithelial cells by priming with interferon-γ.* Scientific Reports, 2023. **13**(1): p. 21067.
365. Laura, G., et al., *ORMDL3 regulates poly I: C induced inflammatory responses in airway epithelial cells.* BMC Pulmonary Medicine, 2021. **21**(1): p. 167.
366. Lee, K.-I., et al., *Tobacco smoking could accentuate epithelial-mesenchymal transition and Th2-type response in patients with chronic rhinosinusitis with nasal polyps.* Immune Network, 2022. **22**(4): p. e35.
367. Pace, E., et al., *Cigarette smoke alters IL-33 expression and release in airway epithelial cells.* Biochimica et Biophysica Acta (BBA)-Molecular Basis of Disease, 2014. **1842**(9): p. 1630-1637.
368. Lee, J.H., et al., *Cigarette smoke triggers IL-33–associated inflammation in a model of late-stage chronic obstructive pulmonary disease.* American Journal of Respiratory Cell and Molecular Biology, 2019. **61**(5): p. 567-574.
369. Nakamura, Y., et al., *Cigarette smoke extract induces thymic stromal lymphopoietin expression, leading to TH2-type immune responses and airway inflammation.* Journal of Allergy and Clinical Immunology, 2008. **122**(6): p. 1208-1214.
370. Jiang, R., et al., *Cigarette smoke extract promotes TIM4 expression in murine dendritic cells leading to Th2 polarization through ERK-dependent pathways.* International Archives of Allergy and Immunology, 2019. **178**(3): p. 219-228.
371. Cooper, P.R., et al., *Involvement of IL-13 in Tobacco Smoke–Induced Changes in the Structure and Function of Rat Intrapulmonary Airways.* American journal of respiratory cell and molecular biology, 2010. **43**(2): p. 220-226.
372. Teng, Y. and Y. Gao, *Tobacco smoking associated with the increases of the bronchoalveolar levels of interleukin-5 and interleukin-1 receptor antagonist in acute eosinophilic pneumonia.* European Review for Medical & Pharmacological Sciences, 2014. **18**(6).
373. Krisiukeniene, A., et al., *Smoking affects eotaxin levels in asthma patients.* Journal of Asthma, 2009. **46**(5): p. 470-476.
374. Montaño-Velázquez, B.B., et al., *Effect of cigarette smoke on counts of immunoreactive cells to eotaxin-1 and eosinophils on the nasal mucosa in young patients with perennial allergic rhinitis.* Brazilian Journal of Otorhinolaryngology, 2017. **83**(4): p. 420-425.
375. Zheng, W., et al., *Pentoxifylline attenuates cigarette smoke-induced overexpression of CXCR3 and IP-10 in mice.* Chinese Medical Journal, 2012. **125**(11): p. 1980-1985.
376. Mortaz, E., et al., *Cigarette smoke induces CXCL8 production by human neutrophils via activation of TLR9 receptor.* European Respiratory Journal, 2010. **36**(5): p. 1143-1154.
377. Mortaz, E., et al., *Cigarette smoke induces the release of CXCL-8 from human bronchial epithelial cells via TLRs and induction of the inflammasome.* Biochimica et Biophysica Acta (BBA)-Molecular Basis of Disease, 2011. **1812**(9): p. 1104-1110.
378. Ilmarinen, P., et al., *Comorbidities and elevated IL-6 associate with negative outcome in adult-onset asthma.* European Respiratory Journal, 2016. **48**(4): p. 1052-1062.

379. Koo, J.B. and J.-S. Han, *Cigarette smoke extract-induced interleukin-6 expression is regulated by phospholipase D1 in human bronchial epithelial cells.* The Journal of toxicological sciences, 2016. **41**(1): p. 77-89.
380. Wu, W., et al., *Human primary airway epithelial cells isolated from active smokers have epigenetically impaired antiviral responses.* Respiratory research, 2016. **17**: p. 1-11.
381. Melgert, B.N., et al., *Short-term smoke exposure attenuates ovalbumin-induced airway inflammation in allergic mice.* American Journal of Respiratory Cell and Molecular Biology, 2004. **30**(6): p. 880-885.
382. Swaroop, A.K., et al., *Navigating IL-6: From molecular mechanisms to therapeutic breakthroughs.* Cytokine & Growth Factor Reviews, 2024.
383. Duffney, P.F., et al., *Cigarette smoke dampens antiviral signaling in small airway epithelial cells by disrupting TLR3 cleavage.* American Journal of Physiology-Lung Cellular and Molecular Physiology, 2018. **314**(3): p. L505-L513.
384. Hudy, M.H., et al., *Cigarette smoke modulates rhinovirus-induced airway epithelial cell chemokine production.* European Respiratory Journal, 2010. **35**(6): p. 1256-1263.
385. Zhang, L. and J. Li, *Unlocking the secrets: the power of methylation-based cfDNA detection of tissue damage in organ systems.* Clinical Epigenetics, 2023. **15**(1): p. 168.
386. Avriel, A., et al., *Prognostic utility of admission cell-free DNA levels in patients with chronic obstructive pulmonary disease exacerbations.* International journal of chronic obstructive pulmonary disease, 2016: p. 3153-3161.
387. Pasupneti, S., et al., *Association of Donor Derived Cell-Free DNA Fractions with Acute Rejection and Pulmonary Infections in Lung Transplant Recipients.* The Journal of Heart and Lung Transplantation, 2024. **43**(4): p. S655-S656.
388. Gregory, C.D. and M.P. Rimmer, *Extracellular vesicles arising from apoptosis: Forms, functions, and applications.* The Journal of Pathology, 2023. **260**(5): p. 592-608.
389. Poon, I.K., et al., *Moving beyond size and phosphatidylserine exposure: evidence for a diversity of apoptotic cell-derived extracellular vesicles in vitro.* Journal of extracellular vesicles, 2019. **8**(1): p. 1608786.
390. Catalano, M. and L. O'Driscoll, *Inhibiting extracellular vesicles formation and release: a review of EV inhibitors.* Journal of extracellular vesicles, 2020. **9**(1): p. 1703244.
391. Aranda, A., et al., *Dichloro-dihydro-fluorescein diacetate (DCFH-DA) assay: a quantitative method for oxidative stress assessment of nanoparticle-treated cells.* Toxicology in vitro, 2013. **27**(2): p. 954-963.
392. Bentley, J.K. and M.B. Hershenson, *Airway smooth muscle growth in asthma: proliferation, hypertrophy, and migration.* Proceedings of the American Thoracic Society, 2008. **5**(1): p. 89-96.
393. Knox, A., et al., *Airway smooth muscle function in asthma.* Clinical & Experimental Allergy, 2000. **30**(5).
394. Bonet, M.L. and A. Palou, *Regulation of gene expression*, in *Principles of Nutrigenetics and Nutrigenomics*. 2020, Elsevier. p. 17-25.
395. Institute, N.H.G.R. *Transcriptome Fact Sheet*. 2020, August; Available from: https://www.genome.gov/about-genomics/fact-sheets/Transcriptome-Fact-Sheet#:~:text=By%20collecting%20and%20comparing%20transcriptomes,reflect%20or%20contribute%20to%20disease.
396. Assis, A.F., et al., *What is the transcriptome and how it is evaluated?* Transcriptomics in Health and Disease, 2014: p. 3-48.
397. Wang, Z., M. Gerstein, and M. Snyder, *RNA-Seq: a revolutionary tool for transcriptomics.* Nature reviews genetics, 2009. **10**(1): p. 57-63.

398. Yue, M., et al., *Transcriptomic profiles in nasal epithelium and asthma endotypes in youth.* JAMA, 2025. **333**(4): p. 307-318.
399. Billatos, E., et al., *The airway transcriptome as a biomarker for early lung cancer detection.* Clinical Cancer Research, 2018. **24**(13): p. 2984-2992.
400. Voic, H., et al., *RNA sequencing identifies common pathways between cigarette smoke exposure and replicative senescence in human airway epithelia.* BMC genomics, 2019. **20**: p. 1-12.
401. Nakamura, M., et al., *TGF-β1 signaling is essential for tissue regeneration in the Xenopus tadpole tail.* Biochemical and biophysical research communications, 2021. **565**: p. 91-96.
402. Lee, S.J., et al., *Gα13 regulates methacholine-induced contraction of bronchial smooth muscle via phosphorylation of MLC20.* Biochemical pharmacology, 2009. **77**(9): p. 1497-1505.
403. Liu, Q., J. Liu, and X. Huang, *Unraveling the mystery: How bad is BAG3 in hematological malignancies?* Biochimica et Biophysica Acta (BBA)-Reviews on Cancer, 2022. **1877**(5): p. 188781.
404. Cao, X., et al., *CXC motif chemokine ligand 9 correlates with favorable prognosis in triple-negative breast cancer by promoting immune cell infiltration.* Molecular Cancer Therapeutics, 2023. **22**(12): p. 1493-1502.
405. Hasegawa, T., et al., *Serum CXCL9 as a potential marker of Type 1 inflammation in the context of eosinophilic asthma.* Allergy, 2019. **74**(12): p. 2515.
406. Xie, M., et al., *IL-27 and type 2 immunity in asthmatic patients: association with severity, CXCL9, and signal transducer and activator of transcription signaling.* Journal of Allergy and Clinical Immunology, 2015. **135**(2): p. 386-394. e5.
407. Feng, J., et al., *Inducible GBP5 mediates the antiviral response via interferon-related pathways during influenza A virus infection.* Journal of innate immunity, 2017. **9**(4): p. 419-435.
408. Zhang, Z. and F. Zhan, *Type 2 cystatins and their roles in the regulation of human immune response and cancer progression.* Cancers, 2023. **15**(22): p. 5363.
409. Liu, H.B., J. Bai, and W.X. Wang, *CST1 promotes the proliferation and migration of PDGF-BB-treated airway smooth muscle cells via the PI3K/AKT signaling pathway.* The Kaohsiung journal of medical sciences, 2023. **39**(2): p. 145-153.
410. Thomas, P.S., *Tumour necrosis factor-α: The role of this multifunctional cytokine in asthma.* Immunology and cell biology, 2001. **79**(2): p. 132-140.
411. Lykouras, D., et al., *Role and pharmacogenomics of TNF-α in asthma.* Mini reviews in medicinal chemistry, 2008. **8**(9): p. 934-942.
412. Wang, B., et al., *Dissecting peroxisome-mediated signaling pathways: A new and exciting research field.* Molecular machines involved in peroxisome biogenesis and maintenance, 2014: p. 255-273.
413. Yu, M., et al., *Aberrant purine metabolism in allergic asthma revealed by plasma metabolomics.* Journal of pharmaceutical and biomedical analysis, 2016. **120**: p. 181-189.
414. Gauthier, M., et al., *CCL5 is a potential bridge between type 1 and type 2 inflammation in asthma.* Journal of Allergy and Clinical Immunology, 2023. **152**(1): p. 94-106. e12.
415. Hizawa, N., et al., *Functional single nucleotide polymorphisms of the CCL5 gene and nonemphysematous phenotype in COPD patients.* European Respiratory Journal, 2008. **32**(2): p. 372-378.
416. Medicine, N.L.o. *SMCO3 single-pass membrane protein with coiled-coil domains 3*. 2025; Available from: https://www.ncbi.nlm.nih.gov/gene/440087/.

417. Badabagni, R., et al., *Thiamine-responsive acute pulmonary hypertension–A case series and review from a pediatric ICU.* Asian Journal of Medical Sciences, 2023. **14**(8): p. 266-271.
418. Komander, D. and M. Rape, *The ubiquitin code.* Annual review of biochemistry, 2012. **81**(1): p. 203-229.
419. Zhang, Z. and L.-Y. Li, *TNFSF15 modulates neovascularization and inflammation.* Cancer Microenvironment, 2012. **5**: p. 237-247.
420. Xie, T., et al., *Cell–cell interactions and communication dynamics in lung fibrosis.* Chinese Medical Journal Pulmonary and Critical Care Medicine, 2024.
421. Imkamp, K., et al., *Gene network approach reveals co-expression patterns in nasal and bronchial epithelium.* Scientific Reports, 2019. **9**(1): p. 15835.
422. Kan, M., et al., *Airway smooth muscle–specific transcriptomic signatures of glucocorticoid exposure.* American journal of respiratory cell and molecular biology, 2019. **61**(1): p. 110-120.
423. Wilhelm, B.T. and J.-R. Landry, *RNA-Seq—quantitative measurement of expression through massively parallel RNA-sequencing.* Methods, 2009. **48**(3): p. 249-257.
424. Johnson, P.R., et al., *Airway smooth muscle cell proliferation is increased in asthma.* American journal of respiratory and critical care medicine, 2001. **164**(3): p. 474-477.
425. O'Sullivan, M., et al., *Airway epithelial cells drive airway smooth muscle cell phenotype switching to the proliferative and pro-inflammatory phenotype.* Frontiers in Physiology, 2021. **12**: p. 687654.
426. De La Cruz-Sigüenza, D., et al., *The non-vesicle cell-free DNA (cfDNA) induces cell transformation associated with horizontal DNA transfer.* Molecular Biology Reports, 2024. **51**(1): p. 174.
427. Wu, J., et al., *Central role of cellular senescence in TSLP-induced airway remodeling in asthma.* PLoS One, 2013. **8**(10): p. e77795.
428. Haj-Salem, I., et al., *Fibroblast-derived exosomes promote epithelial cell proliferation through TGF-β2 signalling pathway in severe asthma.* Allergy, 2018. **73**(1): p. 178-186.
429. Wieczfinska, J. and R. Pawliczak, *Anti-fibrotic effect of ciglitazone in HRV-induced airway remodelling cell model.* Journal of Cellular and Molecular Medicine, 2023. **27**(13): p. 1867-1879.
430. Farea, M., et al., *Synergistic effects of chitosan scaffold and TGFβ1 on the proliferation and osteogenic differentiation of dental pulp stem cells derived from human exfoliated deciduous teeth.* Archives of oral biology, 2014. **59**(12): p. 1400-1411.
431. Pan, Y., et al., *Activation of AMPK inhibits TGF-β1-induced airway smooth muscle cells proliferation and its potential mechanisms.* Scientific reports, 2018. **8**(1): p. 3624.
432. Lv, X., et al., *TGF-β1 induces airway smooth muscle cell proliferation and remodeling in asthmatic mice by up-regulating miR-181a and suppressing PTEN.* International Journal of Clinical and Experimental Pathology, 2019. **12**(1): p. 173.
433. Sakota, Y., et al., *Collagen gel contraction assay using human bronchial smooth muscle cells and its application for evaluation of inhibitory effect of formoterol.* Biological and Pharmaceutical Bulletin, 2014. **37**(6): p. 1014-1020.
434. Kouyama, S., et al., *A contraction assay system using primary cultured mouse bronchial smooth muscle cells.* International Archives of Allergy and Immunology, 2013. **161**(Suppl. 2): p. 93-97.
435. Ramis, J., et al., *Lysyl oxidase like 2 is increased in asthma and contributes to asthmatic airway remodelling.* European Respiratory Journal, 2022. **60**(1).

436. Hou, M., et al., *Comparative analysis of BAG1 and BAG2: Insights into their structures, functions and implications in disease pathogenesis.* International Immunopharmacology, 2024. **143**: p. 113369.
437. Sun, W., et al., *CIRP sensitizes cancer cell responses to ionizing radiation.* Radiation research, 2021. **195**(1): p. 93-100.
438. Liao, Y., et al., *CIRP promotes the progression of non-small cell lung cancer through activation of Wnt/β-catenin signaling via CTNNB1.* Journal of Experimental & Clinical Cancer Research, 2021. **40**(1): p. 275.
439. Callahan, V., et al., *The pro-inflammatory chemokines CXCL9, CXCL10 and CXCL11 are upregulated following SARS-CoV-2 infection in an AKT-dependent manner.* Viruses, 2021. **13**(6): p. 1062.
440. Zhao, C., et al., *Infant RSV infection desensitizes β2-adrenergic receptor via CXCL11-CXCR7 signaling in airway smooth muscle.* bioRxiv, 2025: p. 2025.01. 13.632772.
441. Culley, F.J., et al., *Role of CCL5 (RANTES) in viral lung disease.* Journal of virology, 2006. **80**(16): p. 8151-8157.
442. Nishimura, R., et al., *The role of Smads in BMP signaling.* Front Biosci, 2003. **8**: p. s275-s284.
443. Gao, T., et al., *Aberrant hypomethylation and overexpression of the eyes absent homologue 2 suppresses tumor cell growth of human lung adenocarcinoma cells.* Oncology reports, 2015. **34**(5): p. 2333-2342.
444. Anantharajan, J., et al., *Structural and functional analyses of an allosteric EYA2 phosphatase inhibitor that has on-target effects in human lung cancer cells.* Molecular cancer therapeutics, 2019. **18**(9): p. 1484-1496.
445. Ucche, S., et al., *GSTA4 governs melanoma immune resistance and metastasis.* Molecular Cancer Research, 2023. **21**(1): p. 76-85.
446. Onomoto, K., et al., *Antiviral innate immunity and stress granule responses.* Trends in immunology, 2014. **35**(9): p. 420-428.
447. Guan, Y., et al., *Multiple functions of stress granules in viral infection at a glance.* Frontiers in Microbiology, 2023. **14**: p. 1138864.
448. Niessen, N.M., et al., *Airway monocyte modulation relates to tumour necrosis factor dysregulation in neutrophilic asthma.* ERJ Open Research, 2021. **7**(3).
449. Yeganeh, B., et al., *Asthma and influenza virus infection: focusing on cell death and stress pathways in influenza virus replication.* Iranian Journal of Allergy, Asthma and Immunology, 2013: p. 1-17.
450. Catalanotto, C., et al., *The RNA-binding function of ribosomal proteins and ribosome biogenesis factors in human health and disease.* Biomedicines, 2023. **11**(11): p. 2969.
451. Morita, M. and T. Imanaka, *The function of the peroxisome*, in *Peroxisomes: biogenesis, function, and role in human disease*. 2020, Springer. p. 59-104.
452. Carmichael, R.E. and M. Schrader, *Determinants of peroxisome membrane dynamics.* Frontiers in Physiology, 2022. **13**: p. 834411.
453. Lane, A.N. and T.W. Fan, *Regulation of mammalian nucleotide metabolism and biosynthesis.* Nucleic acids research, 2015. **43**(4): p. 2466-2485.
454. Yao, Y., et al., *Association of HLA-DRB1 gene polymorphism with risk of asthma: A meta-analysis.* Medical science monitor basic research, 2016. **22**: p. 80.
455. Rajagopalan, G., et al., *HLA-DR polymorphism modulates response to house dust mites in a transgenic mouse model of airway inflammation.* Tissue antigens, 2011. **77**(6): p. 589-592.
456. Persson, H., et al., *Transcriptome analysis of controlled and therapy-resistant childhood asthma reveals distinct gene expression profiles.* Journal of Allergy and Clinical Immunology, 2015. **136**(3): p. 638-648.

457. Yang, S., et al., *AIM2 participates in house dust mite (HDM)-induced epithelial dysfunctions and ovalbumin (OVA)-induced allergic asthma in infant mice.* Journal of Asthma, 2024. **61**(5): p. 479-490.
458. Marsango, S. and G. Milligan, *Regulation of the pro-inflammatory G protein-coupled receptor GPR84.* British Journal of Pharmacology, 2024. **181**(10): p. 1500-1508.
459. Tzachanis, D., et al., *The E3 Ubiquitin Ligase TRIM36, a Transcriptional Target of Tob, Is Expressed in Anergic T Cells and Mediates Unresponsiveness through Proteolysis of Signaling Proteins PLC-γ1 and PKC-#.* Blood, 2004. **104**(11): p. 113.
460. Xu, D.W. and M.D. Tate, *Taking AIM at Influenza: The Role of the AIM2 Inflammasome.* Viruses, 2024. **16**(10): p. 1535.
461. Consortium, U., *UniProt: a worldwide hub of protein knowledge.* Nucleic acids research, 2019. **47**(D1): p. D506-D515.
462. Xiang, G., et al., *TGIF1 promoted the growth and migration of cancer cells in nonsmall cell lung cancer.* Tumor Biology, 2015. **36**: p. 9303-9310.
463. Xu, Z., et al., *Bioinformatics analysis and validation of CSRNP1 as a key prognostic gene in non-small cell lung cancer.* Heliyon, 2024. **10**(7).
464. Rusznak, C., et al., *Cigarette smoke potentiates house dust mite allergen–induced increase in the permeability of human bronchial epithelial cells in vitro.* American journal of respiratory cell and molecular biology, 1999. **20**(6): p. 1238-1250.
465. Gahring, L.C., et al., *Lung eosinophilia induced by house dust mites or ovalbumin is modulated by nicotinic receptor α7 and inhibited by cigarette smoke.* American Journal of Physiology-Lung Cellular and Molecular Physiology, 2018. **315**(4): p. L553-L562.
466. Berumen Sánchez, G., et al., *Extracellular vesicles: mediators of intercellular communication in tissue injury and disease.* Cell Communication and Signaling, 2021. **19**: p. 1-18.
467. Gheitasi, H., et al., *Exosome-mediated regulation of inflammatory pathway during respiratory viral disease.* Virology Journal, 2024. **21**(1): p. 30.
468. Caliri, A.W., S. Tommasi, and A. Besaratinia, *Relationships among smoking, oxidative stress, inflammation, macromolecular damage, and cancer.* Mutation Research/Reviews in Mutation Research, 2021. **787**: p. 108365.
469. Wrobel, L.K., et al., *Contractility of single human dermal myofibroblasts and fibroblasts.* Cell motility and the cytoskeleton, 2002. **52**(2): p. 82-90.
470. Wang, M., et al., *Impaired anti-inflammatory action of glucocorticoid in neutrophil from patients with steroid-resistant asthma.* Respiratory research, 2016. **17**: p. 1-9.
471. Jensen, E.J., et al., *Blood eosinophil and monocyte counts are related to smoking and lung function.* Respiratory medicine, 1998. **92**(1): p. 63-69.